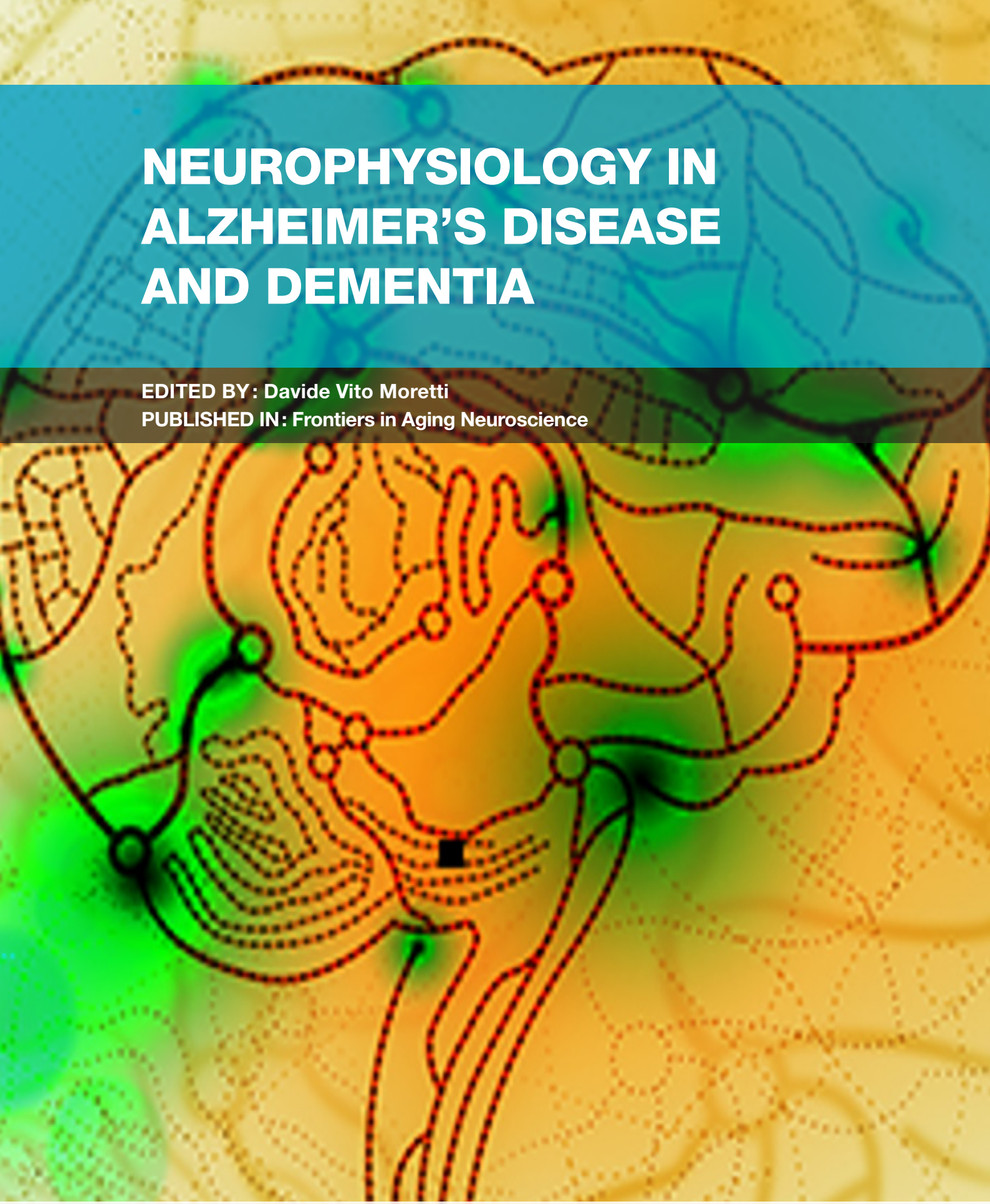

NEUROPHYSIOLOGY IN ALZHEIMER'S DISEASE AND DEMENTIA

EDITED BY: Davide Vito Moretti
PUBLISHED IN: Frontiers in Aging Neuroscience

frontiers Research Topics

frontiers

Frontiers Copyright Statement

© Copyright 2007-2016 Frontiers Media SA. All rights reserved.

All content included on this site, such as text, graphics, logos, button icons, images, video/audio clips, downloads, data compilations and software, is the property of or is licensed to Frontiers Media SA ("Frontiers") or its licensees and/or subcontractors. The copyright in the text of individual articles is the property of their respective authors, subject to a license granted to Frontiers.

The compilation of articles constituting this e-book, wherever published, as well as the compilation of all other content on this site, is the exclusive property of Frontiers. For the conditions for downloading and copying of e-books from Frontiers' website, please see the Terms for Website Use. If purchasing Frontiers e-books from other websites or sources, the conditions of the website concerned apply.

Images and graphics not forming part of user-contributed materials may not be downloaded or copied without permission.

Individual articles may be downloaded and reproduced in accordance with the principles of the CC-BY licence subject to any copyright or other notices. They may not be re-sold as an e-book.

As author or other contributor you grant a CC-BY licence to others to reproduce your articles, including any graphics and third-party materials supplied by you, in accordance with the Conditions for Website Use and subject to any copyright notices which you include in connection with your articles and materials.

All copyright, and all rights therein, are protected by national and international copyright laws.

The above represents a summary only. For the full conditions see the Conditions for Authors and the Conditions for Website Use.

ISSN 1664-8714
ISBN 978-2-88919-930-3
DOI 10.3389/978-2-88919-930-3

About Frontiers

Frontiers is more than just an open-access publisher of scholarly articles: it is a pioneering approach to the world of academia, radically improving the way scholarly research is managed. The grand vision of Frontiers is a world where all people have an equal opportunity to seek, share and generate knowledge. Frontiers provides immediate and permanent online open access to all its publications, but this alone is not enough to realize our grand goals.

Frontiers Journal Series

The Frontiers Journal Series is a multi-tier and interdisciplinary set of open-access, online journals, promising a paradigm shift from the current review, selection and dissemination processes in academic publishing. All Frontiers journals are driven by researchers for researchers; therefore, they constitute a service to the scholarly community. At the same time, the Frontiers Journal Series operates on a revolutionary invention, the tiered publishing system, initially addressing specific communities of scholars, and gradually climbing up to broader public understanding, thus serving the interests of the lay society, too.

Dedication to Quality

Each Frontiers article is a landmark of the highest quality, thanks to genuinely collaborative interactions between authors and review editors, who include some of the world's best academicians. Research must be certified by peers before entering a stream of knowledge that may eventually reach the public - and shape society; therefore, Frontiers only applies the most rigorous and unbiased reviews.
Frontiers revolutionizes research publishing by freely delivering the most outstanding research, evaluated with no bias from both the academic and social point of view.
By applying the most advanced information technologies, Frontiers is catapulting scholarly publishing into a new generation.

What are Frontiers Research Topics?

Frontiers Research Topics are very popular trademarks of the Frontiers Journals Series: they are collections of at least ten articles, all centered on a particular subject. With their unique mix of varied contributions from Original Research to Review Articles, Frontiers Research Topics unify the most influential researchers, the latest key findings and historical advances in a hot research area! Find out more on how to host your own Frontiers Research Topic or contribute to one as an author by contacting the Frontiers Editorial Office: **researchtopics@frontiersin.org**

NEUROPHYSIOLOGY IN ALZHEIMER'S DISEASE AND DEMENTIA

Topic Editor:
Davide Vito Moretti, IRCCS Fatebenefratelli S. John of God Hospital, Italy

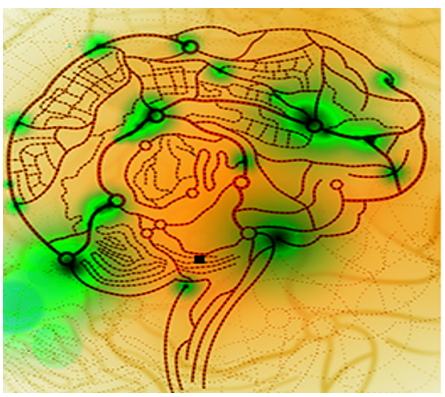

Brain electrical activity.
Figure by Davide Vito Moretti

Alzheimer's disease (AD) and dementia are the most common neurodegenerative disorder. Since the number of individuals with AD and dementia is expected to increase considerably in the near future, reliable treatment and diagnosis are critical. EEG and neurophysiological technique could be used as a cost-effective screening tool for early detection and diagnosis in the Mild Cognitive Impairment (MCI) stage.

The aim in neurophysiology research is to develop signal processing methods that improve the specificity for diagnosing dementia; we wish to discover signal features that not only significantly differ in AD patients, but also allow us to reliably separate AD patients and control subjects. This approach is valuable for clinical purposes (as diagnostic tool for dementia), and it also more fundamentally contributes to a better understanding of brain dynamics of MCI patients. Finally, the development of neurophysiological biomarker could be useful in monitoring pharmacological treatments.

The main focus of this special issue will be on the most recent developments and ideas in the field of EEG and neurophysiology which will enable us to extract features that improve the specificity for diagnosing AD and dementia.

Citation: Moretti, D. V., ed. (2016). Neurophysiology in Alzheimer's Disease and Dementia. Lausanne: Frontiers Media. doi: 10.3389/978-2-88919-930-3

Table of Contents

frontiers in Aging Neuroscience

EDITORIAL
published: 27 June 2016
doi: 10.3389/fnagi.2016.00153

Editorial: Neurophysiology in Alzheimer's Disease and Dementia

Davide V. Moretti *

IRCCS, FBF, Rehabilitation in Alzheimer's Disease Operative Unit, S. John of God Hospital, Brescia, Italy

Keywords: neurophysiology, EEG, alpha rhythm, magntoencefalography, Mismatch Negativity, mild cognitive impairment, Alzheimer's disease, genetics

The Editorial on the Research Topic

Neurophysiology in Alzheimer's Disease and Dementia

The aging of the nervous system is often associated with chronic diseases typical of old age, which can offer in their pathogenesis, and in their susceptibility to particular therapies, the key to understanding the determinants of senescence. In recent years, the need to distinguish normal from pathological aging and the obligation to execute the diagnosis as early as possible, addressed dementia research to the field of biomarkers. The biomarkers are easily recognizable, quantifiable, and reproducible, biological entities, that can identify in a timely manner different profiles of disease. It is widely believed in the scientific community that the diagnosis of Alzheimer's disease (AD) can be made early in the integrated analysis of structural, biological, clinical, and functional biomarkers.

Neurophysiology, and in particular electroencephalography (EEG), has proved a reliable tool in the biomarkers research of dementias. The ability to highlight the state of the underlying brain network, even with very advance, the ease of application, the widespread reproducibility and, not least, the low cost of operation, makes this method very suitable for studies of with a large number of subjects.

In this special issue dedicated to the neurophysiology of dementia, contributions of different cultural origins are presented, contributing to the general richness, and the scientific significance of the issue.

Raymundo Cassani addressed the methodological aspect of removal of artifact from EEG, demonstrating that a wavelet enhanced independent component analysis (wICA) algorithm alone outperforms other methodics, thus opening the doors for fully-automated systems that can assist clinicians with early detection of AD, as well as disease severity progression assessment.

Francesco Di Lorenzo, addressed the basic neurophysiological aspect of the cholinergic system in AD through the theta burst stimulation (TBS) that modulate central cholinergic function using the neurophysiological determination of Short-Latency Afferent Inhibition (SLAI). The SLAI was decreased in AD patients compared to healthy controls (HS). Cerebellar TBS partially restored SLAI in AD patients but did not modify SLAI in healthy subjects. These results demonstrate that cerebellar magnetic stimulation affects cortical cholinergic activity and suggests that the cerebellum could have a direct influence on the cholinergic damage in AD.

A lot of studies addressed the clinical aspect of the early diagnosis in AD.

Christos A. Frantzidis demonstrated an impaired organization of brain networks even in the prodromal phase of Alzheimer's disease (AD) due, in hypothesis, to compensation mechanisms.

Zhijie Bian proposed that the theta/alpha EEG power band ratio recorded in the frontal and temporal region of the left hemisphere could be a diagnostic tool in patients with amnesic mild cognitive impairment (aMCI) affected by diabetes.

OPEN ACCESS

Edited and reviewed by:
Rodrigo Orlando Kuljiš, University of Miami School of Medicine, USA

***Correspondence:**
Davide V. Moretti
davide.moretti@afar.it

Received: *09 April 2016*
Accepted: *13 June 2016*
Published: *27 June 2016*

Citation:
Moretti DV (2016) Editorial: Neurophysiology in Alzheimer's Disease and Dementia. Front. Aging Neurosci. 8:153. doi: 10.3389/fnagi.2016.00153

Simon-Shlomo Poil showed that EEG activity in the beta frequency range (13–30 Hz) could be a helpful prognostic marker to predict the conversion from the MCI state to the overt AD condition. Of note, the authors found that the prediction power is higher (sensitivity of 88% and specificity of 82%) when EEG biomarkers are considered in an integrated way.

Davide V. Moretti demonstrated that the increase of EEG alpha3/alpha2 power ratio is related with prodromal phase of AD. The association with hippocampal atrophy, cortical thickness and reduction of brain regional cerebral perfusion suggests that alpha3/alpha2 power ratio could detect the MCI subjects who will convert to AD.

Very interestingly, Natalya Ponomareva confirmed the reliability of the increase of the EEG alpha3 spectral power investigating the age-related influence of the polymorphism of clusterin (CLU) genotype, associated with AD. In particular, the homozygous variant of CLU C allele is related with the increase of EEG alpha3 power, suggesting a possible susceptibility of this genetic variant carriers to hippocampal atrophy.

Monica Lindin explored the field of event-related potentials demonstrating that the Mismatch Negativity (MMN) amplitude was significantly smaller in aMCI subjects than in healthy controls.

Beyond EEG, also magnetoencephalography (MEG) could be a useful research tool. Pilar Garcés found a pathological alpha slowing in MCI patients when compared to healthy controls investigating the changes in the spatial distribution of the frequency and amplitude values of MEG alpha peak.

Finally, besides AD, Davide V. Moretti found that EEG frequency rhythms are sensible also to different stage of Fronto-Temporal-Dementia (FTD) and could detect changes in brain oscillatory activity affected by progranulin (GRN) mutations.

It is commonly thought that research in neuroscience is the researcher's effort to understand his own brain. If it is true, I want to thank all the authors for helping me to understand also something more of myself.

Somewhere, something incredible is waiting to be discovered (Cari Sagan)

AUTHOR CONTRIBUTIONS

The author confirms being the sole contributor of this work and approved it for publication.

Conflict of Interest Statement: The author declares that the research was conducted in the absence of any commercial or financial relationships that could be construed as a potential conflict of interest.

Copyright © 2016 Moretti. This is an open-access article distributed under the terms of the Creative Commons Attribution License (CC BY). The use, distribution or reproduction in other forums is permitted, provided the original author(s) or licensor are credited and that the original publication in this journal is cited, in accordance with accepted academic practice. No use, distribution or reproduction is permitted which does not comply with these terms.

frontiers in
AGING NEUROSCIENCE

ORIGINAL RESEARCH ARTICLE
published: 25 March 2014
doi: 10.3389/fnagi.2014.00055

The effects of automated artifact removal algorithms on electroencephalography-based Alzheimer's disease diagnosis

Raymundo Cassani[1], Tiago H. Falk[1]*, Francisco J. Fraga[1,2], Paulo A. M. Kanda[3] and Renato Anghinah[3]

[1] *Institut National de la Recherche Scientifique, Centre Énergie, Matériaux, Télécommunications, University of Quebec, Montreal, QC, Canada*
[2] *Engineering, Modelling and Applied Social Sciences Center, Universidade Federal do ABC, São Paulo, Brazil*
[3] *Reference Center of Behavioural Disturbances and Dementia, School of Medicine, Universidade de São Paulo, São Paulo, Brazil*

Edited by:
Davide V. Moretti, IRCCS San Giovanni di Dio Fatebenefratelli, Italy

Reviewed by:
Xiaoli Li, Beijing Normal University, China
Umberto Melia, Universitat Politecnica de Catalunya, Spain

****Correspondence:***
Tiago H. Falk, Institut National de la Recherche Scientifique, Centre Energie, Matériaux, Télécommunications, University of Quebec 800, Rue de la Gauchetire Ouest, Suite 6900 Montreal, QC H5A-1K6, Canada
e-mail: falk@emt.inrs.ca

Over the last decade, electroencephalography (EEG) has emerged as a reliable tool for the diagnosis of cortical disorders such as Alzheimer's disease (AD). EEG signals, however, are susceptible to several artifacts, such as ocular, muscular, movement, and environmental. To overcome this limitation, existing diagnostic systems commonly depend on experienced clinicians to manually select artifact-free epochs from the collected multi-channel EEG data. Manual selection, however, is a tedious and time-consuming process, rendering the diagnostic system "semi-automated." Notwithstanding, a number of EEG artifact removal algorithms have been proposed in the literature. The (dis)advantages of using such algorithms in automated AD diagnostic systems, however, have not been documented; this paper aims to fill this gap. Here, we investigate the effects of three state-of-the-art automated artifact removal (AAR) algorithms (both alone and in combination with each other) on AD diagnostic systems based on four different classes of EEG features, namely, spectral, amplitude modulation rate of change, coherence, and phase. The three AAR algorithms tested are statistical artifact rejection (SAR), blind source separation based on second order blind identification and canonical correlation analysis (BSS-SOBI-CCA), and wavelet enhanced independent component analysis (wICA). Experimental results based on 20-channel resting-awake EEG data collected from 59 participants (20 patients with mild AD, 15 with moderate-to-severe AD, and 24 age-matched healthy controls) showed the wICA algorithm alone outperforming other enhancement algorithm combinations across three tasks: diagnosis (control vs. mild vs. moderate), early detection (control vs. mild), and disease progression (mild vs. moderate), thus opening the doors for fully-automated systems that can assist clinicians with early detection of AD, as well as disease severity progression assessment.

Keywords: Alzheimer's disease, automatic diagnosis, electroencephalogram, amplitude modulation, EEG artifacts, SVM

1. INTRODUCTION

Alzheimer's disease (AD) is a chronic neuro-degenerative disorder that has recently been ranked as the third most expensive disease and the sixth leading cause of death in the United States (Leifer, 2003; Alzheimer Association, 2013). In 2012, the World Health Organization (WHO) stated that between 60–70% of dementia cases around the world were due to AD, making it the most common form of dementia. As such, it called for improved (early) diagnosis, as well as better care and support for patients, their families, and caregivers (WHO and Alzheimer's Disease International, 2012). With regards to the former, today diagnosis is commonly carried out using laboratory tests, medical history, mental status examinations, and more recently, neuroimaging tools such as functional magnetic resonance imaging (fMRI). These clinical assessment methods, however, commonly require experienced clinicians and lengthy sessions, thus can be regarded as non-specific and costly, as well as suffer from long wait times to access an fMRI scanner. In medium- and low-income countries, as well as in rural and remote regions (e.g., the Canadian Arctic), these limitations are further exacerbated, thus hindering the effectiveness of very early disease diagnosis (Sarazin et al., 2012).

Driven by these limitations, quantitative electroencephalography (qEEG, henceforth referred to as "EEG") has emerged as a promising tool capable of assisting physicians in the diagnosis of AD (e.g., Jeong, 2004; Babiloni et al., 2010; Falk et al., 2012). Since the EEG signal reflects functional changes in the cerebral cortex, it can be used to reveal neuronal degeneration and functional impairment long before actual tissue loss can be detected by fMRI (Alzheimer Association, 2013). Over the last decade, several works have demonstrated a neuromodularity deficit with AD via EEG signal analysis (e.g., Jeong, 2004; Dauwels et al., 2011; Moretti et al., 2012). For example, apparent changes in the EEG power spectrum (e.g., slowing of the EEG) have been documented

(Coben et al., 1983, 1985; Brenner et al., 1986; Giaquinto and Nolfe, 1986), as well as reduced spectral coherence between the left and right hemispheres (Leuchter et al., 1987; Besthorn et al., 1994; Dunkin et al., 1994; Sloan et al., 1994; Locatelli et al., 1998). Moreover, EEG signal complexity measures have shown decreased levels with AD, likely due to the reduction in non-linear connections between cortical regions or even neuronal death (Jeong, 2004). More recently, EEG amplitude modulation analysis has also shown to be a powerful tool in EEG diagnosis (Falk et al., 2012; Fraga et al., 2013b). Many such measures have been shown to be related (Dauwels et al., 2011) and to provide diagnostic sensitivity and specificity in line with more complex neuroimaging techniques (Adeli et al., 2005).

Notwithstanding, EEG signals are inherently noisy and susceptible to blink, eye movement, heartbeats, and cranial muscle artifacts, all of which are detrimental to AD diagnosis performance. To overcome this limitation, the majority of the published works have resorted to using artifact-free EEG segments (called epochs) which have been selected by expert clinicians via meticulous visual inspection. Such dependence on human experts, however, hinders the benefits of automated low-cost analysis, as well as introduces possible human biases/errors (Daly et al., 2013). As an alternative, artifact removal algorithms could be employed. Artifact removal algorithms can be classified as 'semi-automated' or 'automated', depending on the need for human intervention, or not, respectively. Component-based methods, such as independent component analysis (ICA), can be regarded as semi-automated methods, as signal components associated with artifacts still need to be manually identified by humans and removed prior to signal reconstruction (Jung et al., 2000; James and Hesse, 2005). On the other hand, wavelet denoising (Zikov et al., 2002; Krishnaveni et al., 2006), blind source separation (De Clercq et al., 2006; Gómez-Herrero et al., 2006), or even simple feature averaging (Fraga et al., 2013b), are fully automated methods that do not require human intervention. Within the scope of EEG-based AD diagnosis, the potential benefits and drawbacks of using automated artifact removal (AAR) algorithms are still unknown. For example, certain algorithms may remove important neurological phenomena needed for accurate diagnosis. The aim of this paper is to fill this gap and explore the (dis)advantages of utilizing AAR for EEG-based AD diagnosis.

Here, three AAR algorithms have been selected after careful screening of the literature for available state-of-the-art methods applicable to our data. The first method, termed statistical artifact rejection (SAR), utilizes statistical characteristics of the signals to make accept/reject decisions over EEG epochs (Delorme et al., 2007). The second method belongs to the widely-used class of blind source separation (BSS) algorithms based on the autocorrelation of independent components (De Clercq et al., 2006; Gómez-Herrero et al., 2006). Lastly, a combined independent components analysis and wavelet denoising algorithm, termed wavelet enhanced ICA (wICA), is used which applies a wavelet thresholding algorithm to replace the human intervention step required with ICA (Castellanos and Makarov, 2006). The three algorithms are tested alone and in combination with each other, as well as in combination with the simple feature averaging approach described by Fraga et al. (2013b). The AAR algorithms are applied to raw EEG data collected from 59 participants (20 patients with mild AD, 15 with moderate-to-severe AD, and 24 age-matched healthy controls). Their effects on four classes of EEG features, namely spectral-, coherence-, phase-, and amplitude modulation-based features are tested and compared to a gold-standard method, which relies on expert human inspection of artifact-free epochs. The ultimate goal of the present paper is to describe the best AAR-feature set combination, thus resulting in a reliable system that can be used to assist clinicians in diagnosis and very early detection of AD, as well to monitor disease progression.

2. MATERIALS AND METHODS

2.1. PARTICIPANTS

Fifty-nine participants were recruited from the Behavioral and Cognitive Neurology Unit of the Department of Neurology and the Reference Center for Cognitive Disorders at the Hospital das Clinicas in São Paulo, Brazil (Kanda et al., 2013). AD diagnosis was made by experienced neurologists according to NINCDS-ADRDA criteria (McKhann et al., 1984) and classified based on the Brazilian version of the Mini-Mental State Examination (MMSE) (Brucki et al., 2003). Participants were divided in three groups. The first group (N) consisted of 24 cognitively healthy controls (12 males; mean age 66.3 years, 8.8 *sd*); the second group ($AD1$) comprised 20 mild-AD patients (9 males, mean age 74.8 years, 6.3 *sd*); the third group ($AD2$) consisted of 15 patients with moderate-to-severe AD symptoms (6 males; mean age 75 years, 11.8 *sd*). Inclusion criteria for the N group included a CDR score $= 0$ and MMSE score ≥ 25 (mean 28.5, 1.7 *sd*), as well as no indication of functional cognitive decline. Inclusion criteria for the $AD1$ group, in turn, included $0.5 \leq \text{CDR} \leq 1$ and $\text{MMSE} \leq 24$ (mean 19.2, 5.2 *sd*); lastly, inclusion criteria for the $AD2$ group were CDR score $= 2$ and $\text{MMSE} \leq 20$ (mean 12.8, 5 *sd*). For inclusion to the two AD groups, an additional criterion used was the presence of functional and cognitive decline over the previous 12 months based on detailed interviews with knowledgeable informants. Patients from the AD cohorts were also screened for diabetes mellitus, kidney disease, thyroid disease, alcoholism, liver disease, lung disease or vitamin B12 deficiency, as these can also cause cognitive decline. Ethics approval was obtained from the Research Ethics Office and participants consented to participate in the study.

2.2. EEG DATA ACQUISITION AND PRE-PROCESSING

Twenty-channel EEG signals were acquired with the participants awake, relaxed, and with their eyes closed for at least 8 min. The Braintech 3.0 instrumentation (EMSA Equipamentos Médicos INC., Brazil) was used with 12-bit resolution and 200 Hz sample rate parameters. Impedance was maintained below 10 kΩ and scalp electrodes were placed according to the international 10–20 system. Bi-auricular referential electrodes were attached, as recommended by the Brazilian Society of Clinical Neurophysiology and the American EEG Society. An infinite impulse response low-pass elliptic filter with a zero at 60 Hz was applied to eliminate power grid interference. Moreover, based on evidence of an interhemispheric disconnection with AD (Jeong, 2004; Trambaiolli et al., 2011b,c; Falk et al., 2012; Fraga et al., 2013b),

we also explore the use of virtual interhemispheric bipolar signals. Interhemispheric bipolar signals refer to the electric potential difference measured between a pair of electrodes symmetrically located in each hemisphere. Moreover, the term "virtual" is used because these signals are mathematically computed as the difference of two recorded unipolar signals rather than directly recorded from the scalp (Nunez, 2006). The eight virtual bipolar signals explored in this work were the interhemispheric signals Fp1-Fp2, F7-F8, F3-F4, T3-T4, C3-C4, T5-T6, P3-P4, and O1-O2.

Unprocessed signals (both per-electrode and bipolar) constitute what will, henceforth, be referred to as the "raw" EEG. The enhanced signals, in turn, will constitute the raw signals processed by the different AAR algorithms described in the next subsection. Lastly, the raw signals have also been visually inspected by two experienced clinicians to obtain several 8-s epochs free of eye blinking, drowsiness, muscle movements, or equipment-related artifacts. This manually-selected data will be used to develop a gold-standard diagnostic system with which the AAR algorithms will be benchmarked against.

2.3. AUTOMATED ARTIFACT REMOVAL (AAR) ALGORITHMS

As mentioned previously, three AAR algorithms are explored within this work and were chosen based on characteristics of our dataset; more specifically, on the electrode layout (international 10–20 system), relatively small number of electrodes (20), absence of electrooculographic (EOG) reference channels, and lack of data from alternate modalities (e.g., accelerometers or gyroscopes). In the subsections to follow, a brief summary of the three AAR algorithms is given, as well as a description of their implementations. References to literature with more detailed descriptions of the algorithms are provided, where appropriate, for the interested reader.

2.3.1. Statistical artifact rejection (SAR)

The SAR method utilizes thresholding on the statistical characteristics of the EEG signals to select epochs that appear to contain artifacts. The implementation of this method was done using the well-known EEGLAB toolbox for Matlab (Delorme and Makeig, 2004). The criteria used to reject epochs included finding: extreme values caused by gross artifacts and amplifier saturation (i.e., greater than $+/-$ 100 μV), abnormally distributed data (i.e., 5 standard deviations from average kurtosis, suggesting peaky or flat distributions) and "improbable data" computed via an online probability-of-occurrence metric. The interested reader is referred to (Delorme et al., 2007) for more details on the SAR algorithm.

2.3.2. Blind source separation (BSS)

The BSS algorithm utilizes spatial filtering to remove ocular and muscular artifacts from EEG data without external references (e.g., EOG or accelerometer signals) (De Clercq et al., 2006; Gómez-Herrero et al., 2006). The basic principle behind BSS is to decompose the EEG signal into different spatial components and then reconstruct the signal based only on the non-artifactual spatial components, which have been found via a suitable automatic criterion. For ocular and muscular artifacts, the EEG signal is decomposed by the so-called second order blind identification (SOBI) and canonical correlation analysis (CCA) methods, respectively. In the SOBI technique (Belouchrani et al., 1997; Gómez-Herrero et al., 2006; Romero et al., 2008), second order statistics are used to find spatial components that have non-zero time-delayed autocorrelations and zero time-delayed cross-correlations. Such approach has been shown to preserve more brain activity relative to other ocular artifact removal methods (Romero et al., 2008). In our simulations, a fractal dimension-based criterion was used to decide which components to use for reconstruction, with the basic premise that EEG artifacts are characterized by higher fractal dimensions (Gómez-Herrero et al., 2006). With CCA, in turn, EEG data is expressed as a combination of maximally autocorrelated and mutually uncorrelated spatial components (De Clercq et al., 2006). Using CCA, spatial components with the lowest autocorrelation values are assumed to be related to muscular artifacts, as muscular activity has been shown to be of wider bandwidth than EEG, thus have more white noise-like properties (De Clercq et al., 2006). For this experiment, BSS AAR refers to the use of the SOBI technique, followed by CCA to remove ocular and muscular artifacts, respectively. The widely-utilized AAR plug-in for EEGLAB was used in our experiments with the following default parameters: for EOG removal, *eigenratio* $= 10^6$, *range* $= 2-4$, and the *no-EOG reference* option selected; for EMG removal, $emg - psd - ratio = 10$, and $femg = 15$. More details about these parameters and the plug-in can be found in (Gómez-Herrero, 2007). For illustration purposes, **Figure 1** depicts a 10-s segment of raw (gray) EEG along with its BSS-processed (green) counterpart for four electrodes affected by eye artifacts: Fp1, Fp2, F7, and F8.

2.3.3. Wavelet-enhanced independent components analysis (wICA)

Wavelet analysis has been used in the past for EEG artifact detection (e.g., Achanccaray and Meggiolaro, 2008) and removal (e.g., Labate et al., 2011) and has recently been combined with ICA for improved artifact removal performance (Castellanos and Makarov, 2006; Akhtar et al., 2012). The so-called wavelet enhanced ICA, or wICA, applies a wavelet thresholding step to the demixed independent components in an attempt to recover any residual neural activity that may be present in components labeled as artifactual (Castellanos and Makarov, 2006). The wICA method can be summarized in five steps: (1) the EEG data is decomposed into independent components (IC); (2) the wavelet transform is applied to the ICs; (3) thresholding of the wavelet coefficients is performed to differentiate between neural and artifactual coefficients; (4) the inverse wavelet transform is applied to the thresholded coefficients, retrieving ICs with only neural activity; and lastly, (5) wavelet-corrected ICs are projected to obtain the artifact-free EEG data. A complete description, as well as a comparative analysis between ICA and wICA is given by Castellanos and Makarov (2006); improved performance and better preservation of EEG spectral and phase coherence properties with wICA are shown. In our experiments, the wICA toolbox described by Makarov (2012) was used with the following parameters: cleaning artifact *tolerance* $= 1.25$ and an IC artifact detection *threshold* $= 4$. **Figure 1** also shows the 10-s noisy EEG segment processed by wICA (black). As can be seen from the highlighted areas, wICA suppresses eye blink/movement artifacts more efficiently than BSS.

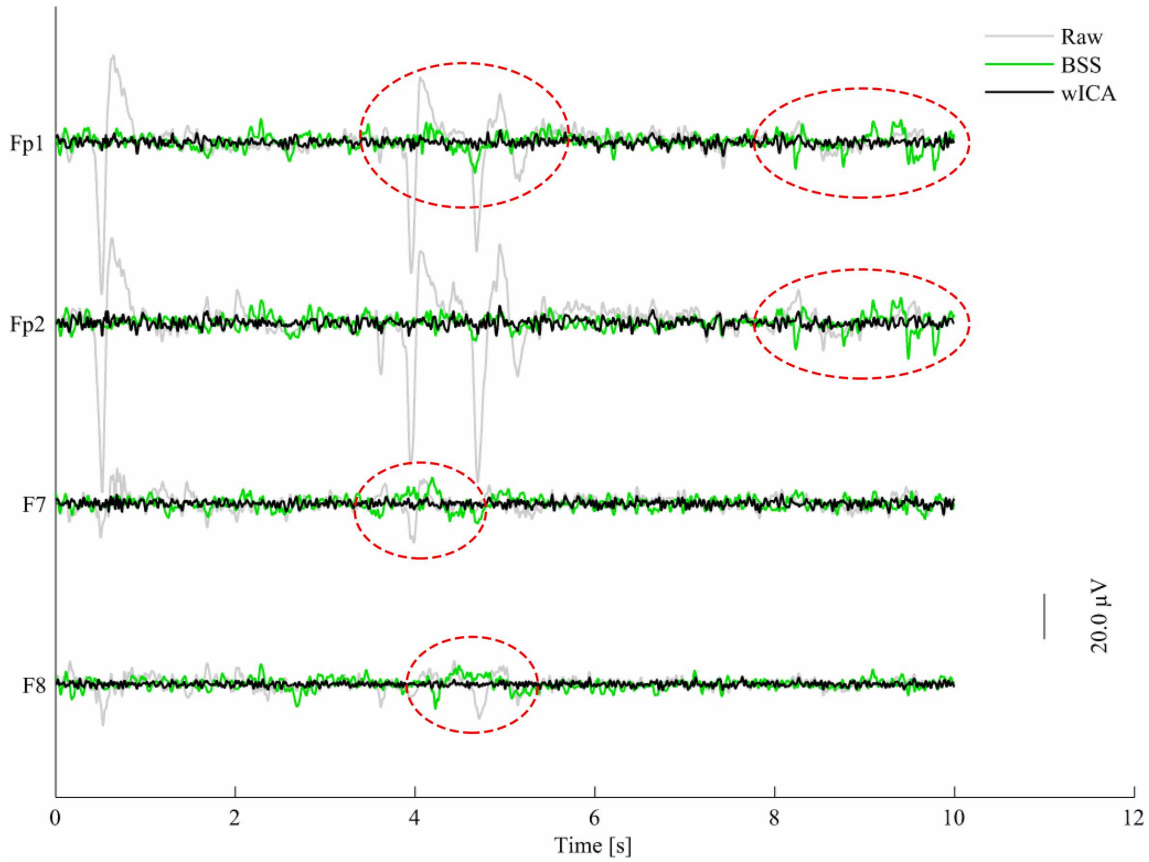

FIGURE 1 | Plots of raw (gray), BSS- (green), and wICA-processed (black) EEG segments for four channels corrupted by eye blinks and movement.

2.3.4. AAR Algorithm Combination

Here, we have tested the three above-mentioned AAR algorithms alone, as well as in cascade; more specifically, we have tested the SAR-BSS and SAR-wICA combinations. Overall, experimental results will be presented using the "raw" data (this will be henceforth refereed to as the "baseline"), the manually-selected artifact-free EEG data (henceforth referred to as the "gold-standard"), and the five "enhanced" EEG datasets (i.e., SAR, BSS, wICA, SAR-BSS, SAR-wICA). To maintain consistency with the gold-standard system, all datasets are segmented into several 8-s epochs.

2.4. EEG FEATURE EXTRACTION AND PROCESSING

Several EEG features have been proposed in the literature over the last decade and shown to accurately discriminate between healthy controls and AD patients. The effects of EEG artifacts on these features, however, are unknown, as are their effects on overall diagnostic performance. Here, we will pursue such an investigation and focus will be placed on four traditional EEG feature categories, namely, spectral power, magnitude square coherence, phase coherence/synchrony, and the recently-proposed EEG amplitude modulation rate-of-change. In the subsections to follow, a brief description of the features will be given. References to literature with more detailed descriptions of the features are provided, where appropriate, for the interested reader.

2.4.1. EEG subband spectral power

The pivotal process to quantify the frequency-domain properties of the EEG signal lies in the estimation of its power spectral density (PSD) function, which is commonly achieved via a discrete Fourier transform (Sörnmo and Laguna, 2005). As the name suggests, spectral power based features measure the power present in the five conventional EEG frequency bands: 0.1–4 Hz (delta), 4–8 Hz (theta), 8–12 Hz (alpha), 12–30 Hz (beta) and, 30–100+ Hz (gamma) (Sörnmo and Laguna, 2005), with some studies further partitioning a band into low (e.g., alpha1: 8–10 Hz) and high (e.g., alpha2: 10–12 Hz) parts. Several studies have shown that changes in EEG power spectra due to AD are reflected as an increase in delta and theta band powers, together with a decrease in alpha and beta band powers, thus suggesting a "slowing" of the EEG signal (Coben et al., 1983, 1985; Penttilä et al., 1985; Soininen et al., 1989; Czigler et al., 2008; Moretti et al., 2009; Babiloni et al., 2010). More recently, other features have been proposed, such as the subband spectral peaks (the most prominent peak inside a frequency band) (Raicher et al., 2008) and the ratio of different bands (e.g., theta/gamma by Moretti et al., 2009, 2011). In this experiment, we compute the so-called relative band power for the five bands for each of the 28 EEG signals (20 electrodes + 8 virtual bipolar signals). The relative band power corresponds to the power of an individual band normalized by the fullband EEG

power. A total of 140 (28 × 5) spectral-based features are thus computed per epoch.

2.4.2. Magnitude square and phase coherence

The magnitude square coherence (MSC), frequently referred to as "coherence," is a measure of co-variance between two power spectra. In EEG studies, the MSC is used as a metric of synchrony in neural activity, which is an indicator of cortical connectivity (Thatcher et al., 1986; Locatelli et al., 1998; Srinivasan et al., 2007). Studies have shown reduced EEG coherence within all EEG subbands during AD (Thatcher et al., 1986; Besthorn et al., 1994; Knott et al., 2000; Adler et al., 2003). The computation of the MSC between signals $x(t)$ and $y(t)$ with $X(f)$ and $Y(f)$ spectra, respectively, for any given frequency band is defined as:

$$MSC(f) = \frac{\left|\langle X(f)\, Y^*(f)\rangle\right|^2}{\left|\langle X(f)\rangle\right|\left|\langle Y(f)\rangle\right|}, \quad (1)$$

where $Y^*(f)$ is the complex conjugate of $Y(f)$, $\langle\ \rangle$ corresponds to the average operator, and the numerator $\langle X(f)Y^*(f)\rangle$ corresponds to the cross-spectral density between signal $x(t)$ and $y(t)$, also called the complex coherence. The imaginary part of the complex coherence, also known as phase coherence, has also been proposed as metric to study brain interactions (Nolte et al., 2004). The phase coherence is given by:

$$\phi(f) = \arg\left\langle X(f)Y^*(f)\right\rangle. \quad (2)$$

In our experiments, we compute both metrics for each of the five EEG frequency bands. Following the recent evidence of an interhemispheric disconnection with AD (Jeong, 2004; Trambaiolli et al., 2011c,b; Falk et al., 2012; Fraga et al., 2013b), the magnitude square and phase coherence measures are computed only for the eight interhemispheric electrodes, namely: Fp1-Fp2, F7-F8, F3-F4, T3-T4, C3-C4, T5-T6, P3-P4, and O1-O2.

2.4.3. Phase synchrony

Global field synchrony (GFS) measures the phase synchrony in a given frequency (or frequency band) for a set of N electrodes. It was first introduced to estimate the functional disorder within the brain for patients with schizophrenia (Koenig et al., 2001). Since AD has also been characterized by a loss of EEG synchrony resultant from the functional interhemispheric disconnection (Jeong, 2004), GFS has been explored as a diagnostic feature (Koenig et al., 2005; Park et al., 2008). Assuming $x_i(k)$, $i = 1, \ldots, N$, are the EEG time-domain signals from electrode 'i' and $X_i(f)$ are their respective frequency responses (obtained via e.g., Fourier transform), the GFS feature is based on the distribution of the real ($X_{\mathbb{R}}(f)$) and imaginary ($X_{\mathbb{I}}(f)$) parts of the frequency-domain representation of all electrode signals. More specifically, it is computed as the difference between the two normalized eigenvalues of the 2×2 auto-correlation matrix between the vectors $X_{\mathbb{R}}(f) = [Re(X_1(f)), \ldots, Re(X_N(f))]$ and $X_{\mathbb{I}}(f) = [Img(X_1(f)), \ldots, Img(X_N(f))]$. More details about the GFS feature can be found in (Koenig et al., 2001). In our experiments, the GFS feature was computed over the 20 electrode signals for each of the five frequency bands, totaling five GFS features per EEG epoch.

2.4.4. EEG amplitude modulation rate-of-change

Amplitude modulation analysis has shown to be a valuable tool for bio-signal processing and analysis (Atlas and Shamma, 2003; Malyska et al., 2005; Falk and Chan, 2008; Falk et al., 2010). For AD analysis, it is particularly useful, as recent experimental evidence has suggested a neuromodulatory deficit with the disease (Moore and Cao, 2008; Laxton et al., 2010). Here, we utilize the EEG amplitude modulation rate-of-change features recently shown to accurately discriminate between different stages of AD (Trambaiolli et al., 2011b; Falk et al., 2012; Fraga et al., 2013a,b). In order to compute the features, three steps are required. First, the fullband EEG is frequency-decomposed into the five bands mentioned above. Second, a Hilbert transform is applied to extract the amplitude modulations of each band. Lastly, in order to characterize the dynamics of the amplitude modulations, a second frequency decomposition is performed on the band envelope signals. To characterize the cross-frequency interactions, this second decomposition utilizes five so-called "modulation bands" that have been designed to coincide with the frequency ranges of the five traditional subbands. To distinguish between frequency and modulation bands, the latter are referred to as *m-delta*, *m-theta*, *m-alpha*, *m-beta* and, *m-gamma*. The normalized energy in each frequency-modulation band is used as a feature. It is important to emphasize, however, that due to properties of the Hilbert transform [e.g., Bedrosian's theorem (Bedrosian, 1963)], not all frequency-modulation band combinations make sense. If we use the notation "*E*(frequency band; modulation band)" to denote the normalized energy in a given frequency and modulation band, only the following scenarios are relevant: *E(delta; m-delta)*, *E(theta; m-delta,m-theta)*, *E(alpha; m-delta, m-theta)*, *E(beta; m-delta, m-theta, m-alpha, m-beta)* and, *E(gamma; m-delta, m-theta, m-alpha, m-beta, m-gamma)*. In our experiments, these 14 features are computed for each of the 28 signals (20 electrodes + 8 virtual bipolar signals). The interested reader is referred to (Trambaiolli et al., 2011b; Falk et al., 2012; Fraga et al., 2013a,b) for complete details of the EEG amplitude modulation rate-of-change features.

2.4.5. Feature sets and set combination

Computed features were grouped into four feature sets: spectral, modulation, coherence (MSC), and phase (phase coherence and phase synchrony). To explore the complementarity of the extracted features, combined feature sets were also investigated. Henceforth, we will refer to the "All" feature set as the set that combines all the extracted features and the "Spec-Mod" set as the set that combines the spectral and amplitude-modulation based features. This latter combined set is motivated by the recent results suggesting the complementary of the two feature domains for AD characterization (Fraga et al., 2013a).

2.4.6. Epoch averaging in the feature domain

As an additional EEG "cleaning" tool, we use epoch averaging in the feature domain as a way of improving the signal-to-noise ratio (SNR) of the extracted features. This procedure was recently shown to improve the clustering of amplitude modulation rate-of-change features, thus leading to higher diagnostic accuracies (Fraga et al., 2013b). This procedure is akin to the epoch averaging step commonly performed in event related potential studies

(Luck, 2005), but differs in the sense that it is performed in the (non-linear) feature domain and not in the time domain. In our experiments, averaging is performed over features extracted from five consecutive epochs, as motivated by Fraga et al. (2013b).

2.5. AUTOMATED SALIENT FEATURE SELECTION AND AD CLASSIFICATION

The machine learning and pattern recognition literature has presented a plethora of possible feature selection and classification algorithms which can be fine-tuned to specific applications and feature sets. For the experiments herein, however, we are interested in understanding the effects of AAR algorithms on different EEG feature sets and on overall diagnostic performance, and not the effects of different selection/classification algorithms and their internal parameters. As such, our experiments are based on a support vector machine (SVM) feature selection and classification algorithm that is widely used in the EEG-based AD diagnosis literature (Lehmann et al., 2007; Trambaiolli et al., 2011a; Falk et al., 2012; Fraga et al., 2013b). The open-source Weka SVM implementation was used in our experiments; default parameters included a polynomial kernel, regularization coefficient $C = 1$, and hyperplane shaping coefficient $\gamma = 0.01$. A description of the SVM-based feature selection and classification algorithm is beyond the scope of this paper, and the interested reader is referred to (e.g., Cristianini and Shawe-Taylor, 2000; Hall et al., 2009) for more details.

In our experiments, 25% of the available data was randomly set aside for feature selection and the remaining 75% was used for classifier training/testing using 10-fold cross validation. Using disjoint sets for feature selection and classifier training reduces any unwanted biases in the reported performance figures. To remain inline with the existing EEG-based AD diagnostic literature, feature selection was used to sift out the 24 most relevant features for AD diagnosis. In this study, we investigate the effects of AAR on AD diagnostic performance using three classification tasks, namely, (a) Task 1: *N* vs. *AD*1 vs. *AD*2; (b) Task 2: *N* vs. *AD*1; and (c) Task 3: *AD*1 vs. *AD*2. The first task explores the impact of AAR on a more challenging 3-class problem discriminating between mild-AD, moderate-AD, and healthy controls. The second, in turn, explores the impact on discrimination capabilities between healthy aging and mild-AD, thus exemplifies the case of early detection. Lastly, the third assesses the impact of AAR on EEG-based disease progression monitoring (i.e., from mild to moderate).

2.6. PERFORMANCE METRICS AND THE "GOLD STANDARD" SYSTEM

In order to assess diagnosis performance, classification accuracy is used as a performance metric. Moreover, for the two 2-class problems described above, diagnosis sensitivity and specificity are also used. Throughout the remainder of this paper we will assess the impact of AAR on AD classification by measuring the performance gains obtained relative to the baseline (i.e., using the "raw" EEG data). The relative performance gain is given by:

$$Gain = \frac{Perf_{AAR} - Perf_{base}}{Perf_{base}} \times 100\%, \quad (3)$$

where "$Perf_{AAR}$" and "$Perf_{base}$" refer to the obtained performances (i.e., accuracy, sensitivity, or specificity) after artifact removal and before, respectively. For comparison purposes, we use a so-called gold-standard system to benchmark the results; the system is based on the manually selected artifact-free EEG dataset and the "All-feature" set with 5-epoch feature averaging. On the 3-class task, the gold standard achieves an accuracy of 83.8%. For the *N* vs. *AD*1 and *AD*1 vs. *AD*2 tasks, in turn, accuracies of 93.2% and 92.8% are obtained, respectively.

3. EXPERIMENTAL RESULTS

Table 1 reports the accuracies achieved with the baseline system in the top row, followed by the relative gains (Equation 3) achieved with the different AAR algorithms for the four feature sets and two combined feature sets (i.e., "All" and "Spec-Mod") for the 3-class task. **Table 2** presents the accuracy, sensitivity, and specificity of the baseline system for all feature sets for the two 2-class tasks. In turn, **Tables 3**, **4** report the relative gains for all AAR-feature set combinations for the *N* vs. *AD*1 and *AD*1 vs. *AD*2 tasks, respectively. Careful analysis of the Tables suggests that for all three tasks, the wICA AAR algorithm combined with the top 24 features selected from the "All-feature" set resulted in the best classification performance. **Tables 5**, **6** show the top-24 selected features for each of the three tasks, for the wICA-AAR and gold standard scenarios, respectively. Feature names are reported as "ELECTRODE_BAND_FEATURE" where "ELECTRODE" represents either the 10–20 electrode positions (e.g., PZ) or the virtual bipolar signal (e.g., P3-P4), "BAND" represents the EEG frequency band (e.g., delta), and "FEATURE" provides a descriptive indication of the feature representation (e.g., "pwr" corresponds to spectral power; "m-alpha" to modulation rate; "cohe_mag/pha" to magnitude/phase coherence).

4. DISCUSSION

4.1. SALIENT FEATURES

The list of top-selected features shown in **Table 5**, **6** show that power spectral and amplitude modulation features are the most salient. Combined, they correspond to 92, 83, and 79% of the top-24 selected features in Tasks 1–3, respectively, for the wICA-AAR

Table 1 | Baseline accuracy per feature set and relative gains obtained after AAR for the 3-class "*N* vs. *AD*1 vs. *AD*2" task.

AAR	Feature sets					
	Spectrum	**Modulation**	**Coherence**	**Phase**	**All**	**Spec-mod**
Baseline (%)	73.2	68.4	60.1	45.7	72.3	73.5
RELATIVE GAINS						
SAR	1.3	−3.6	0.2	1.8	2.5	−0.8
SAR-BSS	−5.9	−10.6	−6.2	−12.2	−1.0	−3.7
SAR-wICA	−0.8	−3.0	7.6	2.6	4.5	2.5
BSS	−4.0	−4.6	−6.5	−12.2	−6.6	−7.4
wICA	3.3	2.9	11.5	5.5	8.4	3.8

Table 2 | Baseline performance values for the two, 2-class tasks.

Task #	Spectrum			Modulation			Coherence			Phase			All			Spec-mod		
	A	*S*	*Sp*	*A*	*S*	*Sp*	*A*	*S*	*Sp*	*A*	*S*	*Sp*	*A*	*S*	*Sp*	*A*	*S*	*Sp*
2	83.6	86.3	80.5	79.6	82.9	75.7	73.3	76.1	70.0	64.9	78.4	48.7	83.0	84.3	81.3	82.6	85.4	79.2
3	89.4	91.3	86.8	85.1	89.5	79.3	78.5	81.9	74.0	69.4	84.9	48.6	89.2	92.2	85.2	88.6	90.9	85.5

Columns labeled "A, S, and Sp" correspond to accuracy, sensitivity, and specificity, respectively.

Table 3 | Relative gains obtained after AAR for the 2-class "*N* vs. *AD*1" task.

AAR	Spectrum			Modulation			Coherence			Phase			All			Spec-mod		
	A	*S*	*Sp*	*A*	*S*	*Sp*	*A*	*S*	*Sp*	*A*	*S*	*Sp*	*A*	*S*	*Sp*	*A*	*S*	*Sp*
SAR	−0.3	−3.0	2.9	3.4	1.9	5.2	2.8	3.3	2.2	3.7	−0.9	11.6	2.2	1.8	2.7	2.5	−1.0	6.7
SAR-BSS	−2.1	−5.5	2.0	−2.9	−1.8	−4.5	−0.3	1.6	−3.0	−2.3	−0.4	−6.3	−2.3	−2.9	−1.5	−0.6	−1.3	0.3
SAR-wICA	4.3	3.2	5.7	−2.0	−3.2	−0.3	1.9	3.8	−0.8	−1.5	0.6	−5.6	4.6	4.1	5.1	3.6	2.8	4.5
BSS	−4.6	−7.2	−1.3	−6.2	−5.4	−7.3	−2.2	0.9	−6.4	−4.7	0.2	−15.7	−4.0	−3.6	−4.6	−1.9	−4.8	1.7
wICA	6.7	5.1	8.8	3.2	3.7	2.4	0.9	4.3	−3.9	4.5	−1.8	14.6	8.7	8.8	8.5	7.7	4.8	11.2

Columns labeled "A, S, and Sp" correspond to accuracy, sensitivity, and specificity, respectively.

Table 4 | Relative gains obtained after AAR for the 2-class "*AD*1 vs. *AD*2" task.

AAR	Spectrum			Modulation			Coherence			Phase			All			Spec-mod		
	A	*S*	*Sp*	*A*	*S*	*Sp*	*A*	*S*	*Sp*	*A*	*S*	*Sp*	*A*	*S*	*Sp*	*A*	*S*	*Sp*
SAR	3.1	2.9	3.3	1.5	1.0	2.3	−1.5	−2.1	−0.6	2.6	0.6	6.9	2.2	−0.4	5.7	2.7	2.2	3.4
SAR-BSS	−3.8	−2.3	−6.0	−5.8	−6.0	−5.5	−2.7	−1.1	−5.2	−2.8	5.3	−28.2	−0.9	−2.4	1.2	−2.2	−1.0	−3.9
SAR-wICA	1.0	1.9	−0.3	0.0	0.7	−1.2	4.3	0.5	9.4	2.2	0.3	6.3	3.2	2.0	5.0	3.9	2.6	5.6
BSS	−5.2	−4.8	−5.8	−7.4	−5.1	−11.0	−2.1	3.7	−12.0	−4.8	3.7	−32.1	−8.1	−8.4	−7.7	−3.9	−3.8	−4.0
wICA	2.1	3.4	0.2	3.8	4.2	3.1	9.3	7.5	11.8	5.0	2.4	10.4	7.4	4.8	10.8	4.7	4.5	4.9

Columns labeled "A, S, and Sp" correspond to accuracy, sensitivity, and specificity, respectively.

scenario. For the gold standard benchmark, such features correspond to 96, 79, and 70% of the entire feature pool for Tasks 1–3, respectively. This corroborates recent findings showing the complementarity of the two modalities for AD diagnosis (Fraga et al., 2013a). Phase features, in turn, were seldom selected in both the wICA-AAR and gold standard scenarios, thus suggesting they play a small role in EEG-based AD diagnosis. The global field synchrony measure, in fact, did not show up in the top-24 feature subsets for any of the three Tasks.

Moreover, when discriminating between the three classes, features from the temporal and parietal regions showed to be important across the two scenarios. For the *N* vs. *AD*1 task, in turn, frontal and temporal regions stood out. For Task 3, features from the temporal and frontal regions were most salient for the wICA-AAR scenario, whereas the temporal and parietal regions stood out for the gold standard. Frontal region data may be corrupted by eye blinks/movement artifacts, thus are likely rejected by human experts. By automatically removing the artifacts from the data, useful discriminatory information may remain in such electrodes, thus assisting in AD diagnosis.

As for frequency bands, in the wICA scenario, delta and beta band features corresponded to roughly 70% of the selected features for each of the three tasks, followed by alpha band features (15%), thus corroborating previous studies that show the slowing of the EEG with AD (e.g., Coben et al., 1983; Elmståhl et al., 1994; Sankari et al., 2012; Waser et al., 2013). In the gold standard scenario, the delta, theta and beta features were most prevalent, amounting to about 80% of the selected features. Theta band features were particularly useful for Task 3, a finding previously reported in the AD severity monitoring literature (Coben et al., 1985). It is important to emphasize that none of the features extracted from the gamma bands were selected. It is hypothesized that this may be due to the fact that such higher frequencies are most sensitive to EEG artifacts, thus are (i) often discarded by human experts and (ii) may be severely distorted by the enhancement algorithms to a point of removing any existing discriminatory information. Lastly, it was observed that of the 24 selected features, roughly 40% corresponded to information extracted from interhemispheric/virtual bipolar signals, thus corroborating evidence of an interhemispheric disconnection with AD (Jeong, 2004).

4.2. EFFECTS OF AAR ON FEATURE DISTRIBUTIONS

In order to characterize the effects of the wICA algorithm on the distribution and statistics of the salient features, we utilize a so-called distribution overlap metric which measures the amount

Table 5 | Selected features used with the wICA-AAR automated system.

Ranking	Tasks		
	N* vs. *AD1* vs. *AD2	***N* vs. *AD1***	***AD1* vs. *AD2***
1	PZ_alpha_pwr*	PZ_alpha_pwr*	P3_P4_delta_pwr
2	C3_C4_delta_pwr	P3_alpha_pwr*	O1_O2_theta_cohe_pha
3	P3_P4_delta_pwr	O1_O2_theta_pwr*	C3_alpha_pwr
4	P3_alpha_pwr*	T3_T4_delta_pwr	F4_delta_pwr
5	P3_P4_delta_m-delta	F7_delta_pwr	T4_delta_pwr
6	FP1_FP2_beta_cohe_mag*	C3_C4_beta_m-beta	T3_T4_beta_pwr*
7	P3_P4_delta_cohe_mag*	F3_delta_pwr	T5_beta_pwr*
8	T3_T4_delta_pwr	O1_O2_delta_m-delta	OZ_beta_pwr
9	P3_delta_pwr	O1_O2_beta_cohe_mag*	FP1_FP2_beta_cohe_mag*
10	O1_alpha_pwr*	FP1_FP2_delta_cohe_mag*	FZ_beta_m-alpha
11	T4_theta_pwr*	FP1_delta_pwr	F3_beta_m-beta
12	T3_delta_pwr	T3_delta_m-delta	T5_theta_pwr*
13	T5_beta_pwr*	C3_delta_m-delta	T3_alpha_pwr*
14	O1_O2_theta_pwr*	P4_alpha_pwr*	T5_T6_delta_cohe_mag*
15	F8_beta_pwr	O1_alpha_pwr*	C4_delta_pwr
16	CZ_beta_pwr	T5_beta_pwr*	C3_C4_delta_cohe_mag*
17	T4_theta_m-theta*	CZ_beta_pwr	O1_O2_beta_m-theta
18	C3_C4_beta_m-beta	F8_beta_pwr	P3_P4_delta_m-delta
19	F7_beta_pwr	T3_T4_beta_m-alpha	F3_F4_beta_m-beta
20	C3_beta_pwr	T3_T4_beta_cohe_mag*	T3_T4_delta_cohe_mag*
21	F3_delta_pwr	F7_F8_beta_cohe_mag*	P4_beta_m-alpha
22	OZ_delta_pwr	FZ_beta_m-alpha	F3_F4_alpha_pwr
23	FZ_beta_m-alpha	T5_T6_theta_pwr*	FP1_theta_pwr*
24	C3_alpha_pwr*	F3_alpha_pwr*	O1_alpha_pwr
NUMBER OF FEATURES PER FEATURE SET			
Spectral power	18 (7)	14 (8)	13 (5)
Modulation	4 (1)	6 (0)	6 (0)
Coherence	2 (2)	4 (4)	4 (4)
Phase	0 (0)	0 (0)	1 (0)
NUMBER OF FEATURES PER BRAIN REGION			
Frontal	5 (1)	8 (3)	7 (2)
Central	5 (1)	3 (0)	3 (1)
Temporal	5 (3)	6 (3)	7 (6)
Parietal	6 (3)	3 (3)	3 (0)
Occipital	3 (2)	4 (3)	4 (0)
NUMBER OF FEATURES PER FREQUENCY BAND			
Delta	9 (1)	8 (1)	8 (3)
Theta	3 (3)	2 (2)	3 (2)
Alpha	4 (4)	5 (5)	4 (1)
Beta	8 (2)	9 (4)	9 (3)
NUMBER OF FEATURES FROM VIRTUAL CHANNELS			
Interhemispheric	8 (3)	9 (6)	11 (5)

Features with an asterisk represent those with an overlap in histograms between pre- and post-AAR ≥ 80%. Last four sections show, from top to bottom, the number of features that belong to each of the four feature sets, brain regions, frequency band, and montage, respectively. Values reported between parentheses represent those with pre-post AAR histogram overlap ≥ 80%.

Table 6 | Selected features used with the gold standard system.

Ranking	Tasks		
	N* vs. *AD1* vs. *AD2	***N* vs. *AD1***	***AD1* vs. *AD2***
1	O1_O2_theta_pwr	O1_O2_theta_pwr	CZ_beta_pwr
2	P3_P4_theta_pwr	PZ_delta_pwr	P4_alpha_m-theta
3	T5_theta_m-theta	CZ_beta_m-theta	P3_P4_delta_pwr
4	F7_F8_alpha_cohe_pha	FP2_beta_pwr	F7_alpha_m-delta
5	T3_theta_m-delta	FP1_beta_m-beta	O1_O2_theta_cohe_pha
6	P3_P4_delta_pwr	O1_O2_alpha_pwr	T3_theta_pwr
7	PZ_alpha_pwr	O1_O2_beta_cohe_pha	OZ_beta_m-alpha
8	O1_O2_alpha_pwr	F7_F8_alpha_cohe_pha	P3_P4_theta_m-theta
9	C4_alpha_m-delta	T6_delta_m-delta	P3_P4_beta_m-alpha
10	FP2_beta_pwr	FP1_delta_pwr	O1_O2_theta_m-theta
11	T3_T4_alpha_m-theta	OZ_beta_m-beta	T4_theta_pwr
12	T5_T6_beta_m-delta	O1_O2_beta_m-theta	T6_theta_m-theta
13	T6_beta_m-delta	T3_T4_beta_m-alpha	P3_P4_beta_m-beta
14	T4_theta_pwr	F7_F8_beta_m-beta	C3_C4_alpha_cohe_mag
15	O1_O2_alpha_m-theta	PZ_alpha_pwr	P3_P4_beta_pwr
16	O1_delta_pwr	OZ_beta_pwr	P3_P4_theta_m-delta
17	P3_P4_beta_m-theta	C4_delta_m-delta	T5_T6_alpha_cohe_mag
18	T3_theta_pwr	CZ_beta_m-alpha	F7_F8_alpha_cohe_mag
19	OZ_beta_pwr	F4_theta_m-delta	P4_beta_m-beta
20	F3_F4_theta_pwr	F3_F4_delta_cohe_mag	T5_T6_delta_cohe_mag
21	T6_delta_pwr	FP1_FP2_beta_cohe_mag	T3_T4_theta_cohe_mag
22	C4_delta_m-delta	P3_P4_delta_cohe_mag	FP1_theta_m-delta
23	T3_T4_beta_m-beta	T5_beta_pwr	T3_theta_m-delta
24	PZ_delta_pwr	FZ_delta_pwr	C3_C4_delta_cohe_pha
NUMBER OF FEATURES PER FEATURE SET			
Spectral power	13	9	5
Modulation	10	10	12
Coherence	0	3	5
Phase	1	2	2
NUMBER OF FEATURES PER BRAIN REGION			
Frontal	3	9	3
Central	2	3	3
Temporal	9	3	7
Parietal	5	3	8
Occipital	5	6	3
NUMBER OF FEATURES PER FREQUENCY BAND			
Delta	5	7	3
Theta	7	2	10
Alpha	6	3	5
Beta	6	12	6
NUMBER OF FEATURES FROM VIRTUAL CHANNELS			
Interhemispheric	11	10	14

Last four sections show, from top to bottom, the number of features that belong to each of the four feature sets, brain regions, frequency band, and montage, respectively.

of overlap between the histogram of a particular feature before and after wICA AAR. The metric is normalized to lie between 0 − 100% with 0 and 100% overlap values suggesting complete change and no change in feature statistics post-AAR, respectively. For simplicity, **Table 5** highlights features which resulted in an overlap greater than 80%, thus can be considered as irrelevant statistical changes. For illustration purposes, **Figure 2** presents the pre- and post-AAR histograms for two features. Subplot (A) is for a feature with an overlap of 83% (FZ_beta_m-alpha) and subplot (B) for a feature with 49% overlap (FZ_beta_m-alpha). As can be seen from **Table 5**, roughly half of the top-24 features did not present relevant modifications in their distributions post wICA-AAR processing. Moreover, coherence features were found to be the least affected, whereas the amplitude modulation ones were most affected. For Tasks 1 and 2, alpha and theta bands features were least affected; however, features from such frequency bands only correspond to roughly 30% of the top-24 selected features. Interestingly, features from such band correspond to 55% and 63% of the features selected manually for Tasks 1 and 3, respectively (see **Table 6**), thus suggesting their robustness to artifacts.

4.3. AUTOMATED vs. HUMAN EXPERT ARTIFACT REMOVAL

From **Tables 1–4**, it can be seen that wICA-AAR combined with classifiers trained on the top-24 features found from the "All-features" pool (see **Tables 5**, **6**) resulted in the best classification performance. For the three-class task, such automated system resulted in an overall classification accuracy of 78.9%, which is significantly higher than chance and inline with what was achieved with the gold standard (i.e., 83.8%). For Task 2, in turn, accuracy, sensitivity, and specificity of 90.8, 92.5, and 88.8% could be achieved, respectively with the automated system. This also compares favorably with the gold standard, which attained performance levels of 93.2, 95, and 91%, respectively. Moreover, the wICA and SAR-wICA combination resulted in substantial improvements for the coherence features, thus corroborating findings from Castellanos and Makarov (2006).

Interestingly, for Task 3 involving AD1 and AD2 patients, the wICA-AAR system outperformed the gold standard, achieving accuracy, sensitivity, and specificity values of 96.3, 96.9, and 95.5%, respectively. The gold standard, in turn, obtained values 92.8, 97.3, and 86.7%, respectively. It is suspected that this improved performance was obtained due to information harnessed from the frontal electrodes, which were often selected by the wICA-processed data and not from the manually-selected data. Frontal electrodes are susceptible to eye-related artifacts and are likely often discarded by human experts. Notwithstanding, the frontal region has been shown in classical studies to be severely affected by disease progression (Mann et al., 1988; DeKosky and Scheff, 1990). These findings show the relevance of an automated system in assisting clinicians with diagnosis.

Moreover, from **Tables 1–4** it can be seen that the BSS algorithm and its combination with SAR resulted in performance decreases relative to the baseline system trained on raw noisy data for all tested feature sets and tasks. This suggests that while BSS can be used to reliably remove ocular artifacts (Gómez-Herrero et al., 2006), its processing also removes important discriminatory information from the raw EEG data. Hence, it is suggested that BSS be avoided in EEG-based AD diagnosis systems.

Lastly, we explored the gains obtained with feature averaging as a simple SNR improvement tool. For Task 1, the accuracy gains relative to the baseline obtained with only feature averaging (i.e., raw EEG data without AAR) were of 3.3, 4.9, 3.4, and 1.9% for the spectral, amplitude modulation, coherence, and phase feature sets, respectively. For Task 2, in turn, these relative accuracy gains were of 1.5, 1.1, 2.6, 2.2%, respectively. Lastly, for Task 3 the relative gains were 3, 0.8, 2.4, and 2% respectively. As can be seen, simple feature averaging (Fraga et al., 2013b) can be used as an effective tool that can be combined with AAR algorithms to further improve diagnostic performance.

4.4. LIMITATIONS

The three enhancement algorithms explored here represented the state-of-the-art applicable to the constraints imposed by

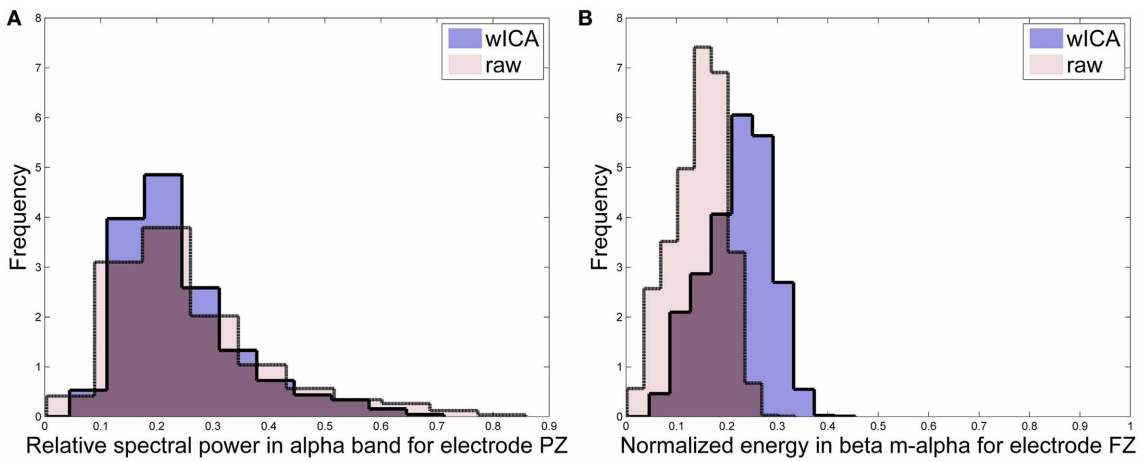

FIGURE 2 | Histograms for features (A) PZ_alpha_pwr and (B) FZ_beta_m-alpha.

our available database, such as small number of channels (20), limited amount of data per participant, and lack of EOG reference channels. For future studies without these limitations, alternate AAR algorithms can be explored. For example, for studies involving EEG with over 64 channels and EOG, the ADJUST (Automatic EEG artifact Detection based on the Joint Use of Spatial and Temporal features) (Mognon et al., 2011) and FASTER (Fully Automated Statistical Thresholding for EEG artifact Rejection) (Nolan et al., 2010) algorithms can be used. On our 20-channel dataset, we found the use of these two algorithms to lead to over rejection of components deemed artifactual, thus negatively impacting diagnostic performance. Alternately, if larger amounts of EEG data are collected per participant, other data-driven methods may be used, such as the weighted support vector machine-based AAR method proposed by Shao et al. (2009). Lastly, if auxiliary signals are recorded simultaneously with EEG data, other multi-channel AAR methods may be applied. Representative examples include the use of EOG or signals from optical eye tracking systems to develop adaptive filtering schemes (e.g., Joyce et al., 2004; Schlögl et al., 2007; Samadi and Cooke, 2013), or even the use of gyroscopes in ambulatory EEG systems to flag EEG segments collected during head movements (ORegan and Marnane, 2013).

5. CONCLUSION

The last decade has seen a rise in the development of EEG-based tools to assist clinicians with AD diagnosis. This paper has evaluated the effects of different state-of-the-art AAR algorithms on diagnosis performance; AAR algorithms were tested both alone and in tandem. Experimental results showed the wavelet enhanced ICA (wICA) AAR algorithm outperforming all other algorithms across four investigated feature sets (spectral, amplitude modulate rate-of-change, coherence, phase), as well as two combined feature sets ("All" and "Spectral-modulation"). In a disease progression monitoring task (Task 3), the automated system was shown to outperform a diagnostic system trained on artifact-free data processed by human experts. Such findings suggest that the discard of useful discriminatory information can be avoided if AAR algorithms are used. Ultimately, it is hoped that such fully-automated diagnostic tools be used to assist clinicians not only with early diagnostics, but also with disease progression monitoring and assessment.

ACKNOWLEDGMENTS

This work was funded by the Natural Sciences and Engineering Research Council of Canada (NSERC) and the Foundation for Research Support of the State of São Paulo (FAPESP). The authors would also like to thank Dr. Justin Dauwels for sharing his scripts to calculate the global field synchrony feature.

REFERENCES

Achanccaray, D. R., and Meggiolaro, M. A. (2008). "Detection of artifacts from EEG data using wavelet transform, high-order statistics and neural networks," in *XVII Brazilian Conference on Automatica* (Juiz de Fora).

Adeli, H., Ghosh-Dastidar, S., and Dadmehr, N. (2005). Alzheimer's disease: models of computation and analysis of EEGs. *Clin. EEG Neurosci.* 36, 131–140. doi: 10.1177/155005940503600303

Adler, G., Brassen, S., and Jajcevic, A. (2003). EEG coherence in Alzheimer's dementia. *J. Neural Transm.* 110, 1051–1058. doi: 10.1007/s00702-003-0024-8

Akhtar, M. T., Mitsuhashi, W., and James, C. J. (2012). Employing spatially constrained ICA and wavelet denoising for automatic removal of artifacts from multichannel EEG data. *Signal Process.* 92, 401–416. doi: 10.1016/j.sigpro.2011.08.005

Alzheimer Association. (2013). 2013 Alzheimer's disease facts and figures. *J. Alzheimer's Assoc.* 9, 208–245. doi: 10.1016/j.jalz.2013.02.003

Atlas, L., and Shamma, S. A. (2003). Joint acoustic and modulation frequency. *EURASIP J. Appl. Signal Process.* 2003, 668–675. doi: 10.1155/S1110865703305013

Babiloni, C., Lizio, R., Vecchio, F., Frisoni, G. B., Pievani, M., Geroldi, C., et al. (2010). Reactivity of cortical alpha rhythms to eye opening in mild cognitive impairment and Alzheimer's disease: an EEG study. *J. Alzheimer's Dis.* 22, 1047–1064. doi: 10.3233/JAD-2010-100798

Bedrosian, E. (1963). A product theorem for Hilbert transforms. *Proc. IEEE* 51, 868–869. doi: 10.1109/PROC.1963.2308

Belouchrani, A., Abed-Meraim, K., Cardoso, J.-F., and Moulines, E. (1997). A blind source separation technique using second-order statistics. *IEEE Trans. Signal Process.* 45, 434–444. doi: 10.1109/78.554307

Besthorn, C., Förstl, H., Geiger-Kabisch, C., Sattel, H., Gasser, T., and Schreiter-Gasser, U. (1994). EEG coherence in alzheimer disease. *Electroencephalogr. Clin. Neurophysiol.* 90, 242–245. doi: 10.1016/0013-4694(94)90095-7

Brenner, R. P., Ulrich, R. F., Spiker, D. G., Sclabassi, R. J., Reynolds III, C. F., Marin, R. S., et al. (1986). Computerized EEG spectral analysis in elderly normal, demented and depressed subjects. *Electroencephalogr. Clin. Neurophysiol.* 64, 483–492. doi: 10.1016/0013-4694(86)90184-7

Brucki, S., Nitrini, R., Caramelli, P., Bertolucci, P. H., and Okamoto, I. H. (2003). Suggestions for utilization of the mini-mental state examination in Brazil. *Arq. Neuropsiquiatr.* 61, 777–781. doi: 10.1590/S0004-282X2003000500014

Castellanos, N. P., and Makarov, V. A. (2006). Recovering EEG brain signals: artifact suppression with wavelet enhanced independent component analysis. *J. Neurosci. Methods* 158, 300–312. doi: 10.1016/j.jneumeth.2006.05.033

Coben, L. A., Danziger, W. L., and Berg, L. (1983). Frequency analysis of the resting awake EEG in mild senile dementia of Alzheimer type. *Electroencephalogr. Clin. Neurophysiol.* 55, 372–380. doi: 10.1016/0013-4694(83)90124-4

Coben, L. A., Danziger, W., and Storandt, M. (1985). A longitudinal EEG study of mild senile dementia of Alzheimer type: changes at 1 year and at 2.5 years. *Electroencephalogr. Clin. Neurophysiol.* 61, 101–112. doi: 10.1016/0013-4694(85)91048-X

Cristianini, N., and Shawe-Taylor, J. (2000). *An Introduction to Support Vector Machines and Other Kernel-Based Learning Methods*. Cambridge, UK: Cambridge University Press.

Czigler, B., Csikós, D., Hidasi, Z., Anna Gaál, Z., Csibri, É., Kiss, É., et al. (2008). Quantitative EEG in early Alzheimer's disease patients—power spectrum and complexity features. *Int. J. Psychophysiol.* 68, 75–80. doi: 10.1016/j.ijpsycho.2007.11.002

Daly, I., Nicolaou, N., Nasuto, S. J., and Warwick, K. (2013). Automated artifact removal from the electroencephalogram: a comparative study. *Clin. EEG Neurosci.* 44, 291–306. doi: 10.1177/1550059413476485

Dauwels, J., Srinivasan, K., Ramasubba Reddy, M., Musha, T., Vialatte, F.-B., Latchoumane, C., et al. (2011). Slowing and loss of complexity in Alzheimer's EEG: two sides of the same coin? *Int. J. Alzheimer's Dis.* 2011:539621. doi: 10.4061/2011/539621

De Clercq, W., Vergult, A., Vanrumste, B., Van Paesschen, W., and Van Huffel, S. (2006). Canonical correlation analysis applied to remove muscle artifacts from the electroencephalogram. *IEEE Trans. Biomed. Eng.* 53, 2583–2587. doi: 10.1109/TBME.2006.879459

DeKosky, S. T., and Scheff, S. W. (1990). Synapse loss in frontal cortex biopsies in Alzheimer's disease: correlation with cognitive severity. *Ann. Neurol.* 27, 457–464. doi: 10.1002/ana.410270502

Delorme, A., and Makeig, S. (2004). EEGLAB: an open source toolbox for analysis of single-trial EEG dynamics including independent component analysis. *J. Neurosci. Methods* 134, 9–21. doi: 10.1016/j.jneumeth.2003.10.009

Delorme, A., Sejnowski, T., and Makeig, S. (2007). Enhanced detection of artifacts in EEG data using higher-order statistics and independent component analysis. *Neuroimage* 34, 1443–1449. doi: 10.1016/j.neuroimage.2006.11.004

Dunkin, J. J., Leuchter, A. F., Newton, T. F., and Cook, I. A. (1994). Reduced EEG coherence in dementia: state or trait marker? *Biol. Psychiatry* 35, 870–879. doi: 10.1016/0006-3223(94)90023-X

Elmståhl, S., Rosén, I., and Gullberg, B. (1994). Quantitative EEG in elderly patients with Alzheimer's disease and healthy controls. *Dement. Geriatr. Cogn. Disord.* 5, 119–124. doi: 10.1159/000106706

Falk, T. H. and Chan, W.-Y. (2008). Modulation filtering for heart and lung sound separation from breath sound recordings. *Conf. Proc. IEEE Eng. Med. Biol. Soc.* 2008, 1859–1862. doi: 10.1109/IEMBS.2008.4649547

Falk, T. H., Chan, W.-Y., Sejdic, E., and Chau, T. (2010). "Spectro-temporal analysis of auscultatory sounds," in *New Developments in Biomedical Engineering*, ed D. Campolo (Rijeka: In-Tech Publishing), 93–104.

Falk, T. H., Fraga, F. J., Trambaiolli, L., and Anghinah, R. (2012). EEG amplitude modulation analysis for semi-automated diagnosis of Alzheimer's disease. *EURASIP J. Adv. Signal Process.* 2012, 1–9. doi: 10.1186/1687-6180-2012-192

Fraga, F. J., Falk, T. H., Kanda, P. A. M., and Anghinah, R. (2013a). Characterizing Alzheimer's disease severity via resting-awake EEG amplitude modulation analysis. *PLoS ONE* 8:e72240. doi: 10.1371/journal.pone.0072240

Fraga, F. J., Falk, T. H., Trambaiolli, L. R., Oliveira, E. F., Pinaya, W. H., Kanda, P. A., et al. (2013b). "Towards an EEG-based biomarker for Alzheimer's disease: improving amplitude modulation analysis features," in *Proceeding IEEE International Conference on Acoustics, Speech and Signal Processing* (Vancouver, BC), 1207–1211.

Giaquinto, S., and Nolfe, G. (1986). The EEG in the normal elderly: a contribution to the interpretation of aging and dementia. *Electroencephalogr. Clin. Neurophysiol.* 63, 540–546. doi: 10.1016/0013-4694(86)90141-0

Gómez-Herrero, G. (2007). *Automatic Artifact Removal (AAR) Toolbox v1. 3 (Release 09.12. 2007) for MATLAB.*

Gómez-Herrero, G., De Clercq, W., Anwar, H., Kara, O., Egiazarian, K., Van Huffel, S., et al. (2006). "Automatic removal of ocular artifacts in the EEG without an EOG reference channel," in *Proceedings Nordic Signal Processing Symposium* (Rejkjavik), 130–133.

Hall, M., Frank, E., Holmes, G., Pfahringer, B., Reutemann, P., and Witten, I. H. (2009). The weka data mining software: an update. *ACM SIGKDD Explor. Newslett.* 11, 10–18. doi: 10.1145/1656274.1656278

James, C. J., and Hesse, C. W. (2005). Independent component analysis for biomedical signals. *Physiol. Meas.* 26, R15. doi: 10.1088/0967-3334/26/1/R02

Jeong, J. (2004). EEG dynamics in patients with Alzheimer's disease. *Clin. Neurophysiol.* 115, 1490–1505. doi: 10.1016/j.clinph.2004.01.001

Joyce, C. A., Gorodnitsky, I. F., and Kutas, M. (2004). Automatic removal of eye movement and blink artifacts from EEG data using blind component separation. *Psychophysiology* 41, 313–325. doi: 10.1111/j.1469-8986.2003.00141.x

Jung, T.-P., Makeig, S., Humphries, C., Lee, T.-W., Mckeown, M. J., Iragui, V., et al. (2000). Removing electroencephalographic artifacts by blind source separation. *Psychophysiology* 37, 163–178. doi: 10.1111/1469-8986.3720163

Kanda, P. A. M., Trambaiolli, L. R., Lorena, A. C., Fraga, F. J., Basile, L. F. I., Nitrini, R., et al. (2013). Clinician's road map to wavelet EEG as an Alzheimer's disease biomarker. *Clin. EEG Neurosci.* doi: 10.1177/1550059413486272. [Epub ahead of print].

Knott, V., Mohr, E., Mahoney, C., and Ilivitsky, V. (2000). Electroencephalographic coherence in Alzheimer's disease: comparisons with a control group and population norms. *J. Geriatr. Psychiatr. Neurol.* 13, 1–8. doi: 10.1177/089198870001300101

Koenig, T., Lehmann, D., Saito, N., Kuginuki, T., Kinoshita, T., and Koukkou, M. (2001). Decreased functional connectivity of EEG theta-frequency activity in first-episode, neuroleptic-naıve patients with schizophrenia: preliminary results. *Schizophr. Res.* 50, 55–60. doi: 10.1016/S0920-9964(00)00154-7

Koenig, T., Prichep, L., Dierks, T., Hubl, D., Wahlund, L., John, E., et al. (2005). Decreased EEG synchronization in Alzheimer's disease and mild cognitive impairment. *Neurobiol. Aging* 26, 165–171. doi: 10.1016/j.neurobiolaging.2004.03.008

Krishnaveni, V., Jayaraman, S., Anitha, L., and Ramadoss, K. (2006). Removal of ocular artifacts from EEG using adaptive thresholding of wavelet coefficients. *J. Neural Eng.* 3, 338. doi: 10.1088/1741-2560/3/4/011

Labate, D., La Foresta, F., Inuso, G., and Morabito, F. C. (2011). "Remarks about wavelet analysis in the EEG artifacts detection," in *Proceedings of the Italian Workshop on Neural Nets* (Vietri sul Mare: IOS Press), 99–106.

Laxton, A. W., Tang-Wai, D. F., McAndrews, M. P., Zumsteg, D., Wennberg, R., Keren, R., et al. (2010). A phase I trial of deep brain stimulation of memory circuits in Alzheimer's disease. *Ann. Neurol.* 68, 521–534. doi: 10.1002/ana.22089

Lehmann, C., Koenig, T., Jelic, V., Prichep, L., John, R. E., Wahlund, L.-O., et al. (2007). Application and comparison of classification algorithms for recognition of Alzheimer's disease in electrical brain activity (EEG). *J. Neurosci. Methods* 161, 342–350. doi: 10.1016/j.jneumeth.2006.10.023

Leifer, B. P. (2003). Early diagnosis of Alzheimer's disease: clinical and economic benefits. *J. Am. Geriatr. Soc.* 51, S281–S288. doi: 10.1046/j.1532-5415.5153.x

Leuchter, A. F., Spar, J. E., Walter, D. O., and Weiner, H. (1987). Electroencephalographic spectra and coherence in the diagnosis of Alzheimer's-type and multi-infarct dementia: a pilot study. *Arch. Gen. Psychiatry* 44, 993. doi: 10.1001/archpsyc.1987.01800230073012

Locatelli, T., Cursi, M., Liberati, D., Franceschi, M., and Comi, G. (1998). EEG coherence in Alzheimer's disease. *Electroencephalogr. Clin. Neurophysiol.* 106, 229–237. doi: 10.1016/S0013-4694(97)00129-6

Luck, S. J. (2005). *An Introduction to the Event-Related Potential Technique*. Cambridge, MA: A Bradford Book.

Makarov, V. A. (2012). *Wavelet Enhanced Independent Component Analysis (wICA) Package For MATLAB*.

Malyska, N., Quatieri, T. F., and Sturim, D. (2005). "Automatic dysphonia recognition using biologically inspired amplitude-modulation features," in *Proceedings ICASSP*, Vol. 1 (Philadelphia, PA), 873–876.

Mann, D., Marcyniuk, B., Yates, P., Neary, D., and Snowden, J. (1988). The progression of the pathological changes of Alzheimer's disease in frontal and temporal neocortex examined both at biopsy and at autopsy. *Neuropathol. Appl. Neurobiol.* 14, 177–195. doi: 10.1111/j.1365-2990.1988.tb00880.x

McKhann, G., Drachman, D., Folstein, M., Katzman, R., Price, D., and Stadlan, E. M. (1984). Clinical diagnosis of Alzheimer's disease report of the NINCDS-ADRDA work group under the auspices of department of health and human services task force on Alzheimer's disease. *Neurology* 34, 939–939. doi: 10.1212/WNL.34.7.939

Mognon, A., Jovicich, J., Bruzzone, L., and Buiatti, M. (2011). Adjust: an automatic EEG artifact detector based on the joint use of spatial and temporal features. *Psychophysiology* 48, 229–240. doi: 10.1111/j.1469-8986.2010.01061.x

Moore, C. I., and Cao, R. (2008). The hemo-neural hypothesis: on the role of blood flow in information processing. *J. Neurophysiol.* 99, 2035–2047. doi: 10.1152/jn.01366.2006

Moretti, D., Fracassi, C., Pievani, M., Geroldi, C., Binetti, G., Zanetti, O., et al. (2009). Increase of theta/gamma ratio is associated with memory impairment. *Clin. Neurophysiol.* 120, 295–303. doi: 10.1016/j.clinph.2008.11.012

Moretti, D., Frisoni, G., Fracassi, C., Pievani, M., Geroldi, C., Binetti, G., et al. (2011). MCI patients' EEGs show group differences between those who progress and those who do not progress to AD. *Neurobiol. Aging* 32, 563–571. doi: 10.1016/j.neurobiolaging.2009.04.003

Moretti, D., Prestia, A., Fracassi, C., Binetti, G., Zanetti, O., and Frisoni, G. (2012). Specific EEG changes associated with atrophy of hippocampus in subjects with mild cognitive impairment and Alzheimer's disease. *Int. J. Alzheimer's Dis.* 2012:253153. doi: 10.1155/2012/253153

Nolan, H., Whelan, R., and Reilly, R. (2010). FASTER: Fully automated statistical thresholding for EEG artifact rejection. *J. Neurosci. Methods* 192, 152–162. doi: 10.1016/j.jneumeth.2010.07.015

Nolte, G., Bai, O., Wheaton, L., Mari, Z., Vorbach, S., and Hallett, M. (2004). Identifying true brain interaction from EEG data using the imaginary part of coherency. *Clin. Neurophysiol.* 115, 2292–2307. doi: 10.1016/j.clinph.2004.04.029

Nunez, P. L. (2006). *Electric Fields of the Brain: the Neurophysics of EEG*. New York, NY: Oxford University Press. doi: 10.1093/acprof:oso/9780195050387.001.0001

ORegan, S., and Marnane, W. (2013). Multimodal detection of head-movement artefacts in eeg. *J. Neurosci. Methods* 218, 110–120. doi: 10.1016/j.jneumeth.2013.04.017

Park, Y.-M., Che, H.-J., Im, C.-H., Jung, H.-T., Bae, S.-M., and Lee, S.-H. (2008). Decreased EEG synchronization and its correlation with symptom severity in Alzheimer's disease. *Neurosci. Res.* 62, 112–117. doi: 10.1016/j.neures.2008.06.009

Penttilä, M., Partanen, J. V., Soininen, H., and Riekkinen, P. (1985). Quantitative analysis of occipital EEG in different stages of Alzheimer's disease. *Electroencephalogr. Clin. Neurophysiol.* 60, 1–6. doi: 10.1016/0013-4694(85)90942-3

Raicher, I., Takahashi, D., Kanda, P., Nitrini, R., and Anghinah, R. (2008). qEEG spectral peak in Alzheimer's disease. *Dement. Neuropsychol.* 2, 9–12.

Romero, S., Mañanas, M. A., and Barbanoj, M. J. (2008). A comparative study of automatic techniques for ocular artifact reduction in spontaneous EEG signals based on clinical target variables: a simulation case. *Comp. Biol. Med.* 38, 348–360. doi: 10.1016/j.compbiomed.2007.12.001

Samadi, M. R. H., and Cooke, N. (2013). "A novel approach for adaptive eeg artefact rejection and eog gaze estimation," in *HCI International 2013-Posters' Extended Abstracts*, ed C. Stephanidis (Las Vegas, NV: Springer), 603–607. doi: 10.1007/978-3-642-39473-7-120

Sankari, Z., Adeli, H., and Adeli, A. (2012). Wavelet coherence model for diagnosis of Alzheimer's disease. *Clin. EEG Neurosci.* 43, 268–278. doi: 10.1177/1550059412444970

Sarazin, M., de Souza, L. C., Lehéricy, S., and Dubois, B. (2012). Clinical and research diagnostic criteria for Alzheimer's disease. *Neuroimaging Clin. N. Am.* 22, 23–32. doi: 10.1016/j.nic.2011.11.004

Schlögl, A., Keinrath, C., Zimmermann, D., Scherer, R., Leeb, R., and Pfurtscheller, G. (2007). A fully automated correction method of EOG artifacts in EEG recordings. *Clin. Neurophysiol.* 118, 98–104. doi: 10.1016/j.clinph.2006.09.003

Shao, S.-Y., Shen, K.-Q., Ong, C. J., Wilder-Smith, E., and Li, X.-P. (2009). Automatic EEG artifact removal: a weighted support vector machine approach with error correction. *IEEE Trans. Biomed. Eng.* 56, 336–344. doi: 10.1109/TBME.2008.2005969

Sloan, E. P., Fenton, G. W., Kennedy, N. S., and MacLennan, J. M. (1994). Neurophysiology and SPECT cerebral blood flow patterns in dementia. *Electroencephalogr. Clin. Neurophysiol.* 91, 163–170. doi: 10.1016/0013-4694(94)90066-3

Soininen, H., Partanen, J., Laulumaa, V., Helkala, E.-L., Laakso, M., and Riekkinen, P. (1989). Longitudinal EEG spectral analysis in early stage of Alzheimer's disease. *Electroencephalogr. Clin. Neurophysiol.* 72, 290–297. doi: 10.1016/0013-4694(89)90064-3

Sörnmo, L., and Laguna, P. (2005). *Bioelectrical Signal Processing in Cardiac and Neurological Applications*. Burlington, MA: Academic Press.

Srinivasan, R., Winter, W. R., Ding, J., and Nunez, P. L. (2007). EEG and MEG coherence: measures of functional connectivity at distinct spatial scales of neocortical dynamics. *J. Neurosci. Methods* 166, 41–52. doi: 10.1016/j.jneumeth.2007.06.026

Thatcher, R., Krause, P., and Hrybyk, M. (1986). Cortico-cortical associations and EEG coherence: a two-compartmental model. *Electroencephalogr. Clin. Neurophysiol.* 64, 123–143. doi: 10.1016/0013-4694(86)90107-0

Trambaiolli, L., Lorena, A., Fraga, F., Kanda, P., Nitrini, R., and Anghinah, R. (2011a). Does EEG montage influence Alzheimer's disease electroclinic diagnosis? *Int. J. Alzheimer's Dis.* 2011:761891. doi: 10.4061/2011/761891

Trambaiolli, L. R., Falk, T. H., Fraga, F. J., Anghinah, R., and Lorena, A. C. (2011b). "EEG spectro-temporal modulation energy: a new feature for automated diagnosis of Alzheimer's disease," in *Proceedings of the International Conference of the IEEE Engineering in Medicine and Biology Society* (Boston, MA), 3828–3831.

Trambaiolli, L. R., Lorena, A. C., Fraga, F. J., Kanda, P. A., Anghinah, R., and Nitrini, R. (2011c). Improving Alzheimer's disease diagnosis with machine learning techniques. *Clin. EEG Neurosci.* 42, 160–165. doi: 10.1177/155005941104200304

Waser, M., Deistler, M., Garn, H., Benke, T., Dal-Bianco, P., Ransmayr, G., et al. (2013). EEG in the diagnostics of Alzheimer's disease. *Stat. Papers* 54, 1095–1107. doi: 10.1007/s00362-013-0538-6

WHO and Alzheimer's Disease International. (2012). *Dementia: A Public Health Priority.* Geneva: Technical report, World Health Organization.

Zikov, T., Bibian, S., Dumont, G. A., Huzmezan, M., and Ries, C. (2002). "A wavelet based de-noising technique for ocular artifact correction of the electroencephalogram," in *Proceedings of the International Conference of the IEEE Engineering in Medicine and Biology Society*, Vol. 1 (Houston, TX), 98–105.

Conflict of Interest Statement: The authors declare that the research was conducted in the absence of any commercial or financial relationships that could be construed as a potential conflict of interest.

Received: 06 December 2013; accepted: 06 March 2014; published online: 25 March 2014.

Citation: Cassani R, Falk TH, Fraga FJ, Kanda PAM and Anghinah R (2014) The effects of automated artifact removal algorithms on electroencephalography-based Alzheimer's disease diagnosis. Front. Aging Neurosci. ***6****:55. doi: 10.3389/fnagi.2014.00055*

This article was submitted to the journal Frontiers in Aging Neuroscience.

Copyright © 2014 Cassani, Falk, Fraga, Kanda and Anghinah. This is an open-access article distributed under the terms of the Creative Commons Attribution License (CC BY). The use, distribution or reproduction in other forums is permitted, provided the original author(s) or licensor are credited and that the original publication in this journal is cited, in accordance with accepted academic practice. No use, distribution or reproduction is permitted which does not comply with these terms.

frontiers in
AGING NEUROSCIENCE

ORIGINAL RESEARCH ARTICLE
published: 04 February 2014
doi: 10.3389/fnagi.2014.00011

Relative power and coherence of EEG series are related to amnestic mild cognitive impairment in diabetes

Zhijie Bian[1], Qiuli Li[2], Lei Wang[2], Chengbiao Lu[1], Shimin Yin[2]* and Xiaoli Li[3,4]*

[1] *Institute of Electrical Engineering, Yanshan University, Qinhuangdao, China*
[2] *Department of Neurology, The Second Artillery General Hospital of PLA, Beijing, China*
[3] *State Key Laboratory of Cognitive Neuroscience and Learning and IDG/McGovern Institute for Brain Research, Beijing Normal University, Beijing, China*
[4] *Center for Collaboration and Innovation in Brain and Learning Sciences, Beijing Normal University, Beijing, China*

Edited by:
Davide V. Moretti, IRCCS San Giovanni di Dio Fatebenefratelli, Italy

Reviewed by:
Francisco J. Fraga, Universidade Federal do ABC, Brazil
Maria E. López, Centre for Biomedical Technology, Spain

****Correspondence:***
Shimin Yin, Department of Neurology, The Second Artillery General Hospital of PLA, Xinjiekou Wai Street No.16, Xicheng District, Beijing 100088, China
e-mail: smyin@126.com;
Xiaoli Li, State Key Laboratory of Cognitive Neuroscience and learning, Beijing Normal University, No.19, XinJieKoWai St., HaiDian District, Beijing,100875, China
e-mail: xiaoli@bnu.edu.cn

Objective: Diabetes is a risk factor for dementia and mild cognitive impairment. The aim of this study was to investigate whether some features of resting-state EEG (rsEEG) could be applied as a biomarker to distinguish the subjects with amnestic mild cognitive impairment (aMCI) from normal cognitive function in type 2 diabetes.

Materials and Methods: In this study, 28 patients with type 2 diabetes (16 aMCI patients and 12 controls) were investigated. Recording of the rsEEG series and neuropsychological assessments were performed. The rsEEG signal was first decomposed into delta, theta, alpha, beta, gamma frequency bands. The relative power of each given band/sum of power and the coherence of waves from different brain areas were calculated. The extracted features from rsEEG and neuropsychological assessments were analyzed as well.

Results: The main findings of this study were that: (1) compared with the control group, the ratios of power in theta band [P(theta)] vs. power in alpha band [P(alpha)] [P(theta)/P(alpha)] in the frontal region and left temporal region were significantly higher for aMCI, and (2) for aMCI, the alpha coherences in posterior, fronto-right temporal, fronto-posterior, right temporo-posterior were decreased; the theta coherences in left central-right central (LC-RC) and left posterior-right posterior (LP-RP) regions were also decreased; but the delta coherences in left temporal-right temporal (LT-RT) region were increased.

Conclusion: The proposed indexes from rsEEG recordings could be employed to track cognitive function of diabetic patients and also to help in the diagnosis of those who develop aMCI.

Keywords: resting-state EEG, amnestic mild cognitive impairment, diabetes, relative power, coherence

INTRODUCTION

That diabetes affects cognitive function was first reported by Mile and Root in the 1920s (Miles and Root, 1922). Diabetes patients were found to have neuronal death and axonal degeneration, a concept of "diabetic encephalopathy" was thus raised in Gispen and Biessels (2000). Epidemiological data showed that the diabetic patients was associated with a 1.5–2.5-fold increased risk of dementia (Strachan et al., 2011).

The MCI is defined as impairment in cognitive functions, particularly memory, with otherwise normal performance of activities of daily living. The MCI lies between and overlaps normal aging and Alzheimer's disease (AD) and is now recognized to be a risk factor for AD (Levey et al., 2006) or an early manifestation of the disease (Morris, 2005). The MCI includes two subtypes: amnestic mild cognitive impairment (aMCI) and non-amnestic MCI (na-MCI). The aMCI patients are the high-risk groups of AD. The percent change of conversion from aMCI to AD was 54% and the conversion duration from initial diagnosis of aMCI to dementia was 28 ± 12 months (Seo et al., 2012).

Type 2 diabetes, is characterized by high blood glucose in the context of insulin resistance and relative insulin deficiency (Kumar et al., 2005). Cognitive impairment such as learning and memory deficiency was seen in type 2 diabetes (Peila et al., 2002). The diabetes may be associated with increased risk of both aMCI and na-MCI (Shimada et al., 2010; Roberts et al., 2014). Therefore, it is critical to explore methods to detect the aMCI of diabetes patients, so that the early interventions to these patients can be provided.

Petersen described the MCI based on clinical criteria (Petersen, 2004), however current proposals also include biomarkers (Albert et al., 2011). By using the ligand-based positron emission tomography (PET), abnormal dosages of the beta amyloid to tau ratio in cerebrospinal fluid (CSF) and deposition of beta amyloid in the brain can be used to diagnose the prodromal stages of AD in MCI subjects; moreover, the neurodegeneration such as atrophy of the hippocampus on magnetic resonance imaging (MRI) and hypometabolism of the posterior cingulate/precuneus, parietal and temporal regions revealed by fluorodeoxyglucose (FDG)-PET are all useful biomarkers for diagnosis of prodromal stages of AD (Albert et al., 2011). However, the sensitivity and specificity of these biomarkers were different for the different international databases (Toussaint et al., 2012; Takahashi et al.,

2013). Moreover, the CSF markers are invasive, the PET markers are costly and expose patients to radiation, and the MRI markers of hippocampus volume are relatively expensive for serial screening of large elderly populations at risk for AD; therefore, a non-invasive and cost-effective tool is needed. It was demonstrated that the cerebral EEG rhythms can reflect the underlying brain network activity (Steriade, 2006), and the resting-state EEG (rsEEG) can be used to perform serial examinations for neurological evolution (Rossini et al., 2007; Schmidt et al., 2013). Recent studies have investigated the rsEEG rhythms in MCI and AD subjects, which may be a promising approach to assess MCI subjects (Babiloni et al., 2014). This technique is low-cost, easy to use, presents a high temporal resolution and is non-invasive.

Spectral power of EEG series and their correlations with neuropsychological tests can provide valuable information in distinguishing normal and diseased brain function (Roh et al., 2011). The theta and delta spectral power tended to increase in the selected brain regions according to cognitive impairment from normal through aMCI to AD, whereas alpha and beta2 power showed a decreasing tendency (Roh et al., 2011). In particular, relative power has been used as a feature to classify the MCI and mild AD patients from age-matched controls (Jelic et al., 1996; Dauwels et al., 2011). In addition, the EEG coherence has been used to evaluate the functionality of cortical connections and to provide information about the synchronization of the regional cortical activity in AD. In Sankari et al. (2011), it was found that decreased coherence indicates a decline in cortical connectivity in AD, which suggests that the coherence of EEG signals have potentials in differentiation of healthy elderly from AD patients. Power and coherence were considered as features for the classification of the AD and control groups, since the classification accuracy reached to 89% (Strijers et al., 1997; Stevens et al., 2001). Therefore, rsEEG indexes may have the potential as a biomarker to distinct the aMCI or AD from controls. In order to seek a better early diagnosis method of aMCI for patients with diabetes, rsEEG indexes (relative power and coherence in different regions and frequencies) were investigated in this study.

MATERIALS AND METHODS

PARTICIPANTS

In this study the participants were 28 right-handed type 2 diabetes patients who satisfied the diagnosis criteria for diabetes (American Diabetes Association, 2013), and they were all voluntary and more than 50 years old. These participants were divided into 2 groups: aMCIs and controls. The aMCI group consisted of 16 patients (5 males and 11 females; mean age 69.7 $\pm$ 8.4 years, range from 52 to 84 years; mean years of diabetes 9.3 $\pm$ 2.4 years, range from 1 to 20 years; mean years of education 12.9 $\pm$ 1.8 years, range from 6 to 16 years), and the control group consisted of 12 patients (6 males and 6 females; mean age 73.3 $\pm$ 4.6 years, range from 63 to 80 years; mean years of diabetes 14.0 $\pm$ 3.1 years, range from 1 to 30 years; mean years of education 13.8 $\pm$ 3.0 years, range from 9 to 19 years). Both groups were matched in age, diabetes duration and education level, but not in gender.

The study was approved by the local ethics committee and all patients gave written informed consent. The experiment was conducted in accordance with the Declaration of Helsinki (1964) and was approved by the Beijing Normal University ethics committee.

NEUROPSYCHOLOGICAL TESTS AND INCLUSION CRITERIA

Based on traditional MMSE (Folstein et al., 1975), and considering the China National State, a modified MMSE proposed by Shanghai Mental Health Center in China (Jia, 2010) was performed to all diabetic participants in this study. The cut-off score for absence of dementia was 24 points for high school and above, 20 points for the primary, and 17 for the illiteracy participants, so the scores of the two groups were all more than 24 points, which included MCI and normal function participants. The MoCA uses a cut-off score 26 points for MCI (Nasreddine et al., 2005). Compared with MMSE, the MoCA appears to be a better screening tool for MCI in the diabetic population because it possesses higher sensitivity (67%) (Alagiakrishnan et al., 2013). Therefore, in this study cognitive disorders were further screened by using MoCA after the preliminary screening of MMSE, which was only used to rule out AD preliminarily.

In this study, besides MMSE and MoCA, Auditory Verbal Learning Test (AVLT) (AVLT-Immediate recall, AVLT-Delayed recall, AVLT-Delayed recognition) (Carlesimo et al., 1996), Wechsler Adult Intelligence Scale Digit Span Test (WAIS-DST) (Orsini et al., 1987), Boston Naming Test (BNT), Trail Making Test (Reitan, 1958), Verbal Fluency Test (Novelli, 1986), Daily Living Test (Lawton and Brody, 1969) were performed to each subject.

The participants were all type 2 diabetes patients, whose vision and hearing were able to complete clinical trials. They underwent MRI examination to rule out the organic brain disease. The depression that can cause cognitive impairment was ruled out using DSM IV criteria for depression (American Psychiatric Association, 1994). No patients in either group reported a history of mental illness, systemic disease (such as liver and kidney dysfunction, heart disease and thyroid disease) and nervous system disease (such as cerebrovascular disease, traumatic brain injury, epilepsy, encephalitis, hydrocephalus, brain tumors, multiple sclerosis, radiation injury) that resulting to cognitive impairment.

The diabetic aMCI patients satisfied the criteria (Petersen, 2004) for the study diagnosis of aMCI. The inclusion criteria were as follows: (1) memory complaint usually coming from the patients or their family; (2) objective memory impairment for age defined by performances $\geq$1.5 standard deviation below the mean value of age- and education-matched controls for the Auditory Verbal Learning Test (Carlesimo et al., 1996); (3) essentially preserved general cognitive function tested using MMSE and MoCA; (4) normal activities of daily living evidenced by Activity of Daily Living Scale (Lawton and Brody, 1969); (5) not demented [the dementia was ruled out by DSM IV criteria for dementia (American Psychiatric Association, 1994)].

EEG RECORDING

The experiment was performed in the Department of Neurology, General Hospital of Second Artillery Corps of PLA, Beijing, China. The participants were asked to wash and brush their hair before the application of the Geodesic Sensor Net (GSN) to their head. During recordings, they were asked to close their eyes and

sit in a comfortable armchair, keeping relaxed and awake for 5 min in a quiet-dim room, with room temperature keeping at $23 \pm 2^{\circ}$C.

The EEG data recording was performed with a high-density 128-channel EGI system of Net Amps 300 amplifiers (Electrical Geodesics Inc. [EGI], Eugene, OR). The EEG was recorded continuously with a 128-channel GSN using the vertex sensor (Cz) as the reference electrode. Direct current acquisition was used and the data were sampled at 1000 Hz during recording. The impedances of all electrodes were kept below 50 kΩ, as recommended for this type of amplifiers by EGI guidelines.

EEG PREPROCESSING

The recorded EEG data were analyzed off-line using NetStation 4.5 software (Electrical Geodesics). First, a band-pass filter of 1–45 Hz was applied; then the data were re-referenced to the average of 57 (left mastoid process) and 100 (right mastoid process) sensors, and the data were re-sampled to 500 Hz. The artifacts (such as ocular and muscular) were removed by visual inspection of the raw EEG data. Finally EEG recordings of 3 min were segmented for further analysis.

The data was recorded using the 128-channel GSN, but in this study, the interested electrodes were circled inside the dashed line (see **Figure 1**), which can throughout the whole brain area. In order to detect EEG power in different regions and inter-/intra-regions coherence, the brain were divided into five regions: frontal (F), left temporal (LT), central (C), right temporal (RT), and posterior (P). For the aim to estimate the left and right hemispheres paired-electrodes coherence, the vertical dashed line (see **Figure 1**) divided the brain into left and right hemispheres (LH and RH) and the frontal region was divided into left frontal (LF) and right frontal (RF), the central region into left central (LC) and right central (RC), the posterior into left posterior (LP) and right posterior (RP).

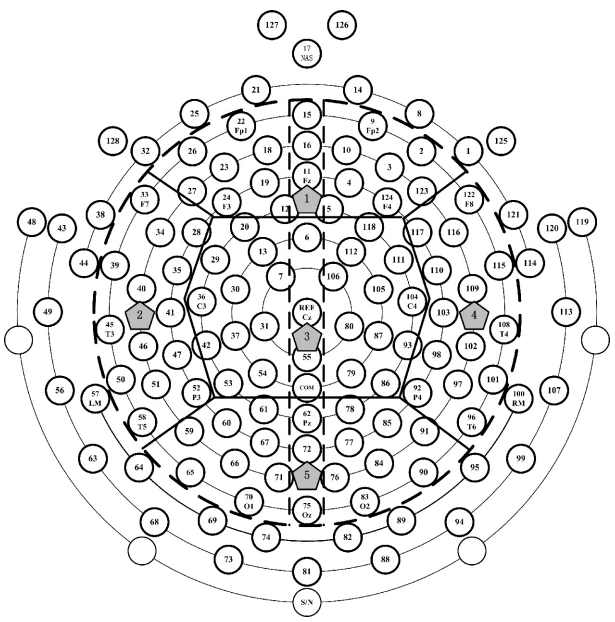

FIGURE 1 | The electrodes distribution of 128-channel Geodesic Sensor Net interested electrodes' partition. The interested electrodes were those inside the black dotted line. Thick solid lines divided the interested electrodes into 5 regions: the number 1, 2, 3, 4, and 5 denote the frontal, left temporal, central, right temporal and posterior regions, respectively. Vertical dotted line divided the brain into left and right hemispheres (LH and RH), left frontal (LF) and right frontal (RF), left central (LC) and right central (RC), and left posterior (LP) and right posterior (RP).

EEG DATA ANALYSIS

In this study, power and coherence were calculated at the five frequency bands: delta (1–4 Hz), theta (4–8 Hz), alpha (8–13 Hz), beta (13–30 Hz), gamma (30–45 Hz). For each band, the relative power and the coherence were obtained. The EEG data of 10 s were divided into overlapping segments using periodic 2-s hamming windows with 50% overlap, then the power spectral density (PSD) and the coherence of were computed using pwelch method (Welch, 1967). Outliers rejection was performed by means of a generalized extreme studentized deviate (GESD) (Seem, 2007) for all epochs.

Relative power

The relative power of each given band/sum of power from 1 to 45 Hz was calculated by

$$RP(f_1, f_2) = \frac{P(f_1, f_2)}{P(1, 45)} \times 100\%$$

where $P(\cdot)$ indicates the power, $RP(\cdot)$ indicates the relative power, and f_1, f_2 indicate the low and high frequency, respectively.

The ratios of power for different frequency bands in each electrode was computed for possible pairs of frequency bands, such as P(delta)/P(theta) [or /P(alpha), or /P(beta), or /P(gamma)], P(theta)/P(alpha) [or /P(beta), or /P(gamma)], P(alpha)/P(beta) [or /P(gamma)] and P(beta)/P(gamma).

The relative power for each band and the ratios of power for different frequency bands were averaged in each region.

Coherence

In this study, the magnitude squared coherence C_{xy} of signals x and y was estimated by using the PSD (P_{xx} and P_{yy}) and the cross PSD (P_{xy}), it is

$$C_{xy}(f) = \frac{\left|P_{xy}(f)\right|^2}{P_{xx}(f) * P_{yy}(f)}$$

where f is the frequency. In this study, Welch's averaged (a modified period-gram method) (Welch, 1967) was used to compute the coherence. Compared with other power spectra estimating methods, it is better to against noise. In the calculation, the frequency resolution was 0.1, and a coherence matrix $\{C_{xy}\}$ for the whole frequency band (1–45 Hz) was obtained. Then the average coherence values for each pair of electrodes over each EEG band were computed by

$$A_{xy} = \frac{1}{U - L} \int_L^U C_{xy}(f) df$$

where U and L were the upper and the lower bound frequencies for each band. The coherence of each pair of electrodes over the five frequency bands for each subject was calculated. After outlier rejection, the remained epochs were averaged. From this point, we called the averaged coherence as coherence.

Table 1 | Neuropsychological assessment scores (mean ± s.e.m.) and *p* values for the tested items in the diabetic aMCI and control groups.

Items	aMCI ($n = 16$)	Control ($n = 12$)	*P* values
MMSE	27.9 ± 0.5	28.8 ± 0.2	0.529
MoCA	22.4 ± 0.5	27.0 ± 0.3	$p < 0.0001$***
AVLT-Immediate recall	5.4 ± 0.4	7.6 ± 0.5	0.002*
AVLT- Delayed recall	4.3 ± 0.9	8.8 ± 1.0	0.005**
AVLT- Delayed recognition	10.9 ± 0.9	13.8 ± 0.3	0.008**
BNT	18.7 ± 0.4	19.8 ± 0.1	0.048*
WAIS-DST	11.5 ± 0.7	14.6 ± 0.6	0.002**
Trail Making Test1	65.4 ± 5.3	58.8 ± 4.9	0.354
Trail Making Test2	112.3 ± 14.3	99.9 ± 10.0	0.699
Verbal Fluency Test	15.6 ± 0.8	18.0 ± 0.1	0.099
Activity of Daily Living Scale	14	14	—

*Key: MMSE, Mini-Mental State Examination; MoCA, Montreal Cognitive Assessment; AVLT, Auditory Verbal Learning Test; BNT, Boston Naming Test; WAIS-DST, Wechsler Adult Intelligence Scale Digit Span Test; aMCI, amnestic mild cognitive impairment; MCI, mild cognitive impairment; s.e.m., Standard Error of the Mean. *$p < 0.05$; **$p < 0.01$; ***$p < 0.001$.*

The intra-/inter-coherence in the five different regions and the paired-electrodes coherence (e.g., 22-9, 26-2, 45-108 and so on) over the left and right hemispheres were calculated.

STATISTICAL ANALYSIS

In this study, Wilcoxon rank sum test was conducted at the 5% significance level including the EEG relative power of each brain area, the inter hemispheric coherence along with the intra-/inter-coherence in the five regions and the neuropsychological scores between aMCI and controls.

In order to determine whether rsEEG can be biomarkers to detect aMCI in diabetes, the correlations between the significantly different neuropsychological items and the EEG indexes over significantly different regions in significantly different bands were analyzed in the diabetic aMCI and control groups. Pearson's linear correlation was employed in this study.

RESULTS

NEUROPSYCHOLOGICAL TESTS

The neuropsychological assessment scores of the aMCIs and controls (the p values for the tested items) were shown in **Table 1**. There were significant differences in scores of MoCA, AVLT-Immediate recall, AVLT-Delayed recall, AVLT-Delayed recognition, BNT, WAIS-DST. The scores of MMSE, Trail Making Test, Verbal Fluency Test, and Daily Living Skills Test were lower in aMCI patients than in controls, but these differences were not statistically significant.

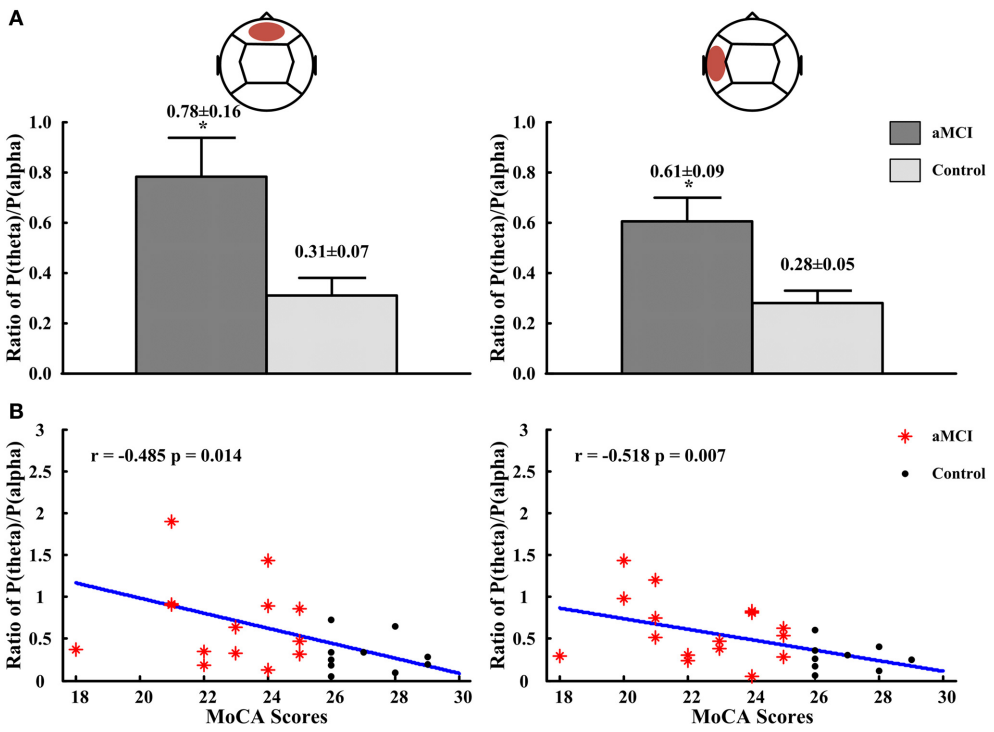

FIGURE 2 | The ratios of P(theta)/P(alpha) in frontal and left temporal regions and the correlations between the ratios of P(theta)/P(alpha) and scores of MMSE and MoCA. (A) The ratios of P(theta)/P(alpha) in frontal region (left panel) and in left temporal region (right panel). **(B)** The correlation between ratios of P(theta)/P(alpha) and scores of MMSE in frontal region (left panel) and in left temporal region (right panel). *$p < 0.05$.

RELATIVE POWER

The relative power for all frequency bands were not significantly different in diabetes between the aMCI and control groups, but the ratios of P(theta)/P(alpha) in the frontal and temporal regions showed statistically significant differences. Compared to the control group, the ratios of P(theta)/P(alpha) in the frontal region (aMCI: 0.78 ± 0.16, control: 0.31 ± 0.07; $p < 0.05$) and the left temporal region (aMCI: 0.61 ± 0.09, control: 0.28 ± 0.05; $p < 0.05$) were significantly higher in the subjects with aMCI (see **Figure 2A**). For the ratios obtained in other regions and at other frequency bands there are no differences between both groups, the significant ratios of relative power obtained were then correlated with those neuropsychological measures in which there were differences between controls and aMCI subjects. **Figure 2B** showed that the ratios of P(theta)/P(alpha) were negatively correlated to the scores of MoCA in the frontal ($r = -0.485$, $p = 0.014$) and left temporal ($r = -0.518$, $p = 0.007$) regions. There were no significant correlations between ratios of relative power and neuropsychological tests.

COHERENCE

In posterior region (intra-region), alpha coherence was lower for subjects with aMCI (0.54 ± 0.02; $p < 0.05$) compared to the controls (0.62 ± 0.02) (see **Figure 3A**). There were no significant differences for coherence at other frequency bands or regions. Then the correlations between significant different intra-region coherence and neuropsychological tests were analyzed. No significant correlation between the alpha coherence and neuropsychological tests was found, including the scores of MoCA ($r = 0.335$, $p = 0.09$) (see **Figure 3B**).

In inter-regions, alpha coherences in fronto-posterior (control: 0.30 ± 0.02, aMCI: 0.24 ± 0.01; $p < 0.01$), right temporo-posterior (aMCI: 0.29 ± 0.01, control: 0.36 ± 0.01; $p < 0.01$) were significantly lower for subjects with aMCI than that with normal cognitive function (**Figure 4A**). No significant differences in inter-regions coherence were found between both groups. The significant different inter-region coherence obtained was then correlated with those neuropsychological measures in which there were differences between controls and aMCI subjects. The alpha coherences in fronto-posterior ($r = 0.496$, $p = 0.009$) and right temporal-posterior ($r = 0.691$, $p = 0.0002$) regions were positively correlated to the scores of MoCA (see **Figure 4B**). There was no significant correlation between alpha coherences and other neuropsychological tests (data not shown).

In inter-hemispheric coherence, aMCI patients showed higher coherence values in delta between LT and RT regions (aMCI: 0.24 ± 0.01, control: 0.20 ± 0.01; $p < 0.05$), and a lower coherence in the theta band in left central-right central (LC-RC) areas (aMCI: 0.66 ± 0.02, control: 0.72 ± 0.02; $p < 0.05$)and in left posterior-right posterior (LP-RP) regions (aMCI: 0.43 ± 0.02, control: 0.54 ± 0.03; $p < 0.05$), than the controls (see **Figure 5A**). There were no significant differences in other inter-hemispheric regions and frequency bands in both groups. The correlation's results between the significant inter-hemispheric coherence and neuropsychological tests which were different in aMCI and controls showed that the delta coherences of left temporal-right temporal (LT-RT) region were negatively correlated to the MoCA scores ($r = -0.474$, $p = 0.019$), and the theta coherences of LC-RC region ($r = 0.441$, $p = 0.024$) and LP-RP region ($r = 0.434$, $p = 0.028$) were positively correlated to the MoCA scores (see **Figure 5B**).

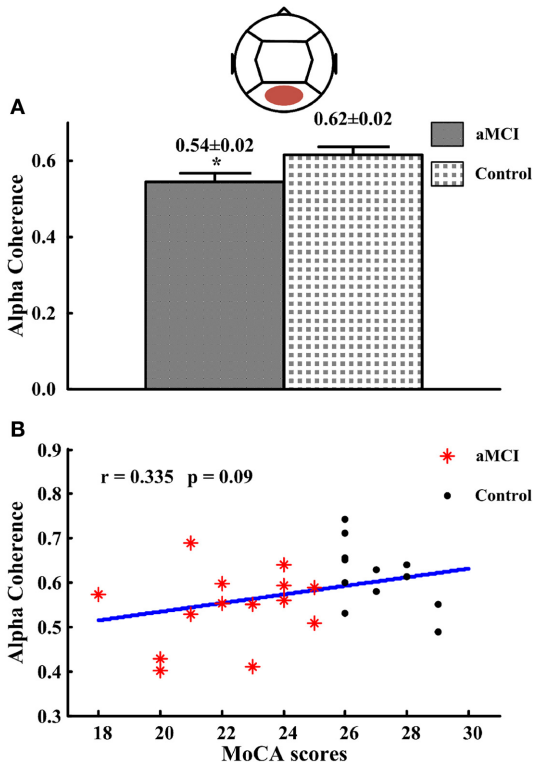

FIGURE 3 | The alpha coherence in posterior region and the correlations between the alpha coherence and the scores of MoCA. **(A)** Alpha coherence in posterior region. **(B)** The correlations between the alpha coherences and the scores of MoCA. *$p < 0.05$.

DISCUSSION

Type 2 diabetes or impairment of glucose metabolism may increase the risk of cognitive impairment and accelerate the progress from MCI to dementia, and it is up to 80% of patients with AD (Ganguli et al., 2004; Busse et al., 2006; Yaffe et al., 2006; Hussain, 2007; Xu et al., 2010; Tuma, 2012; Roberts et al., 2014).

The present study examined whether the ratios of power and the values of coherence of rsEEG data can be used to distinguish aMCI from controls with diabetes. Our findings showed that the ratios of power in theta band vs. power in alpha band [P(theta)/P(alpha)] in the frontal region and left temporal region were significantly higher in aMCI subjects. Besides this, the aMCI group showed lower values of coherence in the alpha band in posterior, fronto-right temporal/fronto-posterior/right temporo-posterior regions and in the theta band in LC-RC and LP-RP regions than the control group. Finally, the aMCI patients exhibited an increase in coherence in delta band in LT-RT regions, compared to the control subjects.

In previous studies, rsEEG absolute power were directly used to evaluate cognitive status of MCI subjects (Luckhaus et al.,

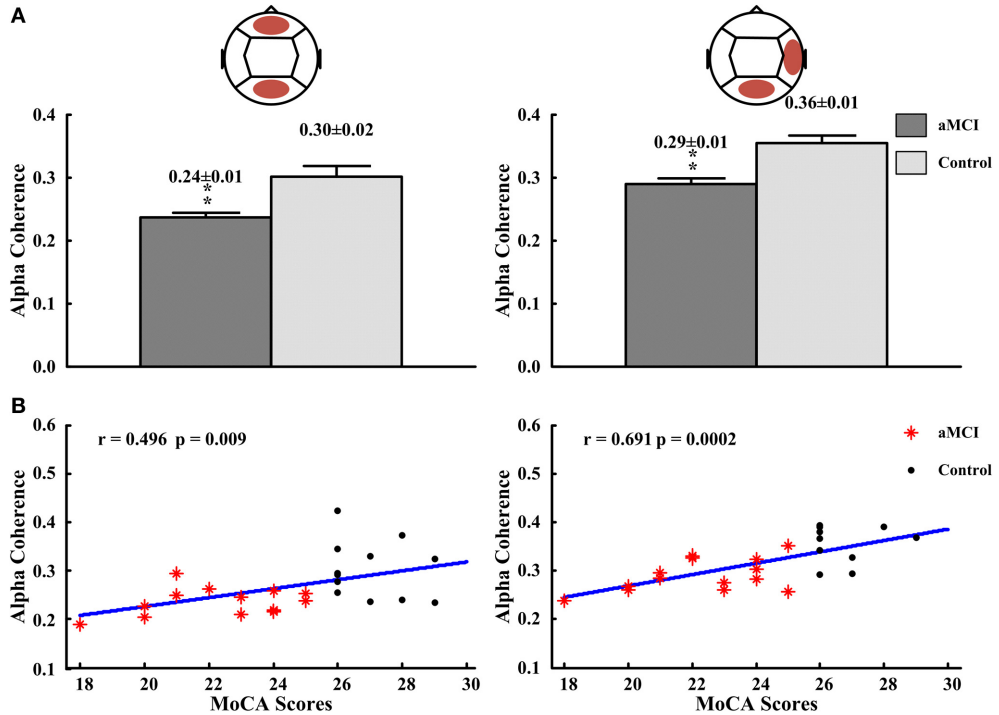

FIGURE 4 | The alpha coherences in fronto-posterior and right temporal-posterior regions and the correlations between the alpha coherences and the scores of MoCA. (A) The alpha coherences in fronto-posterior (left panel) and right temporal-posterior (right panel) regions. **(B)** The correlation between alpha coherences and scores of MoCA in fronto-posterior (left panel) and right temporal-posterior (right panel) regions. $^{**}p < 0.01$.

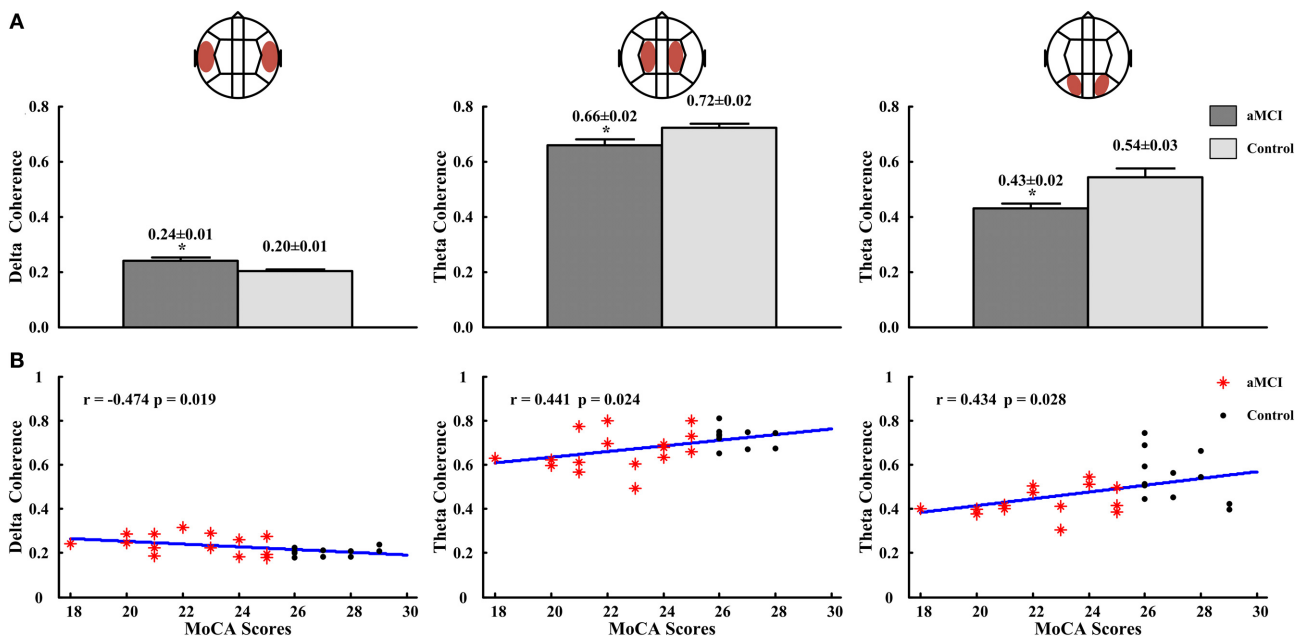

FIGURE 5 | The delta coherences in LT-RT region and theta coherences in LC-RC and LP-RP regions, and the correlations for the delta coherences or (and) theta coherences with the scores of MoCA. (A) The delta coherences in LT-RT region (left panel) and the theta coherences in LC-RC (middle panel) and LP-RP (right panel) regions. **(B)** The correlation between the delta coherences and the scores of MoCA in LT-RT region (left panel), and the correlations between the theta coherences and the scores of MoCA in LC-RC (middle panel) and LP-RP (right panel) regions. $^{*}p < 0.05$.

2008), and specially could reflect neurodegenerative processes in aMCI (Huang et al., 2000; Jelic et al., 2000; Koenig et al., 2005; Babiloni et al., 2006). There were decreased alpha (8–10.5 Hz) power in the parieto-occipital regions (Jelic et al., 1996; Babiloni et al., 2000, 2006; Jelic et al., 2000), significantly increased theta power in the frontal and temporo-parietal regions (Johnson, 2006) and increased delta power widespread over the brain for MCI patients (Babiloni et al., 2006). And the significant correlations between power and neuropsychological assessment scores indicated that aMCI was associated with disruptions in the operation of neuro-cognitive networks (Cummins et al., 2008). Brismar (2007) suggested that the theta rhythm increased in frontal and left central regions, and alpha, beta, and gamma power decreased in temporal region. And it was found that the alpha and beta power was lower in MCI (Rodriguez et al., 2011). The increased slow rhythm power and the reduced fast rhythm power in type 2 diabetic may be associated with cortical damage. However, in this study the absolute power of rsEEG at the different frequency bands was not significantly different between the diabetic aMCI and controls (not shown in the Results section). The possible reason is the rsEEG absolute power was sensitive to non-diabetic's brain performances. The relative power and coherence of rsEEG could be better to indicate aMCI in diabetes.

The relative power of theta and alpha bands was reported as an important predictor for MCI, which correctly classified MCI subjects of 85% (Jelic et al., 2000). However, in this study the relative power for each frequency band was not significantly different between the diabetic aMCI and control groups. Because of the complex structure and richest connections with the hippocampus (Johnson, 2006; Moretti et al., 2007b), the frontal and temporal regions were more sensitive than other regions. Moreover, it has been reported that significant increase in the theta/alpha1 ratio was indicative of cerebrovascular damage (CVD) (Moretti et al., 2007a,b). Our subjects were all diabetic and may be affected by CVD. This may be the reason to support the difference between this study and previous studies. The effects of diabetes on degenerative and CVD may accelerate onset of MCI (Roberts et al., 2014), as insulin-related effects may affect cognitive function (Craft, 2007). Insulin resistance and hyperinsulinemia increased brain intra-neuronal β-amyloid deposition and hyperphosphorylation of tau (Craft, 2005). And the dysregulation of brain insulin signaling may lead to impaired central glucose homeostasis and neurodegeneration. Vascular damage of the brain resulted from diabetes (Craft, 2005; Debette et al., 2011) may contribute to the risk of aMCI (Arvanitakis et al., 2006; Knopman and Roberts, 2010; Roberts et al., 2011). It has been demonstrated that vascular lesions interrupt the cortical cholinergic pathways which may lead to depletion of acetylcholine, resulting in cognitive impairment (Mitrushina et al., 1999). Therefore, this study suggested that the ratios of power at some brain areas can be used as a sensitive index to distinguish aMCI from subjects with normal cognitive function.

Coherence can reflect functional interactions between neural networks (Hogan et al., 2003). In Gomez et al. (2009), it was reported that coherence was lower in all frequency bands in MCI group, and has been used to detect the brain dysfunction thus discriminating MCI patients from controls. In this study, we found that: the alpha coherence decreased in posterior region, fronto-posterior and right temporo-posterior regions; the theta coherence decreased in left and right central and left and right posterior region; and the delta coherence increased in left and right temporal regions in aMCI subjects compared with controls. There are some differences between these findings and the reports in Moretti et al. (2008). The decreased alpha coherence in fronto-posterior and temporo-posterior regions and increased delta in left and right temporal regions have been also reported in previous MCI's studies (Jelic et al., 1996; Jeong, 2004; Babiloni et al., 2008; Moretti et al., 2008). The coherence changes in the alpha and delta bands were associated with aMCI and CVD (Moretti et al., 2008), and authors suggested that the increase of inter-hemispheric coherence in the temporal region was linked to hippocampal atrophy, whereas the decrease of coherence in fronto-parietal regions was linked to subcortical CVD (Moretti et al., 2008). But for other frequency bands, there was regional difference or has no difference between our and their studies (Jeong, 2004; Moretti et al., 2008). In conclusion, this study suggested that the decreased theta, alpha coherence and increased delta coherence in corresponding regions may distinguish aMCI from controls in diabetic.

The results of correlations between scores of MoCA and rsEEG biomarkers indicated that MoCA scores and rsEEG biomarkers among frontal, temporal, and posterior regions are well-correlated. The correlations between other significantly different neuropsychological items and rsEEG biomarkers were not significant. It is worth mentioning that the correlation between the scores of MoCA and alpha coherence was not significant neither. These results suggested that intra-posterior functional connections in alpha band may be relatively preserved in diabetic aMCI. These correlations confirmed the feasibility and value of our studies aimed at detecting aMCI in diabetes by rsEEG biomarkers. And our results evidenced that the sensitivity of MoCA and its utility in diabetic population were better than MMSE (Alagiakrishnan et al., 2013) since this test was usually correlated with the EEG power/coherence.

This study shows the rsEEG may provide efficient methods to monitor the cortical dysfunction associated with the cognitive decline of diabetic patients. The rsEEG measures may be eventually assumed a role in early detecting aMCI or in guiding diagnosis of aMCI in diabetes. Thus, early intervention can be carried out to slow the development pace of aMCI to AD.

However, these results may still be limited, larger prospective studies are necessary to verify the findings in this study.

AUTHOR CONTRIBUTIONS

Zhijie Bian: Acquisition, analysis, interpretation of data for the study and drafting the manuscript. Qiuli Li: Acquisition. Lei Wang: Design of the study and acquisition. Chengbiao Lu: Revising it critically for important intellectual content. Shimin Yin: Design of the study, final approval of the version to be published and agreement to be accountable for all aspects of the study in ensuring that questions related to the accuracy or integrity of any part of the study are appropriately investigated and resolved. Xiaoli Li: Design of the study, revising it critically for important intellectual content, final approval of the version to be published

and agreement to be accountable for all aspects of the study in ensuring that questions related to the accuracy or integrity of any part of the study are appropriately investigated and resolved.

ACKNOWLEDGMENTS

This research was funded in part by National Science Foundation of China (61025019, 31070938, 81230023) and Open project from State Laboratory of Cognitive Neuroscience and Learning, Beijing Normal University.

REFERENCES

Alagiakrishnan, K., Zhao, N., Mereu, L., Senior, P., and Senthilselvan, A. (2013). Montreal Cognitive Assessment is superior to Standardized Mini-Mental Status Exam in detecting mild cognitive impairment in the middle-aged and elderly patients with type 2 diabetes mellitus. *Biomed. Res. Int.* 2013, 186106. doi: 10.1155/2013/186106

Albert, M. S., Dekosky, S. T., Dickson, D., Dubois, B., Feldman, H. H., Fox, N. C., et al. (2011). The diagnosis of mild cognitive impairment due to Alzheimer's disease: recommendations from the National Institute on Aging-Alzheimer's Association workgroups on diagnostic guidelines for Alzheimer's disease. *Alzheimers Dement.* 7, 270–279. doi: 10.1016/j.jalz.2011.03.008

American Diabetes Association. (2013). Diagnosis and classification of diabetes mellitus. *Diabetes Care* 36(Suppl. 1), S67–S74. doi: 10.2337/dc13-S067

Arvanitakis, Z., Schneider, J. A., Wilson, R. S., Li, Y., Arnold, S. E., Wang, Z., et al. (2006). Diabetes is related to cerebral infarction but not to AD pathology in older persons. *Neurology* 67, 1960–1965. doi: 10.1212/01.wnl.0000247053.45483.4e

American Psychiatric Association. (1994). *Diagnostic and Statistical Manual of Mental Disorders, DSM-IV.* 4th Edn. Washington, DC: American Psychiatric Association.

Babiloni, C., Babiloni, F., Carducci, F., Cincotti, F., Del Percio, C., De Pino, G., et al. (2000). Movement-related electroencephalographic reactivity in Alzheimer disease. *Neuroimage* 12, 139–146. doi: 10.1006/nimg.2000.0602

Babiloni, C., Binetti, G., Cassetta, E., Dal Forno, G., Del Percio, C., Ferreri, F., et al. (2006). Sources of cortical rhythms change as a function of cognitive impairment in pathological aging: a multicenter study. *Clin. Neurophysiol.* 117, 252–268. doi: 10.1016/j.clinph.2005.09.019

Babiloni, C., Del Percio, C., Lizio, R., Marzano, N., Infarinato, F., Soricelli, A., et al. (2014). Cortical sources of resting state electroencephalographic alpha rhythms deteriorate across time in subjects with amnesic mild cognitive impairment. *Neurobiol. Aging* 35, 130–142. doi: 10.1016/j.neurobiolaging.2013.06.019

Babiloni, C., Frisoni, G. B., Pievani, M., Toscano, L., Del Percio, C., Geroldi, C., et al. (2008). White-matter vascular lesions correlate with alpha EEG sources in mild cognitive impairment. *Neuropsychologia* 46, 1707–1720. doi: 10.1016/j.neuropsychologia.2008.03.021

Brismar, T. (2007). The human EEG–physiological and clinical studies. *Physiol. Behav.* 92, 141–147. doi: 10.1016/j.physbeh.2007.05.047

Busse, A., Hensel, A., Guhne, U., Angermeyer, M. C., and Riedel-Heller, S. G. (2006). Mild cognitive impairment: long-term course of four clinical subtypes. *Neurology* 67, 2176–2185. doi: 10.1212/01.wnl.0000249117.23318.e1

Carlesimo, G. A., Caltagirone, C., and Gainotti, G. (1996). The Mental Deterioration Battery: normative data, diagnostic reliability and qualitative analyses of cognitive impairment. the group for the standardization of the Mental Deterioration Battery. *Eur. Neurol.* 36, 378–384. doi: 10.1159/000117297

Craft, S. (2005). Insulin resistance syndrome and Alzheimer's disease: age- and obesity-related effects on memory, amyloid, and inflammation. *Neurobiol. Aging* 26(Suppl. 1), 65–69. doi: 10.1016/j.neurobiolaging.2005.08.021

Craft, S. (2007). Insulin resistance and Alzheimer's disease pathogenesis: potential mechanisms and implications for treatment. *Curr. Alzheimer Res.* 4, 147–152. doi: 10.2174/156720507780362137

Cummins, T. D., Broughton, M., and Finnigan, S. (2008). Theta oscillations are affected by amnestic mild cognitive impairment and cognitive load. *Int. J. Psychophysiol.* 70, 75–81. doi: 10.1016/j.ijpsycho.2008.06.002

Dauwels, J., Srinivasan, K., Ramasubba Reddy, M., Musha, T., Vialatte, F. B., Latchoumane, C., et al. (2011). Slowing and loss of complexity in Alzheimer's EEG: two sides of the same coin? *Int. J. Alzheimers Dis.* 2011, 1–10. doi: 10.4061/2011/539621

Debette, S., Seshadri, S., Beiser, A., Au, R., Himali, J. J., Palumbo, C., et al. (2011). Midlife vascular risk factor exposure accelerates structural brain aging and cognitive decline. *Neurology* 77, 461–468. doi: 10.1212/WNL.0b013e318227b227

Folstein, M. F., Folstein, S. E., and McHugh, P. R. (1975). "Mini-mental state." A practical method for grading the cognitive state of patients for the clinician. *J. Psychiatr. Res.* 12, 189–198. doi: 10.1016/0022-3956(75)90026-6

Ganguli, M., Dodge, H. H., Shen, C., and Dekosky, S. T. (2004). Mild cognitive impairment, amnestic type: an epidemiologic study. *Neurology* 63, 115–121. doi: 10.1212/01.WNL.0000132523.27540.81

Gispen, W. H., and Biessels, G. J. (2000). Cognition and synaptic plasticity in diabetes mellitus. *Trends Neurosci.* 23, 542–549. doi: 10.1016/S0166-2236(00)01656-8

Gomez, C., Stam, C. J., Hornero, R., Fernandez, A., and Maestu, F. (2009). Disturbed beta band functional connectivity in patients with mild cognitive impairment: an MEG study. *IEEE Trans. Biomed. Eng.* 56, 1683–1690. doi: 10.1109/TBME.2009.2018454

Hogan, M. J., Swanwick, G. R., Kaiser, J., Rowan, M., and Lawlor, B. (2003). Memory-related EEG power and coherence reductions in mild Alzheimer's disease. *Int. J. Psychophysiol.* 49, 147–163. doi: 10.1016/S0167-8760(03)00118-1

Huang, C., Wahlund, L. O., Dierks, T., Julin, P., Winblad, B., and Jelic, V. (2000). Discrimination of Alzheimer's disease and mild cognitive impairment by equivalent EEG sources: a cross-sectional and longitudinal study. *Clin. Neurophysiol.* 111, 1961–1967. doi: 10.1016/S1388-2457(00)00454-5

Hussain, H. (2007). Conversion from subtypes of mild cognitive impairment to Alzheimer dementia. *Neurology* 69, 409. doi: 10.1212/01.wnl.0000278072.42014.6d

Jelic, V., Johansson, S. E., Almkvist, O., Shigeta, M., Julin, P., Nordberg, A., et al. (2000). Quantitative electroencephalography in mild cognitive impairment: longitudinal changes and possible prediction of Alzheimer's disease. *Neurobiol. Aging* 21, 533–540. doi: 10.1016/S0197-4580(00)00153-6

Jelic, V., Shigeta, M., Julin, P., Almkvist, O., Winblad, B., and Wahlund, L. O. (1996). Quantitative electroencephalography power and coherence in Alzheimer's disease and mild cognitive impairment. *Dementia* 7, 314–323.

Jeong, J. (2004). EEG dynamics in patients with Alzheimer's disease. *Clin. Neurophysiol.* 115, 1490–1505. doi: 10.1016/j.clinph.2004.01.001

Jia, J. (2010). *Chinese Dementia and Cognitive Disorders Treatment Guidelines.* Beijing: People's Medical Publishing House.

Johnson, J. D. (2006). The conversational brain: fronto-hippocampal interaction and disconnection. *Med. Hypotheses* 67, 759–764. doi: 10.1016/j.mehy.2006.04.031

Knopman, D. S., and Roberts, R. (2010). Vascular risk factors: imaging and neuropathologic correlates. *J. Alzheimers Dis.* 20, 699–709. doi: 10.3233/JAD-2010-091555.

Koenig, T., Prichep, L., Dierks, T., Hubl, D., Wahlund, L. O., John, E. R., et al. (2005). Decreased EEG synchronization in Alzheimer's disease and mild cognitive impairment. *Neurobiol. Aging* 26, 165–171. doi: 10.1016/j.neurobiolaging.2004.03.008

Kumar, V., Nelson, F., Abbas, A. K., Cotran, R. S., and Robbins, S. L. (2005). *Robbins and Cotran Pathologic Basis of Disease, 7th Edn*. Philadelphia, PA: Saunders.

Lawton, M. P., and Brody, E. M. (1969). Assessment of older people: self-maintaining and instrumental activities of daily living. *Gerontologist* 9, 179–186. doi: 10.1093/geront/9.3_Part_1.179

Levey, A., Lah, J., Goldstein, F., Steenland, K., and Bliwise, D. (2006). Mild cognitive impairment: an opportunity to identify patients at high risk for progression to Alzheimer's disease. *Clin. Ther.* 28, 991–1001. doi: 10.1016/j.clinthera.2006.07.006

Luckhaus, C., Grass-Kapanke, B., Blaeser, I., Ihl, R., Supprian, T., Winterer, G., et al. (2008). Quantitative EEG in progressing vs stable mild cognitive impairment (MCI): results of a 1-year follow-up study. *Int. J. Geriatr. Psychiatry* 23, 1148–1155. doi: 10.1002/gps.2042

Miles, W. R., and Root, H. F. (1922). Psychologic tests applied to diabetic patients. *Arch. Intern. Med.* 30, 767–777. doi: 10.1001/archinte.1922.00110120086003

Mitrushina, M. N., Boone, K. L., and D'Elia, L. (1999). *Handbook of Normative Data for Neuropsychological Assessment*. New York, NY: Oxford University Press.

Moretti, D. V., Frisoni, G. B., Pievani, M., Rosini, S., Geroldi, C., Binetti, G., et al. (2008). Cerebrovascular disease and hippocampal atrophy are differently linked to functional coupling of brain areas: an EEG coherence study in MCI subjects. *J. Alzheimers Dis.* 14, 285–299.

Moretti, D. V., Miniussi, C., Frisoni, G., Zanetti, O., Binetti, G., Geroldi, C., et al. (2007a). Vascular damage and EEG markers in subjects with mild cognitive impairment. *Clin. Neurophysiol.* 118, 1866–1876. doi: 10.1016/j.clinph.2007.05.009

Moretti, D. V., Miniussi, C., Frisoni, G. B., Geroldi, C., Zanetti, O., Binetti, G., et al. (2007b). Hippocampal atrophy and EEG markers in subjects with mild cognitive impairment. *Clin. Neurophysiol.* 118, 2716–2729. doi: 10.1016/j.clinph.2007.09.059

Morris, J. C. (2005). Mild cognitive impairment and preclinical Alzheimer's disease. *Geriatrics* Suppl. 9–14.

Nasreddine, Z. S., Phillips, N. A., Bedirian, V., Charbonneau, S., Whitehead, V., Collin, I., et al. (2005). The Montreal Cognitive Assessment, MoCA: a brief screening tool for mild cognitive impairment. *J. Am. Geriatr. Soc.* 53, 695–699. doi: 10.1111/j.1532-5415.2005.53221.x

Novelli, G. (1986). Three clinical tests for the assessment of lexical retrieval and production norms from 320 normal subjects. *Arch. Psicol. Neurol. Psichiatr.* 47, 477–506.

Orsini, A., Grossi, D., Capitani, E., Laiacona, M., Papagno, C., and Vallar, G. (1987). Verbal and spatial immediate memory span: normative data from 1355 adults and 1112 children. *Ital. J. Neurol. Sci.* 8, 539–548. doi: 10.1007/BF02333660

Peila, R., Rodriguez, B. L., and Launer, L. J. (2002). Type 2 diabetes, APOE gene, and the risk for dementia and related pathologies: the Honolulu-Asia Aging Study. *Diabetes* 51, 1256–1262. doi: 10.2337/diabetes.51.4.1256

Petersen, R. C. (2004). Mild cognitive impairment as a diagnostic entity. *J. Intern. Med.* 256, 183–194. doi: 10.1111/j.1365-2796.2004.01388.x

Reitan, R. M. (1958). Validity of the trail making test as an indicator of organic brain damage. *Percept. Mot. Skills* 8, 271–276. doi: 10.2466/PMS.8.7.271-276

Roberts, R. O., Kantarci, K., Geda, Y. E., Knopman, D. S., Przybelski, S. A., Weigand, S. D., et al. (2011). Untreated type 2 diabetes and its complications are associated with subcortical infarctions. *Diabetes Care* 34, 184–186. doi: 10.2337/dc10-0602

Roberts, R. O., Knopman, D. S., Geda, Y. E., Cha, R. H., Pankratz, V. S., Baertlein, L., et al. (2014). Association of diabetes with amnestic and nonamnestic mild cognitive impairment. *Alzheimers Dement.* 10, 18–26. doi: 10.1016/j.jalz.2013.01.001

Rodriguez, G., Arnaldi, D., and Picco, A. (2011). Brain functional network in Alzheimer's disease: diagnostic markers for diagnosis and monitoring. *Int. J. Alzheimers Dis.* 2011, 481903. doi: 10.4061/2011/481903

Roh, J. H., Park, M. H., Ko, D., Park, K. W., Lee, D. H., Han, C., et al. (2011). Region and frequency specific changes of spectral power in Alzheimer's disease and mild cognitive impairment. *Clin. Neurophysiol.* 122, 2169–2176. doi: 10.1016/j.clinph.2011.03.023

Rossini, P. M., Rossi, S., Babiloni, C., and Polich, J. (2007). Clinical neurophysiology of aging brain: from normal aging to neurodegeneration. *Prog. Neurobiol.* 83, 375–400. doi: 10.1016/j.pneurobio.2007.07.010

Sankari, Z., Adeli, H., and Adeli, A. (2011). Intrahemispheric, interhemispheric, and distal EEG coherence in Alzheimer's disease. *Clin. Neurophysiol.* 122, 897–906. doi: 10.1016/j.clinph.2010.09.008

Schmidt, M., Kanda, P., Basile, L., da Silva Lopes, H. F., Baratho, R., Demario, J., et al. (2013). Index of alpha/theta ratio of the electroencephalogram: a new marker for Alzheimer's disease. *Front. Aging Neurosci.* 5:60. doi: 10.3389/fnagi.2013.00060

Seem, J. E. (2007). Using intelligent data analysis to detect abnormal energy consumption in buildings. *Energy Build.* 39, 52–58. doi: 10.1016/j.enbuild.2006.03.033

Seo, S. W., Lee, J. H., Jang, S. M., Kim, S. T., Chin, J., Kim, G. H., et al. (2012). Neurochemical alterations of the entorhinal cortex in amnestic mild cognitive impairment (aMCI): a three-year follow-up study. *Arch. Gerontol. Geriatr.* 54, 192–196. doi: 10.1016/j.archger.2011.04.002

Shimada, H., Miki, T., Tamura, A., Ataka, S., Emoto, M., and Nishizawa, Y. (2010). Neuropsychological status of elderly patients with diabetes mellitus. *Diabetes Res. Clin. Pract.* 87, 224–227. doi: 10.1016/j.diabres.2009.09.026

Steriade, M. (2006). Grouping of brain rhythms in corticothalamic systems. *Neuroscience* 137, 1087–1106. doi: 10.1016/j.neuroscience.2005.10.029

Stevens, A., Kircher, T., Nickola, M., Bartels, M., Rosellen, N., and Wormstall, H. (2001). Dynamic regulation of EEG power and coherence is lost early and globally in probable DAT. *Eur. Arch. Psychiatry Clin. Neurosci.* 251, 199–204. doi: 10.1007/s004060170027

Strachan, M. W., Reynolds, R. M., Marioni, R. E., and Price, J. F. (2011). Cognitive function, dementia and type 2 diabetes mellitus in the elderly. *Nat. Rev. Endocrinol.* 7, 108–114. doi: 10.1038/nrendo.2010.228

Strijers, R. L., Scheltens, P., Jonkman, E. J., de Rijke, W., Hooijer, C., and Jonker, C. (1997). Diagnosing Alzheimer's disease in community-dwelling elderly: a comparison of EEG and MRI. *Dement. Geriatr. Cogn. Disord.* 8, 198–202. doi: 10.1159/000106631

Takahashi, R., Ishii, K., Senda, M., Ito, K., Ishii, K., Kato, T., et al. (2013). Equal sensitivity of early and late scans after injection of FDG for the detection of Alzheimer pattern: an analysis of 3D PET data from J-ADNI, a multi-center study. *Ann. Nucl. Med.* 27, 452–459. doi: 10.1007/s12149-013-0704-x

Toussaint, P. J., Perlbarg, V., Bellec, P., Desarnaud, S., Lacomblez, L., Doyon, J., et al. (2012). Resting state FDG-PET functional connectivity as an early biomarker of Alzheimer's disease using conjoint univariate and independent component analyses. *Neuroimage* 63, 936–946. doi: 10.1016/j.neuroimage.2012.03.091

Tuma, I. (2012). Diabetes mellitus and dementia. *Vnitr. Lek.* 58, 305–308.

Welch, P. D. (1967). The use of fast Fourier transform for the estimation of power spectra: a method based on time averaging over short, modified periodograms. *IEEE Trans. Audio Electroacoustics* 15, 70–73. doi: 10.1109/TAU.1967.1161901

Xu, W., Caracciolo, B., Wang, H. X., Winblad, B., Backman, L., Qiu, C., et al. (2010). Accelerated progression from mild cognitive impairment to dementia in people with diabetes. *Diabetes* 59, 2928–2935. doi: 10.2337/db10-0539

Yaffe, K., Petersen, R. C., Lindquist, K., Kramer, J., and Miller, B. (2006). Subtype of mild cognitive impairment and progression to dementia and death. *Dement. Geriatr. Cogn. Disord.* 22, 312–319. doi: 10.1159/000095427

Conflict of Interest Statement: The authors declare that the research was conducted in the absence of any commercial or financial relationships that could be construed as a potential conflict of interest.

Received: 10 November 2013; accepted: 19 January 2014; published online: 04 February 2014.

*Citation: Bian Z, Li Q, Wang L, Lu C, Yin S and Li X (2014) Relative power and coherence of EEG series are related to amnestic mild cognitive impairment in diabetes. Front. Aging Neurosci. **6**:11. doi: 10.3389/fnagi.2014.00011*

This article was submitted to the journal Frontiers in Aging Neuroscience.

Copyright © 2014 Bian, Li, Wang, Lu, Yin and Li. This is an open-access article distributed under the terms of the Creative Commons Attribution License (CC BY). The use, distribution or reproduction in other forums is permitted, provided the original author(s) or licensor are credited and that the original publication in this journal is cited, in accordance with accepted academic practice. No use, distribution or reproduction is permitted which does not comply with these terms.

frontiers in
AGING NEUROSCIENCE

ORIGINAL RESEARCH ARTICLE
published: 03 October 2013
doi: 10.3389/fnagi.2013.00058

Integrative EEG biomarkers predict progression to Alzheimer's disease at the MCI stage

Simon-Shlomo Poil[1], Willem de Haan[2,3], Wiesje M. van der Flier[3,4], Huibert D. Mansvelder[1], Philip Scheltens[3] and Klaus Linkenkaer-Hansen[1]*

[1] Department of Integrative Neurophysiology, Center for Neurogenomics and Cognitive Research, VU University Amsterdam, Amsterdam, Netherlands
[2] Department of Clinical Neurophysiology and MEG, VU University Medical Center, Amsterdam, Netherlands
[3] Department of Neurology, Alzheimer Center, VU University Medical Center, Amsterdam, Netherlands
[4] Department of Epidemiology and Biostatistics, VU University Medical Center, Amsterdam, Netherlands

Edited by:
Davide V. Moretti, S. John of God National Institute of Research and Cure for Mental Disorders and Dementia, Italy

Reviewed by:
Xuemin Xu, The University of Tennessee, USA
Shin Murakami, Touro University-California, USA

***Correspondence:**
Klaus Linkenkaer-Hansen, Department of Integrative Neurophysiology, Center for Neurogenomics and Cognitive Research, VU University Amsterdam, De Boelelaan 1085, 1081 HV Amsterdam, Netherlands
e-mail: klaus.linkenkaer@cncr.vu.nl

Alzheimer's disease (AD) is a devastating disorder of increasing prevalence in modern society. Mild cognitive impairment (MCI) is considered a transitional stage between normal aging and AD; however, not all subjects with MCI progress to AD. Prediction of conversion to AD at an early stage would enable an earlier, and potentially more effective, treatment of AD. Electroencephalography (EEG) biomarkers would provide a non-invasive and relatively cheap screening tool to predict conversion to AD; however, traditional EEG biomarkers have not been considered accurate enough to be useful in clinical practice. Here, we aim to combine the information from multiple EEG biomarkers into a diagnostic classification index in order to improve the accuracy of predicting conversion from MCI to AD within a 2-year period. We followed 86 patients initially diagnosed with MCI for 2 years during which 25 patients converted to AD. We show that multiple EEG biomarkers mainly related to activity in the beta-frequency range (13–30 Hz) can predict conversion from MCI to AD. Importantly, by integrating six EEG biomarkers into a diagnostic index using logistic regression the prediction improved compared with the classification using the individual biomarkers, with a sensitivity of 88% and specificity of 82%, compared with a sensitivity of 64% and specificity of 62% of the best individual biomarker in this index. In order to identify this diagnostic index we developed a data mining approach implemented in the Neurophysiological Biomarker Toolbox (http://www.nbtwiki.net/). We suggest that this approach can be used to identify optimal combinations of biomarkers (integrative biomarkers) also in other modalities. Potentially, these integrative biomarkers could be more sensitive to disease progression and response to therapeutic intervention.

Keywords: Neurophysiological Biomarkers, Alzheimer's disease, mild cognitive impairment (MCI), electroencephalography, predictive analysis, time series analysis, eyes closed resting state

INTRODUCTION

Caused by an increasing average age of the population in the developed world, dementia is becoming a major healthcare problem. Alzheimer's disease is the most common form of dementia and the golden standard for diagnosis is the post-mortem identification of Amyloid Beta 42 depositions and tangles (Blennow et al., 2006; Herrup, 2010). It has been suggested that Alzheimer's disease begins years, maybe even decades before actual cognitive symptoms appear (Sperling et al., 2011). However, normal ageing is also characterized by a slow decline of cognitive functions, which means it can be difficult to disentangle normal ageing from Alzheimer at a very early stage.

Patients with mild cognitive impairment (MCI) are at high risk of developing Alzheimer's disease. The label MCI is given when there is a cognitive complaint (mostly memory), which can also be demonstrated on formal testing, while general cognitive functioning is relatively intact and a patient is still living independently (Flicker et al., 1991; Gauthier et al., 2006; Albert et al., 2011). Therapies that stop the conversion to Alzheimer's disease unfortunately remain to be developed, but it is likely that these drugs or therapies will appear in the future (Prins et al., 2010; Huang and Mucke, 2012). It is plausible that these therapies will be most effective before major brain damage has occurred and it is, therefore, important to develop biomarkers sensitive of this very early stage (Sperling et al., 2011). Early-stage identification may also help the development of new treatments that are more effective at this stage as it can facilitate monitoring of the response to the intervention.

We here focus on biomarkers obtained from electroencephalography (EEG) recordings in the eyes-closed resting state (ECR). EEG biomarkers are optimal for screening purposes because the EEG recording can be obtained using relative cheap and non-invasive equipment, which is widely available and fast to use. Several previous EEG studies of conversion from mild cognitive impairment to Alzheimer's disease have been conducted (Jelic et al., 1996, 2000; Huang et al., 2000; Stam et al., 2003; Schoonenboom et al., 2004; Rombouts et al., 2005; Babiloni et al., 2006, 2011; Kwak, 2006; Rossini et al., 2006, 2008; Lehmann et al., 2007; Moretti et al., 2007a,b, 2008, 2011; Luckhaus et al., 2008) mainly using biomarkers such as spectral measures and

synchronization between brain regions. Machine-learning techniques have been used to explore differences between MCI and AD with varying success (Huang et al., 2000; Bennys et al., 2001; Prichep et al., 2006; Buscema et al., 2007; Lehmann et al., 2007; Prichep, 2007; Rossini et al., 2008), however, only few studies have tried to predict the conversion from MCI to AD (Prichep et al., 2006; Prichep, 2007; Antila et al., 2013). Many studies typically focus on a small number of biomarkers (on the order of 15 marker values), and some do not have adequate validation of their results on independent groups. We perform large-scale data mining of multiple biomarkers (**Figure 1A**) and validate our results on an independent group of subjects.

Our focus is on the EEG measured as part of the initial hospital intake test, combined with longitudinal recordings measured 1 year after the initial intake test. We have mapped several classical EEG biomarkers, such as frequency and power, but also non-classical biomarkers such as detrended fluctuation analysis and oscillation burst analysis (Poil et al., 2008; Montez et al., 2009). By combining several biomarkers, it is often possible to find better separation boundaries between two groups (**Figure 1C**), because each biomarker gives additional information (Lehmann et al., 2007). In this longitudinal study we show that EEG biomarkers from the initial hospital in-take test retrospectively can be used in a classifier algorithm to predict the diagnosis that the patient obtained within the subsequent 2 years.

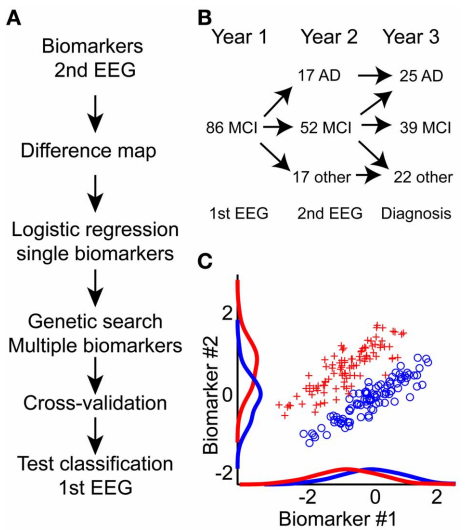

FIGURE 1 | An integrative approach toward improved prediction of mild cognitive impairment to Alzheimer's disease conversion. (A) Diagram of processing flow. We calculate biomarkers on the second year EEG recording; hereafter we mapped all potential differences between MCI and AD using Student's *t*-test (Difference map). Next, we performed logistic regression on each single biomarker. Biomarkers with best single-classification power were seeded to a genetic search algorithm; this algorithm further optimized the combined biomarker set. This biomarker set was then used to predict MCI to AD conversion based on the first-year EEG recording. To evaluate the lower bound on the classification, half-split cross-validation was performed. Finally, the outcome performance was evaluated on the 1st EEG recording. **(B)** Overview of how the MCI patient cohort splits into AD, another diagnosis, or remain MCI one or 2 years after the in-take. **(C)** The integration of multiple biomarkers can reveal hidden separation boundaries. Here, we show two simulated biomarkers where the red and blue groups are overlapping if we only consider the single biomarkers. By combining the biomarkers, we see a clear separation boundary at the diagonal. Classification algorithms aim to identify this boundary, and use it to predict group association for new data.

METHODS AND MATERIALS

SUBJECTS

The study involved 86 mild cognitive impairment (MCI) subjects who were referred to the Alzheimer Center at the VU University Medical Center in Amsterdam, the Netherlands (**Figure 1B**). Upon the first visit at the Alzheimer Center, all subjects underwent a thorough 1-day examination consisting of history taking, physical, and neurological assessment, neuropsychological testing including the Mini Mental State Examination (MMSE) (Folstein et al., 1975), laboratory tests, structural magnetic resonance imaging (MRI), and a routine electroencephalogram (EEG). After reviewing the clinical and ancillary imaging data, a multidisciplinary team established a consensus-based final diagnosis for each patient. The initial diagnosis of MCI was based on the criteria set by (Petersen et al., 1999), consisting of (a) objective memory impairment as seen during neuropsychological evaluation, defined by performances ≥ 1.5 standard deviation below the mean value of education—and that of age matched controls, (b) normal activities of daily living, and (c) a rating score of 0.5 in clinical dementia (Hughes et al., 1982).

All MCI subjects were followed up clinically during an average period of 709 $\pm$ [537:779] days (1.9 years) (median $\pm$ 95% confidence interval). The clinical follow up included medical history and functional status assessment re-examination in order to measure potential changes in the cognitive domain. MCI subjects who showed steady or enhanced cognitive functioning (but still fulfilled the criteria for MCI) during re-assessment were considered as MCI-stable, while MCI subjects who showed impoverished cognitive functioning, and fulfilled the NINDS-ADRDA criteria (McKhann et al., 1984) to be diagnosed with Alzheimer's disease, were considered to belong to the AD-converter group. Exclusion criteria were previous head trauma, history of neurological or psychiatric disease or use of psychotropic medications. Patients progressing from MCI to other disorders than Alzheimer's disease ($n = 22$) were excluded from the analyses reported here. These patients progressed to; "Subjective complaints" ($n = 9$), possible Alzheimer's disease ($n = 1$), frontal lobe dementia ($n = 1$), vascular dementia ($n = 3$), Lewy body dementia ($n = 1$), dementia other ($n = 2$), psychiatric ($n = 2$), or another neurological disorder ($n = 3$). The measurements were approved by the Ethics Committee of the VU University Medical Center, and were in accordance to the Helsinki declaration. All subjects signed an informed consent.

EEG RECORDINGS

Twenty-one channel EEGs were recorded in a sound attenuated, electrically shielded, and dimly lit room. These recordings were performed with OSG digital equipment (Brainlab®) at the following locations of the international 10–20 system: Fp2, Fp1, FT9, FT10, F8, F7, F4, F3, A2, A1, T4, T3, C4, C3, T6, T5, P4, P3, O2, O1, Fz, Cz, and Pz. The recording was referenced to the common

average of all electrodes, excluding Fp1 and Fp2. Sampling frequency was 500 Hz and analogue-digital precision was 16 bit. The impedance of all electrodes was less than 5 kΩ. Recordings were made with a 70 Hz low-pass filter (time constant 1 s). Subjects sat in a reclined chair for approximately 20 min. During this period the subjects kept their eyes closed most of the time, however, at irregular intervals, they were asked to open their eyes when drowsiness was noticed. Approximately 15 min into the recording a memory task, which consisted of remembering pictogram images for 1 min was performed.

EEG CLEANING

The recordings during task and eyes-open were not analyzed. The EEG was viewed in windows of 5 s, and sharp transient artifacts were cut out. On average 17.8 [range (12.4:24.1)] minutes of eyes-closed rest EEG was left. The JADE ICA algorithm was then used to separate the signal into 23 components (Cardoso and Souloumiac, 1993). Eye movements, eye blinks, muscle artifacts, and heartbeat components were rejected, based on abnormal topography, component activation, activity distribution, and spectrum.

BIOMARKERS AND PROCESSING FLOW

The Neurophysiological Biomarker Toolbox (NBT) (http://www.nbtwiki.net/) was used to organize, analyse, and calculate all biomarkers in this study (Hardstone et al., 2012). An EEG biomarker is a quantitative measure derived from the EEG, e.g., the dominant frequency of the beta frequency band (13–30 Hz), to be used as a diagnostic or prognostic predictor of disease (**Figure 2**).

We extracted 177 biomarkers from each EEG trace. We decided to focus on biomarkers we have had good experiences with in other studies, and acknowledge that many more biomarkers could have been selected.

Based on the broadband signal, we computed 28 biomarkers, namely: Hjorth's activity, mobility and complexity parameters (Hjorth, 1970); Time domain Parameters (Goncharova and Barlow, 1990), Wackermann's global field strength, global frequency, and spatial complexity (Wackermann, 1999), Barlow's amplitude, frequency and spectral purity (Goncharova and Barlow, 1990). Alpha peak frequency, peak width, power corrected for 1/f baseline (Poil et al., 2011), when applicable the same parameters where found for double alpha peaks. Alpha-theta transition point (Klimesch, 1999), Beta peak frequency (**Figure 2**), width, power corrected for 1/f baseline (Van Aerde et al., 2009), same for second beta peak if present; Frequency stability was evaluated using different methods, by the standard deviation and interquartile range of the central frequency and maximum wavelet frequency calculated in windows, and by, the distribution parameters of the phase values above zero, and of the number of oscillation cycle peaks per window.

For each of the classical frequency bands—delta (1–3 Hz), theta (4–7 Hz), alpha (8–13 Hz), beta (13–30 Hz), and gamma (30–45 Hz)—we computed 13 biomarkers; namely: The amplitude envelope was extracted using Hilbert transform and characterized extensively. We calculated the spearman correlations of amplitude envelopes in different channels. The distribution

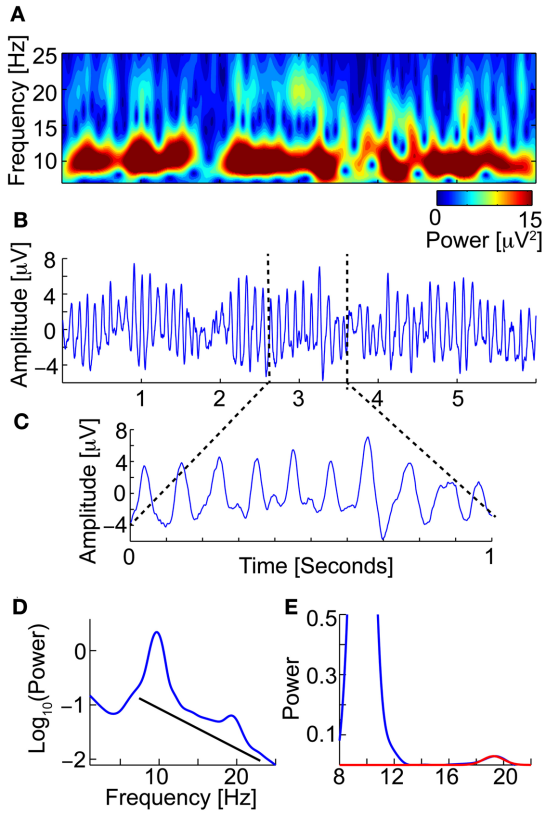

FIGURE 2 | An EEG biomarker is a quantitative measure derived from the EEG. For example the Beta peak frequency. **(A)** Time-frequency (TF-plot) plot of 6 s of an eyes-closed rest EEG signal (from Pz) (Wavelet). The color shows the power. Low-amplitude bursts in the beta-frequency band (13–30 Hz) not directly coupled with the strong alpha are observed. **(B)** The raw EEG signal used to calculate the TF-plot in **(A)**. Clear and strong alpha (8–13 Hz) oscillations are observed. **(C)** Zooming in, we observe small peaks in the space between the strong alpha oscillation peaks, which correspond to the beta oscillations. **(D)** The power spectrum of the full-length EEG signal reveals a beta peak (left). To find the beta peak we first fit a 1/f baseline (right), next we fit a Gaussian to the small beta peak. We now have four biomarkers; Beta peak frequency, Beta peak width, Beta peak corrected power (i.e., minus 1/f baseline), and peak uncorrected power.

of amplitude values was characterized by kurtosis, skewness, interquartile range, median, range, and variance. Furthermore, detrended fluctuation analysis characterizing long-range temporal correlations (Linkenkaer-Hansen et al., 2001; Hardstone et al., 2012; Poil et al., 2012), multifractality spectral width (Kantelhardt et al., 2002; Ihlen, 2012) and oscillation bursts 95th percentile durations and sizes (Montez et al., 2009; Poil et al., 2011) were calculated on the amplitude envelope. The instantaneous phase was also extracted using Hilbert transform, and the 95th percentile duration and size of the stable phase bursts (a phase bursts is defined as the period between phase slips) were calculated. In addition, we computed for all frequency bands and individualized frequency bands, defined as Alpha1 (APF = individually defined Alpha peak frequency): (APF–4 to APF–2) Hz, Alpha2: (APF–2 to APF) Hz, Alpha3: (APF to APF+2) Hz;

Beta: (APF+2 to 30) Hz (Klimesch, 1999), 7 biomarkers: absolute, relative power, and power ratios, furthermore, the central frequency, power in central frequency, bandwidth and spectral edge (Vural and Yildiz, 2010; O'Gorman et al., 2013). In total, we extracted 177 biomarker values from each EEG trace (**Table 1**).

Next, we performed data mining on these biomarkers based on the second EEG recording (**Figure 1A**), to identify biomarkers that reached a significance level of $p < 0.05$ (student's t-test) for the comparison of stable MCI vs. AD-converters (based on the diagnosis after 2 years). We here use student's t-test because this test has best statistical power in most cases under the assumption of normal distributed biomarker values. The biomarkers were tested per channel, and a binomial multiple-comparison correction was performed (Poil et al., 2011). The binomial multiple-comparison correction tests whether a significant number of channels are found (i.e., 3 or more channels, $p < 0.05$). The performance of two different classification algorithms (see below for details) in integrating significant biomarkers into a diagnostic index was then tested using their median values across significant channels.

DEVELOPMENT OF A DIAGNOSTICS INDEX

To move beyond single-biomarker classification we aimed to integrate several EEG biomarkers in a diagnostic index that would classify the AD-converter group from the MCI-stable group better than each individual biomarker. Using one dataset for development and testing is not recommended, because it is theoretically possible to find a perfect separation of two groups if enough biomarkers are included (so-called over-fitting). To counteract this issue we build our classification model based on the second EEG recording (which was obtained in 34 out of a total of 64 subjects that were either MCI-stable or AD-converters), and tested the classification accuracy retrospectively on the first EEG recording. Thirty subjects were not included in the training (22 MCI-stable, 8 AD-converters), because these subjects did not have any second-year recording. These subjects serve as our ultimate classification test. We also used half-split cross-validation to evaluate the stability and lower bound of the solution (see below).

STATISTICS: LOGISTIC REGRESSION WITH GENETIC SEARCH

Binary classification was performed using logistic regression. In logistics regression the binary outcome either AD-converter (1) or MCI-stable (0) is regressed with a linear combination of biomarkers. More specifically we fit a function $f(z)$ using maximum likelihood.

$$f(z) = \frac{1}{1 + e^{-z}}$$

with

$$z = \beta_0 + \sum_{i=1}^{k} \beta_i x_i, \quad (1)$$

and x are the k biomarkers included in the regression (included as medians across significant channels), and β_i are the regression coefficients. The function f represents the probability of Alzheimer's disease. We use the 50% probability as our classification threshold, i.e., if $f \geq 0.5$, the patient belong to the AD-converter group, otherwise the patient belongs to the MCI-stable group. We used a genetic search method to identify biomarkers that combined (using logistic regression) would give the best classification of the outcome MCI-stable vs. AD-converters. Genetic search is considered an efficient method for searching large data sets, instead of the computationally demanding alternative of testing all possible combinations (Koza and Poli, 2005; Zviling et al., 2005). The genetic approach is based around an evolutionary idea where the combined set of biomarkers is "mutated" by different mutation rules; addition of a random biomarker, removal of a biomarker, random selection of a new set of four biomarkers, and random substitution of a biomarker. Each rule was applied 5 times in each generation, leading to 20 new sets of biomarkers. The classifications of these new sets were then compared with the previous optimal set. Only the best biomarker set survived and was used as the base for next generation of mutations. We did not set limits on the maximum or minimum number of biomarkers in each set.

The genetic algorithm was seeded with an initial set of five biomarkers with the highest Matthew correlation coefficient (see outcome evaluation below). The genetic algorithm ran for 100

Table 1 | Thirty-five biomarkers from different signal processing domains were extracted.

Spatial biomarkers	Temporal biomarkers	Spectral biomarkers
Spearman correlations of the amplitude envelope across channels	Detrended fluctuation analysis	Absolute and relative power
	Multifractal spectral width	Central frequency
	Oscillation bursts duration and size	Power in central frequency
	Stable phase bursts duration and size	Bandwidth and spectral edge
	Frequency stability; standard deviation, interquartile range of central frequency, maximum wavelet frequency; distribution parameters of the phase values above zero; number of oscillation cycles per window	Hjorth's activity, complexity, and mobility
		Wackerman's Global Field strength, global frequency, and spatial complexity
		Barlow's amplitude, frequency, and spectral purity
	Amplitude envelope parameters; kurtosis, skewness, interquartile range, median, range, and variance	Alpha peak frequency, peak width
		Alpha peak power corrected for 1/f baseline
		Beta peak frequency, peak width
		Beta peak power corrected for 1/f baseline

generations. At each generation the biomarker set with maximal positive likelihood ratio (see outcome evaluation below) survived. In all cases the logistic regression model was fitted using the second EEG recording, and the classification outcome was measured using the first EEG recording.

STATISTICS: ELASTIC NET LOGISTIC REGRESSION

As an alternative to genetic optimization of biomarkers included in the logistic regression, we employed an elastic net logistic regression algorithm (Zou and Hastie, 2005) as implemented in the GLMnet package for Matlab (http://www-stat.stanford.edu/~tibs/glmnet-matlab/) (Friedman et al., 2010). This algorithm promises a build-in selection of features that optimally can perform much better than the less stable genetic optimization. The elastic net optimizes the number of biomarkers included in the diagnostic index by minimizing both the L1 and L2 norm of the regression coefficients by minimizing the equation

$$L(\lambda_1, \lambda_2, \beta) = |z - X\beta|^2 + \lambda_1 |\beta| + \lambda_2 |\beta|^2$$

where the first term is similar to the logistic regression, and the second and third are the penalizing terms (the elastic net) (Zou and Hastie, 2005). The parameters λ_1 and λ_2 determines the influence of either the L1 or L2 norm penalty. We define a new combined parameter

$$\alpha = \frac{\lambda_2}{\lambda_1 + \lambda_2}$$

which we optimized in 5-split cross-validation based on the best classification by training on second-year data, and testing on the 1/5 left-out subject group on first-year EEG (note that subjects which did not have a second-year EEG were not included, and, therefore, serve as our ultimate test group (see Results) (data not shown). We found the best classification with $\alpha = 0.8$.

STATISTICS: CLASSIFICATION OUTCOME EVALUATION

To evaluate the outcome of our classification we use five different measures:

- Sensitivity (SE): defined as the (number of correctly classified AD-converter patients)/(number of AD-converter patients).
- Specificity (SP): defined as the (number of correctly classified MCI-stable subjects)/(number of MCI-stable subjects).
- Positive predictive value (PPV): defined as (number of correctly classified AD-converter patients)/(number of patients classified as AD-converters).
- Positive likelihood ratio (PLR): defined as (Sensitivity)/(1-Specificity).
- Matthew correlation coefficient (MCC): explains the correlation between the outcome and the expected outcome (Baldi et al., 2000).

A Matthew correlation coefficient higher than 0.20, sensitivity higher than 65%, specificity higher than 65%, positive predictive value higher than 65%, and a positive likelihood ratio higher than 1.6 means that the classification is significantly different from a random classification (Monte Carlo simulation, 5000 iterations, $n = 65$, note these results depends on the sample size making the threshold levels lower for larger sample sizes, $p < 0.05$). Perfect classification would give a Matthew correlation coefficient (MCC) of 1, sensitivity of 100%, specificity of 100%, positive predictive value of 100%, and an infinite positive likelihood ratio.

An issue with these outcome measures is that they only tell how well the classification fits the given subgroup of subjects, but not how well the classification generalizes to other subject populations. We counteract this by three approaches; (1) classification was performed on the second EEG recording, whereas the prediction was tested on the first EEG recording, (2) as the ultimate test we evaluated the prediction on subjects not included for classifier training (because not all subjects had a second EEG recording), and (3) we performed a half-split cross-validation. In the half-split cross-validation the sample was divided randomly in half several times (1000 iterations); the classifier was then trained on the first half, and the outcome was evaluated on the second half. We report the median outcome measures over these splits. Cross-validation gives an estimate of the classification performance on an "unknown" sample (Witten et al., 2011). However, cross-validation also suffers from lower n numbers, which means their outcome should be viewed as a conservative estimate of the average outcome.

STATISTICS: GROUP DIFFERENCES AND CORRELATIONS

We use non-parametric permutation tests based on median (Box and Andersen, 1955; Ernst, 2004) to test for differences between groups. Non-parametric tests are more robust toward non-normal data, but also often have lower power than parametric such as student's t-test. Confidence intervals (95%) were found using non-parametric bias corrected and accelerated bootstrap ($n = 5000$) (DiCiccio and Efron, 1996).

STATISTICS: 2 × 2 TABLE INDEPENDENCE TESTS

To test for dependence of genotype, gender, and patient group we used Barnard's exact test, which is appropriate for low sample statistics compared with Chi-square test, and has better power compared with Fisher's exact test (Barnard, 1947).

STATISTICS: MULTIPLE COMPARISONS

Because we do large-scale mapping of biomarkers, we employ a lenient approach to multiple comparisons correction at the first level of analysis. This means that in the initial mapping of potential difference between the stable MCI and AD-converter groups, we only perform a binomial correction for the number of significant channels in each biomarker (Poil et al., 2011). We do not correct the p-values across different biomarkers. This approach is appropriate since this mapping of potential difference is only used to identify candidate biomarkers for the genetic search algorithm.

RESULTS

PATIENT GROUPS—AGE AND GENDER

Initially 86 subjects (Age: 68.7 [66.5:71.3] years, median [95% confidence interval], age at first EEG, 58 males) were diagnosed with mild cognitive impairment (MCI). After 415 ± [393:478] days, 17 patients (9 males) had converted to Alzheimer's disease. After 709 ± [537:779] days (1.9 years) a total of 25 patients

(14 males) had converted to AD (Age: 69 ± [67:72] years), 39 subjects (28 males) remained MCI (Age: 67 ± [65:71] years), 9 subjects (6 males) were diagnosed with subjective complaints (Age: 67 ± [46:73] years), and 13 patients (10 males) with other disorders (Age: 70 ± [61:74] years) (including frontal lobe and Vascular dementia). No significant difference was found in age and gender between stable MCI and AD-converters (Gender: Barnard's test, $p = 0.16$; Age: permutation test, $p = 0.49$) (**Table 1**). We only focus on the patients diagnosed with AD, and subjects remaining stable MCI. In the following we use the last diagnosis of the subjects for the definition of the MCI-stable and AD-converters groups.

MMSE RESULTS

The MMSE score of the MCI-stable group (28 ± [27:29]) was not significantly different from the score from AD-converter group (27 ± [26:28]) at the intake test (permutation test, $p = 0.8$). At the follow up approximately 1 year later the stable MCI subjects remained at a stable MMSE score of 28 ± [26:29], whereas the MMSE score of the AD-converter group changed to 24 ± [22:24] (permutation test, $p = 0.0044$), which is also lower than the stable MCI group's MMSE scores (permutation test, $p = 0.0002$) (**Table 1**).

APOE STATUS

We observed a significantly higher frequency of E4 allele vs. no E4 allele in AD-converter vs. stable MCI (Barnard test, $p < 0.01$). Only 38% of MCI-stable compared to 64% of AD-converter group had more than one E4 allele (**Table 2**).

SINGLE-BIOMARKER LOGISTIC REGRESSION MODEL OF AD-CONVERTER vs. MCI-STABLE

To show the principle of logistic regression modeling on a single biomarker, we chose the beta peak frequency, because this biomarker showed significantly lower values in MCI (MCI: 17.6 ± [16.8:18.2] Hz, $n = 39$) compared with the AD-converter group (AD: 19.6 ± [18.1:21.0] Hz, $n = 25$) ($p < 0.0005$) in the first measurement (**Figure 3A**), and also significantly lower values in MCI in the second measurement (MCI: 16.9 ± [16.0:17.8] Hz, $n = 17$; AD: 19.3 ± [18.6:20.6] Hz, $n = 17$, $p < 0.005$) (frequency values are averages across the significant channels) (**Figure 3A**).

We fitted a logistic regression model to the second EEG measurement ($n = 17$ in both groups, **Figure 3B**). The model classified the second measurements with a sensitivity (SE) of 76%, 76% specificity (SP), 76% positive predictive value (PPV), 0.5 Matthew correlation coefficient (MCC), and a positive likelihood ratio (PLR) of 3.3. Next, we used this logistic model to retrospectively classify the first EEG measurement (**Figure 3C**). The classification had a SE of 72%, 59% SP, 53% PPV, 0.3 MCC and a PLR of 1.8; thus, as expected, a worse classification power (MCI $n = 39$, AD $n = 25$) (**Figure 3D**).

Table 2 | Overview of patient groups.

Patient group	Age [years]	MMSE 1st year	MMSE 2nd year	Number of APOE E4
MCI-stable	67 ± [65:71]	28 ± [27:29]	28 ± [26:29]	15 out of 39
AD-convert	69 ± [67:72]	27 ± [26:28]	24 ± [22:24]	16 out of 25
Difference (*p*-value)	$p = 0.49$	$p = 0.8$	$p = 0.0002$	$p < 0.01$

MULTIPLE-BIOMARKER LOGISTIC REGRESSION MODEL OF AD-CONVERTER vs. MCI-STABLE

By combining several biomarkers it may be possible to obtain better classification power than the individual biomarkers alone (Schoonenboom et al., 2004; Buscema et al., 2007; Lehmann et al., 2007). However, it is not trivial which combinations of biomarkers are optimal, because of the high number of possible combinations. Here, we employ a genetic search approach and elastic net penalization to assists us in finding these optimal combinations (see Methods and Materials section).

The best set of biomarkers identified by the genetic search was (six biomarkers): Amplitude correlations with Cz in Beta (13–30 Hz), Bandwidth of subject-specific Beta frequency, Peak width of dominant beta peak, range of amplitude values in Beta (13–30 Hz), Ratio between theta and alpha power, and alpha relative power (normalized with 1–45 Hz broadband). The logistic regression training on this biomarker set using the second EEG data yielded a SE of 100%, 94% SP, 94% PPV, 0.94 MCC, and PLR of 17 ($n = 17$ in both groups).

The retrospective testing on first-year data using the classifier model trained on the second-year data gave a SE of 92%, 85% SP, 79% PPV, 0.75 MCC, and PLR of 6 (MCI-stable, $n = 39$; AD-convert, $n = 25$) (**Figures 3F,G**; **Table 3**), which indicates that even at this very early stage differences between AD-converters and MCI-stable can be identified. However, since second-year and first-year data from the same subjects may be strongly correlated we also performed a classification test using only subjects that were not used for training the model (i.e., the subjects without a second EEG recording). We obtained a good classification with a SE of 88%, 82% SP, 64% PPV, 0.64 MCC and a PLR of 4.8 (MCI-stable, $n = 22$; AD-convert, $n = 8$), suggesting the diagnostic index can generally be used for these patient groups. Furthermore, we performed a half-split cross-validation (1000 iterations), with a SE of 75%, 63% SP, 52% PPV, 0.37 MCC, and a PLR of 2, an indication of the average outcome. As expected, the classification powers decrease; however, this is at least partly explained by the lower n number. However, the combined classification is still much better than prediction obtained on the individual biomarkers in the set (**Figures 3E**, **4**). The best single biomarker in the biomarker set (based on sensitivity and specificity) was the peak width of the dominant Beta peak, with a SE of 64%, 62% SP, 52% PPV, 0.24 MCC, and a PLR of 1.7 (MCI-stable, $n = 22$; AD-convert, $n = 8$) (**Table 3**). The logistic regression fitting coefficients for the combined solution were; −2.9 for Amplitude correlations with Cz in Beta, 0.5 for bandwidth of subject specific Beta, 3.4 for Peak width of dominant beta peak, −0.6 for range of amplitude values in Beta, −2.3 for ratio between theta and alpha power, and −0.2 for alpha relative power. This means that the peak width of the dominant beta peak had the greatest

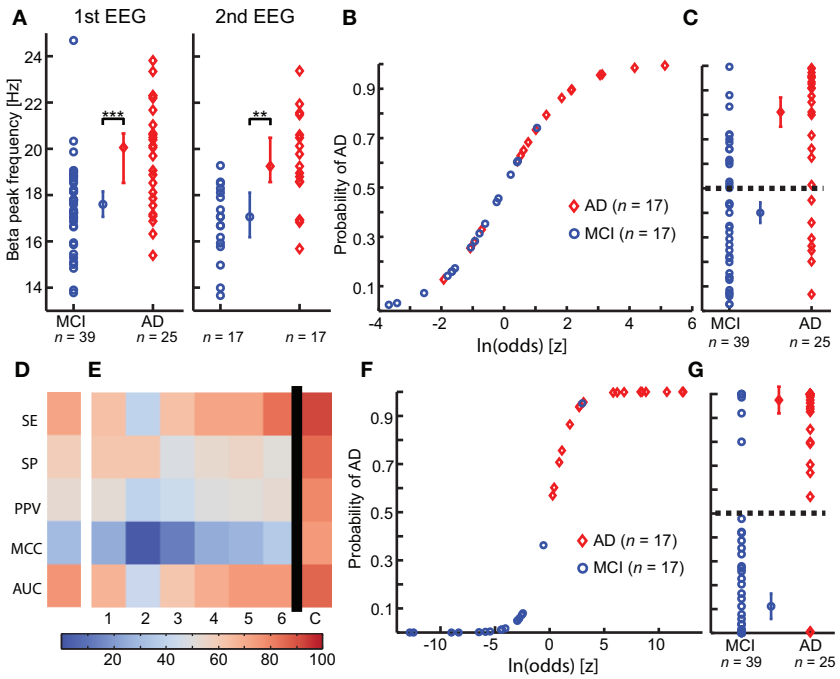

FIGURE 3 | Integration of multiple biomarkers using logistic regression improves the prediction of Alzheimer's disease at the MCI stage. (A) A significant higher Beta peak frequency is observed in Alzheimer's disease converter group (AD) (red) compared with mild cognitive impairment stable group (MCI) (blue), in both first (left) and second (right) year EEG recording. (permutation test on median, binomial corrected, $^{**}p < 0.005$, $^{***}p < 0.0005$) **(B)** The logistic model is fitted to the second-year EEG recording. **(C)** The logistic model is used to predict outcome on the first year EEG recording. Separation plot of AD vs. MCI. **(D)** Outcome evaluation of beta peak frequency using five measures of classification power (warmer is better). SE, Sensitivity; SP, Specificity; PPV, Positive predictive value; MCC, Matthews Correlation Coefficient; AUC, area under the receiver operator curve. **(E)** Outcome evaluation as in **(C)**, but for the "optimal" biomarker set found using genetic search. The first six columns are for classification of the individual biomarkers separately. The last column is the combined classification outcome. We clearly see that the combined outcome is better than the classification using the individual biomarkers. 1, Peak width of dominant beta peak; 2, range of amplitude values in Beta (13–30 Hz); 3, Bandwidth of subject-specific Beta frequency; 4, Ratio between theta and alpha power; 5, alpha relative power (normalized with 1–45 Hz broadband); 6, Amplitude correlations with Cz in Beta (13–30 Hz); **(C)** Combined logistic classification using the biomarkers 1, 2, 3, 4, 5, and 6. **(F)** Logistic curve for combined classification based on first-year EEG. **(G)** Separation plot of MCI vs. AD in first EEG recording using combined classification based on second-year logistic regression coefficients. Note that the recordings used for training in F are different from those used for testing in **(G)**.

Table 3 | Overview of classification results [classification based on testing subjects that were not used for training the classifier (MCI-stable, *n* = 22; AD-convert, *n* = 8)].

Model	Sensitivity (%)	Specificity (%)	Positive predictive value (%)	Matthew correlation coefficient	Positive likelihood ratio
Genetic search 6 biomarkers	88	82	64	0.64	4.8
Single best biomarker	64	62	52	0.24	1.7
Elastic-net 12 biomarkers	75	86	67	0.59	5.5

influence on the outcome, followed by amplitude correlations with Cz.

Taken together, our results show that it is possible to obtain a substantial synergistic effect from the integration of several biomarkers; however, they also show that it is not trivial to identify which combination of biomarkers is most optimal. The major issue with our genetic search is that from run to run we do not obtain the same solution, because the algorithm finds local maxima. We, therefore, employed an elastic net penalized logistic regression algorithm. This algorithm uses a penalization of the weights to optimize the set of biomarkers used for classification. The classification outcome from this algorithm is worse than genetic search optimized logistic regression, with a SE of 75%, 86% SP, 67% PPV, 0.59 MCC, and a PLR of 5.5 (MCI-stable, $n = 22$; AD-convert, $n = 8$) (**Table 3**) based on training on the second-year EEG and testing on the first-year recording of subjects (the test subjects were not used for training). The elastic net logistic regression combined 12 biomarkers (non-zero weights), namely; the amplitude correlations from Cz in Alpha (8–13 Hz) and Beta (13–30 Hz), the range of the generalized multifractal

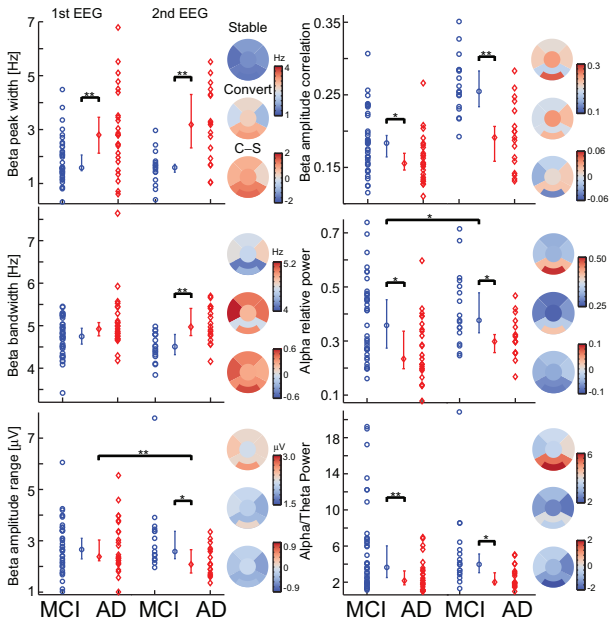

FIGURE 4 | Most biomarkers in the diagnostic index have differences between the MCI-stable (MCI) and AD-converter (AD) groups, and only two have longitudinal changes. For each biomarker, a separation plot is shown for 1st EEG and 2nd EEG. The values are median across channels with significant differences between the MCI-stable (MCI) and AD-converter (AD) groups (Binomial corrected). Topographical plots are of 2nd EEG median value across subjects and channels in 6 regions; Frontal, left/right temporal, Central, Parietal, and Occipital. Asterisk indicates significant differences (permutation test on median, binomial corrected, $^{*}p < 0.05$, $^{**}p < 0.005$).

hurst exponent of the Delta (1–3 Hz) amplitude envelope, the Beta frequency, the power ratio between Gamma (30–45 Hz) and Delta (1–4 Hz), Alpha 1 (Individual Alpha frequency-4: Individual Alpha frequency-2) and Alpha (8–13), Alpha 1 and Beta (13–30 Hz), the spectral edge of the individualized beta-frequency range, the peak width of the beta peak, the second beta peak frequency, the stability of the Delta (1–3 Hz) frequency measured in windows of 5 s, and the Hjorth mobility parameter. The outcome evaluation still shows room for improvement, e.g., by including biomarkers from other modalities.

DISCUSSION

We addressed the challenge of predicting whether an MCI subject would convert to AD within 2 years. To this end, we explored the added value of integrating multiple EEG biomarkers into a diagnostic index using logistic regression in combination with either a genetic search or elastic-net penalization for biomarker selection. From an initial cohort of 86 subjects with mild cognitive impairment, 25 converted to Alzheimer's disease within 2 years. We showed how data mining of 177 EEG biomarkers could be used to identify a set of biomarkers that form a diagnostic index. The analysis was performed using the Neurophysiological Biomarker Toolbox (NBT, http://www.nbtwiki.net/) (Hardstone et al., 2012), which is specifically developed to support data mining and integration of large sets of biomarkers. We found that particularly biomarkers sensitive to changes in the beta frequency (13–30 Hz) band were optimal for classifying the very early EEG recordings of yet to be diagnosed AD patients.

CLASSIFICATION BASED DIAGNOSTICS

Previous studies have shown promise in using machine-learning algorithms to classify between MCI and AD based on EEG recordings (Huang et al., 2000; Bennys et al., 2001; Prichep et al., 2006; Buscema et al., 2007; Lehmann et al., 2007; Prichep, 2007; Rossini et al., 2008). A sensitivity of 89% and specificity of 95% were, e.g., found using the so-called IFAST model (Buscema et al., 2007; Rossini et al., 2008). However, these studies were based on training and testing on the same data, which makes it more difficult to judge the performance. Uniquely to the present study, we performed classification training on the second EEG recording, and retrospectively used this to perform prediction based on the first EEG recording from subjects not used for the training. We note, however, that the drawback of the present procedure is the low number of patients in the smallest patient group (i.e., the eight patients converting to AD) produced a fairly high error margin to the classification estimates (12.5%).

OSCILLATIONS ARE INVOLVED IN COGNITION

Empirical and theoretical evidence suggest that oscillations provide important systems-level mechanisms for normal brain function (Engel and Singer, 2001; Buzsáki and Draguhn, 2004; Axmacher et al., 2006; Klimesch et al., 2007; Palva and Palva, 2007, 2012; Lisman, 2010). For example, oscillations are involved in memory encoding (Raghavachari et al., 2001; Jensen et al., 2002), and are thought to provide a timing mechanism for spike-time dependent plasticity (Engel and Fries, 2010). It, therefore, seem plausible that if oscillations are abnormal in disorders such as MCI and AD, then cognition is also affected. Apart from relative Alpha power and the theta/alpha power ratio, which may reflect early changes toward the well-known slowing of the EEG in AD (Bennys et al., 2001; Rossini et al., 2006), our optimal set of biomarkers is derived from the Beta frequency band (13–30 Hz).

Beta-band changes have previously been observed in Alzheimer's disease, e.g., by a more anterior distribution (Huang et al., 2000). The larger width of the beta peak and bandwidth could potentially be linked with a less stable beta frequency, and, therefore, also a less efficient working memory (Kopell et al., 2011). Beta oscillations are believed to maintain the current sensorimotor and cognitive state (Engel and Fries, 2010). Activity in the beta-frequency range has also traditionally been linked with motor function. Interestingly, it has been found that motor performance is impaired in early-stage Alzheimer's disease but not in mild cognitive impairment (Sheridan et al., 2003; Pettersson et al., 2005), which is a potential explanation of the prominent role of beta-frequency changes in our data. Motor function, e.g., gait control, is a higher cognitive function requiring integration of several cognitive functions, as attention, planning (Hausdorff et al., 2005; Scherder et al., 2007), albeit unrelated to performance in memory tests (Hausdorff et al., 2005). Hyperexcitability of the motor cortex has also been observed in AD (Di Lazzaro et al., 2004), which our finding of higher beta frequency also suggests.

EEG BIOMARKERS AS POTENTIAL INDICATORS OF INFLAMMATION

The standard hypothesis of Alzheimer's disease is the amyloid cascade hypothesis stating that the cause of Alzheimer's should be found in the build up of amyloid and tangles (Hardy and Selkoe, 2002; Huang and Mucke, 2012). It has been hypothesized that Alzheimer's disease is initiated by a micro injury, presumable a vascular event, in the brain with subsequent activation of inflammatory responses that further leads to initiation of the amyloid deposition cycle (De la Torre, 2004; Herrup, 2010).

The theta/(lower alpha) power ratio has previously been associated with vascular damage in AD (Moretti et al., 2007b), and the delta (2–4 Hz) power has been associated with inflammation (Babiloni et al., 2009). EEG power and frequency in general has also been correlated with cerebral perfusion (O'Gorman et al., 2013), which is known to be reduced in Alzheimer's disease (De la Torre, 1999; Kogure et al., 2000; Murray et al., 2011). If we could detect early-stage changes using EEG, we would have a powerful tool that could detect Alzheimer's disease at a point where a possible therapy would be most efficient. Mouse models, e.g., show that Aβ-42 modifying therapy has limited effect after neurodegeneration has begun (Dubois et al., 2007; Sperling et al., 2011). Thus, meaning that diagnosing a patient based on neurodegeneration and cognitive decline may already be too late for a good treatment outcome because the brain damage has already occurred.

It has also been shown that the build-up of Aβ42 influences synaptic transmission, and thus, potentially also give rise to further effects in the EEG (Palop and Mucke, 2009; Verret et al., 2012). Further hippocampal injections of amyloid β in rats have been shown to induce impaired memory performance combined with reduced hippocampal theta oscillations and less activity in GABAergic neurons (GABA, gamma-aminobutyric acid) (Villette et al., 2010). A recent suggestion for a potential improvement of Alzheimer's disease symptoms is transcranial direct current stimulation (tDCS) (Hansen, 2012). This method increased theta and alpha oscillations together with improved working memory performance (Zaehle et al., 2010). Interestingly, it has been suggested these effects may be caused by altered GABA concentration within the stimulated cortex, and potentially by an adjustment of the excitatory/inhibitory balance, which is disturbed in Alzheimer's disease (Di Lazzaro et al., 2004; Rossini et al., 2007; Stagg et al., 2009). This balance may be directly linked to EEG biomarkers that have been shown sensitive to Alzheimer's disease (Montez et al., 2009; Poil et al., 2011, 2012). It thus seems that EEG biomarkers may be sensitive to underlying pathophysiology of AD.

OUTLOOK

We here showed that exploratory data mining and integration of multiple biomarkers might yield many exciting results on the large databases of neuroscience data build up over the years. These studies may identify hidden structures (see schematic **Figure 1C**) and be beneficial for both pre-clinical and clinical research. With recent developments in automatic cleaning of EEG this analysis may potentially be performed immediately after the recording (Nolan et al., 2010; Mognon et al., 2011). This together with the non-invasive character of EEG could make a diagnostic index using EEG biomarkers a powerful tool to support the early-stage clinical assessment. EEG biomarkers, apart from being non-invasive and relative inexpensive, have the advantage of monitoring brain activity in real time, and thus potentially able to identify tiny changes in ongoing cognition. However, we believe the best diagnostic/prognostic performance is achieved if EEG biomarkers are combined with information from other modalities. Future studies should specifically study how the synergistic information of integrative biomarkers can be improved further by the incorporation of different classes of biomarkers, which could range from cognitive markers (Tabert et al., 2006), functional connectivity markers (Stam et al., 2006, 2007), coherence, synchronization, and topographical location markers (Huang et al., 2000; Stam et al., 2005; Rossini et al., 2006) to questionnaire data providing quantitative data on the mental state of the patients during the resting-state EEG recording (Diaz et al., 2013). Improvement in algorithms used for pre-selecting biomarkers could, e.g., be based on measures of interrelatedness between biomarkers or taking scalp topographies into account as opposed to the averaged channel biomarker values used here. We believe the Neurophysiological Biomarker toolbox provides a promising framework for these studies. This could give rise to a better integrative understanding of biomarkers involved with Alzheimer's disease and brain disorders in general (Searls, 2005; Dubois et al., 2007; Schneider, 2010).

ACKNOWLEDGMENTS

This work was supported by Netherlands Organization for Scientific Research (NWO), with a Toptalent grant (Grant nr. 021.002.080) to Simon-Shlomo Poil. The authors would like to acknowledge Emi Saliasi for help with data collection. The authors would like to thank C. J. Stam for sharing the clinical data.

REFERENCES

Albert, M. S., DeKosky, S. T., Dickson, D., Dubois, B., Feldman, H. H., Fox, N. C., et al. (2011). The diagnosis of mild cognitive impairment due to Alzheimer's disease: recommendations from the National Institute on Aging and Alzheimer's Association workgroup. *Alzheimers Dement.* 7, 270–279. doi: 10.1016/j.jalz.2011.03.008

Antila, K., Lötjönen, J., Thurfjell, L., Laine, J., Massimini, M., Rueckert, D., et al. (2013). The PredictAD project: development of novel biomarkers and analysis software for early diagnosis of the Alzheimer's disease. *Interface Focus* 3. doi: 10.1098/rsfs.2012.0072

Axmacher, N., Mormann, F., Fernández, G., Elger, C. E., and Fell, J. (2006). Memory formation by neuronal synchronization. *Brain Res. Rev.* 52, 170–182. doi: 10.1016/j.brainresrev.2006.01.007

Babiloni, C., Binetti, G., Cassetta, E., Forno, G. D., Percio, C. D., Ferreri, F., et al. (2006). Sources of cortical rhythms change as a function of cognitive impairment in pathological aging: a multicenter study. *Clin. Neurophysiol.* 117, 252–268. doi: 10.1016/j.clinph.2005.09.019

Babiloni, C., Frisoni, G. B., Del Percio, C., Zanetti, O., Bonomini, C., Cassetta, E., et al. (2009). Ibuprofen treatment modifies cortical sources of EEG rhythms in mild Alzheimer's disease. *Clin. Neurophysiol.* 120, 709–718. doi: 10.1016/j.clinph.2009.02.005

Babiloni, C., Frisoni, G. B., Vecchio, F., Lizio, R., Pievani, M., Cristina, G., et al. (2011). Stability of clinical condition in mild cognitive impairment is related to cortical sources of alpha rhythms: An electroencephalographic study. *Hum. Brain Mapp.* 32, 1916–1931. doi: 10.1002/hbm.21157

Baldi, P., Brunak, S., Chauvin, Y., Andersen, C. A. F., and Nielsen, H. (2000). Assessing the accuracy of prediction algorithms for classification: an overview. *Bioinformatics rev.* 16, 412–424. doi: 10.1093/bioinformatics/16.5.412

Barnard, G. A. (1947). Significance tests for 2X2 tables. *Biometrika* 34, 123–138.

Bennys, K., Rondouin, G., Vergnes, C., and Touchon, J. (2001). Diagnostic value of quantitative EEG in Alzheimer's disease. *Neurophysiol. Clin. Neurophysiol.* 31, 153–160. doi: 10.1016/S0987-7053(01)00254-4

Blennow, K., de Leon, M. J., and Zetterberg, H. (2006). Alzheimer's disease. *Lancet* 368, 387–403. doi: 10.1016/S0140-6736(06)69113-7

Box, G. E., and Andersen, S. L. (1955). Permutation theory in the derivation of robust criteria and the study of departures from assumption. *J. R. Stat. Soc. Ser. B Methodol.* 17, 1–34.

Buscema, M., Rossini, P., Babiloni, C., and Grossi, E. (2007). The IFAST model, a novel parallel nonlinear EEG analysis technique, distinguishes mild cognitive impairment and Alzheimer's disease patients with high degree of accuracy. *Artif. Intell. Med.* 40, 127–141. doi: 10.1016/j.artmed.2007.02.006

Buzsáki, G., and Draguhn, A. (2004). Neuronal oscillations in cortical networks. *Science* 304, 1926–1929. doi: 10.1126/science.1099745

Cardoso, J. F., and Souloumiac, A. (1993). Blind beamforming for non-Gaussian signals. *IEEE Proc. F* 140, 362–370. doi: 10.1049/ip-f-2.1993.0054

De la Torre, J. C. (1999). Critical threshold cerebral hypoperfusion causes Alzheimer's disease. *Acta Neuropathol.* 98, 1–8. doi: 10.1007/s004010051044

De la Torre, J. C. (2004). Is Alzheimer's disease a neurodegenerative or a vascular disorder. Data, dogma, and dialectics. *Lancet Neurol.* 3, 184–190. doi: 10.1016/S1474-4422(04)00683-0

Di Lazzaro, V., Oliviero, A., Pilato, F., Saturno, E., Dileone, M., Marra, C., et al. (2004). Motor cortex hyperexcitability to transcranial magnetic stimulation in Alzheimer's disease. *J. Neurol. Neurosurg. Psychiatr.* 75, 555–559. doi: 10.1136/jnnp.2003.018127

Diaz, B. A., van der Sluis, S., Moens, S., Benjamins, J. S., Migliorati, F., Stoffers, D., et al. (2013). The Amsterdam Resting-State Questionnaire reveals multiple phenotypes of resting-state cognition. *Front. Hum. Neurosci.* 7:446. doi: 10.3389/fnhum.2013.00446

DiCiccio, T. J., and Efron, B. (1996). Bootstrap confidence intervals. *Stat. Sci.* 11, 189–212.

Dubois, B., Feldman, H. H., Jacova, C., DeKosky, S. T., Barberger-Gateau, P., Cummings, J., et al. (2007). Research criteria for the diagnosis of Alzheimer's disease: revising the NINCDS–ADRDA criteria. *Lancet Neurol.* 6, 734–746. doi: 10.1016/S1474-4422(07)70178-3

Engel, A. K., and Fries, P. (2010). Beta-band oscillations—signalling the status quo. *Curr. Opin. Neurobiol.* 20, 156–165. doi: 10.1016/j.conb.2010.02.015

Engel, A. K., and Singer, W. (2001). Temporal binding and the neural correlates of sensory awareness. *Trends Cogn. Sci.* 5, 16–25.

Ernst, M. D. (2004). Permutation methods: a basis for exact inference. *Stat. Sci.* 19, 676–685. doi: 10.1214/088342304000000396

Flicker, C., Ferris, S. H., and Reisberg, B. (1991). Mild cognitive impairment in the elderly. *Neurology* 41, 1006–1006. doi: 10.1212/WNL.41.7.1006

Folstein, M. F., Folstein, S. E., and McHugh, P. R. (1975). "Mini-mental state". A practical method for grading the cognitive state of patients for the clinician. *J. Psychiatr. Res.* 12, 189–198. doi: 10.1016/0022-3956(75)90026-6

Friedman, J., Hastie, T., and Tibshirani, R. (2010). Regularization paths for generalized linear models via coordinate descent. *J. Stat. Softw.* 33, 1–22.

Gauthier, S., Reisberg, B., Zaudig, M., Petersen, R. C., Ritchie, K., Broich, K., et al. (2006). Mild cognitive impairment. *Lancet* 367, 1262–1270. doi: 10.1016/S0140-6736(06)68542-5

Goncharova, I. I., and Barlow, J. S. (1990). Changes in EEG mean frequency and spectral purity during spontaneous alpha blocking. *Electroencephalogr. Clin. Neurophysiol.* 76, 197–204. doi: 10.1016/0013-4694(90)90015-C

Hansen, N. (2012). Action mechanisms of transcranial direct current stimulation in Alzheimer's disease and memory loss. *Front. Psychiatry* 3:48. doi: 10.3389/fpsyt.2012.00048

Hardstone, R., Poil, S.-S., Schiavone, G., Jansen, R., Nikulin, V. V., Mansvelder, H. D., et al. (2012). Detrended fluctuation analysis: a scale-free view on neuronal oscillations. *Front. Physiol.* 3:450. doi: 10.3389/fphys.2012.00450

Hardy, J., and Selkoe, D. J. (2002). The amyloid hypothesis of Alzheimer's disease: progress and problems on the road to therapeutics. *Science* 297, 353–356. doi: 10.1126/science.1072994

Hausdorff, J. M., Yogev, G., Springer, S., Simon, E. S., and Giladi, N. (2005). Walking is more like catching than tapping: gait in the elderly as a complex cognitive task. *Exp. Brain Res.* 164, 541–548. doi: 10.1007/s00221-005-2280-3

Herrup, K. (2010). Reimagining Alzheimer's disease—an age-based hypothesis. *J. Neurosci.* 30, 16755–16762. doi: 10.1523/JNEUROSCI.4521-10.2010

Hjorth, B. (1970). EEG analysis based on time domain properties. *Electroencephalogr. Clin. Neurophysiol.* 29, 306–310. doi: 10.1016/0013-4694(70)90143-4

Huang, C., Wahlund, L. O., Dierks, T., Julin, P., Winblad, B., and Jelic, V. (2000). Discrimination of Alzheimer's disease and mild cognitive impairment by equivalent EEG sources: a cross-sectional and longitudinal study. *Clin. Neurophysiol.* 111, 1961–1967. doi: 10.1016/S1388-2457(00)00454-5

Huang, L., and Mucke, L. (2012). Alzheimer mechanisms and therapeutic strategies. *Cell* 148, 1204–1222. doi: 10.1016/j.cell.2012.02.040

Hughes, C. P., Berg, L., Danziger, W. L., Coben, L. A., and Martin, R. L. (1982). A new clinical scale for the staging of dementia. *Br. J. Psychiatry* 140, 566–572. doi: 10.1192/bjp.140.6.566

Ihlen, E. A. F. (2012). Introduction to multifractal detrended fluctuation analysis in matlab. *Front. Physiol.* 3:141. doi: 10.3389/fphys.2012.00141

Jelic, V., Johansson, S. E., Almkvist, O., Shigeta, M., Julin, P., Nordberg, A., et al. (2000). Quantitative electroencephalography in mild cognitive impairment: longitudinal changes and possible prediction of Alzheimer's disease. *Neurobiol. Aging* 21, 533–540. doi: 10.1016/S0197-4580(00)00153-6

Jelic, V., Shigeta, M., Julin, P., Almkvist, O., Winblad, B., and Wahlund, L. O. (1996). Quantitative electroencephalography power and coherence in Alzheimer's disease and mild cognitive impairment. *Dement. Geriatr. Cogn. Disord.* 7, 314–323. doi: 10.1159/000106897

Jensen, O., Gelfand, J., Kounios, J., and Lisman, J. E. (2002). Oscillations in the alpha band (9–12 Hz) increase with memory load during retention in a short-term memory task. *Cereb. Cortex* 12, 877–882. doi: 10.1093/cercor/12.8.877

Kantelhardt, J. W., Zschiegner, S. A., Koscielny-Bunde, E., Havlin, S., Bunde, A., and Stanley, H. E. (2002). Multifractal detrended fluctuation analysis of nonstationary time series. *Phys. Stat. Mech. Appl.* 316, 87–114. doi: 10.1016/S0378-4371(02)01383-3

Klimesch, W. (1999). EEG alpha and theta oscillations reflect cognitive and memory performance: a review and analysis. *Brain Res. Rev.* 29, 169–195. doi: 10.1016/S0165-0173(98)00056-3

Klimesch, W., Sauseng, P., and Hanslmayr, S. (2007). EEG alpha oscillations: the inhibition–timing hypothesis. *Brain Res. Rev.* 53, 63–88. doi: 10.1016/j.brainresrev.2006.06.003

Kogure, D., Matsuda, H., Ohnishi, T., Asada, T., Uno, M., Kunihiro, T., et al. (2000). Longitudinal evaluation of early Alzheimer's disease using brain perfusion SPECT. *J. Nucl. Med.* 41, 1155.

Kopell, N., Whittington, M. A., and Kramer, M. A. (2011). Neuronal assembly dynamics in the beta1 frequency range permits short-term memory. *Proc. Natl. Acad. Sci. U.S.A.* 108, 3779–3784. doi: 10.1073/pnas.1019676108

Koza, J., and Poli, R. (2005). "Genetic programming," in *Search Methodologies*, (Heidelberg: Springer), 127–164.

Kwak, Y. T. (2006). Quantitative EEG findings in different stages of Alzheimer's disease. *J. Clin. Neurophysiol.* 23, 457. doi: 10.1097/01.wnp.0000223453.47663.63

Lehmann, C., Koenig, T., Jelic, V., Prichep, L., John, R. E., Wahlund, L. O., et al. (2007). Application and comparison of classification algorithms for recognition of Alzheimer's disease in electrical brain activity (EEG). *J. Neurosci. Methods* 161, 342–350. doi: 10.1016/j.jneumeth.2006.10.023

Linkenkaer-Hansen, K., Nikouline, V. V., Palva, J. M., and Ilmoniemi, R. J. (2001). Long-range temporal correlations and scaling behavior in human brain oscillations. *J. Neurosci.* 21, 1370.

Lisman, J. (2010). Working memory: the importance of theta and gamma oscillations. *Curr. Biol.* 20, R490–R492. doi: 10.1016/j.cub.2010.04.011

Luckhaus, C., Grass-Kapanke, B., Blaeser, I., Ihl, R., Supprian, T., Winterer, G., et al. (2008). Quantitative EEG in progressing vs

stable mild cognitive impairment (MCI): results of a 1-year follow-up study. *Int. J. Geriatr. Psychiatry* 23, 1148–1155. doi: 10.1002/gps.2042

McKhann, G., Drachman, D., Folstein, M., Katzman, R., Price, D., and Stadlan, E. M. (1984). Clinical diagnosis of Alzheimer's disease. *Neurology* 34, 939–939. doi: 10.1212/WNL.34.7.939

Mognon, A., Jovicich, J., Bruzzone, L., and Buiatti, M. (2011). ADJUST: an automatic EEG artifact detector based on the joint use of spatial and temporal features. *Psychophysiology* 48, 229–240. doi: 10.1111/j.1469-8986.2010.01061.x

Montez, T., Poil, S.-S., Jones, B. F., Manshanden, I., Verbunt, J., Van Dijk, B. W., et al. (2009). Altered temporal correlations in parietal alpha and prefrontal theta oscillations in early-stage Alzheimer disease. *Proc. Natl. Acad. Sci. U.S.A.* 106, 1614. doi: 10.1073/pnas.0811699106

Moretti, D. V., Frisoni, G. B., Fracassi, C., Pievani, M., Geroldi, C., Binetti, G., et al. (2011). MCI patients' EEGs show group differences between those who progress and those who do not progress to AD. *Neurobiol. Aging* 32, 563–571. doi: 10.1016/j.neurobiolaging.2009.04.003

Moretti, D. V., Miniussi, C., Frisoni, G. B., Geroldi, C., Zanetti, O., Binetti, G., et al. (2007a) Hippocampal atrophy and EEG markers in subjects with mild cognitive impairment. *Clin. Neurophysiol.* 118, 2716–2729. doi: 10.1016/j.clinph.2007.09.059

Moretti, D. V., Miniussi, C., Frisoni, G., Zanetti, O., Binetti, G., Geroldi, C., et al. (2007b) Vascular damage and EEG markers in subjects with mild cognitive impairment. *Clin. Neurophysiol.* 118, 1866–1876. doi: 10.1016/j.clinph.2007.05.009

Moretti, D. V., Pievani, M., Fracassi, C., Geroldi, C., Calabria, M., De Carli, C. S., et al. (2008). Brain vascular damage of cholinergic pathways and EEG markers in mild cognitive impairment. *J. Alzheimers Dis.* 15, 357–372.

Murray, I. V. J., Proza, J. F., Sohrabji, F., and Lawler, J. M. (2011). Vascular and metabolic dysfunction in Alzheimer's disease: a review. *Exp. Biol. Med.* 236, 772–782. doi: 10.1258/ebm.2011.010355

Nolan, H., Whelan, R., and Reilly, R. B. (2010). FASTER: fully automated statistical thresholding for EEG artifact rejection. *J. Neurosci. Methods* 192, 152–162. doi: 10.1016/j.jneumeth.2010.07.015

O'Gorman, R. L., Poil, S.-S., Brandeis, D., Klaver, P., Bollmann, S., Ghisleni, C., et al. (2013). Coupling between resting cerebral perfusion and EEG. *Brain Topogr.* 26, 442–457. doi: 10.1007/s10548-012-0265-7

Palop, J. J., and Mucke, L. (2009). Epilepsy and cognitive impairments in alzheimer disease. *Arch. Neurol.* 66, 435–440. doi: 10.1001/archneurol.2009.15

Palva, S., and Palva, J. M. (2007). New vistas for Alpha-frequency band oscillations. *Trends Neurosci.* 30, 150–158. doi: 10.1016/j.tins.2007.02.001

Palva, S., and Palva, J. M. (2012). Discovering oscillatory interaction networks with M/EEG: challenges and breakthroughs. *Trends Cogn. Sci.* Available online at: http://www.sciencedirect.com/science/article/pii/S1364661312000472 [Accessed November 3, 2012].

Petersen, R. C., Smith, G. E., Waring, S. C., Ivnik, R. J., Tangalos, E. G., and Kokmen, E. (1999). Mild cognitive impairment: clinical characterization and outcome. *Arch. Neurol.* 56, 303. doi: 10.1001/archneur.56.3.303

Pettersson, A. F., Olsson, E., and Wahlund, L. O. (2005). Motor function in subjects with mild cognitive impairment and early Alzheimer's disease. *Dement. Geriatr. Cogn. Disord.* 19, 299–304. doi: 10.1159/000084555

Poil, S.-S., Hardstone, R., Mansvelder, H. D., and Linkenkaer-Hansen, K. (2012). Critical-state dynamics of avalanches and oscillations jointly emerge from balanced excitation/inhibition in neuronal networks. *J. Neurosci.* 32, 9817–9823. doi: 10.1523/JNEUROSCI.5990-11.2012

Poil, S.-S., Jansen, R., van Aerde, K., Timmerman, J., Brussaard, A. B., Mansvelder, H. D., et al. (2011). Fast network oscillations *in vitro* exhibit a slow decay of temporal auto-correlations. *Eur. J. Neurosci.* 34, 394–403. doi: 10.1111/j.1460-9568.2011.07748.x

Poil, S.-S., van Ooyen, A., and Linkenkaer-Hansen, K. (2008). Avalanche dynamics of human brain oscillations: relation to critical branching processes and temporal correlations. *Hum. Brain Mapp.* 29, 770–777. doi: 10.1002/hbm.20590

Prichep, L. S. (2007). Quantitative EEG and electromagnetic brain imaging in aging and in the evolution of dementia. *Ann. N.Y. Acad. Sci.* 1097, 156–167. doi: 10.1196/annals.1379.008

Prichep, L. S., John, E. R., Ferris, S. H., Rausch, L., Fang, Z., Cancro, R., et al. (2006). Prediction of longitudinal cognitive decline in normal elderly with subjective complaints using electrophysiological imaging. *Neurobiol. Aging* 27, 471–481. doi: 10.1016/j.neurobiolaging.2005.07.021

Prins, N. D., Visser, P. J., and Scheltens, P. (2010). Can novel therapeutics halt the amyloid cascade. *Alzheimers Res. Ther.* 2. Available online at: http://www.biomedcentral.com/content/pdf/alzrt28.pdf (Accessed June 19, 2012).

Raghavachari, S., Kahana, M. J., Rizzuto, D. S., Caplan, J. B., Kirschen, M. P., Bourgeois, B., et al. (2001). Gating of human theta oscillations by a working memory task. *J. Neurosci.* 21, 3175–3183.

Rombouts, S. A. R., Barkhof, F., Goekoop, R., Stam, C. J., and Scheltens, P. (2005). Altered resting state networks in mild cognitive impairment and mild Alzheimer's disease: an fMRI study. *Hum. Brain Mapp.* 26, 231–239. doi: 10.1002/hbm.20160

Rossini, P., Buscema, M., Capriotti, M., Grossi, E., Rodriguez, G., Del Percio, C., et al. (2008). Is it possible to automatically distinguish resting EEG data of normal elderly vs. mild cognitive impairment subjects with HIGH degree of accuracy? *Clin. Neurophysiol.* 119, 1534–1545. doi: 10.1016/j.clinph.2008.03.026

Rossini, P. M., Rossi, S., Babiloni, C., and Polich, J. (2007). Clinical neurophysiology of aging brain: From normal aging to neurodegeneration. *Prog. Neurobiol.* 83, 375–400. doi: 10.1016/j.pneurobio.2007.07.010

Rossini, P., Del Percio, C., Pasqualetti, P., Cassetta, E., Binetti, G., Dal Forno, G., et al. (2006). Conversion from mild cognitive impairment to Alzheimer's disease is predicted by sources and coherence of brain electroencephalography rhythms. *Neuroscience* 143, 793–803. doi: 10.1016/j.neuroscience.2006.08.049

Scherder, E., Eggermont, L., Swaab, D., Van Heuvelen, M., Kamsma, Y., De Greef, M., et al. (2007). Gait in ageing and associated dementias; its relationship with cognition. *Neurosci. Biobehav. Rev.* 31, 485–497. doi: 10.1016/j.neubiorev.2006.11.007

Schneider, L. S. (2010). Organising the language of Alzheimer's disease in light of biomarkers. *Lancet Neurol.* 9, 1044–1045. doi: 10.1016/S1474-4422(10)70246-5

Schoonenboom, N. S. M., Pijnenburg, Y. A. L., Mulder, C., Rosso, S. M., Van Elk, E. J., Van Kamp, G. J., et al. (2004). Amyloid Beta (1–42) and phosphorylated tau in CSF as markers for early-onset Alzheimer disease. *Neurology* 62, 1580–1584. doi: 10.1212/01.WNL.0000123249.58898.E0

Searls, D. B. (2005). Data integration: challenges for drug discovery. *Nat. Rev. Drug Discov.* 4, 45–58. doi: 10.1038/nrd1608

Sheridan, P. L., Solomont, J., Kowall, N., and Hausdorff, J. M. (2003). Influence of executive function on locomotor function: divided attention increases gait variability in Alzheimer's disease. *J. Am. Geriatr. Soc.* 51, 1633–1637. doi: 10.1046/j.1532-5415.2003.51516.x

Sperling, R. A., Aisen, P. S., Beckett, L. A., Bennett, D. A., Craft, S., Fagan, A. M., et al. (2011). Toward defining the preclinical stages of Alzheimer's disease: recommendations from the National Institute on Aging and the Alzheimer's Association workgroup. *Alzheimers Dement.* 7, 280–292. doi: 10.1016/j.jalz.2011.03.003

Stagg, C. J., Best, J. G., Stephenson, M. C., O'Shea, J., Wylezinska, M., Kincses, Z. T., et al. (2009). Polarity-sensitive modulation of cortical neurotransmitters by transcranial stimulation. *J. Neurosci.* 29, 5202–5206.

Stam, C. J., Jones, B. F., Manshanden, I., Van Cappellen van Walsum, A. M., Montez, T., Verbunt, J. P. A., et al. (2006). Magnetoencephalographic evaluation of resting-state functional connectivity in Alzheimer's disease. *Neuroimage* 32, 1335–1344. doi: 10.1016/j.neuroimage.2006.05.033

Stam, C. J., Jones, B. F., Nolte, G., Breakspear, M., and Scheltens, P. (2007). Small-world networks and functional connectivity in Alzheimer's disease. *Cereb. Cortex* 17, 92–99. doi: 10.1093/cercor/bhj127

Stam, C. J., Montez, T., Jones, B. F., Rombouts, S., Van Der Made, Y., Pijnenburg, Y. A. L., et al. (2005). Disturbed fluctuations of resting state EEG synchronization in Alzheimer's disease. *Clin. Neurophysiol.* 116, 708–715. doi: 10.1016/j.clinph.2004.09.022

Stam, C. J., Van der Made, Y., Pijnenburg, Y. A. L., and Scheltens, P. H. (2003). EEG synchronization in mild cognitive impairment and Alzheimer's disease. *Acta Neurol. Scand.* 108, 90–96. doi: 10.1034/j.1600-0404.2003.02067.x

Tabert, M. H., Manly, J. J., Liu, X., Pelton, G. H., Rosenblum, S., Jacobs, M., et al. (2006). Neuropsychological prediction

of conversion to Alzheimer disease in patients with mild cognitive impairment. *Arch. Gen. Psychiatry* 63, 916. doi: 10.1001/archpsyc.63.8.916

Van Aerde, K. I., Mann, E. O., Canto, C. B., Heistek, T. S., Linkenkaer-Hansen, K., Mulder, A. B., et al. (2009). Flexible spike timing of layer 5 neurons during dynamic beta oscillation shifts in rat prefrontal cortex. *J. Physiol.* 587, 5177–5196. doi: 10.1113/jphysiol.2009.178384

Verret, L., Mann, E. O., Hang, G. B., Barth, A. M. I., Cobos, I., Ho, K., et al. (2012). Inhibitory interneuron deficit links altered network activity and cognitive dysfunction in alzheimer model. *Cell* 149, 708–721. doi: 10.1016/j.cell.2012.02.046

Villette, V., Poindessous-Jazat, F., Simon, A., Clement, L., Roullot, E., Bellessort, B., et al. (2010). Decreased rhythmic GABAergic septal activity and memory-associated theta oscillations after hippocampal amyloid-beta pathology in the rat. *J. Neurosci.* 30, 10991–11003. doi: 10.1523/JNEUROSCI.6284-09.2010

Vural, C., and Yildiz, M. (2010). Determination of sleep stage separation ability of features extracted from EEG signals using principle component analysis. *J. Med. Syst.* 34, 83–89. doi: 10.1007/s10916-008-9218-9

Wackermann, J. (1999). Towards a quantitative characterisation of functional states of the brain: from the non-linear methodology to the global linear description. *Int. J. Psychophysiol.* 34, 65–80. doi: 10.1016/S0167-8760(99)00038-0

Witten, I. H., Frank, E., and Hall, M. A. (2011). *Data Mining: Practical Machine Learning Tools and Techniques*. San Francisco: Morgan Kaufmann.

Zaehle, T., Rach, S., and Herrmann, C. S. (2010). Transcranial alternating current stimulation enhances individual alpha activity in human EEG. *PLoS ONE* 5:e13766. doi: 10.1371/journal.pone.0013766

Zou, H., and Hastie, T. (2005). Regularization and variable selection via the elastic net. *J. R. Stat. Soc. Ser. B Stat. Methodol.* 67, 301–320. doi: 10.1111/j.1467-9868.2005.00503.x

Zviling, M., Leonov, H., and Arkin, I. T. (2005). Genetic algorithm-based optimization of hydrophobicity tables. *Bioinformatics* 21, 2651–2656. doi: 10.1093/bioinformatics/bti405

Conflict of Interest Statement: The authors declare that the research was conducted in the absence of any commercial or financial relationships that could be construed as a potential conflict of interest.

Received: 23 July 2013; paper pending published: 22 August 2013; accepted: 11 September 2013; published online: 03 October 2013.

*Citation: Poil S-S, de Haan W, van der Flier WM, Mansvelder HD, Scheltens P and Linkenkaer-Hansen K (2013) Integrative EEG biomarkers predict progression to Alzheimer's disease at the MCI stage. Front. Aging Neurosci. **5**:58. doi: 10.3389/fnagi.2013.00058*

This article was submitted to the journal Frontiers in Aging Neuroscience.

Copyright © 2013 Poil, de Haan, van der Flier, Mansvelder, Scheltens and Linkenkaer-Hansen. This is an open-access article distributed under the terms of the Creative Commons Attribution License (CC BY). The use, distribution or reproduction in other forums is permitted, provided the original author(s) or licensor are credited and that the original publication in this journal is cited, in accordance with accepted academic practice. No use, distribution or reproduction is permitted which does not comply with these terms.

frontiers in
AGING NEUROSCIENCE

ORIGINAL RESEARCH ARTICLE
published: 27 December 2013
doi: 10.3389/fnagi.2013.00100

Brain-wide slowing of spontaneous alpha rhythms in mild cognitive impairment

Pilar Garcés[1,2]*, Raul Vicente[3,4,5], Michael Wibral[3], Jose Ángel Pineda-Pardo[1], Maria Eugenia López[1,6], Sara Aurtenetxe[1,6], Alberto Marcos[7], Maria Emiliana de Andrés[8], Miguel Yus[9], Miguel Sancho[2], Fernando Maestú[1,6] and Alberto Fernández[1,10]

[1] *Laboratory of Cognitive and Computational Neuroscience (UCM-UPM), Centre for Biomedical Technology, Madrid, Spain*
[2] *Department of Applied Physics III, Faculty of Physics, Complutense University of Madrid, Madrid, Spain*
[3] *MEG Unit, Brain Imaging Center, Goethe University, Frankfurt, Germany*
[4] *Max-Planck Institute for Brain Research, Frankfurt, Germany*
[5] *Institute of Computer Science, Faculty of Mathematics and Computer Science, University of Tartu, Tartu, Estonia*
[6] *Department of Basic Psychology II, Complutense University of Madrid, Madrid, Spain*
[7] *Neurology Department, San Carlos Clinical Hospital, Madrid, Spain*
[8] *Memory Decline Prevention Center, Ayuntamiento de Madrid, Madrid, Spain*
[9] *Radiology Department, San Carlos Clinical Hospital, Madrid, Spain*
[10] *Department of Psychiatry and Medical Psychology, Faculty of Medicine, Complutense University of Madrid, Madrid, Spain*

Edited by:
Hari S. Sharma, Uppsala University, Sweden

Reviewed by:
Davide V. Moretti, IRCCSS Centro Giovanni di dio Fatebenefratelli, Italy
Michel J. A. M. van Putten, University of Twente, Netherlands

****Correspondence:***
Pilar Garcés, Laboratory of Cognitive and Computational Neuroscience (UCM-UPM), Centre for Biomedical Technology, Campus de Montegancedo s/n, 28223 Pozuelo de Alarcón, Madrid, Spain
e-mail: pilar.garces@ctb.upm.es

The neurophysiological changes associated with Alzheimer's Disease (AD) and Mild Cognitive Impairment (MCI) include an increase in low frequency activity, as measured with electroencephalography or magnetoencephalography (MEG). A relevant property of spectral measures is the alpha peak, which corresponds to the dominant alpha rhythm. Here we studied the spatial distribution of MEG resting state alpha peak frequency and amplitude values in a sample of 27 MCI patients and 24 age-matched healthy controls. Power spectra were reconstructed in source space with linearly constrained minimum variance beamformer. Then, 88 Regions of Interest (ROIs) were defined and an alpha peak per ROI and subject was identified. Statistical analyses were performed at every ROI, accounting for age, sex and educational level. Peak frequency was significantly decreased ($p < 0.05$) in MCIs in many posterior ROIs. The average peak frequency over all ROIs was 9.68 ± 0.71 Hz for controls and 9.05 ± 0.90 Hz for MCIs and the average normalized amplitude was $(2.57 \pm 0.59) \cdot 10^{-2}$ for controls and $(2.70 \pm 0.49) \cdot 10^{-2}$ for MCIs. Age and gender were also found to play a role in the alpha peak, since its frequency was higher in females than in males in posterior ROIs and correlated negatively with age in frontal ROIs. Furthermore, we examined the dependence of peak parameters with hippocampal volume, which is a commonly used marker of early structural AD-related damage. Peak frequency was positively correlated with hippocampal volume in many posterior ROIs. Overall, these findings indicate a pathological alpha slowing in MCI.

Keywords: mild cognitive impairment, magnetoencephalography, alpha peak, slowing, hippocampal volume

INTRODUCTION

Mild Cognitive Impairment (MCI) is often considered a prodromal stage of Alzheimer's Disease (AD). This is due to the fact that some studies have found that around 10–15% of MCI patients annually progress to AD while it only occurs at a 1–4% rate for the healthy aged population (Petersen, 2001; Petersen and Negash, 2008). MCI patients show objective cognitive alterations but not severe enough to meet the criteria for dementia. In the past years, a great interest has been drawn to MCI, since this condition might help to understand the neurological basis of the "predementia" stages of AD and to maximize the effect of the current available treatments.

Particularly, electrophysiological rhythms have been found relevant in pathological aging. Electroencephalographic (EEG) and magnetoencephalographic (MEG) studies have shown a slowing of the oscillatory rhythms in AD (Berendse et al., 2000; Huang et al., 2000). MCI patients exhibit a reduced mean frequency score in MEG power spectra (Fernández et al., 2006), indicating that the AD-related oscillatory slowing may have its onset in the predementia stage. Additionally, specific spectral profiles have been considered as pathological biomarkers. For example, an increased delta and a decreased alpha1 power were found to be related to a lower cortical gray matter volume (Babiloni et al., 2013). It has also been reported that changes in the high alpha/low alpha ratio or in the theta/gamma ratio are associated with the cognitive status, conversion to AD, hippocampal and amygdalar atrophy or gray matter changes (Moretti et al., 2009a, 2011, 2012).

An essential property of the electrophysiological spectra is the dominant alpha rhythm or alpha peak. Alpha oscillations have been measured over wide regions of the exposed human cortex (Jasper and Penfield, 1949). Sensor-level EEG studies have found that their frequency rises from childhood to adolescence or young adulthood, and then decreases slowly with age (Chiang et al., 2011). Abnormally low alpha peak frequencies can be found in

demented patients (Samson-Dollfus et al., 1997). Some studies of MCI have used the posterior dominant frequency to perform spectral analysis. For instance, (Moretti et al., 2009a, 2011, 2012) used the individual alpha peak to define individual frequency ranges for theta, alpha, and beta bands. Babiloni et al. (2009, 2013) considered the alpha peak frequency as a covariate when performing statistical analysis. Nevertheless, although utilized as an intermediate step in the analysis pipeline of many studies, the importance of alpha peak amplitude and frequency values *per se* to define neurophysiological characteristics in MCI has been scarcely investigated.

In the present study we investigated the spatial distribution of resting state alpha peak frequency and amplitude over the whole brain for MCI patients and age-matched healthy controls. To this aim, beamforming was used to estimate MEG spectral parameters for the alpha peak (frequency and amplitude) in source space. Also, we analyzed how these parameters were modulated by age and sex for each ROI. Finally, we examined the relation between peak parameters and hippocampal volume, which is commonly used as a structural biomarker of AD (Dubois et al., 2007).

MATERIALS AND METHODS

SUBJECTS

27 patients with a diagnosis of amnestic-MCI and 24 controls were included in this study. **Table 1** summarizes their characteristics. MCI patients were recruited at the Geriatric and Neurological Units of the "Hospital Universitario San Carlos," Madrid, Spain, where they were diagnosed by clinical experts. As introduced in Grundman et al. (2004), inclusion criteria for MCI comprised: (1) memory complaint confirmed by an informant, (2) normal cognitive function, (3) no or minimal impairment in activities of daily living, (4) abnormal memory function, (5) not being sufficiently impaired to meet the criteria for dementia.

Additionally, all subjects were in good health and had no history of psychiatric or neurological disorders. They underwent an MRI brain scan to rule out infection, infarction or focal lesions. Subjects meeting any of the following criteria were excluded from the study: Hachinski score (Rosen et al., 1980) higher than 4, Geriatric Depression Scale score (Yesavage et al., 1982) higher than 14, alcoholism, chronic use of anxiolytics, neuroleptics, narcotics, anticonvulsants, or sedative hypnotics. Additionally, MCI patients underwent an exam to rule out possible causes of cognitive decline such as B12 vitamin deficit, thyroid problems, syphilis, or HIV. Drugs that could affect MEG measurements such as cholinesterase inhibitors were removed 48 h before the MEG scan. The investigation was approved by the local Ethics Committee.

MEG RECORDINGS

Three-minute MEG resting state recordings were acquired at the Center for Biomedical Technology (Madrid, Spain) with an Elekta Vectorview system containing 306 sensors (102 magnetometers and 204 planar gradiometers), inside a magnetically shielded room (Vacuumschmelze GmbH, Hanau, Germany). During the measurements, subjects sat with their eyes closed and were instructed to remain calm and move as little as possible. Each subject's head was digitized in 3D with a Fastrak Polhemus system and four coils were attached to the forehead and mastoids, so that the head position with respect to the MEG helmet was continuously determined. Activity in electrooculogram channels was also recorded to keep track of ocular artifacts.

Signals were sampled at 1000 Hz with an online filter of bandwidth 0.1–300 Hz. Maxfilter software (version 2.2., Elekta Neuromag) was used to remove external noise with the temporal extension of the signal space separation method with movement compensation (Taulu and Simola, 2006).

MRI ACQUISITION

3D T1 weighted anatomical brain MRI scans were collected with a General Electric 1.5 T magnetic resonance scanner, using a high-resolution antenna and a homogenization PURE filter [Fast Spoiled Gradient Echo (FSPGR) sequence with parameters: TR/TE/TI = 11.2/4.2/450 ms; flip angle 12°; 1 mm slice thickness, a 256 × 256 matrix and FOV 25 cm]. For volumetric analysis, Freesurfer software package (version 5.1.0) and its automated sub-cortical segmentation tool (Fischl et al., 2002) were employed. For the source analysis, the reference system of the T1 volumes was transformed manually using 3 fiducial points and headshape, until a good match between MEG and T1 coordinates was reached.

SOURCE ANALYSIS

Data analysis was done using both FieldTrip software (Oostenveld et al., 2011) and in-house scripts.

Table 1 | Subjects characteristics.

	Subjects	Age (years)	Gender (M/F)	Educational level	MMSE	Normalized hippocampal volume	
						Left	Right
Control	24	71.8 ± 3.6	6/18	3.8 ± 1.3	29.3 ± 0.9	$(2.62 \pm 0.37)\cdot10^{-3}$	$(2.59 \pm 0.28)\cdot10^{-3}$
MCI	27	73.9 ± 6.3	14/13	2.7 ± 1.3	27.5 ± 2.2	$(2.17 \pm 0.41)\cdot10^{-3}$	$(2.08 \pm 0.49)\cdot10^{-3}$

Data are given as mean ± standard deviation.

M = males, F = females. Educational level was grouped into five levels: 1: Illiterate, 2: Primary studies, 3: Elemental studies, 4: High school studies, 5: University studies.

MMSE = Mini Mental State Examination score. Hippocampal volume was normalized with the overall intracranial volume.

MEG preprocessing

For the definition of artifact-free epochs, the continuous MEG resting state recording was scanned in non-overlapping segments of 4 s. Segments with ocular, jump, or muscular artifacts were identified and discarded. Per subject, a minimum of 20 artifact-free segments (80 s) remained [controls: (25.7 ± 4.8), MCI: (24.6 ± 6.6)]. After filtering of the continuous original data using a finite impulse response filter of order 1000 and a bandwidth of 1–30 Hz, the artifact-free segments of the data identified in the previous step were extracted for further analysis.

Headmodels

First, a regular grid of 2459 points with 1 cm spacing was created in the template Montreal Neurological Institute (MNI) brain. This set of points was transformed to subject's space using a linear normalization between the native T1 image and a standard T1 in MNI space with 2 mm resolution. This grid constituted the source locations. The forward model was solved with a realistic single-shell model (Nolte, 2003).

Beamforming

Source reconstruction was performed with Linearly Constrained Minimum Variance beamformer (Van Veen et al., 1997). For each subject, the covariance matrix was averaged over all trials to compute the spatial filter's coefficients, and then these coefficients were applied to individual trials, obtaining a time series per segment and source location. This reconstruction was performed for magnetometers and gradiometers separately, yielding two different source estimates per subject.

SPECTRAL ANALYSIS

Power spectra were obtained from the time series via a multitaper method with discrete prolate spheroidal sequences as tapers and 1 Hz smoothing for frequencies between 2 and 30 Hz, with a 0.25 Hz step. These spectra were averaged over trials and normalized with the sum of the spectral power in the range (2–30) Hz. Then, an average power spectrum per Region of Interest (ROI) and subject was obtained. Eighty-eight ROIs were used in this study and they were defined in MNI space using the Harvard-Oxford probabilistic atlas (Desikan et al., 2006), as implemented in the fMRIb Software Library (FSL) (Jenkinson et al., 2012). Thirty-seven cortical and 7 subcortical ROIs per hemisphere were included (merging subdivisions within gyri in the Harvard-Oxford atlas).

Then, to extract alpha peak parameters, experimental spectra were fitted with a non-linear least-square procedure to:

$$\log(P(f)) = B - C \cdot \log(f) + A \cdot \exp\left(\frac{-(f - f_p)^2}{\Delta^2}\right)$$

where A,B,C, Δ, and f_p are adjustable parameters and a wide range (4–13) Hz is used for the fitting. Such a Gaussian peak fit with power-law background has been proven useful for alpha rhythm detection in EEG (Chiang et al., 2008; Lodder and van Putten, 2011).

With this procedure, a peak per ROI was identified separately for the reconstructions based on magnetometers and gradiometers. Then, magnetometer and gradiometer data were combined. Thus, the final peak amplitude and frequency per ROI and subject was calculated by averaging the peak values obtained for both types of sensors. In order to optimize the reliability of the alpha peak estimation, two criteria were considered: Peaks with (1) high inter-trial amplitude variability for any sensor type or (2) a frequency difference between the magnetometer and the gradiometer fit bigger than 1 Hz, were considered spurious and removed from the subsequent statistical analysis.

STATISTICAL ANALYSIS

Peak amplitudes and frequencies were compared with univariate ANOVA tests, separately for each ROI. Shapiro-Wilk and Levene tests were used to ensure normality of the data and equal variances across groups. For the peak amplitude, the transformation $x \rightarrow \log(x/(1-x))$ was applied prior to statistical analysis to obtain values following a normal distribution. A four-way ANOVA analysis was performed considering diagnosis, age, sex, and educational level as factors to investigate differences between controls and MCIs and the influence of age and sex on the alpha peak. Finally, we examined whether peak parameters depend on hippocampal volume (which was normalized with the overall intracranial volume). For that, we computed the Pearson correlation coefficient between peak amplitude or frequency and hippocampal volume across all subjects, for every ROI separately. To establish the statistical significance of these correlations, a four-way ANOVA test with hippocampal volume, age, sex, and educational level as factors was used, taking all subjects (Control and MCI) as a single group.

The p-values of all ANOVA tests were corrected for multiple comparisons with a procedure based on clustering and permutations, as introduced by Maris and Oostenveld (2007). For that, spatially adjacent ROIs with $p < 0.05$ were first grouped into clusters. Then, the obtained peak values (frequency or amplitude) were 2000 times randomly assigned to the original groups. The sum of F-values over each cluster in the original dataset was compared with the same measure in the randomized data. For each cluster, the proportion of randomizations with F-values higher than the ones in the original data corresponds to the final p-value.

RESULTS

PEAK FITTING

Peaks were successfully identified for most ROIs and subjects, especially in posterior and temporal ROIs. Overall, the peak was harder to find in anterior areas of the brain, since for around 10–15% of the subjects the criteria for robustness introduced before were not fulfilled in frontal ROIs. On the whole, a peak was fit in 80 ± 14 ROIs (given as mean $\pm$ std) for the control group and in 85 ± 5 ROIs for the MCI group. For the following ROIs, less than 85% of the subjects showed a robust peak: right paracingulate gyrus, right frontal operculum cortex, right inferior and middle frontal gyri, both superior frontal gyri, both supplementary motor cortices and right pallidum. These ROIs were not considered for statistical analysis. The average peak frequency over all ROIs was 9.68 ± 0.71 Hz for controls and 9.05 ± 0.90 Hz

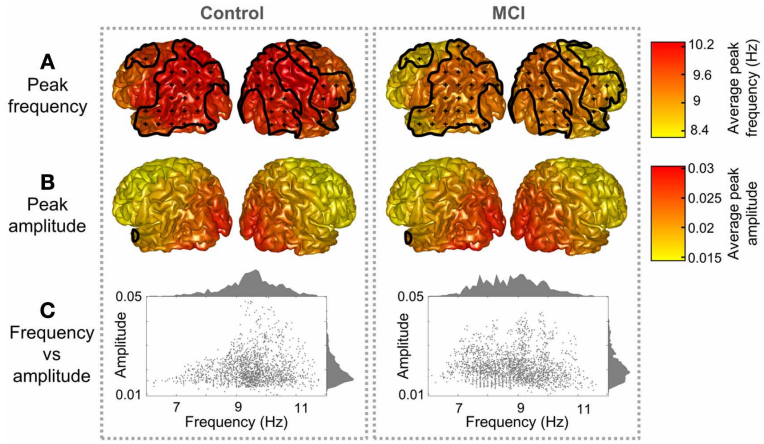

FIGURE 1 | Peak distribution in controls and MCIs. Peak **(A)** frequency and **(B)** amplitude grand averages for controls and MCIs. Clusters with significant differences between controls and MCIs ($p < 0.05$) are enclosed with black lines and scattered with black crosses. **(C)** Represents a scatter plot of the peak parameters (frequency and amplitude) for every region and subject. Frequency and amplitude histograms are projected into the y and x axis respectively.

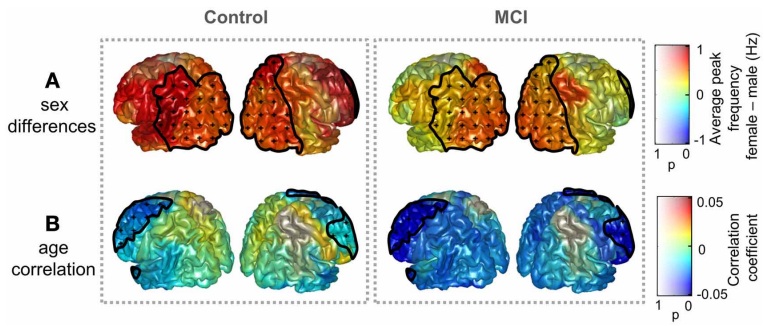

FIGURE 2 | Influence of age and sex on peak frequency in controls and MCIs. (A) Peak frequency difference of grand averages: females—males. **(B)** Correlation coefficient between age and peak frequency. Clusters with significant effect of age or sex upon peak frequencies ($p < 0.05$) are enclosed with black lines and scattered with black crosses. Additionally, the *p*-value specifies the transparency of the plotted intensities: a region with *p*-value of 0 shows a full opaque color, whereas a region with *p*-value of 1 will be transparent.

for MCIs and the average normalized amplitude was $(2.57 \pm 0.59) \cdot 10^{-2}$ for controls and $(2.70 \pm 0.49) \cdot 10^{-2}$ for MCIs.

CONTROL vs. MCI

Both groups presented a similar spatial distribution of peak parameters, with higher amplitude and frequency in posterior ROIs, as shown in **Figure 1**. However, peak frequencies were higher in controls than in MCIs, especially over parietal and temporal ROIs, where differences were statistically significant ($p < 0.05$). Amplitudes were similar in controls and MCIs, although values tended to be higher in MCIs, but this was significant only for six temporal and medial ROIs. As amplitude and frequency values are usually inversely related in electrophysiological power spectra, the amplitude increase in MCIs could be just a consequence of the frequency decrease. To investigate this effect, amplitude values were plotted as a function of frequency (**Figure 1C**). For controls, amplitudes were higher within the 9–11 Hz frequency range, while for MCIs this range seemed to be broader, with high magnitude alpha peaks from 7 to 11 Hz. On the whole, this leads to the idea that alpha peak frequency is reduced in MCI.

AGE AND SEX INFLUENCE

Sex and age did not exert a significant influence on peak amplitude, while significant effects were found for the peak frequency. **Figure 2** displays sex differences and age correlations for peak frequency in Controls and MCIs separately. Peak frequency was higher for females than for males both in controls and MCIs. This trend was present over the whole brain, although only statistically significant ($p < 0.05$) over some posterior and right frontal ROIs. Additionally, peak frequency was found to correlate negatively with age. This correlation was strongest in frontal ROIs, where a significant effect ($p < 0.05$) was found.

HIPPOCAMPAL VOLUME

To further assess whether differences in peak parameters could be considered as a pathological sign, the dependence of peak amplitude and frequency values with hippocampal volume was

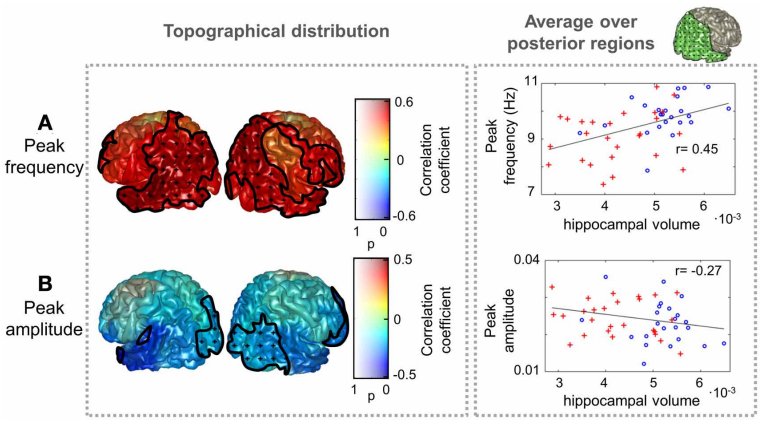

FIGURE 3 | Peak frequency and amplitude correlations with hippocampal volume. The distribution of correlation coefficient between peak **(A)** frequency and **(B)** amplitude with hippocampal volume (normalized with intracranial volume) for all subjects (Controls and MCIs) is shown. Clusters with significant effect of hippocampal volume ($p < 0.05$) are marked as in **Figure 2**. As an example, scatter plots of the average peak frequency and amplitude over posterior ROIs as a function of hippocampal volume are displayed in the right side. The included ROIs are plotted in green in the upper right side of the figure. Controls are represented as blue circles and MCIs as red crosses.

examined. Results are illustrated in **Figure 3**. Peak frequency correlated positively with hippocampal volume, reaching correlation values up to 0.6, which denote a strong association between both measures. This trend was significant ($p < 0.05$) over most of the postrolandic ROIs of the brain and implies that a slowing in the main alpha rhythm is related with a greater atrophy in the medial temporal lobe. The opposite effect was found for the peak amplitude, which correlated negatively with hippocampal volume over the whole brain, especially over occipital and frontal ROIs, where the trend was significant ($p < 0.05$).

DISCUSSION

In this paper the alpha peak parameters (frequency and amplitude) were investigated in a sample of MCI patients and controls. Differences between both groups were examined, as well as the influence of age and sex, and the correlation between peak parameters and hippocampal volume. To attain such goal, a novel method was introduced, that combined beamforming for reconstruction of the power spectra in the source space, and a fitting algorithm that has been successfully used for peak identification with scalp EEG measures in sensor space (Chiang et al., 2011; Lodder and van Putten, 2011).

The alpha peak was robustly identified in most regions and subjects. This is not the first attempt to assess the alpha peak spatial distribution of frequency and amplitude values in resting state, since clusters of alpha peaks in EEG recordings within a large sample of healthy population have been analyzed (Chiang et al., 2011). However, in the present study the MEG source space analysis allows a better understanding of the spatial distribution of this dominant alpha rhythm. Most studies of pathological aging have only focused on the posterior alpha peak (Osipova et al., 2006). Here we intentionally decided to consider sources of alpha rhythm other than the posterior ones, since alpha rhythms have been detected over wide regions of the brain [for a review, see Nunez et al. (2001)].

One of the main findings of our study is that the alpha rhythm of MCIs is slower when compared with a control population, especially over posterior regions. This is not surprising, since abnormally low alpha peak frequencies in AD have already been described (Passero et al., 1995). In the MCI literature less attention has been drawn to the alpha peak, but a reduced mean frequency score has been reported (Fernández et al., 2006). To gain further insight into the meaning of these peak alterations, their relationship with the hippocampal volume was considered. In fact, atrophy in medial temporal structures such as the hippocampus is a pathological marker of AD (Dubois et al., 2007; Prestia et al., 2013). Some studies have related a lower hippocampal volume to a higher delta and theta dipole density in AD (Fernández et al., 2003), lower power in the 8–10.5 Hz range (Babiloni et al., 2009), and an increase in the alpha3/alpha2 ratio (Moretti et al., 2009b). Our results show that hippocampal volumes correlated positively with peak frequencies in temporo-parieto-occipital regions of the brain and negatively with peak amplitude in occipital and frontal regions. This contributes to the idea that the peak frequency slowing is associated with a degenerative process, evolving in parallel with the loss of hippocampal volume. Two different hypotheses have been introduced over the past years to explain the increased low frequency power in AD and MCI. It could be explained through either (1) a slowing down or (2) a redistribution of the oscillatory sources in the theta-alpha frequency range (Osipova et al., 2005, 2006). This study supports the first hypothesis, although bigger samples and an analysis of the possible spatial shift of the sources would be needed to make stronger statements and investigate the second hypothesis.

The exact physiological origin of alpha rhythm remains unclear. Some studies indicate a prominent role of the thalamus (Hughes and Crunelli, 2005; Lőrincz et al., 2009; Bollimunta et al., 2011), while others point out the existence of cortical generators (Flint and Connors, 1996; Bollimunta et al., 2008). With a thalamo-cortical model of EEG generation, (Hindriks and van Putten, 2013) established that the resonance properties of

cortico-thalamo-cortical, intra-cortical, and feedforward circuits determine alpha responses. They found that both a decreased firing of excitatory neuronal populations and an increased firing rate in inhibitory neuronal populations related to a decrease in alpha frequency. This modulation was particularly intense in the intra-cortical circuit: a decreased delay in this circuit produced a strong frequency slowing. Moreover, a decrease in the number of active synapses in thalamic nuclei could also explain an alpha power shift toward lower frequencies, as proved in a recent study with a thalamico-cortical-thalamic neural mass model (Bhattacharya et al., 2011). This model showed that the alpha frequency shift is especially sensitive to damage in inhibitory interneurons in the thalamus. Within this theory, the MCI alpha slowing found in this study would suggest that a synaptic damage is already present in the MCI stage. This in turn could be related with amyloid β, since its deposition has been shown to contribute to synaptic loss in AD (Reddy and Beal, 2008; Bate and Williams, 2011).

Additionally, the peak frequency is not determined exclusively by the pathology, but also depends on other factors like age or sex. In fact, we found a frequency decrease with age, and higher frequency values in females than in males. Such trends have been previously found in studies with large healthy samples (Chiang et al., 2011). In our study, we report that this trend is maintained in MCI patients. Most studies of sex differences in the alpha band have focused on childhood and young age, with mixed outcomes, some of them finding higher frequencies and earlier maturation in girls than boys (Petersén and Eeg-Olofsson, 2008). Our results also show higher frequencies in females than in males, although within a completely different age profile. Dustman et al. (1993) found that a slowing of alpha rhythms and an increase in delta, theta and beta activity are common age-associated changes in EEG spectra. This means that the alpha slowing is normal in healthy aging, and suggests that the MCI disease speeds up the natural aging process.

The methodological procedure followed here enabled the examination of amplitude and frequency shifts of the alpha peak. It combined beamforming of MEG resting state data, alpha peak fitting and ANOVA tests for statistical analysis, corrected for multiple comparisons with a procedure including clustering and permutations. Although it was tested with a rather small sample of subjects, it revealed a slowing of the alpha oscillatory sources in MCI and established that age, sex and hippocampal volume affect peak amplitude and frequency. However, larger samples would be needed to confirm these effects and to evaluate others, such as an interaction between age, sex, or educational level. Additionally, longitudinal follow-up studies could provide insight into the evolution of the slowing process and the onset of the AD-related pathology.

CONCLUSION

In conclusion, we studied the spatial distribution of the alpha peak frequency and amplitude in a sample of controls and MCI patients using MEG resting state spectra in source space. Variations across subjects were found, even at a healthy stage, since peak frequency depended upon age and sex. The alpha peak was altered in the MCI sample when compared to controls: MCIs presented lower peak frequencies. This slowing of the alpha oscillatory sources in MCI could be attributed to an impaired thalamico-cortical circuit or a synaptic loss in thalamic populations. Furthermore, the peak frequency progression to lower frequencies correlated with the degree of hippocampal atrophy, highlighting its pathological meaning.

AUTHOR CONTRIBUTIONS

Conception of the research: Fernando Maestú, Alberto Fernández, and Alberto Marcos. Neuropsychological assessment: Maria Emiliana de Andrés. MCI evaluation: Alberto Marcos. MRI data acquisition: Miguel Yus. Volumetric analysis: Jose Ángel Pineda-Pardo. MEG data acquisition and database organization: Maria Eugenia López and Sara Aurtenetxe. Methods design and data analysis: Pilar Garcés, Raul Vicente, Michael Wibral, and Miguel Sancho. Drafting of the manuscript: Pilar Garcés and Alberto Fernández. Critical revision of the manuscript: Alberto Fernández, Raul Vicente, Michael Wibral, and Fernando Maestú. Every author read and approved the final version of the manuscript.

ACKNOWLEDGMENTS

This work was supported by LOEWE-grant "Neuronale Koordination Forschungsschwerpunkt Frankfurt (NeFF)" and the projects PSI2009-14415-C03-01 and PSI2012-38375-C03-01 from the Spanish Ministry of Science and Economy. Research by Pilar Garcés was supported by a PICATA fellowship of the Moncloa Campus of International Excellence (UCM-UPM).

REFERENCES

Babiloni, C., Carducci, F., Lizio, R., Vecchio, F., Baglieri, A., Bernardini, S., et al. (2013). Resting state cortical electroencephalographic rhythms are related to gray matter volume in subjects with mild cognitive impairment and Alzheimer's disease. *Hum. Brain Mapp.* 34, 1427–1446. doi: 10.1002/hbm.22005

Babiloni, C., Frisoni, G. B., Pievani, M., Vecchio, F., Lizio, R., Buttiglione, M., et al. (2009). Hippocampal volume and cortical sources of EEG alpha rhythms in mild cognitive impairment and Alzheimer disease. *Neuroimage* 44, 123–135. doi: 10.1016/j.neuroimage.2008.08.005

Bate, C., and Williams, A. (2011). Amyloid-β-induced synapse damage is mediated via cross-linkage of cellular prion proteins. *J. Biol. Chem.* 286, 37955–37963. doi: 10.1074/jbc.M111.248724

Berendse, H., Verbunt, J. P., Scheltens, P., van Dijk, B., and Jonkman, E. (2000). Magnetoencephalographic analysis of cortical activity in Alzheimer's disease: a pilot study. *Clin. Neurophysiol.* 111, 604–612. doi: 10.1016/S1388-2457(99)00309-0

Bhattacharya, B. S., Coyle, D., and Maguire, L. P. (2011). A thalamo-cortico-thalamic neural mass model to study alpha rhythms in Alzheimer's disease. *Neural Netw.* 24, 631–645. doi: 10.1016/j.neunet.2011.02.009

Bollimunta, A., Chen, Y., Schroeder, C. E., and Ding, M. (2008). Neuronal mechanisms of cortical alpha oscillations in awake-behaving macaques. *J. Neurosci.* 28, 9976–9988. doi: 10.1523/JNEUROSCI.2699-08.2008

Bollimunta, A., Mo, J., Schroeder, C. E., and Ding, M. (2011). Neuronal mechanisms and attentional modulation of corticothalamic α oscillations. *J. Neurosci.* 31, 4935–4943. doi: 10.1523/JNEUROSCI.5580-10.2011

Chiang, A. K. I., Rennie, C. J., Robinson, P. A., Roberts, J. A., Rigozzi, M. K., Whitehouse, R. W., et al. (2008). Automated characterization of multiple alpha peaks in multi-site electroencephalograms. *J. Neurosci. Methods* 168, 396–411. doi: 10.1016/j.jneumeth.2007.11.001

Chiang, A. K. I., Rennie, C. J., Robinson, P. A., van Albada, S. J., and Kerr, C. C. (2011). Age trends and sex differences of alpha rhythms including split alpha peaks. *Clin. Neurophysiol.* 122, 1505–1517. doi: 10.1016/j.clinph.2011.01.040

Desikan, R. S., Ségonne, F., Fischl, B., Quinn, B. T., Dickerson, B. C., Blacker, D., et al. (2006). An automated labeling system for subdividing the human

cerebral cortex on MRI scans into gyral based regions of interest. *Neuroimage* 31, 968–980. doi: 10.1016/j.neuroimage.2006.01.021

Dubois, B., Feldman, H. H., Jacova, C., Dekosky, S. T., Barberger-Gateau, P., Cummings, J., et al. (2007). Research criteria for the diagnosis of Alzheimer's disease: revising the NINCDS-ADRDA criteria. *Lancet Neurol.* 6, 734–746. doi: 10.1016/S1474-4422(07)70178-3

Dustman, R. E., Shearer, D. E., and Emmerson, R. Y. (1993). EEG and event-related potentials in normal aging. *Prog. Neurobiol.* 41, 369–401. doi: 10.1016/0301-0082(93)90005-D

Fernández, A., Arrazola, J., Maestú, F., Amo, C., Gil-Gregorio, P., Wienbruch, C., et al. (2003). Correlations of hippocampal atrophy and focal low-frequency magnetic activity in Alzheimer disease: volumetric MR imaging-magnetoencephalographic study. *AJNR Am. J. Neuroradiol.* 24, 481–487. Available online at: http://www.ncbi.nlm.nih.gov/pubmed/12637301

Fernández, A., Hornero, R., Mayo, A., Poza, J., Gil-Gregorio, P., and Ortiz, T. (2006). MEG spectral profile in Alzheimer's disease and mild cognitive impairment. *Clin. Neurophysiol.* 117, 306–314. doi: 10.1016/j.clinph.2005.10.017

Fischl, B., Salat, D. H., Busa, E., Albert, M., Dieterich, M., Haselgrove, C., et al. (2002). Whole brain segmentation. *Neuron* 33, 341–355. doi: 10.1016/S0896-6273(02)00569-X

Flint, A. C., and Connors, B. W. (1996). Two types of network oscillations in neocortex mediated by distinct glutamate receptor subtypes and neuronal populations. *J Neurophysiol* 75, 951–957.

Grundman, M., Petersen, R. C., Ferris, S. H., Thomas, R. G., Aisen, P. S., Bennett, D. A., et al. (2004). Mild cognitive impairment can be distinguished from Alzheimer disease and normal aging for clinical trials. *Arch. Neurol.* 61, 59–66. doi: 10.1001/archneur.61.1.59

Hindriks, R., and van Putten, M. J. A. M. (2013). Thalamo-cortical mechanisms underlying changes in amplitude and frequency of human alpha oscillations. *Neuroimage* 70, 150–163. doi: 10.1016/j.neuroimage.2012.12.018

Huang, C., Wahlund, L.-O., Dierks, T., Julin, P., Winblad, B., and Jelic, V. (2000). Discrimination of Alzheimer's disease and mild cognitive impairment by equivalent EEG sources: a cross-sectional and longitudinal study. *Clin. Neurophysiol.* 111, 1961–1967. doi: 10.1016/S1388-2457(00)00454-5

Hughes, S. W., and Crunelli, V. (2005). Thalamic mechanisms of EEG alpha rhythms and their pathological implications. *Neuroscientist* 11, 357–372. doi: 10.1177/1073858405277450

Jasper, H., and Penfield, W. (1949). Zur Deutung des normalen Elektrencephalogramms und selner Veriinderungen. Electroeorticograms in man: effect of voluntary movement upon the electrical activity of the preeentral gyrus *. *Arch. Psychiatr. Z. Neurol.* 174, 163–174. doi: 10.1007/BF01062488

Jenkinson, M., Beckmann, C. F., Behrens, T. E. J., Woolrich, M. W., and Smith, S. M. (2012). FSL. *Neuroimage* 62, 782–790. doi: 10.1016/j.neuroimage.2011.09.015

Lodder, S. S., and van Putten, M. J. A M. (2011). Automated EEG analysis: characterizing the posterior dominant rhythm. *J. Neurosci. Methods* 200, 86–93. doi: 10.1016/j.jneumeth.2011.06.008

Lőrincz, M. L., Kékesi, K. A., Juhász, G., Crunelli, V., and Hughes, S. W. (2009). Temporal framing of thalamic relay-mode firing by phasic inhibition during the alpha rhythm. *Neuron* 63, 683–696. doi: 10.1016/j.neuron.2009.08.012

Maris, E., and Oostenveld, R. (2007). Nonparametric statistical testing of EEG- and MEG-data. *J. Neurosci. Methods* 164, 177–190. doi: 10.1016/j.jneumeth.2007.03.024

Moretti, D. V., Fracassi, C., Pievani, M., Geroldi, C., Binetti, G., Zanetti, O., et al. (2009a). Increase of theta/gamma ratio is associated with memory impairment. *Clin. Neurophysiol.* 120, 295–303. doi: 10.1016/j.clinph.2008.11.012

Moretti, D. V., Pievani, M., Fracassi, C., Binetti, G., Rosini, S., Geroldi, C., et al. (2009b). Increase of theta/gamma and alpha3/alpha2 ratio is associated with amygdalo-hippocampal complex atrophy. *J. Alzheimers Dis.* 17, 349–357. doi: 10.3233/JAD-2009-1059

Moretti, D. V., Frisoni, G. B., Fracassi, C., Pievani, M., Geroldi, C., Binetti, G., et al. (2011). MCI patients' EEGs show group differences between those who progress and those who do not progress to AD. *Neurobiol. Aging* 32, 563–571. doi: 10.1016/j.neurobiolaging.2009.04.003

Moretti, D. V., Paternicò, D., Binetti, G., Zanetti, O., and Frisoni, G. B. (2012). EEG markers are associated to gray matter changes in thalamus and basal ganglia in subjects with mild cognitive impairment. *Neuroimage* 60, 489–496. doi: 10.1016/j.neuroimage.2011.11.086

Nolte, G. (2003). The magnetic lead field theorem in the quasi-static approximation and its use for magnetoencephalography forward calculation in realistic volume conductors. *Phys. Med. Biol.* 48, 3637–3652. doi: 10.1088/0031-9155/48/22/002

Nunez, P. L., Wingeier, B. M., and Silberstein, R. B. (2001). Spatial-temporal structures of human alpha rhythms: theory, microcurrent sources, multiscale measurements, and global binding of local networks. *Hum. Brain Mapp.* 13, 125–164. doi: 10.1002/hbm.1030

Oostenveld, R., Fries, P., Maris, E., and Schoffelen, J.-M. (2011). FieldTrip: open source software for advanced analysis of MEG, EEG, and invasive electrophysiological data. *Comput. Intell. Neurosci.* 2011, 156869. doi: 10.1155/2011/156869

Osipova, D., Ahveninen, J., Jensen, O., Ylikoski, A., and Pekkonen, E. (2005). Altered generation of spontaneous oscillations in Alzheimer's disease. *Neuroimage* 27, 835–841. doi: 10.1016/j.neuroimage.2005.05.011

Osipova, D., Rantanen, K., Ahveninen, J., Ylikoski, R., Häppölä, O., Strandberg, T., et al. (2006). Source estimation of spontaneous MEG oscillations in mild cognitive impairment. *Neurosci. Lett.* 405, 57–61. doi: 10.1016/j.neulet.2006.06.045

Passero, S., Rocchi, R., Vatti, G., Burgalassi, L., and Battistini, N. (1995). Quantitative EEG mapping, regional cerebral blood flow, and neuropsychological function in Alzheimer's disease. *Dement. Geriatr. Cogn. Disord.* 6, 148–156. doi: 10.1159/000106938

Petersén, I., and Eeg-Olofsson, O. (2008). The development of the electroencephalogram in normal children from the age of 1 through 15 years – non-paroxysmal activity. *Neuropediatrics* 2, 247–304. doi: 10.1055/s-0028-1091786

Petersen, R. C. (2001). Current concepts in mild cognitive impairment. *Arch. Neurol.* 58, 1985–1992. doi: 10.1001/archneur.58.12.1985

Petersen, R. C., and Negash, S. (2008). Mild cognitive impairment: an overview. *CNS Spectr.* 13, 45–53. Available online at: http://www.ncbi.nlm.nih.gov/pubmed/18204414

Prestia, A., Caroli, A., van der Flier, W. M., Ossenkoppele, R., Van Berckel, B., Barkhof, F., et al. (2013). Prediction of dementia in MCI patients based on core diagnostic markers for Alzheimer disease. *Neurology* 80, 1048–1056. doi: 10.1212/WNL.0b013e3182872830

Reddy, P. H., and Beal, M. F. (2008). Amyloid beta, mitochondrial dysfunction and synaptic damage: implications for cognitive decline in aging and Alzheimer's disease. *Trends Mol. Med.* 14, 45–53. doi: 10.1016/j.molmed.2007.12.002

Rosen, W. G., Terry, R. D., Fuld, P. A., Katzman, R., and Peck, A. (1980). Pathological verification of ischemic score in differentiation of dementias. *Ann. Neurol.* 7, 486–488. doi: 10.1002/ana.410070516

Samson-Dollfus, D., Delapierre, G., Do Marcolino, C., and Blondeau, C. (1997). Normal and pathological changes in alpha rhythms. *Int. J. Psychophysiol.* 26, 395–409. doi: 10.1016/S0167-8760(97)00778-2

Taulu, S., and Simola, J. (2006). Spatiotemporal signal space separation method for rejecting nearby interference in MEG measurements. *Phys. Med. Biol.* 51, 1759–1768. doi: 10.1088/0031-9155/51/7/008

Van Veen, B. D., van Drongelen, W., Yuchtman, M., and Suzuki, A. (1997). Localization of brain electrical activity via linearly constrained minimum variance spatial filtering. *IEEE Trans. Biomed. Eng.* 44, 867–880. doi: 10.1109/10.623056

Yesavage, J. A., Brink, T. L., Rose, T. L., Lum, O., Huang, V., Adey, M., et al. (1982). Development and validation of a geriatric depression screening scale: a preliminary report. *J. Psychiatr. Res.* 17, 37–49. doi: 10.1016/0022-3956(82)90033-4

Conflict of Interest Statement: The authors declare that the research was conducted in the absence of any commercial or financial relationships that could be construed as a potential conflict of interest.

Received: 09 October 2013; accepted: 15 December 2013; published online: 27 December 2013.

*Citation: Garcés P, Vicente R, Wibral M, Pineda-Pardo JA, López ME, Aurtenetxe S, Marcos A, de Andrés ME, Yus M, Sancho M, Maestú F and Fernández A (2013) Brain-wide slowing of spontaneous alpha rhythms in mild cognitive impairment. Front. Aging Neurosci. **5**:100. doi: 10.3389/fnagi.2013.00100*

This article was submitted to the journal Frontiers in Aging Neuroscience.

Copyright © 2013 Garcés, Vicente, Wibral, Pineda-Pardo, López, Aurtenetxe, Marcos, de Andrés, Yus, Sancho, Maestú and Fernández. This is an open-access article distributed under the terms of the Creative Commons Attribution License (CC BY). The use, distribution or reproduction in other forums is permitted, provided the original author(s) or licensor are credited and that the original publication in this journal is cited, in accordance with accepted academic practice. No use, distribution or reproduction is permitted which does not comply with these terms.

frontiers in
AGING NEUROSCIENCE

ORIGINAL RESEARCH ARTICLE
published: 26 August 2014
doi: 10.3389/fnagi.2014.00224

Functional disorganization of small-world brain networks in mild Alzheimer's Disease and amnestic Mild Cognitive Impairment: an EEG study using Relative Wavelet Entropy (RWE)

Christos A. Frantzidis[1], Ana B. Vivas[2], Anthoula Tsolaki[1,3], Manousos A. Klados[1], Magda Tsolaki[4] and Panagiotis D. Bamidis[1]*

[1] *Laboratory of Medical Physics, Faculty of Health Sciences, Medical School, Aristotle University of Thessaloniki, Thessaloniki, Greece*
[2] *Psychology Department, City College, The University of Sheffield International Faculty, Thessaloniki, Greece*
[3] *Greek Association of Alzheimer's Disease and related Disorders, Thessaloniki, Greece*
[4] *3rd Department of Neurology, Medical School, Aristotle University of Thessaloniki, Thessaloniki, Greece*

Edited by:
Davide V. Moretti, San Giovanni di Dio Fatebenefratelli, Italy

Reviewed by:
Xiaoli Li, Beijing Normal University, China
Sawal Hamid Md Ali, The National University of Malaysia, Malaysia

****Correspondence:***
Panagiotis D. Bamidis, Laboratory of Medical Physics, Faculty of Health Sciences, Medical School, Aristotle University of Thessaloniki, PO Box 376, 54124, Thessaloniki, Greece
e-mail: bamidis@med.auth.gr

Previous neuroscientific findings have linked Alzheimer's Disease (AD) with less efficient information processing and brain network disorganization. However, pathological alterations of the brain networks during the preclinical phase of amnestic Mild Cognitive Impairment (aMCI) remain largely unknown. The present study aimed at comparing patterns of the detection of functional disorganization in MCI relative to Mild Dementia (MD). Participants consisted of 23 cognitively healthy adults, 17 aMCI and 24 mild AD patients who underwent electroencephalographic (EEG) data acquisition during a resting-state condition. Synchronization analysis through the Orthogonal Discrete Wavelet Transform (ODWT), and directional brain network analysis were applied on the EEG data. This computational model was performed for networks that have the same number of edges ($N = 500, 600, 700, 800$ edges) across all participants and groups (fixed density values). All groups exhibited a small-world (SW) brain architecture. However, we found a significant reduction in the SW brain architecture in both aMCI and MD patients relative to the group of Healthy controls. This functional disorganization was also correlated with the participant's generic cognitive status. The deterioration of the network's organization was caused mainly by deficient local information processing as quantified by the mean cluster coefficient value. Functional hubs were identified through the normalized betweenness centrality metric. Analysis of the local characteristics showed relative hub preservation even with statistically significant reduced strength. Compensatory phenomena were also evident through the formation of additional hubs on left frontal and parietal regions. Our results indicate a declined functional network organization even during the prodromal phase. Degeneration is evident even in the preclinical phase and coexists with transient network reorganization due to compensation.

Keywords: Alzheimer Disease, amnestic Mild Cognitive Impairment, electroencephalography, graph analysis, Relative Wavelet Entropy

INTRODUCTION

Alzheimer's Disease (AD) is regarded as a progressive, neurodegenerative disease with a relatively long pre-morbid asymptomatic period (Caselli et al., 2004). Although, no cognitive symptoms may be obvious this pre-morbid period is characterized by abnormal protein (amyloid-β/Aβ and hyperphosphorylated) production which results gradually in the formation of neurofibrillary tangles and neuritic plaques (Buerger et al., 2006). These alterations are particularly evident in brain areas crucial for the functional co-operation of distant brain regions (Delbeuck et al., 2003; Drzezga et al., 2011). Once clinical detection of AD is possible, based mostly on cognitive and daily functioning assessment, brain atrophy and thus functional impairments can be hardly inverted (Citron, 2010). It is therefore reasonable that research on Alzheimer's has focused on the reliable detection of early AD signs that precede functional and cognitive impairment (Sperling et al., 2011). As a result of this research effort, the term *Mild Cognitive Impairment* (MCI) (Petersen et al., 1999; Albert et al., 2011) was introduced to define a transition state between healthy aging and the clinical onset of dementia. It has been proposed that approximately 7% of people diagnosed with MCI eventually progress to Alzheimer's dementia (Mitchell and Shiri-Feshki, 2009). MCI is generally defined as memory impairment, despite normal daily functioning (Petersen, 2004). It has also been suggested that MCI is not a unitary disorder, but it can be further divided into various subtypes, indicating mostly

the etiology: vascular, metabolic, amnestic, etc. (Petersen, 2004). Among them, the amnestic subtype it is considered to be a preclinical stage of AD (Dubois and Albert, 2004; Petersen, 2004; Vos et al., 2013).

The purpose of the present study is to investigate brain functional alterations that may characterize the amnesic subtype of MCI in order to aid to the early diagnosis of AD. Functional analysis can be performed by employing neurophysiological features derived from electroencephalographic (EEG) rhythmic activity (Moretti et al., 2011, 2012, 2013). During the last decade, a new category of metrics, based on the topological architecture of brain connectivity, has been introduced to estimate the organization characteristics of brain networks (Bassett and Bullmore, 2006). Connectomics may provide valuable information regarding the quantification of the network properties (Van Dijk et al., 2010). They employ either structural or functional connectivity to construct brain networks. Network properties are then computed through graph theory analysis (Stam and Reijneveld, 2007). A major notion of graph theory is that of small-world, which describes how efficient and cost-effective the network is. Computation of the small-world value considers both the quality of local information processing and the co-operation of distant brain regions. Therefore, brain networks with large small-world values are densely locally clustered, and at the same time employ the optimal number of distant connections to process information more efficiently and with lower information cost (Bassett and Bullmore, 2006; Bullmore and Sporns, 2009).

During the last few years, several research efforts have provided evidence of loss of "small-worldness" and reorganization of the brain networks due to neurodegeneration (Stam et al., 2009; Sanz-Arigita et al., 2010; Zhao et al., 2012). The majority of these studies have compared healthy adult participants with dementia patients. To the best of our knowledge, only a couple of studies so far have analyzed small-world networks in MCI patients using magnetoencephalography (MEG) (Buldú et al., 2011) and functional MRI (Seo et al., 2013), respectively. Both studies found abnormally increased and decreased synchronization in (pre)frontal and parieto-occipital regions respectively in the MCI patients compared to the healthy adults. More specifically, MCI patients showed an abnormal synchronization increase in comparison to healthy controls during the execution of memory tasks. It was associated with high energy expenditure which may be attributed to the existence of compensatory mechanisms recruited by MCI patients toward the successful execution of cognitive functioning (Buldú et al., 2011). Another study reported loss of functional integration as quantified by the characteristic path length (Seo et al., 2013). However, findings are quite contradictory among studies, since some of them report either no significant changes (Seo et al., 2013) or increased characteristic path lengths for the patients suffering from Alzheimer's (Yao et al., 2010; Zhao et al., 2012). Seo et al. reported diminished information transfer among brain regions for both MCI and MD participants due to functional impairment of the hubs, which are network nodes connecting local networks and facilitating global information processing (Seo et al., 2013).

Binary brain networks are usually constructed by applying a threshold to the metric quantifying the synchronization between two network nodes. A pair of nodes is connected with a network edge when the synchronization degree between these two nodes exceeds the pre-defined threshold. The ratio of the number of network connections (edges) to the number of possible edges is defined as the network's density. The threshold selection is important for the network formation. Application of a fixed threshold value is vulnerable to inter-participant variability, thereby resulting in networks with different density values. The latter influences the network properties (characteristic path length, mean cluster coefficient) and computation of small-worldness cannot be easily performed. Aiming to face this methodological limitation, recent studies adopted the adaptive threshold selection for each participant in order to produce brain networks of fixed density. So, all graphs may have the same number of edges; in this way, group comparison is facilitated. However, there is not yet a gold standard for selecting a fixed density-based threshold. Therefore, the full network analysis is repeated over a density range. Adopting the aforementioned methodological approach, a more recent study recruited a large number of participants (94 controls, 183 MCI patients and 216 MD patients) employing fluorodeoxyglucose positron emission tomography (FDG-PET) (Seo et al., 2013). In addition to the global network analysis through the small-world property, this research investigated the vulnerability of the network hubs. The results showed that both MCI and AD groups had lower local clustering compared to healthy controls. Both pathological groups demonstrated vulnerability of the nodes that are crucial for the information transfer within the brain network (functional hubs). These hubs were mainly associated with the Default Mode Network (DMN).

It has been, therefore, suggested that brain networks are altered in people with neurodegenerative brain disorders, and this alteration is usually evidenced as diminished local processing and disrupted co-operative activity among distant brain regions. However, most focus has so far been placed on the clinical AD phase, while research on functional network analysis during the preclinical (aMCI) phase is scarce. Electroencephalographic (EEG) analysis may provide a direct window of brain functioning. Its excellent temporal resolution could offer a reliable way of quantifying brain co-operative activity during the resting-state condition. Aiming to enhance the understanding of the disease progression and to propose contemporary mathematical tools able to identify early functional disorganization phenomena, this piece of work employs EEG recordings and attempts to answer the following research questions:

1. Is there any evidence of functional disorganization in aMCI, which can be differentiated from healthy aging?
2. Is there a relationship between network architecture and general cognitive state?
3. Are there any significant differences in the network disorganization among aMCI and MD groups? If yes could we also detect any recruitment of additional brain regions during the prodromal phase?

According to previous evidence we expect that aMCI patients will exhibit significant network deficiency as compared to healthy older adults (Buldú et al., 2011; Seo et al., 2013). We also expect

network disorganization in aMCI to result mostly from a reduced local information processing capacity as expressed by *the mean cluster coefficient* value (Seo et al., 2013). Since previous research has shown that the *characteristic path length*, which quantifies information integration and transmission, remains relatively stable across different neurodegenerative phases in AD (Seo et al., 2013), we do not expect this parameter to be affected in the groups of aMCI or MD, relative to the group of healthy controls. The interplay among reduced local processing and relatively stable information transmission is hypothesized to affect the global network functional organization. Since aMCI is regarded as the earliest AD phase, we expect that aMCI individuals would exhibit network deficiencies similar to those of patients suffering from AD and these alterations would be mainly manifested as a disrupted small-world property and abnormal local information processing (Buldú et al., 2011; Seo et al., 2013). It is also expected that the global network architecture would be correlated with neuropsychological tests estimating the generic cognitive status. Finally, the two pathological groups, aMCI and MD, would probably show a vulnerability of network nodes that are crucial for information transfer and cognitive functioning (Seo et al., 2013). These nodes are defined as network hubs and their robustness is estimated by centrality metrics. However, since the aMCI patients relatively preserve their cognitive and daily functioning, compensatory mechanisms may invoke a network reformation in that stage. Therefore, we hypothesize that functional hubs occurred in the healthy brain become less robust and additional hubs are formed during the aMCI phase (Qi et al., 2010).

MATERIALS AND METHODS

PARTICIPANTS

Twenty-three cognitively healthy older adults, 17 aMCI and 24 mild demented (MD) individuals participated in the present study. All of them went through a neuropsychological assessment which was part of the screening process for the *Long Lasting Memories* (LLM) project. LLM was a multi-centric, European Commission-funded project that proposed a computerized intervention of cognitive and physical exercise in order to promote independent living of senior participants (www.longlastingmemories.eu) (Bamidis et al., 2011; González-Palau et al., 2014). Screening took place 1–14 days before the participants' enrollment to the training (Frantzidis et al., 2014). Prior to neurophysiological acquisition, all participants were informed about the study and signed an informed consent form. The study was approved by the ethics committee of the Greek Association of Alzheimer's Disease and Related Disorders.

The following Table (**Table 1**) reports information about the participants' age and generic cognitive status as estimated by the Mini Mental State Examination (MMSE) and the Montreal Cognitive Assessment (MoCA) test (mean values ± standard deviation), and the number of participants per group. The groups were matched on age and male-to female ratios (all $p_s > 0.05$).

Table 1 | Mean age, sex and cognitive status for the participants of each group enrolled in the present study.

Group	Age	Number of participants	MMSE	MoCA
Healthy	68.0 ± 5.5	23 (6 males)	28.0 ± 2.1	26.0 ± 2.4
aMCI	68.6 ± 2.7	17 (4 males)	25.6 ± 2.2	25.6 ± 2.2
MD	72.3 ± 6.3	24 (7 males)	22.3 ± 2.5	17.3 ± 4.3

NEUROPSYCHOLOGICAL EXAMINATION

The neuropsychological examination included a complete set of tests aiming to assess the participant's generic cognitive status as well as other specific cognitive domains (verbal memory, executive functions, independent living, etc.) that are essential to the diagnostic procedure and the group formation. A detailed list may be found in Bamidis et al. (2012).

MEDICAL EXAMINATION

Medical examination consisted of a full blood count, biochemical tests and examination of various parameters such as thyroid hormones, anti-thyroid auto-antibodies, homocysteine and folic acid levels. The Erythrocyte Sedimentation Rate (ESR) was also estimated. Neuroimaging examination either through MRI or Computerized Tomography (CT) was adopted to exclude participants suffering from various parameters that may influence the study results (e.g., cancer of the central nervous system, hypercholesterolemia, etc.). Finally, the participants visited a doctor involved in the current study. Their medical and family history as well as their current and past medication were recorded.

DIAGNOSTIC PROCEDURE

A dementia expert neurologist performed the diagnosis of each participant considering the aforementioned examinations. AD diagnosis was performed according to both the DSM-IV and the criteria of the National Institute of Neurological and Communicative Disorders and Alzheimer's Disease and Related Disorders (NINCDS-ADRDA) (McKhann et al., 1984). Patients suffering from aMCI, met Petersen's criteria (Petersen, 2004). The study groups were matched according to the baseline demographic variables (age and sex). This study was focused on MCI patients suffering from multiple domains and having as major problem that of memory impairment (Petersen, 2004). This group of patients would be referred as aMCI in the remaining of the manuscript, but merely for briefness, as the most appropriate term is that of multiple domain + amnestic MCI (Petersen, 2004).

EEG ANALYSIS

Data acquisition and pre-processing

Neurophysiological data acquisition was performed through a Nihon Kohden JE-207A. The device was equipped with 57 active electrodes attached on a cap fitted to the scalp (EASYCAP). There were also 2 reference electrodes attached to the mastoids and a ground electrode placed at a left anterior position. Both vertical and horizontal electrooculograms (EOG) and electrocardiographic (ECG) activity were recorded through bipolar electrodes. Electrode impendances of brain signals, ground electrode and references were kept lower than 2 KΩs. The sampling rate was set at 500 Hz. Participants were sitting in a comfortable armed chair located in a quiet room with minimal ambient light. They were

instructed to remain calm, with their eyes closed, for 5 min at least.

The brain electrodes were re-referenced using the two reference electrodes located on the mastoids in a way described also in Frantzidis et al. (2014). Then, Butterworth digital filtering of 3rd order was performed through a high pass filter with cut-off frequency at 1 Hz and a notch filter centered on 50 Hz. Independent Component Analysis (ICA) was then employed to remove artifactual components. Finally, visual inspection was performed to eliminate data segments contaminated with noise. The aforementioned pre-processing procedure was performed through the Matlab Signal Processing Toolbox and the EEGLAB graphic user interface (Delorme and Makeig, 2004).

Synchronization analysis

The synchronization analysis involved 75 epochs of artifact-free, continuous data of high quality (**Figure 1**; Step "A"). The duration of each epoch was set at 20 s, since it was demonstrated in a previous work that this time interval is sufficient for extracting the synchronization degree in a robust way (Gudmundsson et al., 2007; Hsu et al., 2012; Frantzidis et al., 2014). Aiming to avoid methodological and sampling errors, the epoch selection was performed in a completely randomized way. More specifically, a random number generator output choices of continuous, artifact-free epochs to be used for the unbiased synchronization analysis.

Synchronization analysis (**Figure 1**; Steps "B-D") aimed firstly at the robust extraction of activity for each frequency band for every electrode (Step "B"), its relative energy contribution (Step "C") and finally at the quantification of the co-operative degree among pairs of electrodes (Step "D") by employing wavelet analysis through the Orthogonal Discrete Wavelet Transform (ODWT). Wavelets were subjected to scaling and translation in order to extract both frequency and time-dependent components with optimal resolution. ODWT also involved an iterative decomposition scheme through recursive low-pass filtering for computing the wavelet coefficients of the five frequency bands in a way that discarded redundant information, while allowing the perfect reconstruction of the whole EEG. Wavelet coefficient amplitudes indicated the degree of correlation among the wavelet and the signal, while the sign of each coefficient represented the type of correlation (positive/negative). All computations were implemented through Matlab functions (Wavelet Toolbox).

The family of 5th order bi-orthogonal wavelets was selected as the mother wavelet (Frantzidis et al., 2010, 2014). This specific type of wavelets was selected due to its resemblance with common EEG waveforms and its attractive mathematical properties (e.g., semi-orthogonality, symmetry, smoothness and maximum time-frequency resolution). Therefore, phase distortion and discontinuity effects are avoided (Unser et al., 1992; Quian Quiroga and Schürmann, 1999; Frantzidis et al., 2010). Each epoch was divided in non-overlapping windows of 128 ms duration and computations were performed for each window, in which the first step was the computation of the wavelet coefficients using a decomposition scheme of $j = 1 \ldots 5$ levels. Multiple coefficients ($k = 1 \ldots K$) were calculated for each decomposition level, except of the last one ($j = 5$). The energy of each frequency band (E_j)

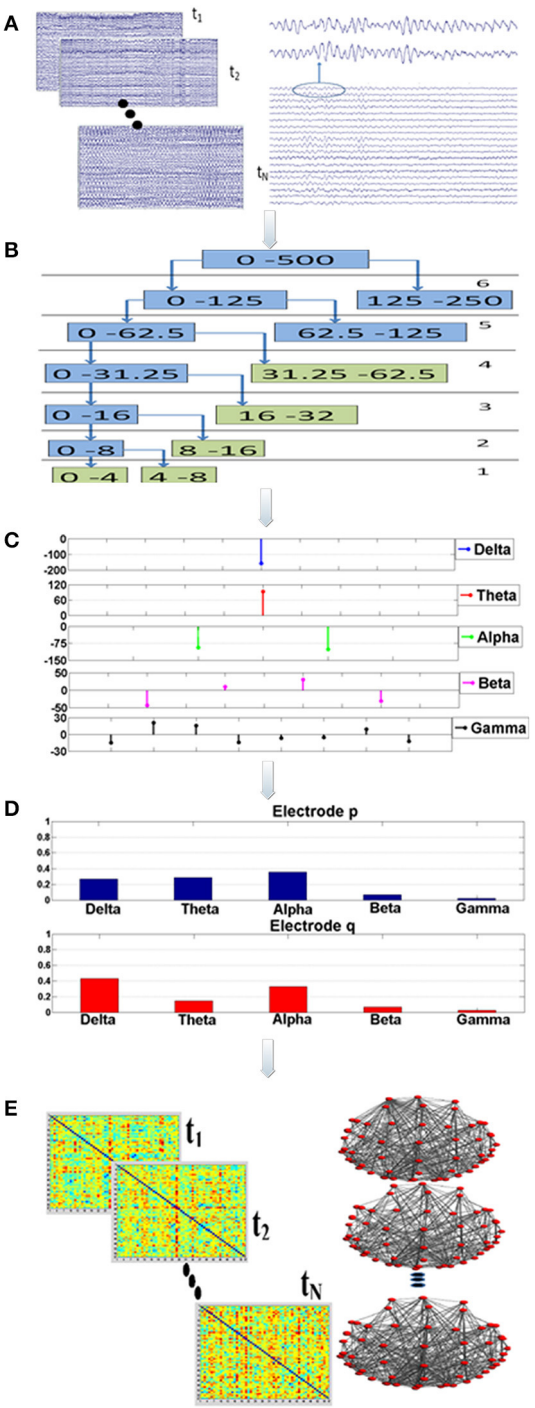

FIGURE 1 | Visualization of the proposed analysis framework: there are five main analysis steps (A–E). Firstly, a randomization, bootstrap technique* is employed during step "A" to select ($N = 75$) multiple, artifact free data epochs. This bootstrap technique is implemented through a generator of random numbers which produces choices of data epochs. Each epoch lasts for 20 s. For each data segment and for each electrode the Orthogonal Discrete Wavelet Transform (ODWT) is applied through an iterative, recursive decomposition scheme (Step "B"). The ODWT framework results in the estimation of the wavelet coefficients for each frequency band and for each epoch. The computations are performed on

(Continued)

FIGURE 1 | Continued
128 ms intervals, resulting in one (1) wavelet coefficient for the slow (delta, theta rhythms), two (2) coefficients for the alpha, four (4) for beta and eight (8) for gamma (Step "C"). These coefficients are then squared in order to express the rhythm's energy. So, the relative energy contribution of each frequency band is then computed by dividing the energy of each rhythm by the total EEG energy during Step "D." The Relative Wavelet Entropy (RWE) is then computed for each electrode pair. The RWE provides a directed metric of the co-operative degree among two electrodes. Then, synchronization matrices based on the RWE values are formed. These matrices are then thresholded and directed, non-weighted networks are formed. These networks are employed toward the estimation of both global (small-world, characteristic path length, mean cluster coefficient) and local (relative betweenness centrality) characteristics.

was estimated by firstly squaring and then summing the wavelet coefficients (C_k) corresponding to each rhythm:

$$E_j = \sum_{k=1}^{K} \left| C_k^2 \right|, \mathrm{j} = 1 \ldots 5 \quad (1)$$

A simple summation of all energies for each frequency band provided the total EEG energy:

$$E_{tot} = \sum_{j=1}^{5} E_j \quad (2)$$

Relative energies at each frequency band were estimated by dividing each absolute energy value E_j with the total energy E_{tot}.

These computations involved the 57 brain electrodes that formed 3192 electrode pairs. The number of electrode pairs was computed as follows: each one of the 57 electrodes was compared with all the other electrodes. Since the metric is a directional one the electrode pair (p, q) is different from the pair (q, p). Therefore, we had $57 \times 57 = 3249$ comparisons. Among these there are 57 pairs that compare the same electrode (p, p). That electrode pairs are not meaningful and were subtracted. Therefore, the total number of electrode pairs is $3249-57 = 3192$. The mathematical framework resulted in a probabilistic energy distribution (**Figure 1**; Step "D") for each one of the 57 electrodes participating in the 3192 electrode pairs. The probabilistic energy distribution of each electrode was consisting of contributions of each frequency band (a positive number) to the total energy of a specific electrode for a given time period (window duration). Since, these numbers quantify the energy ratio of each frequency band to the total EEG energy, their summation was equal to one (Rosso et al., 2001; Frantzidis et al., 2010, 2014). Finally, the synchronization degree among each electrode pair was computed through the notion of the Relative Wavelet Entropy (RWE) which represented the co-operation degree of the generalized rhythmic activity among two distinct electrode sites (**Figure 1**; Step "E"). Since there were $N = 57$ electrodes, the dimension of the synchronization matrix is $N \times N = 57 \times 57$. In case of two electrodes with energy distributions p_j and q_j, the synchronization degree (RWE value) was given by the following formula (the smaller the RWE value, the greater the synchronization):

$$RWE = \sum_{j=1}^{5} p_j \times \ln\left(\frac{p_j}{q_j}\right) \quad (3)$$

Therefore, the main diagonal of the synchronization matrix contained zero values (comparison of a signal with itself). As mentioned earlier, these 57 electrode pairs do not participate in the computations.

NETWORK ANALYSIS

Synchronization matrix thresholding

Synchronization matrices were then passed through a threshold to be transformed into binary, directed brain graphs (**Figure 1**; Step "E"). Aiming to avoid the influence of methodological limitations posed by brain networks of varying density, the selection of an adaptive threshold was preferred. This choice ensured that the brain network of each participant would have the same number of edges. So, both global and local network properties (small-word value, characteristic path length, mean cluster coefficient, global efficiency and normalized relative betweenness) were quantified for each participant and for four (4) fixed density ranges (500, 600, 700, 800 edges). The number of edges corresponded to 15.39, 18.47, 21.55, and 24.62% density values, respectively. Analysis, over a wide density range was preferred since there is lack of a golden standard for density selection. It was also unknown whether the influence of neurodegeneration phenomena could be detected in both low and high density networks. The following section provides a brief description of these network characteristics.

Description of network parameters

A network is represented by a graph that consists of nodes and edges. Each electrode represents a node, which is connected with another one through an edge (Bassett and Bullmore, 2006). These edges may be directed (directed graphs) or not (undirected graphs). The size of a graph depends on the total number of nodes, while its degree is the mean value of edges per node. The distance between two nodes is computed by the total number of edges of the shortest path needed to reach from one node to another. The *characteristic path length* (L) is computed by the mean (or in some cases median) value of the shortest paths among all pairs of nodes (Bassett and Bullmore, 2006; Stam and Reijneveld, 2007; Bullmore and Sporns, 2009; Stam et al., 2009).

To calculate the *cluster coefficient, C*, for each node, a 3-step procedure is followed:

- Immediate neighbors of (those directly connected with) a given node are identified.
- The number of connections among immediate neighbors is computed (existing connections).
- C, for a given vertex/node, is then computed as the ratio of the number of existing connections to the total number of all possible connections in the immediate vertex neighborhood, ranging from zero to one. Finally, the mean cluster coefficient is computed as the mean value of all cluster coefficient values (Lithari et al., 2012).

The small-world property, introduced by Watts and Strogatz (1998), is usually employed to characterize network architectures by means of dense clustering of local connections, as well as, short characteristic path lengths achieved by a few long-range connections, thereby facilitating the fast and efficient information transfer among all network nodes. Thus, small-network topologies offer an attractive model for brain network connectivity quantification, since they combine strong local information processing (high cluster coefficient value) with fast and efficient, global information transfer through small characteristic path length (Sanz-Arigita et al., 2010; Buldú et al., 2011; De Haan et al., 2012; Lithari et al., 2012; Seo et al., 2013); estimating the small-world property involves computation of the network characteristic path length (L) and mean cluster coefficient (C), as well as, the comparison with the corresponding properties (L_{rand} and C_{rand}) of a random graph containing the same number of nodes (N), edges (K) and degree of distribution as shown by formulae (4) and (5):

$$L_{rand} = \frac{\ln(N)}{\ln\left(\frac{k}{N} - 1\right)} \quad (4)$$

$$C_{rand} = \frac{\left(\frac{k}{N}\right)}{N} \quad (5)$$

Then the ratios $\lambda = L/L_{rand}$ and $\gamma = C/C_{rand}$ are combined to retrieve the small world property (sigma), sigma $= \gamma/\lambda$. Small-world networks exhibit sigma values greater than one (Bassett and Bullmore, 2006).

The local nodal metric of betweenness centrality, B_i (for each node $i = 1 \ldots N$), is also employed to investigate whether the age-related neuro-degeneration affects nodes with a functionally significant role (hubs) or not. B_i is defined as the number of shortest paths from all nodes to all others that run through node i. Therefore, it quantifies the amount of information transferred through node i. To normalize raw B_i values, the value for each node is divided by the mean B_i value of the whole network. In this way, and when B_i is greater than 1.5, a node can be regarded as a functional hub. This parameter setting was adopted from a previous study (Seo et al., 2013). The threshold value, which was a strict one, was the same.

RESULTS

GLOBAL CHARACTERISTICS AND THEIR ALTERATIONS IN AMCI AND MD

All groups (Healthy, aMCI, MD) demonstrated small-world characteristics ($\sigma > 1$) over the entire range of densities. Tables S1–S3 in Supplementary Material show means and standard deviation as a function of group and density for each network characteristic. **Figure 2** illustrates the mean (grand average) brain networks for each one of the three groups (Healthy, aMCI, MD) as well as the networks with the strongest (1%) connections only. The visualization is performed for the entire density range employed in the study ($N = 500, 600, 700, 800$).

To analyze the data we conducted a 3×4 by (3) MANOVA with group (Healthy, aMCI, and MD) as the between subject factor, density (500, 600, 700, 800) as the within subject factor,

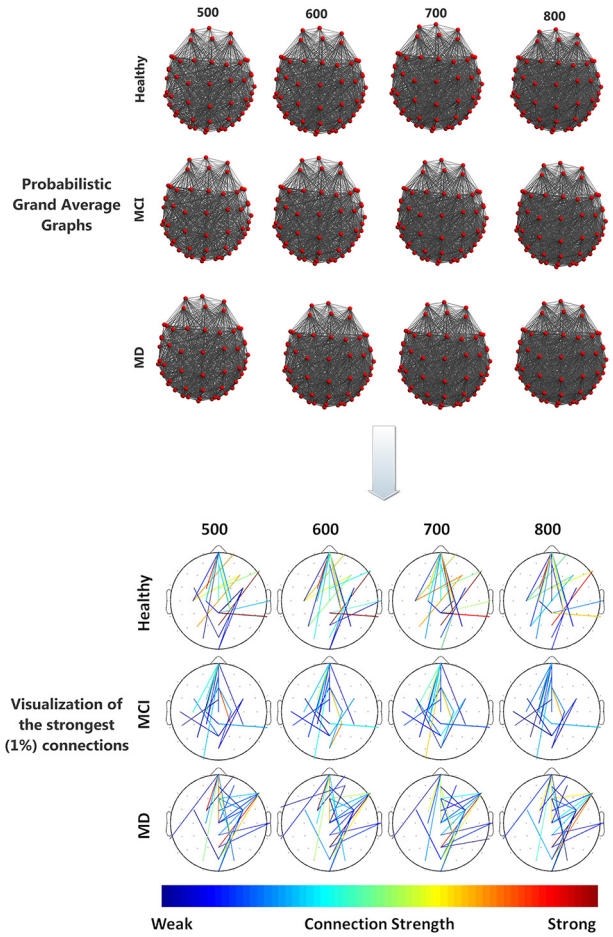

FIGURE 2 | (Top) Visualization of grand average brain graphs for each one of the three study groups (Healthy, MCI, MD) and for each edge density value (500, 600, 700, 800). **(Bottom)** visualization of the strongest (1%) network connections and their (edge) strengths, depicted through a colorbar.

and the 3 interrelated dependent variables (small-world value, C and L). Using Pillai' trace, there were significant effects of group [$V = 0.44, F_{(6,\ 120)} = 5.63, p < 0.0001$], and density [$V = 0.999, F_{(9,\ 53)} = 8766.855, p < 0.0001$], and a significant group by density interaction [$V = 0.541, F_{(18,\ 108)} = 2.225, p = 0.006$] on small world property, Cluster Coefficient and Length path. Separate 2×4 ANOVAs on the 3 outcomes variables revealed a significant[1] main effect of group for the small world property, $F_{(2,\ 61)} = 17.92$; $p < 0.0001$, and the Cluster Coefficient $F_{(2,\ 61)} = 10.83$; $p < 0.0001$. Also there was a main effect of density for the three outcomes variables, small world property, $F_{(3,\ 183)} = 4236.71$, $p < 0.0001$; cluster coefficient, $F_{(3,\ 183)} = 524.28$; $p < 0.0001$, and path length, $F_{(3,\ 183)} = 529.10$; $p < 0.0001$. Tukey HSD *post-hoc* comparisons for the group factor showed significant differences between the Healthy controls

[1]Notice: to correct for multiple analyses we adopted a stricter significance criterion, $p = 0.01$ *Bootstrapping involves the resampling of an observed dataset by randomly sampling it with replacement.

group (2.217) and the aMCI (2.146) and MD groups (2.099) for the Small World property, $p = 0.005$ and $p = 0.0001$, respectively. There were no significant differences between the aMCI and the MD groups. Similarly, for the Cluster Coefficient, there were significant differences between the Healthy controls group (0.549) and the aMCI (0.521), and MD groups (0.508), $p = 0.01$ and $p = 0.0002$, respectively. Again, there were no significant differences between the aMCI and the MD groups. For the Small World property, Tukey HSD *post-hoc* comparisons showed significant differences between the four density values, 500 (2.609), 600 (2.245), 700 (1.977), and 800 (1.784), all *p*s < 0.0001. That is, the Small World property value decreased as the density value increased. The same pattern was observed for the Path length ($Mean_{500} = 2.357$, $Mean_{600} = 2.199187$, $Mean_{700} = 2.071634$, $Mean_{800} = 1.962972$). The Path Length value decreased as the density value increased, all *p*s < 0.0001. Finally, for the Cluster Coefficient, Tukey HSD *post-hoc* comparisons showed again significant different between all density conditions ($Mean_{500} = 0.489$, $Mean_{600} = 0.518$, $Mean_{700} = 0.539$, $Mean_{800} = 0.559$), all *p*s < 0.0001. However, the Cluster Coefficient value increased as the density increased. The statistically significant results regarding the graph parameter differences for the three groups are visualized in **Figure 3**.

In order to test if there was a linear relationship between cognitive status as measured with the MMSE and the MOCA, and the small-world property value we computed Pearson's correlations. The analyses showed a significant positive correlation between the MMSE scores and the Small World property, $r = 0.367$, $df = 63$, $p = 0.003$, and between the MoCA scores and the Small World property, $r = 0.470$, $df = 63$, $p < 0.0001$. **Figure 4** illustrates these correlations through scatter plots of the MoCA/MMSE data distributions against the Small-World data. More specifically, the horizontal axis (Small-World value) was estimated as the mean of the four small-world values of each edge density range ($N = 500$, 600, 700, 800). Since this metric quantifies the linear correlation among two variables, the statistically significant results indicate a linear correlation of medium strength among the network architecture and the performance on the generic neuropsychological estimation. This finding may demonstrate that the degree of network performance may reflect deficiency in generic cognitive processing.

FUNCTIONAL HUB IDENTIFICATION

Following the work of Seo et al. (2013), electrodes were identified as functional hubs based on their standardized Bi value ($Bi \geq 1.5$). The identification procedure was performed for each one of the three groups (Healthy, aMCI, MD) for the density condition $N = 500$ edges. Visualization of the functional hubs is presented in **Figure 5**.

The mean normalized B_i value of the identified hubs of the healthy group computed for all participants and all groups (**Table 2**). These values were then submitted to One-Way ANOVA with group as the between subject factor. Results showed

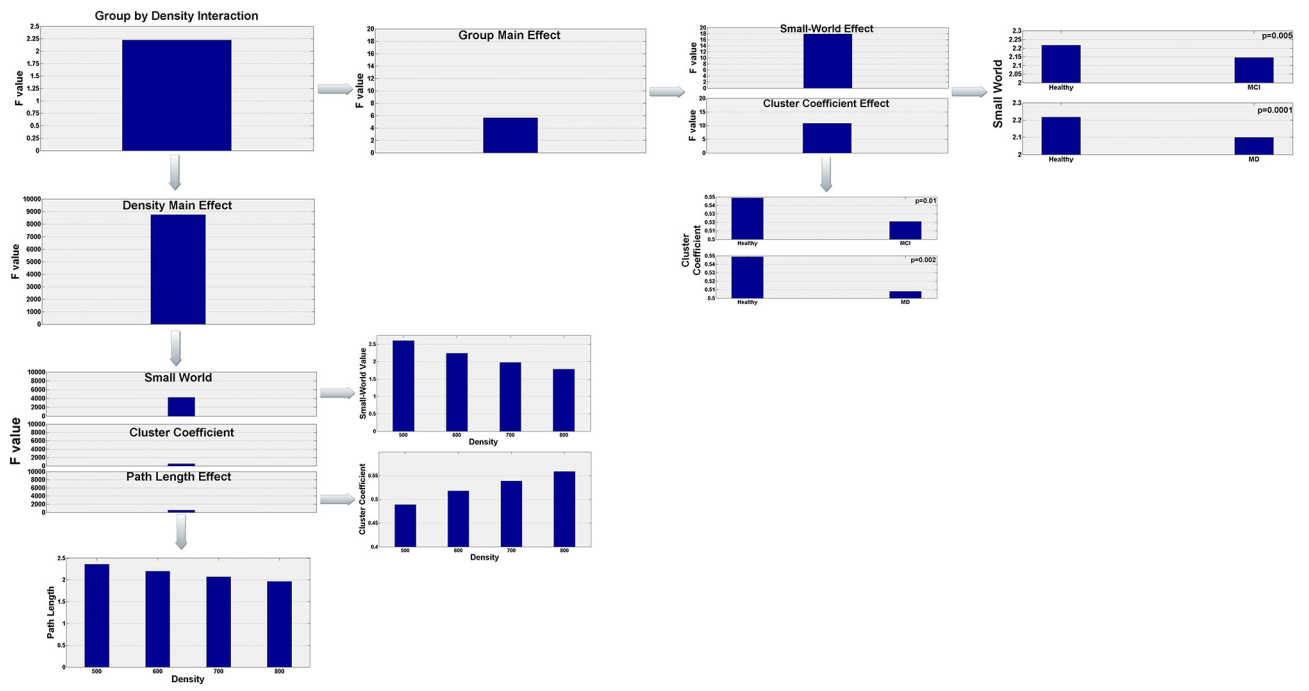

FIGURE 3 | Visualization of the statistically significant network parameters results (Small-World, Characteristic Path Length, Cluster Coefficient). Results refer to network differences among the three groups (Healthy, aMCI, MD) and are dependent on the density parameter ($N = 500$, 600, 700, 800). More specifically, statistical analysis demonstrated a significant group by density interaction. Both group and density main effects were further analyzed in order to highlight how global network characteristics differ among the three groups and how these parameters are affected by the density of the graph.

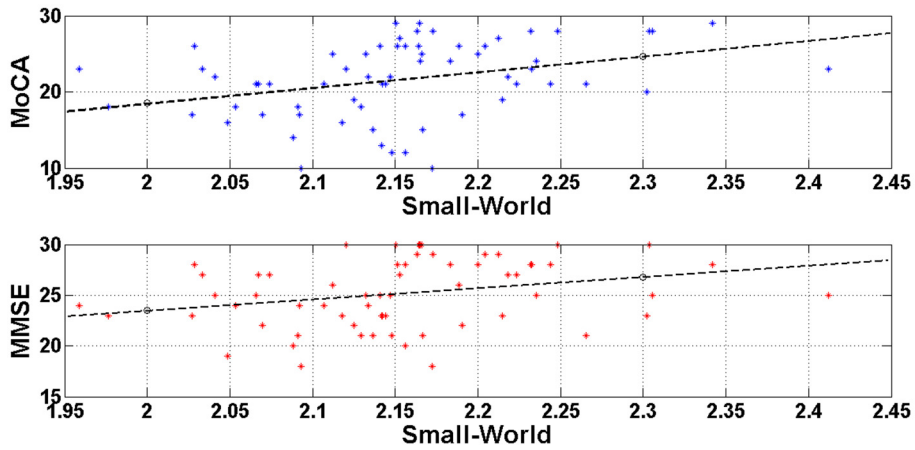

FIGURE 4 | Visualization of the linear correlation among the network architecture (Small-World) with the generic neuropsychological tests. The correlation degree was estimated through the Pearson coefficient and was greater for the MoCA ($r = 0.470$) and lower for the MMSE ($r = 0.367$). Both correlations would be characterized of medium strength and may indicate that deficient generic cognition may be attributed to disturbances of the resting-state brain networks.

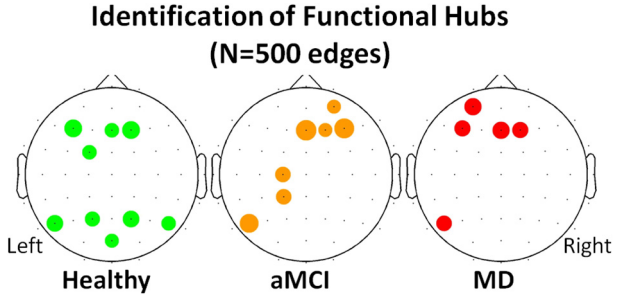

FIGURE 5 | Visualization of the functional hubs identified for each one of the three groups (Healthy, aMCI and MD). The hub identification was based on the normalized relative betweenness centrality value. According to a previous study, a node is defined as a hub when its centrality value is greater or equal to 1.5 (Seo et al., 2013). This threshold is a strict one. Therefore, the analysis was performed on the lower density range ($N = 500$). A small density value is more likely to result in a greater number of functional hubs. The hubs (names and locations) are visualized in a sensor level for each group. The hub strength is also reported through its relative betweenness centrality (b_i) value.

Table 2 | Description of the functional hubs identified in the three (Healthy controls, aMCI, MD) groups.

Electrode	Healthy	aMCI	MD
	Relative betweenness centrality (B_i)		
F3	1.9149		1.8843
Fz	1.5812	2.2090	1.7431
FC1	1.6167		
POz	1.5173		
F2	1.9143	2.1717	1.8704
P1	1.6265		
P2	1.8004		
P5	1.8483	2.0669	1.6949
P6	1.5940		
F4		1.5521	
CP1		1.5511	
C1		1.7077	
AF4		1.6829	
AF3			1.7343

The functional hubs were identified in terms of their normalized relative betweenness centrality value (B_i). Nine (9) hubs covering mainly frontal and parietal areas were identified in the healthy controls. Seven (7) hubs located mainly on right frontal and left posterior areas were identified in the aMCI patients. Five (5) hubs located mainly on frontal and on left parietal areas were identified in the MD group.

a significant main effect of group, $F_{(2,\ 61)} = 5.87$; $p = 0.005$. Tukey HSD *post-hoc* comparisons showed significant differences between the Healthy Controls group (Mean = 1.849; $SD = 0.463$) and the aMCI (Mean = 1.365; $SD = 0.523$) and MD groups (Mean = 1.503; $SD = 0.435$), $p = 0.006$, and $p = 0.037$, respectively. There were no significant differences between the aMCI and the MD groups. That is, both aMCI and MD groups had significantly lower nodal strength of functional hubs as compared to healthy controls.

To investigate whether neurodegeneration induced the additional recruitment of anterior, bilateral regions we proposed the computation of the Anterior Hub Ratio (AHR) as the ratio of the nodal significance of *left anterior/right anterior* functional hubs in terms of relative betweenness centrality. This AHR metric quantifies the functional interplay among anterior hemispheres. It was based on the hub identification described previously. So, the nominator included the left anterior hubs (F3, FC1, AF3, F1, FC3) and the denominator included the right anterior hubs (F2, F4, Fz, Afz, FCz, FC2, FC4). One-Way ANOVA with group as the between subject factor showed a significant main effect of group [$F_{(2,\ 61)} = 3.27$, $p = 0.045$]. Tukey HSD *post-hoc* comparisons showed significant differences

only between the group of Healthy controls (Mean = 0.517; $SD = 0.327$) and the group of aMCI (Mean = 1.179, $SD = 1.279$), $p = 0.0430$. There were no significant differences between the MD group (Mean = 0.943, $SD = 0.868$) and the other groups.

DISCUSSION

To investigate functional network organization in aMCI and MD, we employed graph analysis of resting-state electroencephalographic data. The results of the global characteristics indicated that all three (3) groups demonstrated small-world characteristics. However, both aMCI and MD patients showed reduced global network properties (small-world value and mean cluster coefficient) in comparison with the healthy controls. This result is in agreement with previous studies that showed a loss of optimal network organization in AD patients (Stam et al., 2007; He et al., 2008; Supekar et al., 2008; Zhao et al., 2012) and the general category of MCI (Yao et al., 2010; Seo et al., 2013).

Previous studies with MCI participants yielded contradictory results. Specifically, Yao et al. performed cortical network analysis through gray matter volume characteristics obtained from MRI (Yao et al., 2010). The study design included 98 healthy controls, 113 MCI participants and 91 AD patients. The MCI group exhibited intermediate small-world values. Further analysis, revealed that comparison of the MCI network characteristics (cluster coefficient and characteristic path length) either with the healthy or the AD group did not reach statistical significance. Nevertheless, in a more recent study recruiting 94 healthy controls, 183 MCI and 216 AD patients, graph analysis was performed through FDG-PET data. It was found that both MCI and AD patients demonstrated lower cluster coefficient than healthy controls, while the characteristic path length was not affected. The study also reported that MCI participants exhibited the lower cluster coefficient values. (Seo et al., 2013). Aiming to avoid the heterogeneity of the entire MCI spectrum, we tested only patients suffering from the amnestic subtype which is considered to be a pre-stage of AD (Dubois and Albert, 2004; Petersen, 2004). Our results support that there are no differences between aMCI and MD patients in terms of network function (small-world, mean cluster coefficient and characteristic path length). That is, both groups of patients showed the same pattern of network property breakdown as compared to Healthy controls. Since these two groups are diagnostically different, we consider these results in terms of compensatory mechanisms. That is, we propose that compensatory mechanisms are preserved in aMCI, and that loss of these mechanisms may lead to progression to mild dementia. This hypothesis would be in agreement with our finding of additional hub formations in the group of aMCI.

However, absence of statistically significant findings regarding the characteristic path length seems to be in contradiction with the only other (prior) study that has investigated network organization in a group of 37 aMCI patients (Wang et al., 2013). That study employed fMRI recordings combined with frequency-dependent wavelet based correlation analysis and reported abnormally increased *path length characteristic* in the group of aMCI. This contradiction may be attributed to the much smaller number of participants that our study enrolled in both groups. Another possible explanation may be that Wang et al. extracted frequency-dependent brain networks, while our methodology received the entire EEG range as input and computed the co-operative degree in terms of frequency-based similarity of the probability distribution among electrode pairs.

In addition, we found a statistically significant positive correlations between small-worldness and cognitive status as measured with MMSE and MoCA. That is, the more cognitively deteriorated (lower scores in MMSE and MoCA) the patients are, the less optimal the network organization is (lower small world values). This finding is also in agreement with a previous finding of a positive correlation between characteristic path length values and MMSE scores in a group of AD patients (De Haan et al., 2009). We deem our findings to be important in this sense, as we extended those results to small-world property which better quantifies the global network performance. In addition we included a larger sample with healthy adults, aMCI and MD individuals. Overall, these findings suggest network analysis may be used as a tool for detecting age-related pathological disorders due to neurodegeneration.

Local network analysis was performed through the identification of those nodes that were important for the network organization. Those nodes were named functional hubs. The hub definition was based on the amount of information flow the nodes transfer. The normalized betweenness centrality was previously proposed to be a robust metric of the hub strength (Seo et al., 2013). The results demonstrated that healthy hubs seem to be preserved to some extent during the aMCI and mild dementia phase. However, they are functionally impaired, as it is demonstrated by statistically significant decreases in terms of betweenness centrality. This finding may be indicative of deficiency due to neurodegeneration and impaired functional connection of distant brain regions. Apart from hub strength reductions, aMCI participants formed additional hubs especially in the left frontal and parietal regions. The hub formation may be attributed to compensatory mechanisms (Cabeza et al., 2002; Hämäläinen et al., 2007; Qi et al., 2010); according to these studies healthy elderly recruit additional frontal and parietal regions during memory processes (Cabeza et al., 2002), while increased frontal activation of MCI patients compared to controls is observed through fMRI recordings even in the resting state condition (Hämäläinen et al., 2007). A more recent study employing aMCI patients and fMRI during resting state reported diminished anterior DMN symmetry due to increased left frontal activation (Qi et al., 2010). The results derived from the proposed local characteristic analysis (strength of healthy hubs and additional hub formation in the pathological groups) are in line with previous findings, thereby implying a reorganization of the brain's architecture during early neurodegeneartion. The additional hubs are mainly evident in the preclinical (aMCI) phase and attenuate during the onset of the clinical AD phase. This temporal pattern seems to enhance the compensatory hypothesis.

The current piece of research employed brain network analysis on EEG recordings. Despite its excellent temporal resolution,

which facilitates the understanding of functional interactions among distant brain regions, EEG's spatial resolution is extremely low in comparison to other recording modalities (fMRI, PET, MEG). Moreover, it faces the problem of volume conduction especially, when analysis is not performed on the source level. Therefore, the interpretation of results, especially in the case of local characteristics analysis, should be supported by neuroimaging studies (Hämäläinen et al., 2007; Qi et al., 2010). To this extent, any synergy between EEG and fMRI with simultaneous recordings may be able to reliably track transient network alterations and their locations. However, the analysis performed herein with regards to estimating the brain network reorganization and the quantification of the underlying compensatory mechanisms was based on the definition of a Region of Interest (ROI). The ROI identification was based on the previous analysis step (identification of functional hubs) and on a priori hypothesis of an increased frontal symmetry (Hämäläinen et al., 2007; Qi et al., 2010). Despite the positive results and validating previous neuroimaging evidence (Qi et al., 2010), this point may be regarded as a current limitation, since it introduces a methodological bias posed by the study hypothesis. Finally, estimation of the disease progression was performed by forming three separate groups of participants and analyzing their brain network characteristics. However, longitudinal studies employing the same participants and investigating their network alterations during different temporal phases may estimate the disease progression much more accurately.

To sum up, this piece of work proposed a mathematical model consisting of both wavelet and brain network analysis to study neuropathological alterations due to AD and the disease progression. It provided evidence that AD evolution from its preclinical phase (aMCI) to the dementia phase is accompanied by a gradual loss of optimal brain network organization as quantified by the small-world property. This mainly occurs due to the reductions of local information processing, as expressed by lower values of the mean cluster coefficient. The degree of non-economical wiring was correlated with the amount of cognitive decline as estimated by generic neuropsychological testing (MMSE and MoCA). The functional disorganization of the EEG-based brain network is apparent during the aMCI phase. It often coexists with compensatory mechanisms involving the formation of additional hubs located mainly on left frontal and parietal regions. However, these mechanisms are transient and attenuate when progressing to the clinical AD phase. Then, the global brain network characteristics (small-world property and cluster coefficient) deteriorate much more. This computational framework seems to be a robust and reliable tool, which may be used toward the identification of functional alterations preceding structural isolation/atrophy in senior citizens facing increased risk of future progression to the clinical AD phase.

ACKNOWLEDGMENT

This research was partially funded by the European CIP-ICT-PSP.2008.1.4 Long Lasting memories (LLM) project (Project No. 238904) (www.longlastingmemories.eu).

SUPPLEMENTARY MATERIAL

The Supplementary Material for this article can be found online at: http://www.frontiersin.org/journal/10.3389/fnagi.2014.00224/abstract

REFERENCES

Albert, M. S., DeKosky, S. T., Dickson, D., Dubois, B., Feldman, H. H., Fox, N. C., et al. (2011). The diagnosis of mild cognitive impairment due to Alzheimer's Disease: recommendations from the national institute on Aging-Alzheimer's association workgroups on diagnostic guidelines for Alzheimer's Disease. *Alzheimers Dement.* 7, 270–279. doi: 10.1016/j.jalz.2011.03.008

Bamidis, P. D., Konstantinidis, E. I., Billis, A., Frantzidis, C., Tsolaki, M., Hlauschek, W., et al. (2011). "A Web services-based exergaming platform for senior citizens: the long lasting memories project approach to e-health care," in *Proceedings of the Annual International Conference of the IEEE Engineering in Medicine and Biology Society, EMBS, Art. No. 6090694* (Boston, MA), 2505–2509.

Bamidis, P. D., Baker, N., Franco, M., Losada, R., Papageorgiou, S., and Pattichis, C. S. (2012). *Long Lasting Memories Project Deliverable D1.4 Final Report.* Available online at: http://www.longlastingmemories.eu/sites/default/files/LLM_D1.4_final_report_public_v2.2doc.pdf, July 2012.

Bassett, D. S., and Bullmore, E. D. (2006). Small-world brain networks. *Neuroscientist* 12, 512–523. doi: 10.1177/1073858406293182

Buerger, K., Ewers, M., Pirttilä, T., Zinkowski, R., Alafuzoff, I., Teipel, S. J., et al. (2006). CSF phosphorylated tau protein correlates with neocortical neurofibrillary pathology in Alzheimer's Disease. *Brain* 129, 3035–3041. doi: 10.1093/brain/awl269

Buldú, J. M., Bajo, R., Maestú, F., Castellanos, N., Leyva, I., Gil, P., et al. (2011). Reorganization of functional networks in mild cognitive impairment. *PLoS ONE* 6:e19584. doi: 10.1371/journal.pone.0019584

Bullmore, E., and Sporns, O. (2009). Complex brain networks: graph theoretical analysis of structural and functional systems. *Nat. Rev. Neurosci.* 10, 186–198. doi: 10.1038/nrn2575

Cabeza, R., Anderson, N. D., Locantore, J. K., and McIntosh, A. R. (2002). Aging gracefully: compensatory brain activity in high-performing older adults. *Neuroimage* 17, 1394–1402. doi: 10.1006/nimg.2002.1280

Caselli, R. J., Reiman, E. M., Osborne, D., Hentz, J. G., Baxter, L. C., Hernandez, J. L., et al. (2004). Longitudinal changes in cognition and behavior in asymptomatic carriers of the APOE e4 allele. *Neurology* 62 1990–1995. doi: 10.1212/01.WNL.0000129533.26544.BF

Citron, M. (2010). Alzheimer's Disease: strategies for disease modification. *Nat. Rev. Drug Discov.* 9, 387–398. doi: 10.1038/nrd2896

De Haan, W., Pijnenburg, Y. A., Strijers, R. L., Van Der Made, Y., Van Der Flier, W. M., Scheltens, P., et al. (2009). Functional neural network analysis in frontotemporal dementia and Alzheimer's Disease using EEG and graph theory. *BMC Neurosci.* 10:101. doi: 10.1186/1471-2202-10-101

De Haan, W., Van Der Flier, W. M., Koene, T., Smits, L. L., Scheltens, P., and Stam, C. J. (2012). Disrupted modular brain dynamics reflect cognitive dysfunction in Alzheimer's Disease. *Neuroimage* 59, 3085–3093. doi: 10.1016/j.neuroimage.2011.11.055

Delbeuck, X., Van der Linden, M., and Collette, F. (2003). Alzheimer's Disease as a disconnection syndrome? *Neuropsychol. Rev.* 13, 79–92. doi: 10.1023/A:1023832305702

Delorme, A., and Makeig, S. (2004). EEGLAB: an open source toolbox for analysis of single-trial EEG dynamics including independent component analysis. *J. Neurosci. Methods* 134, 9–21. doi: 10.1016/j.jneumeth.2003.10.009

Drzezga, A., Becker, J. A., Van Dijk, K. R., Sreenivasan, A., Talukdar, T., Sullivan, C., et al. (2011). Neuronal dysfunction and disconnection of cortical hubs in non-demented subjects with elevated amyloid burden. *Brain* 134, 1635–1646. doi: 10.1093/brain/awr066

Dubois, B., and Albert, M. L. (2004). Amnestic MCI or prodromal Alzheimer's Disease? *Lancet Neurol.* 3, 246–248. doi: 10.1016/S1474-4422(04)00710-0

Frantzidis, C. A., Bratsas, C., Papadelis, C. L., Konstantinidis, E., Pappas, C., and Bamidis, P. D. (2010). Toward emotion aware computing: an integrated approach using multichannel neurophysiological recordings and affective visual stimuli. *IEEE Trans. Inf. Technol. Biomed.* 14, 589–597. doi: 10.1109/TITB.2010.2041553

Frantzidis, C. A., Ladas, A.-K. I., Vivas, A. B., Tsolaki, M., and Bamidis, P. D. (2014). Cognitive and physical training for the elderly: evaluating outcome efficacy by

means of neurophysiological synchronization. *Int. J. Psychophysiol.* 93, 1–11. doi: 10.1016/j.ijpsycho.2014.01.007

González-Palau, F., Franco, M., Bamidis, P. D., Losada, R., Parra, E., Papageorgiou, S., et al. (2014). The effects of a computer-based cognitive and physical training program in a healthy and mildly cognitive impaired aging sample. *Aging Ment. Health*. 18, 838–846. doi: 10.1080/13607863.2014.899972

Gudmundsson, S., Runarsson, T. P., Sigurdsson, S., Eiriksdottir, G., and Johnsen, K. (2007). Reliability of quantitative EEG features. *Clin. Neurophysiol*. 118, 2162–2171 doi: 10.1016/j.clinph.2007.06.018

Hämäläinen, A., Pihlajamäki, M., Tanila, H., Hänninen, T., Niskanen, E., Tervo, S., et al. (2007). Increased fMRI responses during encoding in mild cognitive impairment. *Neurobiol. Aging* 28, 1889–1903. doi: 10.1016/j.neurobiolaging.2006.08.008

He, Y., Chen, Z., and Evans, A. (2008). Structural insights into aberrant topological patterns of large-scale cortical networks in Alzheimer's Disease. *J. Neurosci*. 28, 4756–4766. doi: 10.1523/JNEUROSCI.0141-08.2008

Hsu, Y. F., Huang, Y. Z., Lin, Y. Y., Tang, C. W., Liao, K. K., Lee, P. L., et al. (2012). Intermittent theta burst stimulation over ipsilesional primary motor cortex of subacute ischemic stroke patients: a pilot study. *Brain Stimul*. 6, 166–174. doi: 10.1016/j.brs.2012.04.007

Lithari, C., Klados, M. A., Pappas, C., Albani, M., Kapoukranidou, D., Kovatsi, L., et al. (2012). Alcohol Affects the Brain's Resting-State Network in Social Drinkers. *PLoS ONE* 7:e48641. doi: 10.1371/journal.pone.0048641

McKhann, G., Drachman, D., Folstein, M., Katzman, R., Price, D., and Stadlan, E. M. (1984). Clinical diagnosis of Alzheimer's Disease report of the NINCDS—ADRDA work group* under the auspices of department of health and human services task force on Alzheimer's Disease. *Neurology* 34, 939–939. doi: 10.1212/WNL.34.7.939

Mitchell, A. J., and Shiri-Feshki, M. (2009). Rate of progression of mild cognitive impairment to dementia–meta-analysis of 41 robust inception cohort studies. *Acta Psychiatr. Scand*. 119, 252–265. doi: 10.1111/j.1600-0447.2008.01326.x

Moretti, D. V. D., Paternic, ò, Binetti, G., Zanetti, O., and Frisoni, G. B. (2013). EEG upper/low alpha frequency power ratio relates to temporo-parietal brain atrophy and memory performances in mild cognitive impairment. *Front. Aging Neurosci.* 5:63. doi: 10.3389/fnagi.2013.00063

Moretti, D. V., Frisoni, G. B., Fracassi, C., Pievani, M., Geroldi, C., Binetti, G., et al. (2011). MCI patients' EEGs show group differences between those who progress and those who do not progress to AD. *Neurobiol. Aging* 32, 563–571. doi: 10.1016/j.neurobiolaging.2009.04.003

Moretti, D. V., Prestia, A., Fracassi, C., Binetti, G., Zanetti, O., and Frisoni, G. B. (2012). Specific EEG changes associated with atrophy of hippocampus in subjects with mild cognitive impairment and Alzheimer's Disease. *Int. J. Alzheimers Dis*. 2012:253153. doi: 10.1155/2012/253153

Petersen, R. C. (2004). Mild cognitive impairment as a diagnostic entity. *J. Intern. Med*. 256, 183–194. doi: 10.1111/j.1365-2796.2004.01388.x

Petersen, R. C., Smith, G. E., Waring, S. C., Ivnik, R. J., Tangalos, E. G., and Kokmen, E. (1999). Mild cognitive impairment: clinical characterization and outcome. *Arch. Neurol*. 56, 303. doi: 10.1001/archneur.56.3.303

Qi, Z., Wu, X., Wang, Z., Zhang, N., Dong, H., Yao, L., et al. (2010). Impairment and compensation coexist in amnestic MCI default mode network. *Neuroimage* 50, 48–55. doi: 10.1016/j.neuroimage.2009.12.025

Quian Quiroga, R., and Schürmann, M. (1999). Functions and sources of event-related EEG alpha oscillations studied with the wavelet transform. *Clin. Neurophysiol.* 110, 643–654. doi: 10.1016/S1388-2457(99)00011-5

Rosso, O. A., Blanco, S., Yordanova, J., Kolev, V., Figliola, A., Schurmann, M., et al. (2001). Wavelet entropy: a new tool for analysis of short duration brain electrical signals. *J. Neurosci. Methods* 105, 65–76. doi: 10.1016/S0165-0270(00)00356-3

Sanz-Arigita, E. J., Schoonheim, M. M., Damoiseaux, J. S., Rombouts, S. A., Maris, E., Barkhof, F., et al. (2010). Loss of 'small-world'networks in Alzheimer's Disease: graph analysis of FMRI resting-state functional connectivity. *PLoS ONE* 5:e13788. doi: 10.1371/journal.pone.0013788

Seo, E. H., Lee, D. Y., Lee, J. M., Park, J. S., Sohn, B. K., Lee, D. S., et al. (2013). Whole-brain functional networks in cognitively normal, mild cognitive impairment, and Alzheimer's Disease. *PLoS ONE* 8:e53922. doi: 10.1371/journal.pone.0053922

Sperling, R. A., Aisen, P. S., Beckett, L. A., Bennett, D. A., Craft, S., Fagan, A. M., et al. (2011). Toward defining the preclinical stages of Alzheimer's Disease: recommendations from the national institute on Aging-Alzheimer's association workgroups on diagnostic guidelines for Alzheimer's Disease. *Alzheimers Dement*. 7, 280–292. doi: 10.1016/j.jalz.2011.03.003

Stam, C. J., De Haan, W., Daffertshofer, A., Jones, B. F., Manshanden, I., van Walsum, A. V. C., et al. (2009). Graph theoretical analysis of magnetoencephalographic functional connectivity in Alzheimer's Disease. *Brain* 132, 213–224. doi: 10.1093/brain/awn262

Stam, C. J., Jones, B. F., Nolte, G., Breakspear, M., and Scheltens, P. (2007). Small-world networks and functional connectivity in Alzheimer's Disease. *Cereb. Cortex* 17, 92–99. doi: 10.1093/cercor/bhj127

Stam, C. J., and Reijneveld, J. C. (2007). Graph theoretical analysis of complex networks in the brain. *Nonlinear Biomed. Phys*. 1:3. doi: 10.1186/1753-4631-1-3

Supekar, K., Menon, V., Rubin, D., Musen, M., and Greicius, M. D. (2008). Network analysis of intrinsic functional brain connectivity in Alzheimer's Disease. *PLoS Comput. Biol*. 4:e1000100. doi: 10.1371/journal.pcbi.1000100

Unser, M., Akram, A., and Murray, E. (1992). On the asymptotic convergence of B-spline wavelets to Gabor functions. *IEEE Trans. Inf. Theory* 38, 864–872. doi: 10.1109/18.119742

Van Dijk, K. R., Hedden, T., Venkataraman, A., Evans, K. C., Lazar, S. W., and Buckner, R. L. (2010). Intrinsic functional connectivity as a tool for human connectomics: theory, properties, and optimization. *J. Neurophysiol*. 103, 297–321. doi: 10.1152/jn.00783.2009

Vos, S. J., van Rossum, I. A., Verhey, F., Knol, D. L., Soininen, H., Wahlund, L. O., et al. (2013). Prediction of Alzheimer disease in subjects with amnestic and nonamnestic MCI. *Neurology* 80, 1124–1132. doi: 10.1212/WNL.0b013e318288690c

Wang, J., Zuo, X., Dai, Z., Xia, M., Zhao, Z., Zhao, X., et al. (2013). Disrupted functional brain connectome in individuals at risk for Alzheimer's Disease. *Biol. Psychiatry* 73, 472–481. doi: 10.1016/j.biopsych.2012.03.026

Watts, D. J., and Strogatz, S. H. (1998). Collective dynamics of 'small-world'networks. *Nature* 393, 440–442. doi: 10.1038/30918

Yao, Z., Zhang, Y., Lin, L., Zhou, Y., Xu, C., and Jiang, T. (2010). Abnormal cortical networks in mild cognitive impairment and Alzheimer's Disease. *PLoS Computat. Biol*. 6:e1001006. doi: 10.1371/journal.pcbi.1001006

Zhao, X., Liu, Y., Wang, X., Liu, B., Xi, Q., Guo, Q., et al. (2012). Disrupted small-world brain networks in moderate Alzheimer's Disease: a resting-state FMRI study. *PLoS ONE* 7:e33540. doi: 10.1371/journal.pone.0033540

Conflict of Interest Statement: The authors declare that the research was conducted in the absence of any commercial or financial relationships that could be construed as a potential conflict of interest.

Received: 16 April 2014; accepted: 08 August 2014; published online: 26 August 2014.
*Citation: Frantzidis CA, Vivas AB, Tsolaki A, Klados MA, Tsolaki M and Bamidis PD (2014) Functional disorganization of small-world brain networks in mild Alzheimer's Disease and amnestic Mild Cognitive Impairment: an EEG study using Relative Wavelet Entropy (RWE). Front. Aging Neurosci. **6**:224. doi: 10.3389/fnagi.2014.00224*
This article was submitted to the journal Frontiers in Aging Neuroscience.
Copyright © 2014 Frantzidis, Vivas, Tsolaki, Klados, Tsolaki and Bamidis. This is an open-access article distributed under the terms of the Creative Commons Attribution License (CC BY). The use, distribution or reproduction in other forums is permitted, provided the original author(s) or licensor are credited and that the original publication in this journal is cited, in accordance with accepted academic practice. No use, distribution or reproduction is permitted which does not comply with these terms.

frontiers in Aging Neuroscience

ORIGINAL RESEARCH
published: 20 March 2015
doi: 10.3389/fnagi.2015.00031

Theta and alpha EEG frequency interplay in subjects with mild cognitive impairment: evidence from EEG, MRI, and SPECT brain modifications

Davide V. Moretti *

Istituto di Ricovero e Cura a Carattere Scientifico San Giovanni di Dio – Fatebenefratelli, Brescia, Italy

Background: Temporo-parietal and medial temporal cortex atrophy are associated with mild cognitive impairment (MCI) due to Alzheimer disease (AD) as well as the reduction of regional cerebral blood perfusion in hippocampus. Moreover, the increase of EEG alpha3/alpha2 power ratio has been associated with MCI due to AD and with an increase in theta frequency power in a group of subjects with impaired cerebral perfusion in hippocampus.

Methods: Seventy four adult subjects with MCI underwent clinical and neuropsychological evaluation, electroencephalogram (EEG) recording and high resolution 3D magnetic resonance imaging (MRI). Among the patients, a subset of 27 subjects underwent also perfusion single-photon emission computed tomography and hippocampal atrophy evaluation. Alpha3/alpha2 power ratio as well as cortical thickness was computed for each subject. Three MCI groups were detected according to increasing tertile values of alpha3/alpha2 power ratio and difference of cortical thickness among the groups estimated.

Results: Higher alpha3/alpha2 power ratio group had wider cortical thinning than other groups, mapped to the Supramarginal and Precuneus bilaterally. Subjects with higher alpha3/alpha2 frequency power ratio showed a constant trend to a lower perfusion than lower alpha3/alpha2 group. Moreover, this group correlates with both a bigger hippocampal atrophy and an increase of theta frequency power.

Conclusion: Higher EEG alpha3/alpha2 power ratio was associated with temporo-parietal cortical thinning, hippocampal atrophy and reduction of regional cerebral perfusion in medial temporal cortex. In this group an increase of theta frequency power was detected inMCI subjects. The combination of higher EEG alpha3/alpha2 power ratio, cortical thickness measure and regional cerebral perfusion reveals a complex interplay between EEG cerebral rhythms, structural and functional brain modifications.

Keywords: theta, alpha, EEG, SPECT, MRI, midl cognitive impairment

OPEN ACCESS

Edited by:
Gemma Casadesus, Case Western Reserve University, USA

Reviewed by:
Pablo Billeke, Universidad del Desarrollo, Chile
Carlos Beas-Zarate, Universidad de Guadalajara Mexico, Mexico

***Correspondence:**
Davide V. Moretti, Istituto di Ricovero e Cura a Carattere Scientifico San Giovanni di Dio – Fatebenefratelli, Via Pilastroni 4, Brescia, Italy, davide.moretti@afar.it

Received: *12 June 2014*
Accepted: *27 February 2015*
Published: *20 March 2015*

Citation:
Moretti DV (2015) Theta and alpha EEG frequency interplay in subjects with mild cognitive impairment: evidence from EEG, MRI, and SPECT brain modifications. Front. Aging Neurosci. 7:31. doi: 10.3389/fnagi.2015.00031

Introduction

The MCI commonly represent the 'at-risk' state of developing dementia. In neurodegenerative disorders, like AD or other dementias, the brain networks modifies many years before clinical manifestations (Dubois et al., 2007; Hampel et al., 2007; Albert et al., 2011; Galluzzi et al., 2013). Recent MRI studies have demonstrated that a large neural network is altered in subjects with prodromal AD, including precuneus, medial temporal, parietal, and frontal cortices (Frisoni et al., 2006, 2007, 2008, 2009; Van Strien et al., 2009; Frisoni, 2012). In particular, subjects with cognitive decline have shown early atrophy and loss of gray matter in cortical specific brain areas (Frisoni et al., 2007, 2009), including hippocampal, medial temporal and parietal lobes. In the conceptual frame of the integration of biomarkers for an early and highly predictive diagnosis, the EEG could be a reliable tool (Missonnier et al., 2010). Indeed, it is widely accepted that the cerebral EEG rhythms reflect the underlying brain network activity (Steriade, 2006). As a consequence, modifications in EEG rhythms could be an early sign of disease associated with AD-related structural and functional networks. In particular, the study of alpha rhythm seems to be a very suitable tool to detect relationship between structural and functional brain networks. Previous studies has convincingly demonstrated that there are thalamo-cortical and cortico-cortical components which interact in the generation of cortical alpha rhythms (Lopes da Silva et al., 1980). According to the seminal paper of Lopes Da Silva, the disrupture of long-range network, inpinguing on low alpha frequency, is replaced by an increase in higher frequency (upper alpha) synchronization, which is based on narrower cell assemblies activity. Furthermore, the dynamic behavior of alpha rhythm is apparently due to some combination of global and local processes. The global processes appear to be analogous to large-scale coherent EEG observed in low alpha frequency, whereas the local processes seem to be analogous to the smaller (mesoscopic) scale columnar dynamics, observed in upper alpha frequency (Ingber and Nunez, 2011). Given the well-known loss of brain network complexity in AD pathology (Nunez, 1989; Stam et al., 2005), it is highly conceivable an impairment of long-range connectivity pathways, replaced by short-range, downsized, cell assemblies connections, resulting in a decrease of low alpha and an increase of upper alpha frequency power. Recent single-photon emission computed tomography (SPECT) studies have demonstrated that a large neural network is altered in subjects with prodromal AD, including precuneus, medial temporal, parietal and frontal cortices (Rodriguez et al., 1999). For instance, selective regional cerebral blood perfusion (rCBF) reductions in the left hippocampus and parahippocampal gyrus and in extended areas of cerebral association cortex were demonstrated in a 2-years follow-up clinical study with rCBF-SPECT (Pupi et al., 2005). Cross-sectional studies have shown rCBF and regional metabolic rates of glucose (rCMRgl) reductions in the resting state throughout the cortex in AD, involving distinctive brain structures such as the posterior cingulate/precuneus, temporoparietal, and frontal cortices (Frisoni, 2012). A positive SPECT scan raised the likelihood of diagnosing pathological AD from 84%, as defined by clinical diagnosis, to 92% (Frisoni, 2012). Recent results show that there is a hippocampal rCBF hypoperfusion in patients with mild AD (Moretti et al., 2012b), as well as that baseline SPECT can support outcome prediction in subjects with MCI (Pupi et al., 2005). Of note, rCBF (bilateral parietal perfusion) and qEEG (especially the slowest frequencies, i.e., 2–5.5 Hz) are confirmed to be good descriptors of AD severity. It is especially noteworthy that bilateral hippocampal rCBF reduction was the perfusional index best correlated with both cognitive performance and qEEG (Rodriguez et al., 1999). Recent studies confirms the relationship of higher alpha3/alpha2 frequency power ratio with a smaller hippocampal volume and a lower cerebral perfusion (Moretti et al., 2013b). Recently, it has been demonstrated that temporo-parietal and medial temporal cortex atrophy are associated with mild cognitive impairment (MCI) due to Alzheimer disease (AD) as well as the reduction of regional cerebral perfusion in hippocampus. Moreover, the increase of EEG alpha3/alpha2 power ratio has been associated with MCI due to AD and with an increase in theta frequency power in a group of subjects with impaired cerebral perfusion in hippocampus (Moretti et al., 2009, 2011a,b, 2012a,b, 2013a,b).

In this study, we investigated the possible interactions between brain rhythms and their associations with data morphostructural in an attempt to investigate the anatomical and pathophysiological alterations at the base of the prodromal phase of AD.

Materials and Methods

Subjects

For the present study, 74 subjects with MCI were recruited from the memory Clinic of the Scientific Institute for Research and Care (IRCCS) of Alzheimer's and psychiatric diseases 'Fatebenefratelli' in Brescia, Italy. All experimental protocols had been approved by the local ethics committee. Informed consent was obtained from all participants or their caregivers, according to the Code of Ethics of the World Medical Association (Declaration of Helsinki).

Diagnostic Criteria

Patients were selected from a prospective study on the natural history of cognitive impairment (the translational outpatient memory clinic—TOMC study) carried out in the outpatient facility of the National Institute for the Research and Care of Alzheimer's Disease (IRCCS Istituto Centro San Giovanni di Dio Fatebenefratelli, Brescia, Italy). The diagnosis of prodromal AD has been made according recent guidelines (Dubois et al., 2007; Albert et al., 2011; Galluzzi et al., 2013).

The project was aimed to study the natural history of non-demented persons with apparently primary cognitive deficits, i.e., deficits not due to psychic (anxiety, depression, etc.) or physical (hypothyroidism, vitamin B12 and folate deficiency, uncontrolled heart disease, uncontrolled conditions (diabetes, etc.) in the absence of functional impairment. The selection criteria has the aim to include as much as possible primary prodromal dementia due to neurodegenerative disorders. Demographic and cognitive features of the subjects in study are summarized in **Table 1**.

TABLE 1 | Demographic and cognitive characteristics in the whole sample, according to increased levels of alpha3/alpha2 Numbers denote mean ± SD, number, and [range].

	Alpha3/alpha2			
	High	**Middle**	**Low**	***p***
Demographic and clinical futures				
Number of subjects	18	38	18	—
Age, years	70.4 ± 6.7 [60–85]	68.4 ± 8.2 [52–83]	70.4 ± 7.4 [57–80]	0.55
Sex, female	13 (%)	24 (%)	14 (%)	0.51
Education, years	6.6 ± 3.6 [4–18]	7.6 ± 3.7 [3–17]	8.3 ± 4.7 [3–18]	0.42
Mini Mental State Exam	27 ± 1.7	27.4 ± 1.3	26.9 ± 1.2	0.46
Alpha3/alpha2	1.29 ± 0.1 [1.17–1.52]	1.08 ± 0.0 [1–1.16]	0.9 ± 0.1 [0.77–0.98]	**0.000**

p denotes significance on ANOVA. Bold value indicates statistical significant results.

Patients were rated with a series of standardized diagnostic and severity instruments, including the Mini-Mental State Examination (MMSE; Folstein et al., 1975), the Clinical Dementia Rating Scale (CDRS; Hughes et al., 1982), the Hachinski Ischemic Scale (HIS; Rosen et al., 1980) and the Instrumental and Basic Activities of Daily Living (IADL, BADL; Lawton and Brodie, 1969). In addition, patients underwent diagnostic neuroimaging procedures (magnetic resonance imaging, MRI), and laboratory testing to rule out other causes of cognitive impairment. These inclusion and exclusion criteria for MCI were based on previous seminal studies (Petersen et al., 2001; Portet et al., 2006; Dubois et al., 2007). Inclusion criteria of the study were all of the following: (i) complaint by the patient, or report by a relative or the general practitioner, of memory or other cognitive disturbances; (ii) MMSE score of 24–27/30, or MMSE of 28 and higher plus low performance (score of 2–6 or higher) on the clock drawing test (Lezak et al., 2004); (iii) sparing of IADL, BADL or functional impairment steadily due to causes other than cognitive impairment, such as physical impairments, sensory loss, gait or balance disturbances, etc. Exclusion criteria were any one of the following: (i) patients aged 90 years and older (no minimum age to participate in the study); (ii) history of depression (from mild to moderate or major depression) or juvenile-onset psychosis; (iii) history or neurological signs of major stroke; (iv) other psychiatric diseases, overt dementia, epilepsy, drug addiction, alcohol dependence; (v) use of psychoactive drugs, including acetylcholinesterase inhibitors or other drugs enhancing brain cognitive functions or biasing EEG activity; and (vi) current or previous uncontrolled or complicated systemic diseases (including diabetes mellitus), or traumatic brain injuries. All subjects were right-handed.

All patients underwent: (i) semi-structured interview and – whenever possible – with another informant (usually, the patient's spouse or a child of the patient) by a geriatrician or neurologist; (ii) physical and neurological examinations; (iii) performance-based tests of physical function, gait and balance; (iv) neuropsychological battery assessing memory (Babcock Story Recall – Rey–Osterrieth Complex Figure, Recall – Auditory-Verbal Learning Test, immediate and delayed recall; Lezak et al., 2004) verbal and non-verbal memory, attention and executive functions (Trail Making Test B, A and B-A; Inverted Motor Learning-Clock Drawing Test; Lezak et al., 2004), abstract reasoning thinking (Raven Colored Progressive Matrices; Lezak et al., 2004), frontal functions (Inverted Motor Learning); language (Phonological and Semantic fluency-Token test; Lezak et al., 2004), and apraxia and visuo-constructional abilities (Rey–Osterrieth Complex Figure, Rey figure copy, Clock Drawing Test; Rosen et al., 1980); (v) assessment of depressive symptoms by means of the Center for Epidemiologic Studies Depression Scale (CES-D; Radloff, 1977). All the neuropsychological tests were standardized on Italian population, thus scores were compared to normative values with age, education and gender corrections in an Italian population.

EEG and MRI

EEG Recordings

The EEG activity was recorded, continuously from 19 sites by using electrodes set in an elastic cap (Electro-Cap International, Inc.) and positioned according to the 10–20 international systems (Fp1, Fp2, F7, F3, Fz, F4, F8, T3, C3, Cz, C4, T4, T5, P3, Pz, P4, T6, O1, and O2). The patients were instructed to stay sit with closed eyes and relaxed. In order to keep constant the level of vigilance, an operator controlled on-line the subject and the EEG traces, alerting the subject any time there were signs of behavioral and/or EEG drowsiness. The ground electrode was placed in front of Fz. The left and right mastoids served as reference for all electrodes. The recordings were used off-line to re-reference the scalp recordings to the common average. Re-referencing was done prior to the EEG artifact detection and analysis. Data were recorded with a band-pass filter of 0.3–70 Hz, and digitized at a sampling rate of 250 Hz (BrainAmp, BrainProducts, Germany). Electrodes-skin impedance was set below 5Ω. Horizontal and vertical eye movements were detected by recording the electrooculogram (EOG). The recording lasted 5 min, with subjects with closed eyes. Longer recordings would have reduced the variability of the data, but they would also have increased the possibility of slowing of EEG oscillations due to reduced vigilance and arousal. EEG data were then analyzed and fragmented off-line in consecutive epochs of 2 s, with a frequency resolution of 0.5 Hz. The average number of epochs analyzed was 140, ranging from 130 to 150. The epochs with ocular, muscular and other types of

artifacts were discarded by two skilled electroencephalographists (Moretti et al., 2003).

Analysis of Individual Frequency Bands

All recordings were obtained in the morning with subjects resting comfortably. Vigilance was continuously monitored in order to avoid drowsiness. A digital FFT-based power spectrum analysis (Welch technique, Hanning windowing function, no phase shift) computed – ranging from 2 to 45 Hz – the power density of EEG rhythms with a 0.5 Hz frequency resolution. Two anchor frequencies were selected according to the literature guidelines (Klimesch, 1997; Moretti et al., 2004), that is, the theta/alpha transition frequency (TF) and the individual alpha frequency (IAF) peak. IAF and TF were computed for each subject in the study. These anchor frequencies were computed on the power spectra averaged across all recording electrodes. This "collapsed spectrum method" allows to identify a robust and reliable IAF, being a normalized scalp spectrum. The TF marks the TF between the theta and alpha bands, and represents an estimate of the frequency at which the theta and alpha spectra intersect. TF was computed as the minimum power in the alpha frequency range, since our EEG recordings were performed at rest. The IAF represents the frequency with the maximum power peak within the extended alpha range (5–14 Hz). Based on TF and IAF, we estimated the frequency band range for each subject, as follows: delta from TF-4 to TF- 2, theta from TF-2 to TF, low alpha band (alpha1 and alpha2) from TF to IAF, and high alpha band (or alpha3) from IAF to IAF + 2. The alpha1 and alpha2 bands were computed for each subject as follows: alpha1 from TF to the middle point of the TF-IAF range, and alpha2 from such middle point to the IAF peak (Fischl et al., 1999; Bazanova and Vernon, 2013). The mean frequency range computed in MCI subjects considered as a whole are: delta 2.9–4.9 Hz; theta 4.9–6.9 Hz; alpha1 6.9–8.9 Hz; alpha2 8.9–10.9 Hz; alpha3 10.9–12.9 Hz. Finally, in the frequency bands determined on an individual basis, we computed the relative power spectra for each subject. The relative power density for each frequency band was computed as the ratio between the absolute power and the mean power spectra from 2 to 45 Hz. The relative band power at each band was defined as the mean of the relative band power for each frequency bin within that band. The alpha3/alpha2 was computed in all subjects and three groups were obtained according to increasing tertiles values of alpha3/alpha2: low ($a3/a2 < 1$) middle ($1 \leq a3/a2 \leq 1.16$) and high ($a3/a2 \geq 1.17$). The three groups of MCI has been demonstrated in previous studies to be different in nature. In particular, the high alpha3/alpha2 EEG power ratio MCI group is at major risk to convert to Alzheimer's disease (Frisoni, 2012), as well as to have different pattern of hippocampal atrophy (Moretti et al., 2011b) and basal ganglia and thalamus gray matter lesions (Moretti et al., 2009) as compared to the other alpha3/alpha2 power ratio MCI groups. Moreover, this group subdivision has been chosen for reason of homogeneity and comparability with the previous studies. As the aim of our study was to evaluate the relationship only between functional and morphostructural biomarkers in a group of MCI who has major probability to develop AD, we did not consider the clinical subtype of MCI, i.e., amnesic, or non-amnesic, single or multiple domains.

MRI Scans

For each subject, a high-resolution sagittal T1 weighted volumetric MR scan was acquired at the Neuroradiology Unit of the 'Citta` di Brescia' Hospital, Brescia, by using a 1.0 T Philips Gyroscan scanner, with a gradient echo 3D technique: TR = 20 ms, TE = 5 ms, flip angle = 30, field of view = 220 mm, acquisition matrix 256 · 256, slice thickness 1.3 mm.

Cortical Thickness Estimation Steps

Cortical thickness measurements for 74 MCI patients were made using a fully automated MRI-based analysis technique: FreeSurfer, a set of software tools for the study of cortical and subcortical anatomy. Briefly, in the cortical surface stream, the models of the boundary between white matter and cortical gray matter as well as the pial surface were constructed. Once these surfaces are known, an array of anatomical measures becomes possible, including: cortical thickness, surface area, curvature, and surface normal at each point on the cortex. In addition, a cortical surface-based atlas has been defined based on average folding patterns mapped to a sphere and surfaces from individuals can be aligned with this atlas with a high-dimensional non-linear registration algorithm. The surface-based pipeline consists of several stages previous described in detail (Fischl and Dale, 2000; Gronenschild et al., 2012).

Single Subject Analysis

For each subjects the T1-weighted, anatomical 3-D MRI dataset were converted from Dicom format into .mgz format, then intensity variations are corrected and a normalized intensity image is created. The volume is registered with the Talairach atlas through an affine registration. Next, the skull is stripped using a deformable template model (Segonne et al., 2004) and extracerebral voxels are removed. The intensity normalized, skull-stripped image is then operated on by a segmentation procedure based on the geometric structure of the gray–white interface. Voxels are classified as white or gray matter, cutting planes are chosen to separate the hemispheres from each other. A white matter surface is then generated for each hemisphere by tiling the outside of the white matter mass for that hemisphere. This initial surface is then refined to follow the intensity gradients between the white and gray matter. The white surface is then nudged to follow the intensity gradients between the gray matter and CSF, obtaining the pial surface. Cortical thickness measurements were obtained by calculating the distance between those surfaces (white and pial surface) at each of ∼160,000 points per hemisphere across the cortical mantle (Dale et al., 1999).

Group Analysis

In order to relate and compare anatomical features across subjects, it is necessary to establish a mapping that specifies a unique correspondence between each location in one brain and the corresponding location in another. Thus, the pial surface of an individual subject is inflated to determine the large-scale folding patterns of the cortex and subsequently transformed into a sphere to minimize metric distortion. The folding patterns of the

individual are then aligned with an average folding pattern using a high-resolution surface-based averaging. Thickness measures were mapped to the inflated surface of each participant's brain reconstruction allowing visualization of data across the entire cortical surface. Finally, cortical thickness was smoothed with a 20-mm full width at half height Gaussian kernel to reduce local variations in the measurements for further analysis.

Test–Retest Reproducibility of Cortical Thickness Analysis

Previous studies have investigated the reliability of the cortical thickness measurements: some of these addressed the effect of scanner-specific parameters, including field strength, pulse sequence, scanner upgrade, and vendor. The use of a different pulse sequence had a larger impact, as did different parameters employed in data processing. The within-scanner variability of global cortical thickness measurements reported in previous studies was 0.03–0.07 in average (Rosas et al., 2002; Kuperberg et al., 2003; Pennanen et al., 2005; Han et al., 2006). Scanner upgrade did not increase variability nor introduce bias while measurements across field strength were slightly biased (thicker at 3 T). In the study by Han et al. (2006) the variability was 0.15 and 0.17 mm in average, respectively, for cross-scanner (Siemens/GE) and cross-field strength (1.5 T/3 T) comparisons. The recent study by Gronenschild et al. (2012) also investigated the effects of data processing conditions such as FreeSurfer version, workstation, and Macintosh operating system version. The authors reported significant differences between FreeSurfer version (average: 2.8–3%) and a smaller differences between workstation and operating system version. On the whole, the results suggest that MRI-derived cortical thickness measures are highly reliable, however it is important to keep consistent the MRI parameters and data processing factors within any given structural neuroimaging study (DeCarli et al., 2005; Markesbery et al., 2006; McKhann et al., 2011).

Radial Atrophy Mapping for Hippocampal Atrophy Computation

The 3D parametric surface mesh models were created from the manual tracings of hippocampal boundaries (DeCarli et al., 2005). This procedure allows measurements to be made at corresponding surface locations in each subject, which are then compared statistically in 3D (DeCarli et al., 2005). To assess hippocampal morphology, a medial curve was automatically defined as the 3D curve traced out by the centroid of the hippocampal boundary in each image slice. The radial size of each hippocampus at each boundary point was assessed by automatically measuring the radial 3D distance from the surface points to the medial curve defined for individual's hippocampal surface model.

The analysis of variance ANOVA was performed in order to verify the difference of hippocampal volume among groups.

EEG and SPECT

MCI Patients

Mild cognitive impairment patients were taken from a prospective project on MCI ("Mild Cognitive Impairment in Brescia, MCIBs"), aimed to study the natural history of persons without dementia with apparently primary cognitive deficits, i.e., not due to psychic or physical conditions, the same of MRI-EEG project. The study protocol was approved by the local ethics committee and all participants signed an informed participation consent. Details on inclusion/exclusion criteria and on physical and neurological examinations, performance-based tests of physical function, gait and balance and performed neuropsychological battery have been previously published and are at disposal elsewhere (Caroli et al., 2007; Moretti et al., 2013b) and described above. Among the 56 MCI patients who agreed to undergo MRI and SPECT scan, all consecutive 27 who agreed also to undergo EEG recording were further considered.

Normal Controls

We enrolled all 17 healthy subjects from a previous study on cerebral perfusion correlates of conversion to AD with both an MRI and a SPECT scan available (Caroli et al., 2007; Moretti et al., 2013b). Briefly, subjects were consecutive normal volunteers picked among those undergoing brain MRI scan at the Neuroradiology Unit of the "Città di Brescia" Hospital in Brescia from October 2004 to June 2006 for reasons unrelated to cognition, or were healthy volunteers aged 65 years or older, among MCI patients' spouses, friends of them, and researchers' acquaintances. All scans of enrolled subjects were normal on visual assessment by a neuroradiologist. Subjects underwent multidimensional assessment including clinical, neurological, and neuropsychological evaluations, and drawing of a blood sample (not used for the purposes of the present study). Data coming from normal controls were used only to compute *W* scores in each selected perfusion Region of Interest (ROI).

SPECT Scan

Both patients and normal controls underwent SPECT scan in the nuclear medicine department of the Ospedali Riuniti in Bergamo. Each patient received an intravenous injection of 925 MBq of technetium- 99 m ethylcysteinate dimer (99mTc-ECD) in resting conditions, lying supine with eyes closed in a quiet, dimly lit room. Forty to sixty minutes after injection, brain SPECT was performed using a dual-head rotating gamma camera (GE Elscint Helix) equipped with low energy-high resolution, parallel hole collimators. A 128 × 128 pixel matrix, zoom = 1.5, was used for image acquisition with 120 views over a 360° orbit (in 3° steps) with a pixel size and slice thickness of 2.94 mm. Butterworth filtered-back projection (order = 7, cut-off = 0.45 cycles/cm) was used for image reconstruction, and attenuation correction was performed using Chang's method (attenuation coefficient = 0.11 cm-1). Images were exported in DICOM format.

SPECT Processing Protocol

To achieve a precise normalization, we generated a study-specific SPECT template using both SPECT and MRI scans of all patients and normal controls under study, following a procedure described in detail elsewhere (Caroli et al., 2007) and schematically represented in **Figure 1**. Briefly, we created a customized high-definition MRI template, we converted

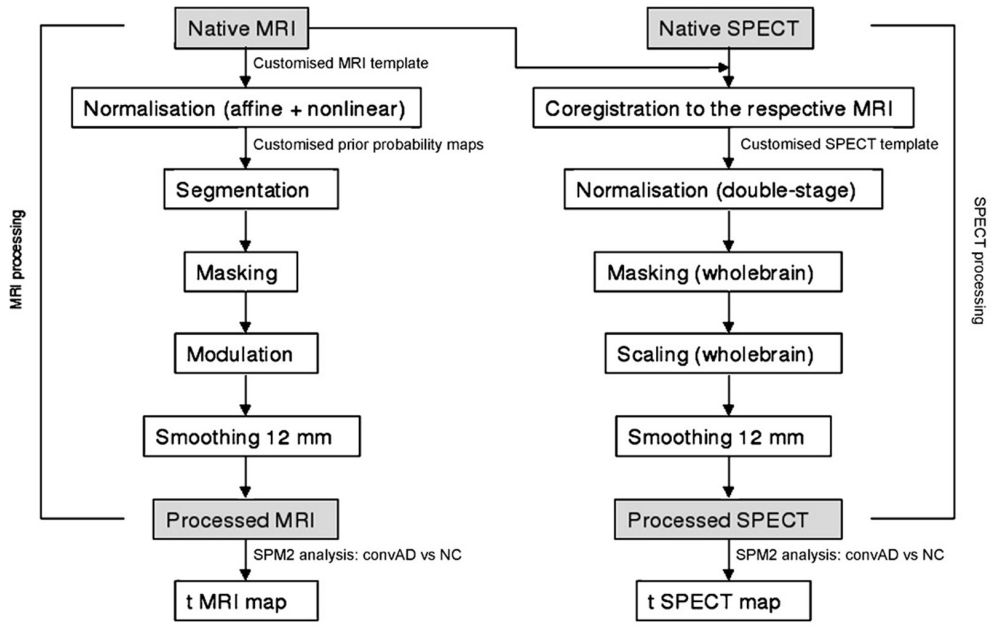

FIGURE 1 | Flow chart summarizing the whole MRI-SPECT processing protocol.

SPECT scans to Analyze format using MRIcro (Rorden and Brett, 2000), and we coregistered them to their respective MRI scans with SPM2 (SPM, Statistical Parametric Mapping, version 2,2002. London: Functional Imaging Laboratory. Available at: http://www.fil.ion.ucl.ac.uk/spm/software/spm2). We normalized each MRI to the customized MRI template through a non-linear transformation (cut-off 25 mm), and we applied the normalization parameters to the coregistered SPECT. We obtained the customized SPECT template as the mean of all the latter normalized SPECT images. The creation of a study-specific template allows for better normalization, since low uptake in ventricular structures and cortical hypoperfusion effects are frequently present in elderly patients. For each coregistered SPECT scan, we set the origin to the anterior commissure, using the respective MRI image as a reference, and we processed all scans with SPM2 according to an optimized processing protocol described in detail elsewhere (Caroli et al., 2007). Brain perfusion correlates of medial temporal lobe atrophy and white matter hyperintensities in MCI were obtained as follows: (I) we smoothed each scan with a 10 mm full width at half maximum (FWHM) Gaussian, and spatially normalized it with an affine deformation to the customized SPECT template; we applied the same deformation to the unsmoothed images; (II) we masked the unsmoothed normalized images from I to remove scalp activity using SPM2's "brainmask." We smoothed with a 10 mm FWHM Gaussian, and warped them to the customized template with a non-linear transformation (cut-off 25 mm); we applied the same transformation to the unsmoothed masked images; (III) we smoothed the normalized unsmoothed images from II with a 12 mm FWHM Gaussian. The following ROI were chosen for perfusion analyses in each hemisphere from the Pick atlas by a sub-routine implemented on SPM2: frontal, parietal and temporal lobes, the thalamus and the hippocampal-amygdalar complex (Maldjian et al., 2003). The choice of these regions was based on previous SPECT and PET studies in subjects with MCI (Staffen et al., 2009; Alegret et al., 2012; Yoon et al., 2012).

The whole cerebellum was chosen for normalization of ROI counts. Since perfusion values in selected ROIs did not account for age, pertinent age corrected perfusion values (hereafter called *W* scores), were computed in each selected ROI, following a previously published procedure (Alegret et al., 2012).

Statistical Analysis for MRI and EEG

Differences between groups in sociodemographic and neuropsychological features were analyzed using SPSS version 13.0 (SPSS, Chicago, IL, USA) performing an analysis of variance (ANOVA) for continuous variables and paired χ^2 test for dichotomous variables. For continuous variables, post-hoc pairwise comparisons among groups were performed with the Games-Howell or Bonferroni tests depending on homogeneity of variance tested with Levene's test.

Concerning the neuroimaging analysis, the Qdec interface in Freesurfer software was used: a vertex-by-vertex analysis was carried out performing a general linear model to analyze whether any difference in mean cortical thickness existed between groups (low a3/a2 $< 1\ \mu V^2$;) middle ($1 \leq$ a3/a2 $\leq 1.16\ \mu V^2$ and high (a3/a2 $\geq 1.17\ \mu V^2$). The following comparisons were carried out: High vs. Low, High vs. Middle, and Middle vs. Low. Age, sex, education, global cognitive level (MMSE score) The value of cortical thickness estimation in middle and low was averaged and compared to the high alpha3/alpha2 power ratio. When a statistical threshold at $p \leq 0.05$ corrected was applied, there were no significant results. So we choose to apply an uncorrected but more restrictive significance threshold than 0.05 ($p \leq 0.001$) and we

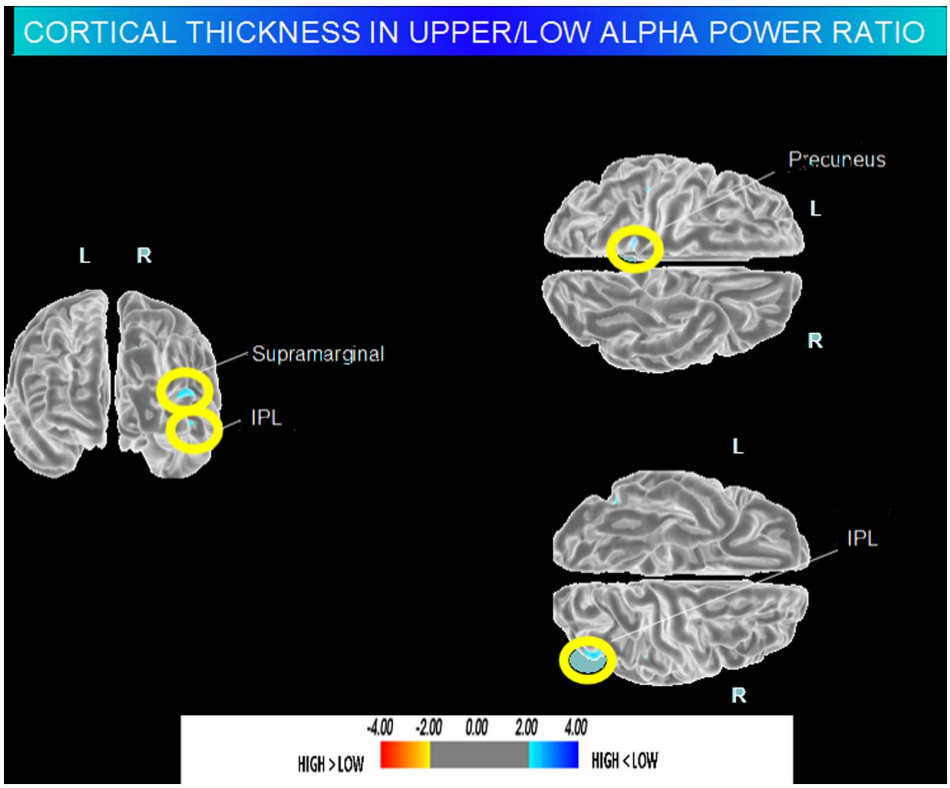

FIGURE 2 | Brain regions with significant regional cortical thickness differences in MCI with high a3/a2 ratio compared to MCI with low averaged with middle a3/a2 ratio ($p < 0.01$ uncorrected). The color-coding for p values is on a logarithmic scale. Warmer color represents cortical thinning, cooler color represents cortical thickening. Results are presented on the pial cortical surface of brain: dark gray regions represent sulci and light gray regions represent gyri.

considered as significant only the clusters which also were wide equal or major to 30 mm^{2}. Finally a surface map was generated to display the results on an average brain. For illustrative purpose significance was set to a p-value of ≤ 0.01 uncorrected for multiple comparisons.

Statistical Analysis for SPECT AND EEG

All statistical analyses were performed using SPSS software version 13.0. We investigated significance of the difference between the two groups (MCI at low and at high risk to develop AD) in socio-demographic, clinical and cognitive features using $\chi 2$ test for categorical variables (sex, and ApoE carriers) and Student's independent t test for continuous variables (volumetric, perfusion features and EEG frequencies). In all cases we set the significant threshold at $p < 0.05$. Since native SPECT scans were coregistered to their respective MRI images, and the study-specific SPECT template was coregistered to the high-definition MRI template, all the normalized SPECT and MRI images used for the statistical analysis were coregistered to the SPM standard anatomical space. Moreover, Pearson's r correlations were assessed between the selected perfusion ROIs (in terms of age corrected W scores) and the acquired EEG frequencies in both groups. Moreover, a correlation analysis was computed between theta and alpha brain rhythms.

Results

MRI-EEG

Table 1 shows the sociodemographic and neuropsychological characteristics of MCI subgroups defined by the tertile values of alpha3/alpha2. The ANOVA analysis showed that there was not statistically significant differences between groups which resulted well paired for age, sex, education, and global cognitive level. Anyway, age, sex, education, global cognitive level (MMSE score) alpha3/alpha2 ratio levels were significant at Games-Howell *post hoc* comparisons ($p = 0.000$).

Pattern of Cortical Thickness between Groups

High vs. Middle and Low averaged thickness (named low): when compared to subjects with low a3/a2 ratios, patients with high a3/a2 ratio show thinning in the right Supramarginal and IPL and in the left Precuneus cortex, (**Figure 2**; **Table 2**).

SPECT-EEG

Twenty seven MCI patients were enrolled for the present study and they were classified as at high risk (when the a3/a2 EEG rhythm median was above 1.17) or at low risk (when the a3/a2 EEG rhythm median was under 1.17) to develop AD. The two

TABLE 2 | Brain regions with significant regional cortical thickness differences in MCI with high a3/a2 ratio compared to MCI with low averaged with middle a3/a2 ratio.

High a3/a2<averaged middle and low a3/a2								
Cluster size (mm^2)	Region	Side	Stereotaxc coordinate			*P*	Thickness (mm^2)	
			x	*y*	*z*		High	Low+middle
55	Precuieus	L	−14	−48	58	0.00001	1.35 ± 0.14	2.57 ± 0.24
76	Supra marginal	R	49	−29	27	00.01.00	1.53 ± 0.18	2.67 ± 0.56
93	Inferior parietal	R	46	−75	10	0.001	1.54 ± 0.22	3.07 ± 0.35

Cluster size represents the extension of contiguous significant voxels in the cluster obtained at $p < 0.01$ uncorrected (cluster size > 30 mm^2). Stereotaxic coordinates reveal the position of the most significant voxel of the cluster, and side denotes its localization on the left (L) or right (R) brain hemisphere. Thickness denotes the average cortical thickness and SD values within the cluster in high and low + middle a3/a2 groups. P denotes the significance level of the differences in thickness between groups.

TABLE 3 | Demographic and cognitive characteristics in the whole sample, disaggregated for increased levels of alpha3/alpha2 Numbers denote mean ± SD, number, and [range].

	At low-risk MCI	At high-risk MCI	*P* value
N	14	13	
Age (years) [range]	69.1 ± 7.6 [57÷83]	70.6 ± 5.5 [62÷78]	0.555
Gender (females)	6 (43%)	9 (69%)	0.168
Education (years) [range]	8.2 ± 4.3 [4-18]	7.9 ± 4.5 [3÷18]	0.865
MMSE score [range]	27.9 ± 1.6 [25÷30]	27.2 ± 1.9 [24÷29]	0.309
3 Left hippocampal volume (mm^3)[Range]	2,606 ± 353 [1,923÷3,017]	2,073 ± 412 [1,234÷2,641]	0.001
3 Right hippocampal volume (mm^3)[range]	2,581 ± 473 [1,549÷3,150]	2,296 ± 501 [1,589÷3,086]	0.141
Wahlund total score [Range]	3.58 ± 3.29 [0.0÷10.0]	3.78 ± 2.63 [0.0÷7.0]	0.886

p denotes significance on ANOVA.

groups (AD high risk, $N = 13$, AD low risk, $N = 14$) were similar for age ($p = 0.56$), education in years ($p = 0.87$), gender ($p = 0.17$), ApoE genotype ($p = 0.15$), MMSE scores ($p = 0.31$) and white matter lesions load ($p = 0.88$; **Table 3**). **Figure 1** shows the visual rating scale of the SPECT scans representative of normal control, MCI with low and MCI with high risk to convert in AD, respectively. ANOVA results show that the selected cut-off was effective in detecting two different groups: patients with high risk to develop AD show significantly higher alpha3/alpha2 power ratio than patients with low risk ($p = 0.0001$). Moreover, a control analysis was performed on the single frequencies. The results show that the increase of alpha3/alpha2 frequency power ratio was due to both increase of alpha3 ($p = 0.001$) and decrease of alpha2 ($p = 0.0001$) and not to the modification of a single frequency. This control analysis was performed because the change of only one frequency could be due to the chance. But it was not the case.

Although the mean perfusion in all the selected ROIs was similar between groups (all $p > 0.38$), in the group with high alpha3/alpha2 frequency ratio there is a constant trend to a lower perfusion (see **Figure 3**). Moreover, left hippocampal volumes were lower for AD-high risk patients respect to low risk ones ($p < 0.001$; **Table 3**). Data coming from normal controls were used only to compute *W* scores in each selected perfusion ROI. In patients at low risk to develop AD, significant Pearson's R negative correlation was found between perfusion in the hippocampal complex ROI and theta rhythm ($r = -0.544$, $p = 0.044$).

In patients at high risk to develop AD otherwise, more and dissimilar correlations were found: a positive correlation, inverted respect to patients at low risk, between the perfusion in the hippocampal complex ROI and theta rhythm ($r = 0.729$, $p = 0.005$). No other significant correlations were found in both groups between perfusion ROIs and other EEG rhythms or hippocampal volumes. Moreover, no significant correlations were found between hippocampal complex ROI and theta rhythm pooling low and high risk patients together ($r = 0.086$, $p = 0.671$). The correlation analysis between theta and alpha rhythm showed a positive correlation between the ghigher alpha3/alpha2 power ratio and the theta brain rhythms ($r = 0.67$, $p < 0.03$).

Discussion

Association between EEG Markers and MRI Changes

In the present study the relationship between an EEG marker (the alpha3/alpha2 power ratio) and the cortical thickness in subjects with MCI was investigated. The alpha3/alpha2 power ratio has been chosen because in previous works it has been demonstrated that MCI subjects with higher alpha3/alpha2 ratio are at major risk to develop AD (Moretti et al., 2009, 2011b, 2013b; Frisoni, 2012). Our results show that the MCI group with higher alpha3/alpha2 ratio has a greater global cortical atrophy than the other subgroups, thus confirming a large body of literature (Frisoni et al., 2007; Frisoni, 2012). Furthermore, the

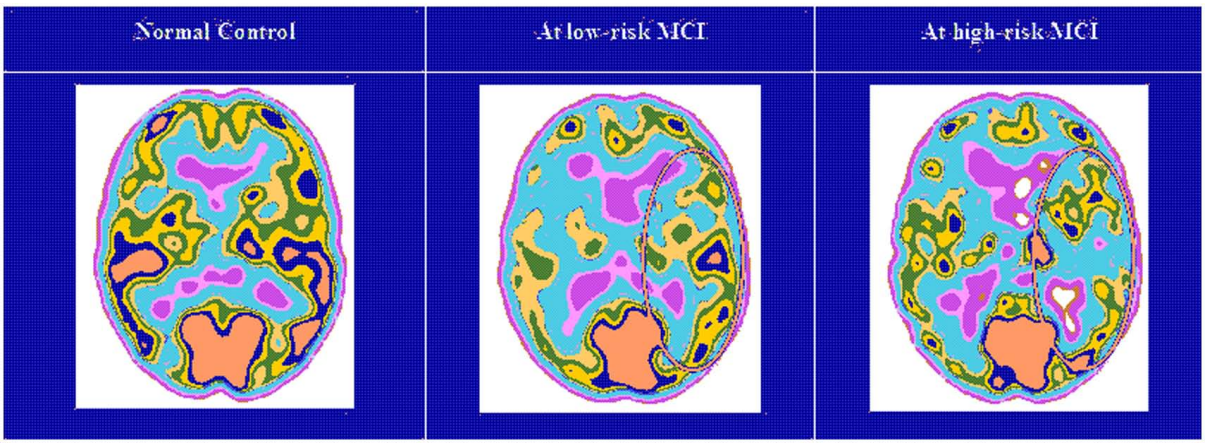

FIGURE 3 | Single-photon emission computed tomography (SPECT) visual rating. The output shows a SPECT visual inspection of glucose uptake metabolism: the white square denotes an area of mild-to-moderate (purple to blue) temporparietal hypometabolism in one of the 14 at low risk and in one of the 13 at high risk MCI patient respect to one of the 17 enrolled controls.

greater atrophy is significant in two specific brain areas: precuneus and supramarginal gyrus (a brain area belonging to the inferior parietal lobule), both in left and right hemisphere. These results was largely expected considering previous studies. Indeed, structural and functional abnormalities of the precuneus were observed in MCI (Ryu et al., 2010) as well a in Azheimer's disease (Sperling et al., 2010) so that the atrophy of precuneus has been considered as a pathognomonic marker of early AD. Recent studies suggest that the pathophysiological process of AD exerts specific deleterious effects on distributed memory circuits, even prior to clinical manifestations of significant memory impairment. Specific regions, namely the precuneus and posterior cingulate, together with the medial temporal lobe, are selectively vulnerable to early amyloid deposition in AD pathology (Sperling et al., 2010; De Haan et al., 2012). Recent studies have demonstrated that during the successful encoding of new items there is a desynchronization in the temporo-parietal memory-related networks whereas a synchronization prevent a successful semantic encoding (Ryu et al., 2010; Pievani et al., 2011). The deleterious role of synchronization has been recently demonstrated by an interesting study facing the intriguing relationship between functional and structural degeneration in AD (Sperling et al., 2010). The authors detected some hub regions (heteromodal associative regions) selectively vulnerable in AD pathology, due to the damage of inhibitory interneurons providing a loss of inhibition at cellular level. According to the authors, the disinhibition provokes an increasing amount of neural activity at network level, giving as a final result an hypersynchronization of brain areas. Of note, this overactivity is excitotoxic and determines cellular apoptosis and brain atrophy. Also, Palop and Mucke (2010) emphasize the role of inhibitory interneuron dysfunction, leading to hypersynchronization (Jones et al., 2011; Brier et al., 2012; Chatwal and Sperling, 2012). Our results are in line with these previous influential studies. A possible integrative view of all the results could be as follows: (1) the higher neuronal activity in the hub regions starts from a disfunction of cellular inhibition; (2) the consequent disinhibition drives neural network to an oversynchronization; (3) this oversynchronization is peculiar of the hub regions with higher amyloid burden; (4) these overactivated regions are prone to degeneration and atrophy; (5) a possible neurophysiologic sign of this oversynchronization is the increase of the alpha3/alpha2 power ratio we have found in typical hub regions (Stam et al., 2003; Rossini et al., 2008; Bhattacharya et al., 2011; Wu et al., 2011). It is of great interest that there is an overlapping between the brain regions associated with increase of EEG alpha3/alpha2 power ratio (hypersynchronization of upper alpha) in our study and the regions associated with higher amyloid burden related to memory processes (Palop and Mucke, 2010; Chatwal and Sperling, 2012). Moreover, in the present study, there is a very interesting result. The atrophy of precuneus is coupled with the atrophy in supramarginal gyrus and, at lesser extent, with inferior parietal, insula and superior temporal gyrus. This atrophy pattern is clearly expressed in the group of MCI subjects with higher alpha3/alpha2 power ratio. This finding fits well with the results of a recent study (Wonderlick et al., 2009), investigating the functional connectivity of human precuneus by resting state fMRI. The authors found that there is a preferential pathway of connectivity of the dorsal precuneus with supramarginal gyrus, parietal cortex, superior temporal gyrus and insula. As a consequence, the atrophy we detected in the MCI group with higher alpha3/alpha2 ratio power could be hypothesized as the loss of GM in an entire anatomo-functional network more than atrophy of isolated brain areas. Of note, it is widely accepted that AD is the result of a cortical network impairment more than the atrophy of single cortical areas (Zhang and Li, 2012). In subjects with low or middle alpha3/alpha2 power ratio the cognitive impairment is possibly due to cerebro-vascular impairment or non-AD degenerative process. Although rigid selection criteria were adopted to include in the study only patients with primary cognitive deficits, in the clinical practice is not infrequent to have MCI subjects not due to AD.

Association between EEG Markers and SPECT Changes

The EEG alpha3/alpha2 frequency ratio in previous studies has proved useful in identifying a group at greater risk of converting in AD (Stam et al., 2005). This group has the higher alpha3/alpha2 EEG frequency power ratio, at an orientative cut-off of about 1.17. The choice of a cut-off allows the individuation of a particular population inside the group of patients with MCI. It is a very important issue of the study and makes it different from other works, usually distinguishing the MCI subjects on clinical, structural or functional aspects but not on a neurophysiological marker. The particular group individuated by the higher alpha3/alpha2 power ratio is at major risk to develop AD. The possibility to detect this risk not only in a group but also in the single patient through a cut-off is also an original contribution of this study. To be validated this EEG marker needs correlation study with morphostructural or functional milestones peculiar of AD, like as rCBF. These present results confirm that the relationship alpha3/alpha2 identifies two distinct groups: the higher ratio characterizes a group with a smaller hippocampal volume and a constant trend of lower cerebral perfusion, even if it does not reach significance. These results confirm previous studies which have shown that patients with high risk of developing AD have left hippocampal atrophy and reduced SPECT perfusion (Frisoni, 2012). Actually, amyloid plaques deposition, NFT formation, neuronal loss, decrease in dendritic extent, and synaptic depletion are thought to disturb the communication among various cortical areas, resulting in anatomic isolation and decreased perfusion of many cortical zones (Golde, 2003). The lack of a significant difference is an obvious limitation of the work. One possible explanation is the relatively small sample size of the two groups. Given that the trend is constant, a larger sample in both groups could exploit a significant statistical difference. On the other side, it is possible that when considering two groups of patients, both with a MCI, the rCBF is not so sensible to evidence little difference. On the contrary, previous studies have demonstrated that metabolic, but not perfusional, patterns were related to severity of cognitive impairment and were more sensible in detecting prodromal MCI due to AD (Mielke et al., 1994). Further studies, with larger sample size, are mandatory to confirm these results. The present study shows a correlation between cerebral perfusion and theta rhythm. Anyway, the correlation emerges only when considering the different groups individuated on the alpha3/alpha2 frequency power ratio. This is confirmed by the finding that when the groups are merged, no correlation could be found. This is the main aspect of the study and the peculiar novelty of the results. The patients at lower risk to develop AD, who have a constant trend toward a higher brain regional blood perfusion, maintains low levels of hippocampal theta power while in patients at higher risk, with a basically lower cerebral blood perfusion, theta rhythm tends to be higher. This latter finding is also confirmed by the increased ratio of theta/gamma frequency power ratio in the temporal region, adjacent to the hippocampus. A lot of previous studies have shown an increase of theta rhythm in patients with mild AD (Rodriguez et al., 2011), so that the increase of theta power is a robust features of AD. Theta rhythms are usually not appreciated in normal awakening EEG. However, a theta power increase is observed over the frontal and temporal areas during learning and memory tasks. The theta rhythms that are recorded during these tasks are thought to be produced by the activation of septal-hippocampal system. On the other hand, it should be taken in mind that EEG measures electrical field variations, and a number of clinical conditions can disturb the normal electrical field of the brain. For instance, electrolyte changes may alter the appearance and time variation of the brain-generated electrical fields, and medications can slow the posterior dominant rhythm. Moreover, in assessing the frequency of the theta rhythm, cerebrovascular lesions should be considered as a possible cause of increase. By means of observations in patients with ischemic lesions, it has been suggested that delays in cortico-cortical fiber propagation may play a global role in determining human EEG frequencies, increasing the amount of theta activity (Thatcher et al., 1998). Increased T2 relaxation times in cortical gray matter and white matter were correlated with a shift in relative EEG power to lower frequencies in the theta range (4–7 Hz) and reduced cognitive performance (Rodriguez et al., 2011). Anyway, none of our patients suffered from acute ischemic lesions and there was no difference in the cerebrovascular load between the two groups. Moreover, the EEG frequency details of patients with chronic cerebrovascular load has been recently investigated (Moretti et al., 2004) and they are not compatible with an high alpha3/alpha2 frequency ratio increase. So, we are confident the our results are of neurodegenerative origin. On the whole, it emerges a picture in which it is not the simple cerebral blood perfusion rate nor a single brain rhythm that reflect the complexity of functional alteration in AD. A previous work already found that none of the regions of interest of the SPECT scans were significantly correlated with clinical severity (Müller et al., 1997; Wenderoth et al., 2005).

Theta and Alpha Frequency Interplay in MCI Due to AD

Klimesch et al. (1996) and Klimesch (1997, 1999) have convincingly demonstrated that that the upper alpha band (10–13 Hz) specifically reflects encoding memory processes. Recent EEG and magnetoencephalography (MEG) studies have confirmed that a correct functioning of memory, both in encoding and in retrieval, requires the high alpha rhythm desynchronization (or power decrease; Kilner et al., 2005; Wyart and Tallon-Baudry, 2008; Spitzer et al., 2009; Staudigl et al., 2010; Moretti et al., 2012b). From a neurophysiological point of view the synchronization (or power increase) of EEG alpha power has been associated with the inhibition timing hypothesis (Moretti et al., 2012b) and with poor information transmission, according to he entropy's theory (Hanslmayr et al., 2010; Moretti et al., 2013b). The increases in alpha amplitudes reflect inhibition of cortical brain regions (Hanslmayr et al., 2012; Moretti et al., 2012a, 2013a). Similarly, the entropy's theory stated that synchronization is disadvantageous for storing information, as it reduces the flow of information (Moretti et al., 2013b). Entropy is a measure of the richness of information encoded in a sequence of events. Applying this concept to the neural networks, it has been demonstrated (Wonderlick et al., 2009) that the degree of

information that is encoded in neural assemblies increases as a function of desynchronization and decreases as a function of synchronized firing patterns (Jensen and Mazaheri, 2010; Norman, 2010). This hypothesis has been confirmed in clinical studies in patients with memory deficits (Schneidman et al., 2011). as well as during states where there is little cognitive processing (e.g., epileptic seizures or slow wave sleep; Goard and Dan, 2009; Wonderlick et al., 2009; Kurimoto et al., 2012) As regards cognitive impairment due to AD, the typical synaptic loss could prevent the physiological flexibility of brain neural assemblies, impeding the desynchronizing downstream modulation of the brain activity. As a consequence, it could be hypothesized that the disruption of cortical network due to degenerative disease, inducing cortical atrophy, could determine an oversynchronization of the brain oscillatory activity. The synchronization state of the high alpha power could prevent the creation of a semantic sensory code and, consequently, of the episodic memory trace (Barlow, 1961; Bialek et al., 1991; Bazanova and Aftanas, 2008; Chalk et al., 2010). In previous seminal studies, high alpha frequency has been specifically related to semantic memory processes (Craik, 2002; Moretti et al., 2003; Hanslmayr et al., 2009). Of note, in subjects with early cognitive decline, the impairment of the semantic features of memory has been recently accepted as a hallmark for the early AD diagnosis. (Dubois et al., 2007; Albert et al., 2011). Indeed, according to the new diagnostic criteria of AD, the measurement of sensitivity to semantic cueing can successfully differentiate patients with AD from healthy controls, even when patients are equated to controls on MMSE scores or when disease severity is very mild. Our results are generally in line with this hypothesis, suggesting that increase in power of high alpha brain oscillations reflects a block of information processes. However, the present study goes one step further, linking the increase of high alpha synchronization to the atrophy of a specific brain network, correlated with impairment in memory performances. Hippocampus has a cholinergic innervation originating from basal forebrain, the medial septum, and the vertical limb of the diagonal band of Broca. Populations of GABAergic and glutamatergic neurons have also been described in several basal forebrain structures. The synchronized depolarization of hippocampal neurons produces field potentials that have a main frequency of 3–12 Hz and are usually known as hippocampal theta rhythm (Bland and Colom, 1993; Craik, 2002). A cholinergic–glutamatergic hypothesis of AD, in which most symptoms may be explained by cholinergic–glutamatergic deficits, has been advanced. Neuronal injury/loss may include an excitotoxic component that possibly contributes to the early cholinergic deficit. This excitotoxic component may occur, at least in part, at the septal level where somas of cholinergic neurons are found. This insult may modify septal networks and contribute to the abnormal information processing observed in AD brain, including its hyperexcitability states. According to this theory, the increased theta production in AD would derive from hyperexcitability of the septal-hippocampal system (Bland and Colom, 1993; Colom, 2006; Moretti et al., 2007, 2008). Of note, such pattern of decreased cerebral blood flow activity and increased excitability was found even prior to the onset of cognitive impairment and cortical atrophy (Moretti et al., 2012a).

A recent study, confirms the major role of the interplay of theta and alpha frequency in the cognitive impairment evaluating the global field synchronization and power spectral analysis (Abuhassan et al., 2014).

This study have investigated the interplay between various synaptic degeneration and compensation mechanisms, and abnormal cortical oscillations based on a large-scale network model consisting of 100,000 neurons exhibiting several cortical firing patterns, 8.5 million synapses, short-term plasticity, axonal delays and receptor kinetics.

The structure of the model is inspired by the anatomy of the cerebral cortex. The results of the modeling study suggest that cortical oscillations respond differently to compensation mechanisms. In particular, the local compensation preserves the baseline activity of theta and alpha oscillations. Deactivating local compensation mechanisms will result in rapid decline (cognitive deficit) of the network dynamics at theta and alpha bands. Therefore, methods which can enhance local compensation could play a major role in the stimulation of neural processes and cognitive functions that are associated with these frequency bands. As compensating for synaptic loss is speculated to differ from one cortical area to another, the study suggests that activating an inappropriate compensation mechanism in a particular area may fail to recover the network dynamics and/or may induce secondary pathological changes in the network. This speculation is supported by the observation that local compensation fails at recovering/maintaining the baseline delta and beta oscillations whilst theta and alpha oscillations are least preserved with global compensation.

Clinical Implications

The associations between neurophysiological, functional and morphostructural biomarkers may open new perspectives in terms of early diagnosis of Alzheimer's disease. In addition, the correlation of these biomarkers with peculiar cognitive performance can be a valuable prognostic tool and a mean to identify a particular group of subjects with MCI who may participate in clinical trials in which new therapies are tested. This would allow a more accurate diagnosis, better planning for the future by the patient and his family, and optimization of health care spending. Of course, the next step is to move away from population studies to studies on single subject.

Study Limitations

There are some limitations due to the obvious explorative nature of the present study: (1) further studies are needed to confirm our result on larger samples and applying an appropriate multiple comparison correction; (2) the pattern of cortical thickness should be investigated on the remaining EEG frequency measures; (3) finally the retrospective nature of the study prevented a direct assessment of whether subjects with increase of a3/a2 EEG power ratio will convert to Alzheimer's or other neurodegenerative disease; (4) the conservative $p < 0.001$ used here is not necessarily sufficient given the number of comparisons. Anyway,

given the explorative nature of the study it is plausible a permissive approach in order to avoid to reject possibly interesting results.

It remains clear that further studies with less permissive statistical approach are mandatory to confirm results.

Conclusion

The present results show that that synchronization (or increase in power) of high alpha is associated with greater cortical atrophy. The greater cortical atrophy is present both the whole brain volume and in a peculiar memory-related network, including precuneus and temporo-parietal cortices. The combination of EEG alpha3/alpha2 ratio and cortical thickness measure could be useful for identifying individuals at risk for progression to AD dementia and may be of value in clinical context.

Acknowledgment

The work is funded by Fatebenefratelli Association for Research.

Disclosure Statement

I declare that appropriate approval and procedures were used concerning human subjects.

References

Abuhassan, K., Coyle, D., Belatreche, A., and Maguire, L. (2014). Compensating for synaptic loss in Alzheimer's disease. *J. Comput. Neurosci.* 36, 19–37. doi: 10.1007/s10827-013-0462-8

Albert, M. S., DeKosky, S. T., Dickson, D., Dubois, B., Feldman, H. H., Fox, N. C., et al. (2011). The diagnosis of mild cognitive impairment due to Alzheimer's disease: recommendations from the National Institute on Aging-Alzheimer's Association workgroups on diagnostic guidelines for Alzheimer's disease. *Alzheimers Dement.* 7, 270–279. doi: 10.1016/j.jalz.2011.03.008

Alegret, M., Cuberas-Borrós, G., Vinyes-Junqué, G., Espinosa, A., Valero, S., Hernández, I., et al. (2012). A two-year follow-up of cognitive deficits and brain perfusion in mild cognitive impairment and mild Alzheimer's disease. *J. Alzheimers Dis.* 30, 109–120. doi: 10.3233/JAD-2012-111850

Barlow, H. B. (1961). "The coding of sensory messages," in *Current Problems in Animal Behaviour*, eds W. H. Thorpe and O. L. Zangwill (Cambridge: Cambridge University Press), 331–360.

Bazanova, O. M., and Aftanas, L. I. (2008). Individual measures of electroencephalogram alpha activity and non-verbal creativity. *Neurosci. Behav. Physiol.* 38, 227–235. doi: 10.1007/s11055-008-0034-y

Bazanova, O. M., and Vernon, D. (2013). Interpreting EEG alpha activity. *Neurosci. Biobehav. Rev.* 44, 94–110. doi: 10.1016/j.neubiorev.2013.05.007

Bhattacharya, B. S., Coyle, D., and Maguire, L. P. (2011). Alpha and theta rhythm abnormality in Alzheimer's disease: a study using a computational model. *Adv. Exp. Med. Biol.* 718, 57–73. doi: 10.1007/978-1-4614-0164-3_6

Bialek, W., Rieke, F., de Ruytervan Steveninck, R. R., and Warland, D. (1991). Reading a neural code. *Science* 252, 1854–1857. doi: 10.1126/science.2063199

Bland, B. H., and Colom, L. V. (1993). Extrinsic and intrinsic properties underlying oscillation and synchrony in limbic cortex. *Prog. Neurobiol.* 41, 157–208. doi: 10.1016/0301-0082(93)90007-F

Brier, M. R., Thomas, J. B., Snyder, A. Z., Benzinger, T. L., Zhang, D., Raichle, M. E., et al. (2012). Loss of intranetwork and internetwork resting state functional connections with Alzheimer's disease progression. *J. Neurosci.* 32, 8890–8899. doi: 10.1523/JNEUROSCI.5698-11.2012

Caroli, A., Testa, C., Geroldi, C., Nobili, F., Barnden, L. R., Guerra, U. P., et al. (2007). Cerebral perfusion correlates of conversion to Alzheimer's disease in amnestic mild cognitive impairment. *J. Neurol.* 254, 1698–1707. doi: 10.1007/s00415-007-0631-7

Chalk, M., Herrero, J. L., Gieselmann, M. A., Delicato, L. S., Gotthardt, S., and Thiele, A. (2010). Attention reduces stimulus-driven gamma frequency oscillations and spike field coherence in V1. *Neuron* 66, 114–125. doi: 10.1016/j.neuron.2010.03.013

Chatwal, J. P., and Sperling, R. A. (2012). Functional MRI of mnemonic networks across the spectrum of normal aging, mild cognitive impairment, and Alzheimer's disease. *J. Alzheimers Dis.* 31, S155–S167. doi: 10.3233/JAD-2012-120730

Colom, L. V. (2006). Septal networks: relevance to theta rhythm, epilepsy and Alzheimer's disease. *J. Neurochem.* 96, 609–623. doi: 10.1111/j.1471-4159.2005.03630.x

Craik, F. I. M. (2002). Levels of processing: past, present and future? *Memory* 10, 305–318. doi: 10.1080/09658210244000135

Dale, A. M., Fischl, B., and Sereno, M. I. (1999). Cortical surface- based analysis. I. Segmentation and surface reconstruction. *Neuroimage* 9, 179–194. doi: 10.1006/nimg.1998.0395

DeCarli, C., Fletcher, E., Ramey, V., Harvey, D., and Jagust, W. J. (2005). Anatomical mapping of white matter hyperintensities (WMH): exploring the relationships between periventricular WMH, deep WMH, and total WMH burden. *Stroke* 36, 50–55. doi: 10.1161/01.STR.0000150668.58689.f2

De Haan, W., Mott, K., van Straaten, E. C., Scheltens, P., and Stam, C. J. (2012). Activity dependent degeneration explains hub vulnerability in Alzheimer's disease. *PLoS Comput. Biol.* 8:e1002582. doi: 10.1371/journal.pcbi.1002582

Dubois, B., Feldman, H. H., Jacova, C., Dekosky, S. T., Barberger-Gateau, P., Cummings, J., et al. (2007). Research criteria for the diagnosis of Alzheimer's disease: revising the NINCDS-ADRDA criteria. *Lancet Neurol.* 6, 734–746. doi: 10.1016/S1474-4422(07)70178-3

Fischl, B., and Dale, A. M. (2000). Measuring the thickness of the human cerebral cortex using magnetic resonance images. *Proc. Natl. Acad. Sci. U.S.A.* 97, 11044–11049. doi: 10.1073/pnas.200033797

Fischl, B., Sereno, M. I., and Dale, A. M. (1999). Cortical surface- based analysis. II. Inflation, flattening, and a surface-based coordinate system. *Neuroimage* 9, 195–207. doi: 10.1006/nimg.1998.0396

Folstein, M. F., Folstein, S. E., and McHugh, P. R. (1975). 'Mini mental state': a practical method for grading the cognitive state of patients for the clinician. *J. Psychiatr. Res.* 12, 189–198. doi: 10.1016/0022-3956(75)90026-6

Frisoni, G. B. (2012). Alzheimer disease: biomarker trajectories across stages of Alzheimer disease. *Nat. Rev. Neurol.* 8, 299–300. doi: 10.1038/nrneurol.2012.8

Frisoni, G. B., Ganzola, R., Canu, E., Rub, U., Pizzini, F. B., Alessandrini, F., et al. (2008). Mapping local hippocampal changes in Alzheimer's disease and normal ageing with MRI at 3 tesla. *Brain* 131, 3266–3276. doi: 10.1093/brain/awn280

Frisoni, G. B., Pievani, M., Testa, C., Sabattoli, F., Bresciani, L., Bonetti, M., et al. (2007). The topography of grey matter involvement in early and late onset Alzheimer's disease. *Brain* 130, 720–730. doi: 10.1093/brain/awl377

Frisoni, G. B., Prestia, A., Rasser, P. E., Bonetti, M., and Thompson, P. M. (2009). In vivo mapping of incremental cortical atrophy from incipient to overt Alzheimer's disease. *J. Neurol.* 256, 916–924. doi: 10.1007/s00415-009-5040-7

Frisoni, G. B., Sabattoli, F., Lee, A. D., Dutton, R. A., Toga, A. W., Thompson, P. M., et al. (2006). In vivo neuropathology of the hippocampal formation in AD: a radial mapping MR-based study. *Neuroimage* 32, 104–110. doi: 10.1016/j.neuroimage.2006.03.015

Galluzzi, S., Geroldi, C., Amicucci, G., Bocchio- Chiavetto, L., Bonetti, M., Bonvicini, C., et al. (2013). Translational outpatient memory clinic working group: supporting evidence for using biomarkers in the diagnosis of MCI due to AD. *J. Neurol.* 260, 640–650. doi: 10.1007/s00415-012-6694-0

Goard, M., and Dan, Y. (2009). Basal forebrain activation enhances cortical coding of natural scenes. *Nat. Neurosci.* 12, 1444–1449. doi: 10.1038/nn.2402

Golde, T. E. (2003). Alzheimer disease therapy: can the amyloid cascade be halted? *J. Clin. Invest.* 111, 11–18. doi: 10.1172/JCI200317527

Gronenschild, E. H., Habets, P., Jacobs, H. I., Mengelers, R., Rozendaal, N., van Os, J., et al. (2012). The effects of FreeSurfer version, workstation type, and Macintosh operating system version on anatomical volume and cortical thickness measurements. *PLoS ONE* 7:e38234. doi: 10.1371/journal.pone.0038234

Hampel, H., Burger, K., Teipel, S. J., Bokde, A. L., Zetterberg, H., and Blennow, K. (2007). Core candidate neurochemical and imaging biomarkers of Alzheimer's disease. *Alzheimers Dement.* 4, 38–48. doi: 10.1016/j.jalz.2007.08.006

Han, X., Jovicich, J., Salat, D., van der Kouwe, A., Quinn, B., Czanner, S., et al. (2006). Reliability of MRI-derived measurements of human cerebral cortical thickness: the effects of field strength, scanner upgrade and manufacturer. *Neuroimage* 32, 180–194. doi: 10.1016/j.neuroimage.2006.02.051

Hanslmayr, S., Spitzer, B., and Bauml, K.-H. (2009). Brain oscillations dissociate between semantic and non-semantic encoding of episodic memories. *Cereb. Cortex* 19, 1631–1640. doi: 10.1093/cercor/bhn197

Hanslmayr, S., Staudigl, T., Aslan, A., and Bauml, K.-H. (2010). Theta oscillations predict the detrimental effects of memory retrieval. *Cogn. Affect. Behav. Neurosci.* 10, 329–338. doi: 10.3758/CABN.10.3.329

Hanslmayr, S., Staudigl, T., and Fellner, M. C. (2012). Oscillatory power decreases and long-term memory: the information via desynchronization hypothesis. *Front. Hum. Neurosci.* 6:74. doi: 10.3389/fnhum.2012.00074

Hughes, C. P., Berg, L., Danziger, W. L., Cohen, L. A., and Martin, R. L. (1982). A new clinical rating scale for the staging of dementia. *Br. J. Psychiatry* 140, 1225–1230. doi: 10.1192/bjp.140.6.566

Ingber, L., and Nunez, P. L. (2011). Neocortical dynamics at multiple scales: EEG standing waves, statistical mechanics, and physical analogs. *Math. Biosci.* 229, 160–173. doi: 10.1016/j.mbs.2010.12.003

Jensen, O., and Mazaheri, A. (2010). Shaping functional architecture by oscillatory alpha activity: gating by inhibition. *Front. Hum. Neurosci.* 4:186. doi: 10.3389/fnhum.2010.00186

Jones, D. T., Machulda, M. M., Vemuri, P., McDade, E. M., Zeng, G., Senjem, M. L., et al. (2011). Age-related changes in the default mode network are more advanced in Alzheimer disease. *Neurology* 77, 1524–1531. doi: 10.1212/WNL.0b013e318233b33d

Kilner, J. M., Mattout, J., Henson, R., and Friston, K. J. (2005). Hemodynamic correlates of EEG: a heuristic. *Neuroimage* 28, 280–286. doi: 10.1016/j.neuroimage.2005.06.008

Klimesch, W. (1997). EEG-alpha rhythms and memory processes. *Int. J. Psychophysiol.* 26, 319–340. doi: 10.1016/S0167-8760(97)00773-3

Klimesch, W. (1999). EEG alpha and theta oscillations reflect cognitive and memory performance: a review and analysis. *Brain Res. Rev.* 29, 169–195. doi: 10.1016/S0165-0173(98)00056-3

Klimesch, W., Schimke, H., Doppelmayr, M., Ripper, B., Schwaiger, J., and Pfurtscheller, G. (1996). Event-related desynchronization (ERD) and the Dm effect: does alpha desynchronization during encoding predict late recall performance? *Int. J. Psychophysiol.* 24, 47–60. doi: 10.1016/S0167-8760(96)00054-2

Kuperberg, G. R., Broome, M. R., McGuire, P. K., David, A. S., Eddy, M., Ozawa, F., et al. (2003). Regionally localized thinning of the cerebral cortex in schizophrenia. *Arch. Gen. Psychiatry* 60, 878–888. doi: 10.1001/archpsyc.60.9.878

Kurimoto, R., Ishii, R., Canuet, L., Ikezawa, K., Iwase, M., Azechi, M., et al. (2012). Induced oscillatory responses during the Sternberg's visual memory task in patients with Alzheimer's disease and mild cognitive impairment. *Neuroimage* 59, 4132–4140. doi: 10.1016/j.neuroimage.2011.10.061

Lawton, M. P., and Brodie, E. M. (1969). Assessment of older people: self maintaining and instrumental activity of daily living. *J. Gerontol.* 9, 179–186. doi: 10.1093/geront/9.3_Part_1.179

Lezak, M., Howieson, D., and Loring, D. W. (2004). *Neuropsychological Assessment*, 4th Edn. Oxford: Oxford University Press.

Lopes da Silva, F. H., Vos, J. E., Mooibroek, J., and van Rotterdam, A. (1980). Relative contributions of intracortical and thalamo-cortical processes in the generation of alpha rhythms, revealed by partial coherence analysis. *Electroencephalogr. Clin. Neurophysiol.* 50, 449–456. doi: 10.1016/0013-4694(80)90011-5

Maldjian, J. A., Laurienti, P. J., Kraft, R. A., and Burdette, J. H. (2003). An automated method for neuroanatomic and cytoarchitectonic atlas-based interrogation of fMRI data sets. *Neuroimage* 19, 1233–1239. doi: 10.1016/S1053-8119(03)00169-1

Markesbery, W. R., Schmitt, R. A., Kryscio, R. J., Davis, D., Smith, C., and Wekstein, D. (2006). Neuropathologic substrate of mild cognitive impairment. *Arch. Neurol.* 63, 38–46. doi: 10.1001/archneur.63.1.38

McKhann, G. M., Knopman, D. S., Chertkow, H., Hyman, B. T., Jack, C. R. Jr., Kawas, C. H., et al. (2011). The diagnosis of dementia due to Alzheimer's disease: recommendations from the National Institute on Aging-Alzheimer's Association workgroups on diagnostic guidelines for Alzheimer's disease. *Alzheimers Dement.* 7, 263–269. doi: 10.1016/j.jalz.2011.03.005

Mielke, R., Pietrzyk, U., Jacobs, A., Fink, G. R., Ichimiya, A., Kessler, J., et al. (1994). HMPAO SPET and FDG PET in Alzheimer's disease and vascular dementia: comparison of perfusion and metabolic pattern. *Eur. J. Nucl. Med.* 21, 1052–1060. doi: 10.1007/BF00181059

Missonnier, P., Herrmann, F. R., Michon, A., Fazio-Costa, L., Gold, G., and Giannakopoulos, P. (2010). Early disturbances of gamma band dynamics in mild cognitive impairment. *J. Neural. Transm.* 117, 489–498. doi: 10.1007/s00702-010-0384-9

Moretti, D. V., Babiloni, C., Binetti, G., Cassetta, E., Dal Forno, G., Ferreri, F., et al. (2004). Individual analysis of EEG frequency and band power in mild Alzheimer's disease. *Clin. Neurophysiol.* 115, 299– 308. doi: 10.1016/S1388-2457(03)00345-6

Moretti, D. V., Babiloni, F., Carducci, F., Cincotti, F., Remondini, E., Rossini, P. M., et al. (2003). Computerized processing of EEG-EOGEMG artifacts for multi-centric studies in EEG oscillations and event-related potentials. *Int. J. Psychophysiol.* 47, 199–216. doi: 10.1016/S0167-8760(02)00153-8

Moretti, D. V., Frisoni, G. B., Fracassi, C., Pievani, M., Geroldi, C., Binetti, G., et al. (2011a). MCI patients' EEGs show group differences between those who progress and those who do not progress to AD. *Neurobiol. Aging* 32, 563–571. doi: 10.1016/j.neurobiolaging.2009.04.003

Moretti, D. V., Prestia, A., Fracassi, C., Geroldi, C., Binetti, G., Rossini, P., et al. (2011b). Volumetric differences in mapped hippocampal regions correlate with increase of high alpha rhythm in Alzheimer's disease. *Int. J. Alzheimers Dis.* 2011:208218. doi: 10.4061/2011/208218

Moretti, D. V., Miniussi, C., Frisoni, G., Zanetti, O., Binetti, G., Geroldi, C., et al. (2007). Vascular damage and EEG markers in subjects with mild cognitive impairment. *Clin. Neurophysiol.* 118, 1866–1876. doi: 10.1016/j.clinph.2007.05.009

Moretti, D. V., Paternico, D., Binetti, G., Zanetti, O., and Frisoni, G. B. (2012a). EEG markers are associated to gray matter changes in thalamus and basal ganglia in subjects with mild cognitive impairment. *Neuroimage* 60, 489–496. doi: 10.1016/j.neuroimage.2011.11.086

Moretti, D. V., Prestia, A., Fracassi, C., Binetti, G., Zanetti, O., and Frisoni, G. B. (2012b). Specific EEG changes associated with atrophy of hippocampus in subjects with mild cognitive impairment and Alzheimer's disease. *Int. J. Alzheimers Dis.* 2012:253153. doi: 10.1155/2012/253153

Moretti, D. V., Paternico, D., Binetti, G., Zanetti, O., and Frisoni, G. B. (2013a). Relationship between EEG alpha3/ alpha2 Ratio and the nucleus accumbens in subjects with mild cognitive impairment. *J. Neurol. Neurophysiol.* 4, 1–6.

Moretti, D. V., Prestia, A., Binetti, G., Zanetti, O., and Frisoni, G. B. (2013b). Increase of theta frequency is associated with reduction in regional cerebral blood flow only in subjects with mild cognitive impairment with higher upper alpha/low alpha EEG frequency power ratio. *Front. Behav. Neurosci.* 7:188. doi: 10.3389/fnbeh.2013.00188

Moretti, D. V., Pievani, M., Fracassi, C., Binetti, G., Rosini, S., Geroldi, C., et al. (2009). Increase of theta/gamma and alpha3/ alpha2 ratio is associated with amygdalohippocampal complex atrophy. *J. Alzheimers Dis.* 120, 295–303.

Moretti, D. V., Pievani, M., Fracassi, C., Geroldi, C., Calabria, M., De Carli, C. S., et al. (2008). Brain vascular damage of cholinergic pathways and EEG markers in mild cognitive impairment. *J. Alzheimers Dis.* 15, 357–372.

Müller, T. J., Thome, J., Chiaramonti, R., Dierks, T., Maurer, K., Fallgatter, A. J., et al. (1997). A comparison of qEEG and HMPAO-SPECT in relation to the clinical severity of Alzheimer's disease. *Eur. Arch. Psychiatry Clin. Neurosci.* 247, 259–263. doi: 10.1007/BF02900304

Norman, K. A. (2010). How hippocampus and cortex contribute to recognition memory: revisiting the complementary learning systems model. *Hippocampus* 20, 1217–1227. doi: 10.1002/hipo.20855

Nunez, P. (1989). Generation of human EEG rhythms by a combination of long and short-range neocortical interactions. *Brain Topogr.* 1, 199–215. doi: 10.1007/BF01129583

Palop, J. J., and Mucke, L. (2010). Synaptic depression and aberrant excitatory network activity in Alzheimer's disease: two faces of the same coin? *Neuromol. Med.* 12, 48–55. doi: 10.1007/s12017-009-8097-7

Pennanen, C., Testa, C., Laasko, M. P., Hallikainen, M., Helkala, E. L., Hanninen, T., et al. (2005). A voxel based morphometry study on mild cognitive impairment. *J. Neurol. Neurosurg. Psychiatry* 76, 11–14. doi: 10.1136/jnnp.2004.035600

Petersen, R. C., Doody, R., Kurz, A., Mohs, R. C., Morris, J. C., Rabins, P. V., et al. (2001). Current concepts in mild cognitive impairment. *Arch. Neurol.* 58, 1985–1992. doi: 10.1001/archneur.58.12.1985

Pievani, M., de Haan, W., Wu, T., Seeley, W. W., and Frisoni, G. B. (2011). Functional network disruption in the degenerative dementias. *Lancet Neurol.* 10, 829–843. doi: 10.1016/S1474-4422(11)70158-2

Portet, F., Ousset, P. J., Visser, P. J., Frisoni, G. B., Nobili, F., Scheltens, P., et al. (2006). Mild cognitive impairment (MCI) in medical practice: a critical review of the concept and new diagnostic procedure. Report of the MCI Working Group of the European Consortium on Alzheimer's Disease. *J. Neurol. Neurosurg. Psychiatry* 77, 714–718. doi: 10.1136/jnnp.2005.085332

Pupi, A., Mosconi, L., Nobili, F. M., and Sorbi, S. (2005). Toward the validation of functional neuroimaging as a potential biomarker for Alzheimer's disease: implications for drug development. *Mol. Imaging Biol.* 7, 59–68. doi: 10.1007/s11307-005-0953-8

Radloff, L. S. (1977). The CES-D scale: a self-report depression scale for research in the general population. *Appl. Psychol. Measure* 1, 385–401. doi: 10.1177/014662167700100306

Rodriguez, G., Arnaldi, D., and Picco, A. (2011). Brain functional network in Alzheimer's disease: diagnostic markers for diagnosis and monitoring. *Int. J. Alzheimers Dis.* 2011:481903. doi: 10.4061/2011/481903

Rodriguez, G., Nobili, F., Copello, F., Vitali, P., Gianelli, M. V., Taddei, G., et al. (1999). 99mTc-HMPAO regional cerebral blood flow and quantitative electroencephalography in Alzheimer's disease: a correlative study. *J. Nucl. Med.* 40, 522–529.

Rorden, C., and Brett, M. (2000). Stereotaxic display of brain lesions. *Behav. Neurol.* 12, 191–200. doi: 10.1155/2000/421719

Rosas, H. D., Liu, A. K., Hersch, S., Glessner, M., Ferrante, R. J., Salat, D. H., et al. (2002). Regional and progressive thinning of the cortical ribbon in Huntington's disease. *Neurology* 58, 695–701. doi: 10.1212/WNL.58.5.695

Rosen, W. G., Terry, R. D., Fuld, P. A., Katzman, R., and Peck, A. (1980). Pathological verification of ischemic score in differentiation of dementias. *Ann. Neurol.* 7, 486–488. doi: 10.1002/ana.410070516

Rossini, P. M., Buscema, M., Capriotti, M., Grossi, E., Rodriguez, G., Del Percio, C., et al. (2008). Is is possible to automatically distinguish resting EEG data of normal elderly vs mild cognitive impairment subjects with high degree of accuracy? *Clin. Neurophysiol.* 119, 1534–1545. doi: 10.1016/j.clinph.2008.03.026

Ryu, S. Y., Kwon, M. J., Lee, S. B., Yang, D. W., Kim, T. W., Song, I. U., et al. (2010). Measurement of precuneal and hippocampal volumes using magnetic resonance volumetry in Alzheimer's disease. *J. Clin. Neurol.* 6, 196–203. doi: 10.3988/jcn.2010.6.4.196

Schneidman, E., Puchalla, J. L., Segev, R., Harris, R. A., Bialek, W., and Berry, M. J. (2011). Synergy from silence in a combinatorial neural code. *J. Neurosci.* 31, 15732–15741. doi: 10.1523/JNEUROSCI.0301-09.2011

Segonne, F., Dale, A. M., Busa, E., Glessner, M., Salat, D., Hahn, H. K., et al. (2004). A hybrid approach to the skull stripping problem in MRI. *Neuroimage* 22, 1060–1075. doi: 10.1016/j.neuroimage.2004.03.032

Sperling, R. A., Dickerson, B. C., Pihlajamaki, M., Vannini, P., LaViolette, P. S., Vitolo, O. V., et al. (2010). Functional alterations in memory networks in early Alzheimer's disease. *Neuromol. Med.* 12, 27–43. doi: 10.1007/s12017-009-8109-7

Spitzer, B., Hanslmayr, S., Opitz, B., Mecklinger, A., and Bauml, K.-H. (2009). Oscillatory correlates of retrievalinduced forgetting in recognition memory. *J. Cogn. Neurosci.* 21, 976–990. doi: 10.1162/jocn.2009.21072

Staffen, W., Bergmann, J., Schönauer, U., Zauner, H., Kronbichler, M., Golaszewski, S., et al. (2009). Cerebral perfusion (HMPAO-SPECT) in patients with depression with cognitive impairment versus those with mild cognitive impairment and dementia of Alzheimer's type: a semiquantitative and automated evaluation. *Eur. J. Nucl. Med. Mol. Imaging* 36, 801–810. doi: 10.1007/s00259-008-1028-2

Stam, C. J., Montez, T., Jones, B. F., Rombouts, S. A., van der Made, Y., Pijnenburg, Y. A., et al. (2005). Disturbed fluctuations of resting state EEG synchronization in Alzheimer's disease. *Clin. Neurophysiol.* 116, 708–715. doi: 10.1016/j.clinph.2004.09.022

Stam, C. J., van der Made, Y., Pijnenburg, Y. A., and Scheltens, P. (2003). EEG synchronization in mild cognitive impairment and Alzheimer's disease. *Acta Neurol. Scand.* 108, 90–96. doi: 10.1034/j.1600-0404.2003.02067.x

Staudigl, T., Hanslmayr, S., and Bauml, K.-H. T. (2010). Theta oscillations reflect the dynamics of interference in episodic memory retrieval. *J. Neurosci.* 30, 11356–11362. doi: 10.1523/JNEUROSCI.0637-10.2010

Steriade, M. (2006). Grouping of brain rhythms in corticothalamic systems. *Neuroscience* 137, 1087–1106. doi: 10.1016/j.neuroscience.2005.10.029

Thatcher, R. W., Biver, C., McAlaster, R., and Salazar, A. (1998). Biophysical linkage between MRI and EEG coherence in closed head injury. *Neuroimage* 8, 307–326. doi: 10.1006/nimg.1998.0365

Van Strien, N. M., Cappaert, N. L., and Witter, M. P. (2009). The anatomy of memory: an interactive overview of the parahippocampal-hippocampal network. *Nat. Rev. Neurosci.* 10, 272–282. doi: 10.1038/nrn2614

Wenderoth, N., Debaere, F., Sunaert, S., and Swinnen, S. P. (2005). The role of anterior cingulate cortex and precuneus in the coordination of motor behaviour. *Eur. J. Neurosci.* 22, 235–246. doi: 10.1111/j.1460-9568.2005.04176.x

Wonderlick, J. S., Ziegler, D. A., Hosseini-Varnamkhasti, P., Locascio, J. J., Bakkour, A., van der Kouwe, A., et al. (2009). Reliability of MRI-derived cortical and subcortical morphometric measures: effects of pulse sequence, voxel geometry, and parallel imaging. *Neuroimage* 44, 1324–1333. doi: 10.1016/j.neuroimage.2008.10.037

Wu, X., Li, R., Fleisher, A. S., Reiman, E. M., Guan, X., Zhang, Y., et al. (2011). Altered default mode network connectivity in Alzheimer's disease – a resting functional MRI and bayesian network study. *Hum. Brain Mapp.* 32, 1868–1881. doi: 10.1002/hbm.21153

Wyart, V., and Tallon-Baudry, C. (2008). Neural dissociation between visual awareness and spatial attention. *J. Neurosci.* 28, 2667–2679. doi: 10.1523/JNEUROSCI.4748-07.2008

Yoon, H. J., Park, K. W., Jeong, Y. J., and Kang, D. Y. (2012). Correlation between neuropsychological tests and hypoperfusion in MCI patients: anatomical labeling using xjView and Talairach Daemon software. *Ann. Nucl. Med.* 26, 656–664. doi: 10.1007/s12149-012-0625-0

Zhang, S., and Li, C. S. (2012). Functional connectivity mapping of the human precuneus by resting state fMRI. *Neuroimage* 59, 3548–3562. doi: 10.1016/j.neuroimage.2011.11.023

Conflict of Interest Statement: The author declares that the research was conducted in the absence of any commercial or financial relationships that could be construed as a potential conflict of interest.

Copyright © 2015 Moretti. This is an open-access article distributed under the terms of the Creative Commons Attribution License (CC BY). The use, distribution or reproduction in other forums is permitted, provided the original author(s) or licensor are credited and that the original publication in this journal is cited, in accordance with accepted academic practice. No use, distribution or reproduction is permitted which does not comply with these terms.

frontiers in
AGING NEUROSCIENCE

ORIGINAL RESEARCH ARTICLE
published: 20 November 2013
doi: 10.3389/fnagi.2013.00079

Mismatch negativity (MMN) amplitude as a biomarker of sensory memory deficit in amnestic mild cognitive impairment

Mónica Lindín*, Kenia Correa, Montserrat Zurrón and Fernando Díaz

Laboratorio de Psicofisioloxía e Neurociencia Cognitiva, Facultade de Psicoloxía, Universidade de Santiago de Compostela, Santiago de Compostela, Spain

Edited by:
Davide V. Moretti, IRCCS Fatebenefratelli, Italy

Reviewed by:
Daniel Ortuño-Sahagun, Centro Universitario de Ciencias Biológicas y Agropecuarias, Mexico
Olga Bazanova, Siberian branch of the Russian Academy of Medical Sciences, Russia

****Correspondence:***
Mónica Lindín, Laboratorio de Psicofisioloxía e Neurociencia Cognitiva, Departamento de Psicoloxía Clínica e Psicobioloxía, Universidade de Santiago de Compostela, Rúa de Xosé María Suárez Núñez, S/N, 15782 Santiago de Compostela, Spain
e-mail: monica.lindin@usc.es

It has been suggested that changes in some event-related potential (ERP) parameters associated with controlled processing of stimuli could be used as biomarkers of amnestic mild cognitive impairment (aMCI). However, data regarding the suitability of ERP components associated with automatic and involuntary processing of stimuli for this purpose are not conclusive. In the present study, we studied the Mismatch Negativity (MMN) component, a correlate of the automatic detection of changes in the acoustic environment, in healthy adults and adults with aMCI (age range: 50–87 years). An auditory-visual attention-distraction task, in two evaluations separated by an interval of between 18 and 24 months, was used. In both evaluations, the MMN amplitude was significantly smaller in the aMCI adults than in the control adults. In the first evaluation, such differences were observed for the subgroup of adults between 50 and 64 years of age, but not for the subgroup of 65 years and over. In the aMCI adults, the MMN amplitude was significantly smaller in the second evaluation than in the first evaluation, but no significant changes were observed in the control adult group. The MMN amplitude was found to be a sensitive and specific biomarker of aMCI, in both the first and second evaluation.

Keywords: amnestic mild cognitive impairment, Alzheimer's disease, event-related potentials, mismatch negativity, sensory memory, biomarkers

INTRODUCTION

Mild cognitive impairment (MCI) is a heterogeneous clinical entity characterized by objective evidence of cognitive decline, without any notable impairment in the performance of daily activities. It is also considered as an intermediate stage between the cognitive changes associated with healthy aging and early clinical features of dementia (Petersen, 2004; Winblad et al., 2004). Among the different subtypes of MCI, amnestic MCI (aMCI) is the most likely to progress to Alzheimer's disease (AD) (Petersen et al., 2001, 2009; Petersen, 2004; Winblad et al., 2004; Albert et al., 2011), which is the most prevalent form of dementia in the elderly (Papaliagkas et al., 2009).

The establishment of aMCI biomarkers would be of benefit to clinicians as the biomarkers could be used as objective diagnostic tools, thus allowing early or pre-symptomatic identification of AD, aiding treatment decisions, monitoring disease progress, and providing opportunities for prevention by population screening (Henry et al., 2012). The methods used to search for biomarkers of MCI include neuroimaging techniques (Small et al., 2006; Hämäläinen et al., 2007), cerebrospinal fluid analysis (Perneczky et al., 2011), genetic analysis (Zhang et al., 2012) and electroencephalography (EEG), both quantitative EEG (see Jackson and Snyder, 2008) and event-related potentials (ERPs; see Jackson and Snyder, 2008 and Vecchio and Määttä, 2011).

The use of ERP technique in the search for aMCI biomarkers is founded on three essential characteristics designated as ideal (see Hampel et al., 2010): it is non-invasive, simple to measure and inexpensive. Moreover, the technique has good temporal resolution and allows the study of neurophysiological correlates of sensory-perceptive and pre-attentive processes, the integrity of which are essential for the efficient functioning of higher-level processes and thus the final performance.

Some ERP studies have shown a larger deficit in the controlled processing of information (such as the evaluation of stimuli in working memory) in adults with aMCI than in healthy adults (Golob et al., 2001; Bennys et al., 2007; Missonnier et al., 2007; Lai et al., 2010; Li et al., 2010; Parra et al., 2012). This deficit appears to be more evident in aMCI adults that progress to AD than in those who do not develop AD (Golob et al., 2007; Missonnier et al., 2007). However, studies concerning ERP correlates of involuntary and automatic processing of stimuli in adults with MCI are scarce and the results are inconclusive.

The mismatch negativity (MMN) component is probably the most widely studied ERP component in healthy and clinical populations, in relation to automatic and pre-attentive processing of stimuli. Mismatch negativity was first described for the auditory modality (Näätänen et al., 1978), but has also been reported for other sensory modalities (for a review see Näätänen et al., 2007).

Auditory MMN is a negative wave commonly derived by subtracting the ERP waveform evoked by the standard stimulus from that evoked by the deviant stimulus in passive oddball tasks (which do not require the participant's attention). In young adults, the MMN latency is between 100 and 200 ms, and the amplitude is maximal at frontocentral sites (reversing polarity

at mastoid electrodes). In fact, MMN is considered a correlate of pre-attentive processes, which are triggered when the sensory input does not match the echoic memory representation of a prevalent standard stimulus. Therefore, auditory MMN is an objective index of auditory discrimination (automatic detection of changes in the acoustic environment) and an indirect measure of the accuracy of the neural representation of a standard stimulus (see Näätänen and Alho, 1997).

Among the neural generators of MMN, the bilateral supratemporal cortices and predominantly right frontal cortex have been consistently identified (Näätänen et al., 2007). It has been suggested that the supratemporal component is involved in the automatic detection of auditory change and that the frontal component is related to the involuntary attention switch caused by auditory change (Giard et al., 1990; Rinne et al., 2000).

Some studies have shown that the MMN amplitude decreases significantly with age in healthy adults. This has been observed both when the deviant stimulus differs from the standard in duration (Pekkonen et al., 1996; Cooper et al., 2006) or tonal frequency (Czigler et al., 1992; Gaeta et al., 1998; Cooper et al., 2006) and when novel stimuli are presented (Gaeta et al., 1998). It has also been observed with long interstimulus intervals (ISIs) (Czigler et al., 1992; Pekkonen et al., 1996), but not with short ISIs (2.4 s. or less; Pekkonen et al., 1996; Amenedo and Díaz, 1998; Raggi et al., 2013; but also see Czigler et al., 1992; Gaeta et al., 1998; Cooper et al., 2006). In a rather less consistent manner, the latency of MMN also increases with age (Gaeta et al., 1998; Cooper et al., 2006).

Two possible explanations for age-related changes in MMN parameters have been proposed: (i) the sensory memory trace may be poorer or more degraded in older than in younger subjects, reflecting an inaccurate representation of standard stimuli by the brain, and/or (ii) a deficient comparator mechanism fails to detect a mismatch between the representation of the standard and the deviant stimuli (Gaeta et al., 1998).

In studies with AD patients, changes in MMN have been observed under some task conditions. For ISIs of 1.3 s or less, no significant differences between control adults and adults with AD were observed in the MMN amplitude elicited by changes in tonal frequency (Pekkonen et al., 1994; Kazmerski et al., 1997; Gaeta et al., 1999; Brønnick et al., 2010) or by presentation of novel stimuli (Kazmerski et al., 1997; Gaeta et al., 1999). However, in AD patients the MMN amplitude was significantly smaller for an ISI of 3 s than for the shorter ISI condition (1 s), while in control adults the MMN amplitude was stable across both ISIs (Pekkonen et al., 1994). These results suggest that sensory memory trace decays faster in AD patients than in healthy controls, although auditory discrimination was not affected (Pekkonen et al., 1994).

In the only published study to date evaluating the effect of MCI on MMN parameters, Mowszowski et al. (2012) recorded ERPs in a sample of 14 healthy adults and 28 adults with MCI, in a passive oddball task in which the standard and deviant stimuli differed in duration (standard: 50 ms, deviant: 100 ms). In the MCI group, all participants showed impairment in several cognitive domains. Of these, half were amnestic subtype (aMCI) Multiple Domain and half non-amnestic subtype (naMCI) Multiple Domain. The authors found no differences between the MCI and control groups in MMN amplitude or latency, or between the aMCI and naMCI subtypes at frontocentral locations. However, they did observe that at mastoid locations, the MMN amplitude was smaller in the MCI group than in the control group, which the authors considered reflect of the inefficiency of processing information in an early pre-attentional stage in the MCI group.

The recent study by Mowszowski et al. (2012) provided some interesting results, but also presented some limitations. Thus, the differences in MMN amplitude between MCI and control adults were obtained at mastoid electrodes, but not at the frontocentral locations, where MMN is typically identified and analyzed. Moreover, the analysis did not take into account the possible effects of interactions between the Age and Group factors, although previous studies have reported age effects on MMN amplitude to changes of stimuli duration (Pekkonen et al., 1996; Gaeta et al., 1998; Cooper et al., 2006). Moreover, the MCI group was heterogeneous, as it included both amnestic and non-amnestic multidomain MCI patients.

The aims of the present study were as follows: (1) to determine any differences in MMN parameters between healthy adults and adults with aMCI; (2) to evaluate whether such differences between healthy adults and adults with aMCI are affected by age, by considering two age subgroups (50–64 years and 65 years and over); (3) to determine whether the differences in MMN parameters between healthy and aMCI adults are maintained in a second evaluation, conducted 18–24 months after the first evaluation, and (4) to evaluate whether MMN changes associated with aMCI are sensitive and specific biomarkers of this syndrome.

We used an auditory-visual attention-distraction task [based on the task designed by Escera et al. (1998), see Methods section]. This task was presented to a sample of healthy control adults and adults with aMCI during two evaluations separated by an interval of between 18 and 24 months. Auditory MMN was obtained by subtracting the ERP waveform evoked by standard stimuli from the waveform evoked by the deviant or novel stimuli (deviant *minus* standard, and novel *minus* standard).

To our knowledge, this is the first study designed to determine whether MMN parameters (amplitude and/or latency) are sensitive and specific biomarkers of aMCI, whether their effectiveness in identifying adults with this syndrome interacts with age, and also whether the MMN parameters change over time in healthy control and aMCI adults.

MATERIALS AND METHODS

PARTICIPANTS

Participants were 56 healthy adult volunteers (35 women, 21 men; age range: 50–87 years old; mean = 65.7 years, SD = 9.1), recruited from Primary Care Health Centres in Santiago de Compostela and Vigo (Galicia, Spain) and referred to our research group by their general practitioners (GPs). The participants had no history of clinical stroke, traumatic brain injury, motor-sensory defects, or alcohol or drug abuse/dependence, and they were not diagnosed with any significant medical or psychiatric illnesses. To control for the effects of depression, adults with a score of more than 10 in depression screening (Geriatric Depression Scale, GDS; Yesavage et al., 1983) were excluded from the study. All participants had normal audition and normal or

corrected-to-normal vision. Most of them were right-handed, as assessed by the Edinburgh inventory (Oldfield, 1971), except for one left-handed and one ambidextrous participant.

After giving their written informed consent, participants were referred by their GPs to the Psychogerontology Group (see Juncos-Rabadán et al., 2013) with whom we participate in a collaborative research project. They conducted the neuropsychological evaluation and the clinical diagnosis of MCI. The participants were then referred to our laboratory for psychophysiological (ERP) evaluation.

The participants provided us with information about years of education, as well as socioeconomic, medical and personal data, received extensive psychological and neuropsychological evaluations, and were diagnosed and classified as control or aMCI. They underwent the following tests: (1) The Mini-Mental State Examination (MMSE, Folstein et al., 1975; Spanish version, MEC by Lobo et al., 1999), which assesses general cognitive functioning; (2) The Californian Verbal Learning Test [CVLT, Delis et al., 1987; Spanish version, TAVEC by Benedet and Alejandre (1998)], which assesses short-delay free recall, short-delay recall with semantic cues, and long-delay free recall; (3) The Spanish version of the Cambridge Cognitive Examination (CAMCOG-R), which assesses deterioration in specific domains such as language, attention-calculation, praxis, perception, and executive functioning (Huppert et al., 1996) and is sensitive to MCI detection (Gallagher et al., 2010); and (4) The Spanish version of the vocabulary test of the Wechsler Adult Intelligence Scale (WAIS, Wechsler, 1988).

Two evaluations, separated by an interval of between 18 and 24 months, were carried out. In the first evaluation, the Control group (CG) comprised 30 adults aged between 50 and 84 years (mean: 63.9 years, *SD*: 8.4) with normal cognitive and memory functioning, and the aMCI group comprised 26 adults aged between 51 and 87 years (mean: 67.8 years, *SD*: 9.3). In the second evaluation, only 27 (18 control and 9 aMCI) of the initial sample of 56 participants agreed to participate in the ERP recordings. Two of the 18 control adults and 1 of the 9 aMCI adults were excluded because of excessive artifacts in their recording, and 1 aMCI adult died. Nine of the 16 control adults with valid recordings were selected with the aim of matching their ages with the aMCI group. Consequently, the final sample in the second evaluation consisted of 16 adults: 9 control adults (range age: 59–73 years) and 7 aMCI adults (range age: 62–89 years), whose diagnosis was maintained between evaluations.

In both evaluations, control adults scored higher than the cut-off on memory, general cognitive functioning, and specific cognitive domain tests. The aMCI subjects met the general criteria for MCI outlined by Albert et al. (2011) and the criteria for aMCI proposed by Petersen and colleagues (Petersen, 2004; Dubois et al., 2007).

The aMCI adults fulfilled the following criteria: (1) memory complaints corroborated by an informant; (2) performance of less than 1.5 *SD*s below age norms for the CVLT; (3) no significant impact on daily living activities; and (4) without dementia, according to the National Institute of Neurological and Communicative Diseases and Stroke/Alzheimer's Disease and Related Disorders Association (NINCDS-ADRDA) and the Diagnostic and Statistical Manual of Mental Disorders (DMS-IV) criteria. The Lawton and Brody Index (Lawton and Brody, 1969) was used to evaluate instrumental activities of daily living (IADL). Nine of the aMCI adults fulfilled criteria for multiple domain amnestic MCI (mda-MCI), and 17 subjects fulfilled criteria for single domain amnestic MCI (sda-MCI). With respect to general cognitive functioning, the mda-MCI subjects scored less than 1.5 *SD*s below age- and education-related norms in the MEC and in at least two cognitive subscales of the CAMCOG-R. For the analysis of the present study, the two subgroups of aMCI were not differentiated, because they did not show any differences in MMN parameters (see Results section), and they were consequently regrouped into a single group of adults with aMCI.

The research project was approved by the Galician Clinical Research Ethics Committee (CEIC) and performed in accordance with the ethical standards established in the 1964 Declaration of Helsinki (Lynöe et al., 1991).

STIMULI AND TASK

An auditory-visual attention-distraction task adapted from Escera et al. (1998, 2001) was used. This included a passive auditory oddball task and an active Go/NoGo three-stimuli visual oddball task. Participants were presented with 500 auditory-visual (A-V) stimuli pairs (divided in two blocks separated by a 2-min rest interval). Each pair included an auditory stimulus (150 ms duration) followed by a visual stimulus (200 ms duration), with an interval of 300 ms (onset-to-onset) between them, and a 2-s interval between each pair. Participants were asked to attend to the visual stimuli and ignore the auditory stimuli.

Auditory stimuli were sounds, presented binaurally via headphones, with 75 dB SPL intensity. Three kinds of sounds were presented: 70% were standard stimuli (tone bursts, 1000 Hz), 15% were deviant stimuli (tone bursts, 2000 Hz), and 15% were novel stimuli (different each time: glass crashing, ringing, etc . . .). Visual stimuli were numbers (2, 4, 6, or 8), letters (a, e, c, or u) or triangles (pointing up, down, right, or left). Participants were asked to respond to the numbers (33%) with one hand and to the letters (33%) with the other hand, by pressing a different button in each case (Go condition), and they were asked to inhibit their responses to triangles (34%, NoGo condition). Response buttons were counterbalanced among participants. For this task, each participant underwent two evaluations separated by an interval of between 18 and 24 months.

ELECTROENCEPHALOGRAPHIC (EEG) RECORDING

The participants were seated on a comfortable chair in a Faraday chamber, with attenuated levels of light and noise, and were instructed to move as little as possible during the recording. Visual stimuli were presented with a subtended visual angle of $1.7° \times 3.3°$ of arc, on a 19″ flat screen monitor with a vertical refresh rate of 120 Hz. The monitor was located one meter away from the participant. The electroencephalogram was recorded from 49 ring electrodes placed in an elastic cap (Easycap, GmbH), according to the International 10-10 system. All electrodes were referenced to an electrode attached to the tip of the nose, and an electrode positioned at Fpz served as ground. The horizontal electro-oculogram (EOG) was recorded from two electrodes

placed at the outer canthi of both eyes, and the vertical EOG was recorded from two electrodes placed supra and infra-orbitally on the right eye. The EEG was continuously digitized at a rate of 500 Hz (bandpass 0.01–100 Hz), and electrode impedances were kept below 10 kΩ.

Once the signal was stored, ocular artifacts were corrected and the EEG was then segmented by extraction of -100 to 650 ms epochs, synchronized with each auditory stimuli. These were then classified *a posteriori* as Standard, Deviant and Novel, depending on the type of auditory stimulus. The signal was passed through a digital 0.1–30 Hz (24 dB/octave slope) bandpass filter and epochs were corrected to the mean voltage of the 100-ms pre-stimulus recoding period. EEG segments exceeding ±100 μV and the first five epochs of each block were automatically excluded from the averages. Finally, to identify and measure MMN, we obtained the deviant *minus* standard (D-S) and novel *minus* standard (N-S) difference waveforms.

DATA ANALYSES

The MMN component was identified as a negative wave in the 125–260 ms interval, and it was evaluated at the Cz electrode site (where the amplitude was maximal). The polarity of the component was reversed at temporal (TP9 and TP10) electrode sites (see **Figure 1**).

In the first evaluation, the MMN component was identified in the N-S and D-S difference waveforms, for the two groups of participants (CG and aMCI group). In the second evaluation, MMN was also identified in the N-S and D-S difference traces for

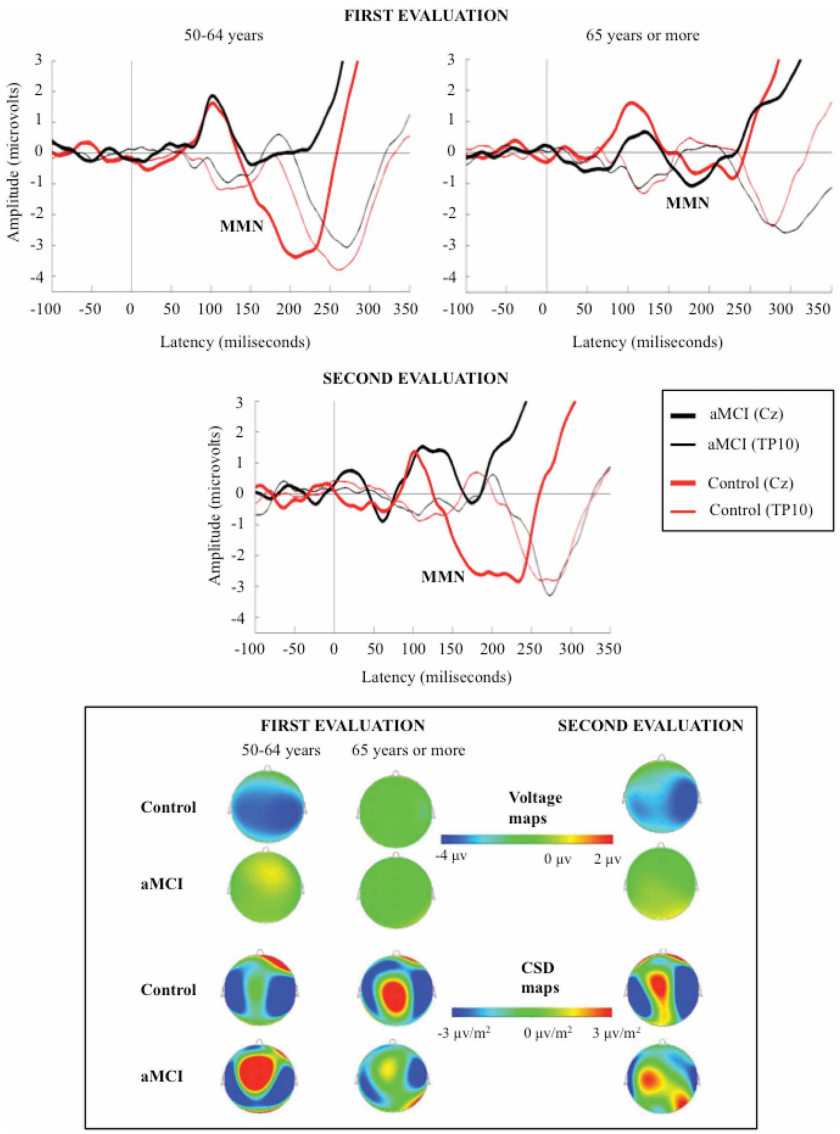

FIGURE 1 | Grand-average event-related potentials waveforms, measured at Cz (top), during the 350 ms after the stimulus, and voltage and current source density (CSD) maps for MMN maximum peak (bottom), in the novel minus standard difference waveforms, for control and aMCI adults, in the first (for the two age subgroups) and second evaluations.

the control adults; however, for the aMCI adults, MMN was only identified in the N-S difference trace and it was absent in the D-S difference trace.

The MMN amplitude (in microvolts, from the maximum peak to the baseline) and latency (in milliseconds, from the auditory stimulus onset to the maximum peak) were measured. Current source density (CSD) and voltage maps were also obtained for topographic analysis.

STATISTICAL ANALYSES

In the first evaluation, one-factor analysis of variance (ANOVA) was used to investigate the effect of the Group factor on the MMN amplitude and latency (measured at Cz) in the N-S and D-S difference waveforms. The analysis considered a dependent variable (MMN amplitude or latency) and an independent factor (Group, three levels: CG, sda-MCI, and mda-MCI groups). As there were no significant differences between aMCI subgroups for MMN parameters, both subgroups were regrouped as a single aMCI group for the following analysis.

Two-factor ANOVAs was used to investigate the effect of Group and Age factors on the MMN amplitude and latency (measured at Cz) in the N-S and D-S waveforms. The analysis included a dependent variable (MMN amplitude or latency) and two independent factors, Group (two levels: CG, and aMCI) and Age (two levels: middle-aged adults: 50–64 years, and older adults: 65 years and over).

In the second evaluation, a one-factor ANOVAs (Group) was used to investigate the Group factor effect on the MMN amplitude and latency (measured at Cz) in the N-S difference waveforms. The Age factor was not evaluated because of the small number of participants (9 in the CG and 7 in the aMCI group). In this evaluation, the effect of the Group factor on MMN in the D-S difference was not evaluated because no MMN component was observed in this difference waveform in aMCI adults.

Finally, *t*-tests for related samples were used to evaluate the changes in the MMN parameters (in the N-S difference waveform) between the first and the second evaluation, in each group of participants (9 control adults and 7 aMCI adults).

When the ANOVAs revealed significant factor and interactions effects, further comparisons of the mean values were carried out by paired multiple comparisons (adjusted to Bonferroni correction). Differences were considered significant at $p < 0.05$.

The receiver-operating characteristics (ROC) method was used to assess the capacity of MMN parameters to discriminate aMCI adults from control adults. A line diagram was constructed with the sensitivity (true positive rate) plotted on the vertical axis and the false positive rate (1 minus specificity) on the horizontal axis. The ROC curve was constructed by finding the sensitivity and specificity for a range of values of the continuous variable (MMN parameters). The tests were considered to be ideal when the area under the curve (AUC) was higher than 0.7.

All statistical analyses were performed with IBM SPSS Statistics package v.19 for Windows.

RESULTS

DEMOGRAPHIC AND NEUROPSYCHOLOGICAL DATA

In both evaluations, the groups were matched according to age and level of education. The demographic and neuropsychological measurements are summarized in **Table 1**, together with the between-group differences calculated by the corresponding analysis. For an extensive description of the global samples, the inclusion/exclusion criteria, the tests used, and the diagnosis and classification criteria, see Juncos-Rabadán et al. (2013).

Table 1 | Mean values and standard deviations (in parentheses) of the demographic and neuropsychological measures, for control and amnestic MCI (aMCI) adults.

	Control	aMCI	*p*<	
FIRST EVALUATION	***N* = 30**	***N* = 26**		
Age	63.9 (8.4)	67.8 (9.3)	NS	
Years of education	9.4 (4.4)	10.15 (4.7)	NS	
Gender (F/M)	21/9	14/12		
WAIS, vocabulary	49.9 (11.7)	46.7 (13.4)	NS	
MMSE	28.5 (0.9)	25.8 (2.1)	0.001	Control > aMCI
CVLT (short-delay free recall)	10.2 (2.3)	3.9 (1.8)	0.001	Control > aMCI
CVLT (short-delay cued recall)	12 (2.3)	5.8 (2.2)	0.001	Control > aMCI
CVLT (long-delay free recall)	11.4 (2.2)	4.5 (3)	0.001	Control > aMCI
Depression (GDS)	2.9 (2.1)	3.8 (3.1)	NS	
SECOND EVALUATION	***N* = 9**	***N* = 7**		
Age	66.6 (5.5)	74.4 (10.1)	NS	
Years of education	8.2 (4.3)	11.1 (4.5)	NS	
Gender (F/M)	(7/2)	(3/4)		
WAIS, vocabulary	46.4 (9)	49 (16.7)	NS	
MMSE	28.1 (1.2)	23.3 (5.1)	0.01	Control > aMCI
CVLT (short-delay free recall)	11.6 (2.9)	2.7 (2.6)	0.001	Control > aMCI
CVLT (short-delay cued recall)	13 (1.9)	5 (2.5)	0.001	Control > aMCI
CVLT (long-delay free recall)	12.3 (3.3)	4.7 (3.6)	0.001	Control > aMCI
Depression (GDS)	2.2 (0.9)	2.7 (1.1)	NS	

The ANOVA results for the Group factor are also shown.

ERPs

The factors under consideration did not have any significant effects on the MMN latency or amplitude in the D-S difference waveforms. Therefore, we will report only the results obtained for MMN in the N-S difference waveforms, for both the first and the second evaluation.

The mean MMN amplitudes (μV) and latencies (ms) obtained in both evaluations are shown in **Table 2**. The grand average ERP waveforms of the N-S difference traces and the voltage and CSD maps for MMN maximum amplitude peaks in the first and the second evaluations are shown in **Figure 1**. Voltage maps for MMN revealed larger amplitudes for the CG than for the aMCI group. In both groups, the CSD maps showed bilateral sinks at temporoparietal scalp regions and a right frontal source. However, between-group topographical differences in CSD maps were also observed. During the first evaluation, a widespread centroparietal source was observed in control adults in the older age subgroup (65 years and over) and in aMCI adults in the middle-aged

Table 2 | Mean values and standard deviations (in parentheses) of the auditory MMN amplitudes (in μV) and latencies (in ms), measured at the Cz electrode, in the novel minus standard (N-S) and deviant minus standard (D-S) difference waveforms, for the two diagnostic groups (control and amnestic MCI adults).

Group	Age	N-S MMN		D-S MMN	
		Amplitude	Latency	Amplitude	Latency
FIRST EVALUATION					
Control adults ($N = 30$)	50–64 ($N = 15$) (M: 56.8 years, *SD*: 3.9)	−5.3 (3.3)	207 (27)	−1.9 (2.0)	228 (25)
	≥65 ($N = 15$) (M: 71.1 years, *SD*: 4.9)	−2.6 (2.2)	202 (33)	−1.1 (1.5)	207 (32)
aMCI adults ($N = 26$)	50–64 ($N = 10$) (M: 58.8 years, *SD*: 4.3)	−2.1 (2.8)	187 (35)	−1.2 (1.2)	208 (27)
	≥65 ($N = 16$) (M: 73.5 years, *SD*: 6.7)	−2.5 (2.2)	186 (34)	−2.2 (2.1)	201 (33)
SECOND EVALUATION					
Control adults ($N = 9$)	59–73 (M: 66.6 years, *SD*: 5.5)	−4.7 (3.5)	205 (56)	−1.9 (1.2)	210 (35)
aMCI adults ($N = 7$)	62–89 (M: 74.4 years, *SD*: 10.1)	−1.1 (2.0)	192 (34)	–	–

In the first evaluation, the data for the two age subgroups (50–64 years and 65 years and over) in each group (control and aMCI) are shown.
M: mean, SD: standard deviations.

subgroup (50–64 years); however, this source was not observed in the middle-aged control adults or in the older adults with aMCI.

First evaluation

For MMN latency, the two-factor ANOVA (Group × Age) showed significant effects of the Group factor [$F_{(1, 52)} = 4.1$, $p < 0.048$], as latency was significantly shorter in the aMCI group than in the CG. For MMN amplitude, the two-factor ANOVA revealed significant effects of the Group factor [$F_{(1, 52)} = 5.4$, $p < 0.023$] and the Group × Age interaction [$F_{(1, 52)} = 4.9$, $p < 0.031$], because the amplitude was significantly larger ($p < 0.004$) in the CG than in the aMCI group, only for the middle-aged subgroup (50–64 years). Furthermore, for the CG, the amplitude was significantly larger ($p < 0.008$) in the middle-aged than in the older adults.

Second evaluation

For MMN latency, the one-factor ANOVA revealed no significant factor (Group) effect. For MMN amplitude, the ANOVA showed significant effect of the Group factor [$F_{(1, 14)} = 5.66$, $p < 0.032$], as the amplitude was significantly larger for the CG than for the aMCI group.

First vs. Second evaluation

The *t*-test for related samples did not show any significant differences for the MMN latency between the first and second evaluations. However, for the MMN amplitude, the analysis revealed significant differences within the aMCI group, as the MMN amplitude was significantly smaller in the second evaluation (−1.1 μV) than in the first evaluation (−2.8 μV) [$t_{(6)} = -2.9$, $p < 0.027$]. The MMN amplitude and latency in the control group did not differ significantly between the first and second evaluations (see **Figure 2**).

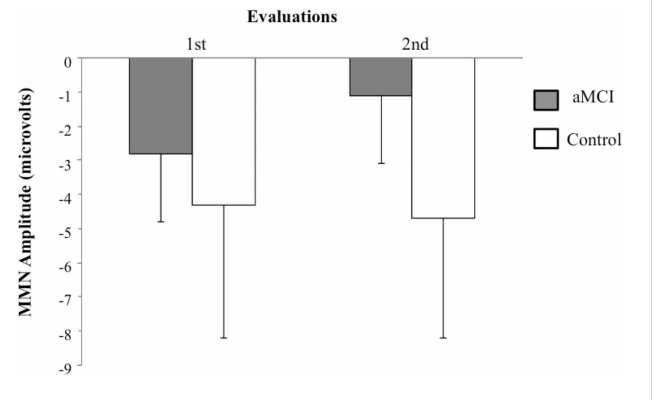

FIGURE 2 | Means and standard deviations for MMN amplitudes (in μV) in the novel minus standard difference, in the first and the second evaluations, for control ($N = 9$) and aMCI ($N = 7$) adults.

SENSITIVITY AND SPECIFICITY

The ROC curves for MMN amplitudes (N-S difference waveforms), in the first and second evaluations, for the aMCI group and CG comparisons are shown in **Figure 3**.

In the first evaluation, MMN amplitude showed 0.7 sensitivity and 0.66 specificity (AUC = 0.76) for the discrimination between aMCI and control middle-aged adults. However, the MMN latency showed very low sensitivity and specificity (AUC = 0.34). In the second evaluation, the MMN amplitude was also sensitive

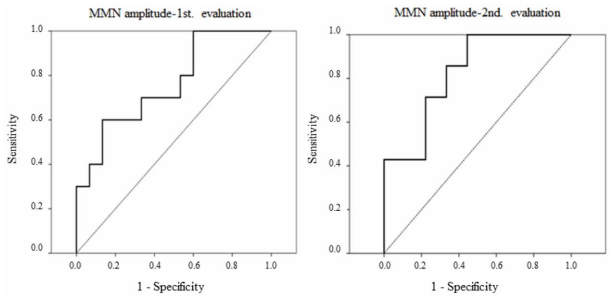

FIGURE 3 | Receiver-operating characteristics (ROC) curves are represented for MMN amplitudes in novel minus standard difference, in the first and the second evaluations, for the aMCI and control adults comparison. Left: MMN amplitude for the middle-aged subgroup in the first evaluation. **Right:** MMN amplitude in the second evaluation.

and specific in discrimination between aMCI and control groups, with 0.71 sensitivity and 0.78 specificity (AUC = 0.82).

DISCUSSION

Mismatch negativity (MMN) component was identified in both groups of participants (control and aMCI). As expected, CSD maps showed bilateral sinks at temporal scalp regions and a right frontal source for this component, presumably reflecting the MMN generator activity, located in the auditory supratemporal cortices and the frontal cortex, respectively (see Näätänen et al., 2007).

Control and aMCI adults showed differences for MMN component of the N-S difference waveforms in two evaluations separated by an interval of between 18 and 24 months. In the first evaluation, the MMN amplitude was significantly smaller in the aMCI adults than in the control adults, though only for the middle-aged subgroup (between 50 and 64 years of age). The MMN latency was significantly shorter in the aMCI group than in the CG. In the second evaluation, the MMN amplitude was also significantly smaller in the aMCI group than in the CG, and the aMCI group showed a decrease in MMN amplitude from the first to the second evaluation, whereas the CG did not show significant changes between evaluations.

MMN LATENCY

In the first evaluation, the MMN latency was significantly shorter in the aMCI group than in the CG. In the second evaluation, although the mean values and SD for both groups were similar to those of the first evaluation, the Group factor was not statistically significant, probably because the sample size was smaller in the second evaluation. This result is intriguing because no significant differences in MMN latencies were observed in other MMN studies comparing AD patients and healthy control subjects (Kazmerski et al., 1997; Gaeta et al., 1999; Brønnick et al., 2010) or in the only previous study comparing a MCI group with a control group (Mowszowski et al., 2012).

Although the shorter MMN latency in the aMCI group than in the CG in the first evaluation of this study must be considered with caution. Interestingly, Mowszowski et al. (2012) also observed slightly shorter (but non-significant) MMN latencies (measured at Fz and Cz electrodes) in the MCI than in the control group (see Table 2, page 214, of the cited study). We tentatively speculate that in participants with aMCI, earlier closure of the comparison (in echoic memory) of each novel stimulus with the stored model of a standard stimulus may occur, resulting in a mismatch. This early closure may be premature and related to the deterioration of echoic memory. However, this hypothesis must be addressed in greater detail in future studies.

MMN AMPLITUDE

In the first evaluation, the MMN amplitude was significantly larger in the CG than the aMCI group, only for the middle-aged subgroup (50–64 years). This may indicate some impairment, in the middle-age aMCI adults, of the automatic detection mechanism of disparities when the novel stimuli are presented. This mechanism depends on maintaining an echoic memory trace of the standard stimulus, with which it automatically compares each novel (or deviant) stimuli presented. Näätänen et al. (2011, 2012) suggested that MMN deficits may be at least partly explained by dysfunction of the N-methyl-D-aspartate (NMDA) receptor system, which usually binds to the neurotransmitter glutamate. Consequently, reduced MMN in aMCI adults may signify a more general functional deficiency involving glutamatergic dysfunction, as suggested by Mowszowski et al. (2012).

The ROC analysis for the first evaluation showed that MMN amplitude could be considered a biomarker of aMCI in middle-aged adults, discriminating between the two groups with a sensitivity of 0.70 and specificity of 0.66 (AUC = 0.76, in ROC curves).

For adults 65 years old or more, there were no differences in MMN amplitude between the control and aMCI groups. This is probably due to a significant age-related decrease in MMN amplitude in the CG, as also found by Gaeta et al. (1998). For the aMCI group, the MMN amplitude did not differ between the two age subgroups. Thus, in the older adults (65 years and over), the lack of differences between the CG and the aMCI group may be due to an age-related decline in the mechanism for echoic memory trace maintenance and/or the pre-attentional mechanisms involved in the automatic detection of differences in the acoustic environment, which may mask the effects of aMCI on that parameter.

The CSD maps for MMN showed similar sources and sinks in control and aMCI adults. These maps also revealed differences in the first evaluation, which are consistent with the results obtained for the MMN parameters in the present work. Thus, they revealed a centroparietal source in middle-aged adults (50–64 years) with aMCI, but not in the middle-aged control adults, which is consistent with the significant between-group differences (control and aMCI adults) for MMN amplitude. Moreover, in accordance with the observed effects of aging on the MMN amplitude in the control group, this source was also observed in the older control adults (65 years and over). Within the framework of the Scaffolding Theory of Aging and Cognition (STAC) proposed by Park and Reuter-Lorenz (2009), we believe that the said source may reflect a brain that is adapting, through neural scaffolding,

to the functional and structural changes that appear, either due to aMCI in middle–aged adults or to healthy aging.

The present ERP results are partly consistent with those obtained by Mowszowski et al. (2012) for the MMN amplitude evoked by deviant stimuli, which differed from the standard stimuli in duration (100 and 50 ms, respectively). These authors observed a larger MMN amplitude in healthy adults than in a multi-domain MCI group (for an age range of 50–90 years in both groups), although only at mastoid locations, where MMN shows polarity reversal, but not at the frontocentral locations, where the amplitude of this negative component is maximal.

Our results are also consistent with those reported by Pekkonen et al. (1994) for AD patients and healthy controls. These authors observed a significant decrease in MMN amplitude, in the AD group, from an ISI of 1 s to an ISI of 3 s, which they interpreted as a weakening of echoic memory trace with increasing ISI in people with AD. In the present study, the interval between auditory stimuli was 2.35 s. We also presented visual stimuli between the auditory stimuli, which required attention and often response. The combination of both factors may have affected the maintenance of echoic memory trace of standard auditory stimuli in aMCI participants, but not in CG participants.

In the second evaluation (conducted between 18 and 24 months after the first), comparison of the MMN parameters in a subsample of participants again showed a significantly larger MMN amplitude in control adults than in adults with aMCI. As found in the first evaluation, the MMN amplitude may be considered a biomarker of aMCI, discriminating between the two groups with 0.71 sensitivity and 0.78 specificity (AUC = 0.82, in ROC curves). Moreover, the characteristics of the MMN component make it an ideal biomarker: it is an automatic ERP component, which is not dependent on the attention given by the subject to the task and, moreover, it is obtained in a non-invasive manner and is simple and inexpensive to measure.

The MMN amplitude was also significantly smaller in the second evaluation than in the first in the group with aMCI, while it did not differ between evaluations in the CG. This may indicate a progressive deterioration, in aMCI adults, of the neural mechanisms involved in the maintenance of sensory trace and/or the pre-attentive mechanisms for automatic detection of changes in the acoustic environmental. The findings highlight the importance of longitudinal studies in determining the evolution of deficits detected in a first assessment in participants with aMCI, as well as the diagnostic and prognostic value of psychophysiological markers.

This study is not without limitations, mainly due to the small sample size in the second evaluation. Future studies, with a large sample of participants in all follow-up evaluations, should (1) confirm the effect of the interaction between age and diagnostic group on MMN amplitude, and (2) determine any differences in how the MMN amplitude decreases over time in adults with MCI who progress to AD and in adults with MCI who do not develop AD.

Despite these limitations, the present study showed that the MMN amplitude was smaller in adults with aMCI than in control adults (in the middle-aged subgroup in the first evaluation and in the whole sample in the second evaluation, conducted between 18 and 24 months after the first). In addition, in participants with aMCI, the MMN amplitude was smaller in the second evaluation than in the first, whereas no difference was observed in the control group. The results of this study suggest that MMN amplitude can be a fairly sensitive and specific psychophysiological biomarker for the identification of adults with aMCI.

ACKNOWLEDGMENTS

The authors thank the participants and their relatives. They also thank S. Galdo, A. Buján, J. Cespón, D. Pinal, M. Ramos, C. Libisch, and S. Cid for help in the sample selection, electroencephalographic recordings and ERP processing. This work was financially supported by funds from the Spanish Ministerio Economía y Competitividad (PSI2010-22224-C03-03), and from the Galician Government: Consellería de Industria e Innovación/Economía e Industria (PGIDIT07PXIB211018PR, 10 PXIB 211070 PR), and Consellería de Educación e Ordenación Universitaria (Axudas para a Consolidación e Estruturación de unidades de investigación competitivas do sistema universitario de Galicia. Modalidade: Grupos con potencial de crecimento. Ref: CN 2012/033).

REFERENCES

Albert, M. S., DeKosky, S. T., Dickson, D., Dubois, B., Feldman, H. H., Fox, N. C., et al. (2011). The diagnosis of mild cognitive impairment due to Alzheimer's disease: recommendations from the National Institute on Aging-Alzheimer's Association workgroups on diagnostic guidelines for Alzheimer's disease. *Alzheimers Dement*. 7, 270–279. doi: 10.1016/j.jalz.2011.03.008

Amenedo, E., and Díaz, F. (1998). Automatic and effortful processes in auditory memory reflected by event-related potentials. Age-related findings. *Electroencephalogr. Clin. Neurophysiol.* 108, 361–369. doi: 10.1016/S0168-5597(98)00007-0

Benedet, M. J., and Alejandre, M. A. (1998). *TAVEC: Test de Aprendizaje Verbal España-Complutense*. Madrid: TEA Ediciones.

Bennys, K., Portet, F., Touchon, J., and Rondouin, G. (2007). Diagnostic value of event-related evoked potentials N200 and P300 subcomponents in early diagnosis of Alzheimer's disease and mild cognitive impairment. *J. Clin. Neurophysiol.* 24, 405–412. doi: 10.1097/WNP.0b013e31815068d5

Brønnick, K. S., Nordby, H., Larsen, J. P., and Aarsland, D. (2010). Disturbance of automatic auditory change detection in dementia associated with Parkinson's disease: a mismatch negativity study. *Neurobiol. Aging* 31, 104–113. doi: 10.1016/j.neurobiolaging.2008.02.021

Cooper, R. J., Todd, J., McGill, K., and Michie, P. T. (2006). Auditory sensory memory and the aging brain: a mismatch negativity study. *Neurobiol. Aging* 27, 752–762. doi: 10.1016/j.neurobiolaging.2005.03.012

Czigler, I., Csibra, G., and Csontos, A. (1992). Age and inter-stimulus interval effects on event-related potentials to frequent and infrequent auditory stimuli. *Biol. Psychol.* 33, 195–206. doi: 10.1016/0301–0511(92)90031-O

Delis, D. C., Kramer, J. H., Kaplan, E., and Ober, B. A. (1987). *California Verbal Learning Test: Adult Version*. San Antonio, TX: The Psychological Corporation.

Dubois, B., Feldman, H. H., Jacova, C., Dekosky, S. T., Barberger-Gateau, P., Cummings, J., et al. (2007). Research criteria for the diagnosis of Alzheimer's disease: revising the NINCDS–ADRDA criteria. *Lancet Neurol.* 6, 734–746. doi: 10.1016/S1474-4422(07)70178-3

Escera, C., Alho, K., Winkler, I., and Näätänen, R. (1998). Neural mechanisms of involuntary attention to acoustic novelty and change. *J. Cogn. Neurosci.* 10, 590–604. doi: 10.1162/089892998562997

Escera, C., Yago, E., and Alho, K. (2001). Electrical responses reveal the temporal dynamics of brain events during involuntary attention switching. *Eur. J. Neurosci.* 4, 877–883. doi: 10.1046/j.0953-816x.2001.01707.x

Folstein, M. F., Folstein, S. E., and McHugh, P. R. (1975). "Mini-mental state." A practical method for grading the cognitive state of patients for the clinician. *J. Psychiatr. Res.* 12, 189–198. doi: 10.1016/0022-3956(75)90026-6

Gaeta, H., Friedman, D., Ritter, W., and Cheng, J. (1998). An event-related potential study of age-related changes in sensitivity to stimulus deviance. *Neurobiol. Aging* 19, 447–459. doi: 10.1016/S0197-4580(98)00087-6

Gaeta, H., Friedman, D., Ritter, W., and Cheng, J. (1999). Changes in sensitivity to stimulus deviance in Alzheimer's disease: an ERP perspective. *Neuroreport* 10, 281–287.

Gallagher, D., Mhaolain, A. N., Coen, R., Walsh, C., Kilrov, D., Belinski, K., et al. (2010). Detecting prodromal Alzheimer's disease in mild cognitive impairment: utility of the CAMCOG and other neuropsychological predictors. *Int. J. Geriatr. Psychiatry* 25, 1280–1287. doi: 10.1002/gps.2480

Giard, M. H., Perrin, F., Pernier, J., and Bouchet, P. (1990). Brain generators implicated in the processing of auditory stimulus deviance: a topographic event-related potential study. *Psychophysiology* 27, 627–640. doi: 10.1111/j.1469-8986.1990.tb03184.x

Golob, E., Irimajiri, R., and Starr, I. (2007). Auditory cortical activity in amnestic mild cognitive impairment: relationship to subtype and conversion to dementia. *Brain* 130, 740–752. doi: 10.1093/brain/awl375

Golob, E., Johnson, J. K., and Starr, I. (2001). Auditory event-related potentials during target detection are abnormal in mild cognitive impairment. *Clin. Neurophysiol.* 113, 151–161. doi: 10.1016/S1388-2457(01)00713-1

Hämäläinen, A., Pihlajamäki, M., Tanila, H., Hänninen, T., Niskanen, E., Tervo, S., et al. (2007). Increased fMRI responses during encoding in mild cognitive impairment. *Neurobiol. Aging* 28, 1889–1903. doi: 10.1016/j.neurobiolaging.2006.08.008

Hampel, H., Shen, Y., Walsh, D. M., Aisen, P., Shaw, L. M., Zetterberg, H., et al. (2010). Biological markers of amyloid beta-related mechanisms in Alzheimer's disease. *Exp. Neurol.* 223, 334–346. doi: 10.1016/j.expneurol.2009.09.024

Henry, M. S., Passmore, A. P., Todd, S., McGuinness, B., Craig, D., and Johnston, J. A. (2012). The development of effective biomarkers for Alzheimer's disease: a review. *Int. J. Geriatr. Psychiatry* 28, 331–340. doi: 10.1002/gps.3829

Huppert, F. A., Jorm, A. F., Brayne, C., Girling, D. M., Barkley, C., Beardsall, L., et al. (1996). Psychometric properties of the CAMCOG and its efficacy in the diagnosis of dementia. *Aging Neuropsychol. Cogn.* 3, 201–214. doi: 10.1080/13825589608256624

Jackson, C. E., and Snyder, P. J. (2008). Electroencephalography and event-related potentials as biomarkers of mild cognitive impairment and mild Alzheimer's disease. *Alzheimers Dement.* 4, S137–S143. doi:10.1016/j.jalz.2007.10.008

Juncos-Rabadán, O., Facal, D., Lojo-Seoane, C., and Pereiro, A. X. (2013). Does tip-of-the-tongue for proper names discriminate amnestic mild cognitive impairment? *Int. Psychogeriatr.* 25, 627–634. doi: 10.1017/S1041610212002207

Kazmerski, V. A., Friedman, D., and Ritter, W. (1997). Mismatch negativity during attend and ignore conditions in Alzheimer's disease. *Biol. Psychiatry* 42, 382–402. doi: 10.1016/S0006-3223(96)00344-7

Lai, C. L., Lin, R. T., Liou, L. M., and Liu, C. K. (2010). The role of event-related potentials in cognitive decline in Alzheimer's disease. *Clin. Neurophysiol.* 121, 194–199. doi: 10.1016/j.clinph.2009.11.001

Lawton, M. P., and Brody, E. M. (1969). Assessment of older people: self-maintaining and instrumental activities of daily living. *Gerontologist* 9, 179–186. doi: 10.1093/geront/9.3_Part_1.179

Li, X., Shao, X., Wang, N., Wang, T., Chen, G., and Zhou, H. (2010). Correlation of auditory event-related potentials and magnetic resonance spectroscopy measures in mild cognitive impairment. *Brain Res.* 1346, 204–212. doi: 10.1016/j.brainres.2010.04.078

Lobo, A., Saz, P., Marcos, G., Día, J. L., de la Cámara, C., Ventura, T., et al. (1999). Revalidation and standardization of the cognition mini-exam (first Spanish version of the Mini-Mental Status Examination) in the general geriatric population. *Med. Clin.* 112, 767–774.

Lynöe, N., Sandlund, M., Dahlqvist, G., and Jacobsson, L. (1991). Informed consent: study of quality of information given to participants in a clinical trial. *BMJ* 303, 610–613.

Missonnier, P., Deiber, M. P., Gold, G., Herrmann, F. R., Millet, P., Michon, A., et al. (2007). Working memory load-related electroencephalographic parameters can differentiate progressive from stable mild cognitive impairment. *Neuroscience* 150, 346–356. doi: 10.1016/j.neuroscience.2007.09.009

Mowszowski, L., Hermens, D. F., Diamond, K., Norrie, L., Hickie, I. B., Lewis, S. J., et al. (2012). Reduced mismatch negativity in mild cognitive impairment: associations with neuropsychological performance. *J. Alzheimers Dis.* 30, 209–219. doi: 10.3233/JAD-2012-111868

Näätänen, R., and Alho, K. (1997). Mismatch negativity-the measure for central sound representation accuracy. *Audiol. Neurootol.* 2, 341–353. doi: 10.1159/000259255

Näätänen, R., Gaillard, A. W. K., and Mäntysalo, S. (1978). Early selective-attention effect on evoked potential reinterpreted. *Acta Psychol.* 42, 313–329. doi: 10.1016/0001-6918(78)90006-9

Näätänen, R., Kujala, T., Escera, C., Baldeweg, T., Kreegipuu, K., Carlson, S., et al. (2012). The mismatch negativity (MMN) – a unique window to disturbed central auditory processing in ageing and different clinical conditions. *Clin. Neurophysiol.* 123, 424–458. doi: 10.1016/j.clinph.2011.09.020

Näätänen, R., Kujala, T., Kreegipuu, K., Carlson, S., Escera, C., Baldeweg, T., et al. (2011). The mismatch negativity: an index of cognitive decline in neuropsychiatric and neurological diseases and in ageing. *Brain* 134, 3435–3453. doi: 10.1093/brain/awr064

Näätänen, R., Paavilainen, P., Rinne, T., and Alho, K. (2007). The mismatch negativity (MMN) in basic research of central auditory processing: a review. *Clin. Neurophysiol.* 118, 2544–2590. doi: 10.1016/j.clinph.2007.04.026

Oldfield, R. C. (1971). The assessment and analysis of handedness: the Edinburgh inventory. *Neuropsychologia* 9, 97–113. doi: 10.1016/0028-3932(71)90067-4

Papaliagkas, V. T., Anogianakis, G., Tsolaki, M. N., Koliakos, G., and Kimiskidis, V. K. (2009). Progression of mild cognitive impairment to Alzheimer's disease: improved diagnostic value of the combined use of N200 latency and beta-amyloid (1-42) levels. *Dement. Geriatr. Cogn. Disord.* 28, 30–35. doi: 10.1159/000229023

Park, D. C., and Reuter-Lorenz, P. (2009). The adaptive brain: aging and neurocognitive scaffolding. *Annu. Rev. Psychol.* 60, 173–196. doi: 10.1146/annurev.psych.59.103006.093656

Parra, M. A., Ascensio, L. L., Urquina, H. F., Manes, F., and Ibáñez, A. M. (2012). P300 and neuropsychological assessment in mild cognitive impairment and Alzheimer dementia. *Front. Neurol.* 3:172. doi: 10.3389/fneur.2012.00172

Pekkonen, E., Jousmäki, V., Könönen, M., Reinikainen, K., and Partanen, J. (1994). Auditory sensory memory impairment in Alzheimer's disease: an event-related potential study. *Neuroreport* 5, 2537–2540. doi: 10.1097/00001756-199412000-00033

Pekkonen, E., Rinne, T., Reinikainen, K., Kujala, T., Alho, K., and Näätänen, R. (1996). Aging effects on auditory processing: an event-related potential study. *Exp. Aging Res.* 22, 171–184. doi:10.1080/03610739608254005

Perneczky, R., Tsolakidou, A., Arnold, A., Diehl-Schmid, J., Grimmer, T., Förstl, H., et al. (2011). CSF soluble amyloid precursor proteins in the diagnosis of incipient Alzheimer disease. *Neurology* 77, 35–38. doi: 10.1212./WNL.0b013e318221ad47

Petersen, R. C. (2004). Mild cognitive impairment as a diagnostic entity. *J. Intern. Med.* 256, 183–194. doi: 10.1111/j.1365-2796.2004.01388.x

Petersen, R. C., Doody, R., Kurz, A., Mohs, R. C., Morris, J. C., Rabins, P. V., et al. (2001). Current concepts in mild cognitive impairment. *Arch. Neurol.* 58, 1985–1992. doi: 10.1001/archneur.58.12.1985

Petersen, R. C., Roberts, R. O., Knopman, D. S., Boeve, B. F., Geda, Y. E., Ivnik, R. J., et al. (2009). Mild cognitive impairment: ten years later. *Arch. Neurol.* 66, 1447–1455. doi: 10.1001/archneurol.2009.266

Raggi, A., Tasca, D., Rundo, F., and Ferri, R. (2013). Stability of auditory discrimination and novelty processing in physiological aging. *Behav. Neurol.* 27, 193–200. doi: 10.3233/BEN-120261

Rinne, T., Alho, K., Ilmoniemi, R. J., Virtanen, J., and Näätänen, R. (2000). Separate time behaviors of the temporal and frontal mismatch negativity sources. *Neuroimage* 12, 14–19. doi: 10.1006/nimg.2000.0591

Small, G. W., Kepe, V., Ercoli, L. M., Siddarth, P., Bookheimer, S. Y., Miller, K. J., et al. (2006). PET of brain amyloid and tau in mild cognitive impairment. *N. Engl. J. Med.* 355, 2652–2663. doi: 10.1016/S1388-2457(00)00337-0

Vecchio, F., and Määttä, S. (2011). The use of auditory event-related potentials in Alzheimer's disease diagnosis. *Int. J. Alzheimers Dis.* 2011:653173. doi: 10.4061/2011/653173

Wechsler, D. (1988). *WAIS-R: Wechsler Adult Intelligence Scale- Revised.* Oxford: Psychological Corporation.

Winblad, B., Palmer, K., Kivipelto, M., Jelic, V., Fratiglioni, L., Wahlund, L. O., et al. (2004). Mild cognitive impairment–beyond controversies, towards a consensus: report of the international working group on mild cognitive impairment. *J. Intern. Med.* 256, 240–246. doi:10.1111/j.1365-2796.2004.01380.x

Yesavage, J. A., Brink, T. L., Rose, T. L., Lum, O., Huang, V., Adey, M., et al. (1983). Development and validation of a geriatric depression screening scale: a preliminary report. *J. Psychiatr. Res.* 17, 37–49. doi: 10.1016/0022-3956(82)90033-4

Zhang, Z., Deng, L., Yu, H., Shi, Y., Bai, F., Xie, C., et al. (2012). Association of angiotensin-converting enzyme functional gene I/D polymorphism with amnestic mild cognitive impairment. *Neurosci. Lett.* 514, 131–135. doi: 10.1016/j.neulet.2012.02.074

Conflict of Interest Statement: The authors declare that the research was conducted in the absence of any commercial or financial relationships that could be construed as a potential conflict of interest.

Received: 31 July 2013; paper pending published: 20 August 2013; accepted: 04 November 2013; published online: 20 November 2013.

*Citation: Lindín M, Correa K, Zurrón M and Díaz F (2013) Mismatch negativity (MMN) amplitude as a biomarker of sensory memory deficit in amnestic mild cognitive impairment. Front. Aging Neurosci. **5**:79. doi: 10.3389/fnagi.2013.00079*

This article was submitted to the journal Frontiers in Aging Neuroscience.

Copyright © 2013 Lindín, Correa, Zurrón and Díaz. This is an open-access article distributed under the terms of the Creative Commons Attribution License (CC BY). The use, distribution or reproduction in other forums is permitted, provided the original author(s) or licensor are credited and that the original publication in this journal is cited, in accordance with accepted academic practice. No use, distribution or reproduction is permitted which does not comply with these terms.

frontiers in
AGING NEUROSCIENCE

ORIGINAL RESEARCH ARTICLE
published: 13 December 2013
doi: 10.3389/fnagi.2013.00086

Age-dependent effect of Alzheimer's risk variant of *CLU* on EEG alpha rhythm in non-demented adults

Natalya Ponomareva*[1]*, *Tatiana Andreeva*[2,3], *Maria Protasova*[2], *Lev Shagam*[2], *Daria Malina*[1], *Andrei Goltsov*[2], *Vitaly Fokin*[1], *Andrei Mitrofanov*[4] and *Evgeny Rogaev*[2,3,5]

[1] *Brain Research Department, Research Center of Neurology Russian Academy of Medical Science, Moscow, Russia*
[2] *Vavilov Institute of General Genetics, Russian Academy of Sciences, Moscow, Russia*
[3] *Center of Brain Neurobiology and Neurogenetics, Institute of Cytogenetics and Genetics, Russian Academy of Sciences, Novosibirsk, Russia*
[4] *Institute of Psychiatry, Moscow, Russia*
[5] *University of Massachusetts Medical School, Department of Psychiatry, BNRI, Worcester, MA, USA*

Edited by:
Davide V. Moretti, Istituto Di Ricovero e Cura a Carattere Scientifico, Italy

Reviewed by:
Bogdan O. Popescu, University Hospital Bucharest, Romania
Maria Eugenia Lopez, Centre for Biomedical Technology, Spain

***Correspondence:**
Natalya Ponomareva, Brain Research Department, Research Center of Neurology Russian Academy of Medical Science, Obucha-by-street 5, 105064 Moscow, Russia
e-mail: ponomare@yandex.ru;
Evgeny Rogaev, Vavilov Institute of General Genetics, Russian Academy of Sciences, Moscow, Russia. Center of Brain Neurobiology and Neurogenetics, Institute of Cytogenetics and Genetics, Russian Academy of Sciences, Novosibirsk, Russia. University of Massachusetts Medical School, Department of Psychiatry, BNRI, 303 Belmont Street, Worcester, MA 01604, USA
e-mail: Evgeny.Rogaev@umassmed.edu

Polymorphism in the genomic region harboring the *CLU* gene (rs11136000) has been associated with the risk for Alzheimer's disease (AD). *CLU C* allele is assumed to confer risk for AD and the *allele T* may have a protective effect. We investigated the influence of the AD-associated *CLU* genotype on a common neurophysiological trait of brain activity (resting-state alpha-rhythm activity) in non-demented adults and elucidated whether this influence is modified over the course of aging. We examined quantitative electroencephalography (EEG) in a cohort of non-demented individuals (age range 20–80) divided into young (age range 20–50) and old (age range 51–80) cohorts and stratified by *CLU* polymorphism. To rule out the effect of the apolipoprotein E *(ApoE)* genotype on EEG characteristics, only subjects without the *ApoE ε4* allele were included in the study. The homozygous presence of the AD risk variant *CLU CC* in non-demented subjects was associated with an increase of alpha3 absolute power. Moreover, the influence of *CLU* genotype on alpha3 was found to be higher in the subjects older than 50 years of age. The study also showed age-dependent alterations of alpha topographic distribution that occur independently of the *CLU* genotype. The increase of upper alpha power has been associated with hippocampal atrophy in patients with mild cognitive impairment (Moretti et al., 2012a). In our study, the *CLU CC*-dependent increase in upper alpha rhythm, particularly enhanced in elderly non-demented individuals, may imply that the genotype is related to preclinical dysregulation of hippocampal neurophysiology in aging and that this factor may contribute to the pathogenesis of AD.

Keywords: Alzheimer's disease, aging, clusterin, genetic predisposition, EEG, alpha rhythm

INTRODUCTION

Alzheimer's disease (AD) is the major cause of dementia in the elderly. It is estimated that 35.6 million people worldwide currently suffer from dementia, with the prevalence projected to increase to 65.7 million by 2030 and 115.4 million by 2050. Two-thirds of these people will likely develop AD (http://www.alz.co.uk/research/files/WorldAlzheimerReportExecutiveSummary.pdf). The incidence and prevalence of AD begins to rise as individuals reach the age of 65, so that by the time they are in their 80s and 90s the risk of clinical dementia is nearly 50%.

Alzheimer's disease has a strong genetic basis with heritability estimates of up to 80% (Gatz et al., 2006). Mutations in the amyloid precursor protein gene (chr21), presenilin 1 (chr14), and presenilin 2 (chr1) genes are causative factors for familial AD (Goate et al., 1991; Levy-Lahad et al., 1995; Rogaev et al., 1995; Sherrington et al., 1995). A common polymorphism in the apolipoprotein E gene (*ApoE*), located on chromosome 19, has been established as the most common genetic risk factor for AD in Caucasian ethnic groups, including the Russian population (Saunders et al., 1993; Schmechel et al., 1993; Farrer et al., 1997; Rogaev, 1999).

Recent genome-wide association studies (GWAS) studies have provided evidence that polymorphisms of the clusterin (*CLU)* (chr8) and *PICALM* (chr11) genes are also associated with AD risk (Harold et al., 2009; Lambert et al., 2009; Golenkina et al., 2010). Carriers of the *CLU* rs1113600 *C* allele have 1.16 greater odds of developing late-onset AD than carriers of the potentially protective *T* allele. Although the AD-association with *CLU* polymorphism alone was not confirmed in some studied populations, the putative epistatic interaction of the *CLU* genotype with *APOE ε4* in risk for AD has been demonstrated (Golenkina et al., 2010). Approximately 36% of Caucasians carry two copies of the risk-conferring allele (Bertram et al., 2007), which imply significance of this gene for public health.

The *CLU* gene encodes glycoprotein clusterin, also known as apolipoprotein J, which shares several properties with ApoE. Clusterin and ApoE both act as amyloid-β (Aβ) chaperones to alter Aβ aggregation and/or clearance (Killick et al., 2012; Ling et al., 2012). Clusterin and ApoE are involved in the transport of cholesterol

and phospholipids, and modulate AD-related pathways such as inflammation and apoptosis (Bettens et al., 2012; Ling et al., 2012). Clusterin is upregulated during different physiological and pathological states, such as senescence, type-2 diabetes mellitus, AD, and in various neoplasms (Song et al., 2012; Tang et al., 2013).

In order to identify early preclinical markers for AD, it is vital to find specific genotype–phenotype characteristics in individuals with hereditary risk for AD at different stages of the pathological process, including the preclinical period. Such biomarkers can be helpful for estimating the effect of potential therapies for preventing or delaying onset of neurodegenerative diseases (Illarioshkin et al., 2004; Feigin et al., 2007; Masdeu et al., 2012; Suslina, 2012). At present, there is still a mismatch between the known genetic factors of AD, and the biomarkers reflecting the development of the pathological process.

Electroencephalography (EEG) patterns are considered to be valuable as an endophenotype – a more basic biological trait that more directly reflects the influence of the genome (Gottesman and Gould, 2003). The heritability of EEG patterns has been shown to be in the range 70–90% (van Beijsterveldt et al., 1996). Multiple genes may modulate the alpha phenotype. Recent studies indicated that the catechol-*O*-methyl transferase (*COMP)* genotype and the gene encoding gamma-aminobutyric acid B ($GABA_B$) receptor both influence alpha voltage (Enoch et al., 2003; Winterer et al., 2003; Bodenmann et al., 2009).

Testing the association of the AD risk alleles with EEG endophenotypes can help understand where in the brain, in which stage, and during what type of information processing the genetic variant has a role.

Quantitative EEG (qEEG) has been shown to be a reliable diagnostic tool in dementia research (Stam et al., 2003; Jeong, 2004; Babiloni et al., 2006b, 2011a, 2014; Dauwels et al., 2010; Moretti et al., 2012a). Slowing of EEG in AD is a uniform finding. Patients with mild AD are characterized by higher delta and theta, and lower alpha and beta power than normal elderly subjects (Huang et al., 2000; Lizio et al., 2011). In patients with mild cognitive impairment (MCI), which is considered to be a prodromic stage of AD, EEG parameters have presented magnitudes intermediate between those observed in normal subjects and in AD patients (Babiloni et al., 2006b). Longitudinal studies have revealed qEEG-based predictors of future decline in patients with MCI and even in normal elderly subjects (Prichep et al., 2006; Van der Hiele et al., 2008; Babiloni et al., 2011b).

Alterations of alpha rhythm in particular were found to be related to AD development. In a resting-state condition, posterior alpha rhythms showed a power decrement in patients with MCI as compared with healthy elderly subjects (Huang et al., 2000; Jelic et al., 2000; Koenig et al., 2005; Babiloni et al., 2006b, 2014). It has been reported that, in contrast to the decrease of alpha1 (6.9–8.9 Hz) and alpha2 (8.9–10.9 Hz) relative power, the alpha3 (10.9–12.9 Hz) relative power increased in patients with MCI (Moretti et al., 2007, 2011, 2012a,b).

Recent studies have demonstrated the association between the AD genetic risk variant *ApoE ε4* and EEG in patients with AD, MCI, and healthy subjects (Jelic et al., 1997; Lehtovirta et al., 2000; Babiloni et al., 2006b; Ponomareva et al., 2008, 2012; Lee et al., 2012). It was shown that AD patients carrying the *ApoE ε4* genotype have lower alpha power and lower alpha coherence as compared to non-carriers (Jelic et al., 1997; Lehtovirta et al., 2000; Ponomareva et al., 2008). Similarly, alpha1 and alpha2 sources in occipital, temporal and limbic areas as examined by LORETA was demonstrated to have lower amplitude in AD and MCI patients with *ApoE ε4* genotype compared with those non-carrying *ApoE ε4* (Babiloni et al., 2006b). The authors suggested that these neurophysiological abnormalities might reflect greater impairment of the cholinergic basal forebrain, hippocampal, and thalamocortical networks. In young healthy women, Lee et al. (2012) noticed a consistent trend across the brain, in which *ApoE ε4* carriers possessed lower regional power at the alpha band.

The effect of *CLU* polymorphism on EEG characteristics has not been previously investigated, although several morphofunctional alterations associated with the *CLU* gene risk variant were recently identified. Young healthy carriers of *CLU C* allele demonstrated lower white matter integrity in multiple brain regions, including several which are known to degenerate in AD (Braskie et al., 2011). Elderly cognitively normal carriers of the *CLU* risk allele showed significant dose-dependent longitudinal increases in resting-state regional cerebral blood flow (rCBF) in the brain regions intrinsic to memory processes, and faster rates of decline in verbal memory performance scores (Thambisetty et al., 2013). EEG activity and alpha rhythm in particular are closely related to the rCBF (Jann et al., 2010).

The purpose of this study was to examine the possible effects of the *CLU* genotype on resting-state alpha activity in non-demented adults and to estimate whether this effect is modified over the course of aging.

We tested the hypothesis that healthy adult carriers of the AD risk variant *CLU C* (homozygous *CLU CC* genotype) would show age-dependent alpha-rhythm alterations relative to carriers of the protective *T* allele (heterozygous *CLU CT* and homozygous *CLU TT* genotypes).

MATERIALS AND METHODS

PARTICIPANTS

The enrolled cohort included 87 non-demented individuals (33 men and 54 women, age range 20–80 years). All subjects were of Russian origin from Moscow and the Moscow region. Participants underwent a neurological examination and cognitive screening. The recruited subjects were free of dementia and other medical, psychiatric, and neurological conditions. Exclusion criteria included a personal history of mental illness, signs of clinical depression or anxiety, physical brain injury, neurological disorder, or other medical condition (e.g., hypertension, diabetes, cardiac disease, and thyroid disease), and a personal history of drug or alcohol addiction. The Spielberger state-trait anxiety inventory (Spielberger, 1983) and Hamilton rating scale for depression (Hamilton, 1960) were used to examine anxiety and depression. Subjects were evaluated with the mini-mental state examination (MMSE) and Clinical Dementia Rating (CDR) scale (Hughes et al., 1982). Only subjects with MMSE scores of 28 and more and CDR scale 0 cases were included in the study. All subjects were right-handed.

Informed written consent was obtained from all participants. The experimental protocol of this study was approved by the local Ethics Committee.

ApoE genotyping was performed on all participants, and to exclude the effect of the *ApoE* genotype on EEG characteristics, only subjects without the *ApoE ε4* allele were included in the study.

All subjects were divided into subgroups according to *CLU* (*CLU CC* and *CLUCT*&*TT*) polymorphism. The homozygous *CLU CC* group included subjects with two *C* alleles of *CLU*, and the *CLU CT*&*TT* group consisted of subjects with heterozygous *CLU CT* or homozygous *CLU TT* genotypes. The participants with *CLU CC* as well as with *CLU CT*&*TT* genotypes were also divided into cohorts of those younger and older than 50 years of age.

EEG RECORDING

All recordings were obtained in the afternoon at 3–4 pm. During the experiments, the subjects sat comfortably in a chair. They were asked to close their eyes and to relax during the recording. The technician watched the subject's vigilance state continuously by monitoring the EEG and observing the subject.

The registration and evaluation of EEG has been carried out in accordance with the International Pharmaco-EEG Society (IPEG) guidelines (Versavel et al., 1995; Jobert et al., 2012). EEGs were recorded during resting with eyes closed on a Nihon Kohden 4217 G EEG using a time constant of 0.3 s. The 16 Ag/AgCl electrodes were placed according to the international 10–20 system at O2, O1, P4, P3, C4, C3, F4, F3, Fp2, Fp1, T6, T5, T4, T3, F8, and F7 positions. Linked ears served as the reference. Electrode impedance did not exceed 10 kΩ. During the recording, 180 s of EEG in resting conditions were simultaneously sampled at 256 Hz and stored on a computer for further analysis off-line. The records were digitally filtered with a band-pass filter of 1.0–45.0 Hz prior to analysis. Periods of artifact were eliminated from subsequent analysis. Identification and removal of artifacts (ocular, cardiac, muscular, sweating and respiratory, electrode movements) were performed by two expert electroencephalographists (P.N.V., M.D.D.) in accordance with criteria thoroughly described elsewhere (Moretti et al., 2003; Tatum et al., 2011; Jobert et al., 2012).

DATA ANALYSIS

Thirty-six to forty artifact-free 4-s epochs of resting EEG were processed by fast Fourier transform. Absolute power for the frequencies of interest: alpha1 (7.5–8.99), alpha2 (9.00–10.99), alpha3 (11–12.99), and for the regions of interest (ROI): occipital (O2, O1), frontal 1 (F4, F3), frontal 2 (Fp2, Fp1), temporal 1 (T6, T5), and temporal 2 (T4, T3) were calculated.

These alpha band frequencies were chosen by averaging those used in previous relevant EEG studies on aging, genetic influences, and dementia (Babiloni et al., 2006a,b; Bodenmann et al., 2009; Moretti et al., 2012a,b). This allowed better comparison of our results with the previous literature on aging and genetics, but it did not account for individual alpha frequencies peak (Klimesch, 1999).

Log transformations of the absolute power of the various bandwidths in each derivation were calculated in order to compensate for data skewness, as recommended by John et al. (1980).

GENETIC ANALYSIS

Genomic DNA was isolated from peripheral venous blood by the standard phenol–chloroform extraction methodology, or by using a Qiagen kit for DNA isolation. Genotyping was performed by polymerase chain reaction (PCR) and followed by restriction fragment length polymorphism (RFLP) analysis. Amplification was performed according to the manufacturer's instructions using both the Tercyc DNA amplifier (DNA technology, Russia) and the GeneAmp PCR System 9700 Thermal Cycler (Applied Biosystems).

To genotype the *APOE* gene locus, the following oligonucleotide primers were used: 5′_CGGCTGGGCGCG_GACATGGAGGA and 5′_TCGCGGGCCCCGGC_CTGGTACAC. The PCR protocol was as follows: preliminary denaturation at 95°C for 4 min; 5 cycles: 95°C for 45 s, 54°C for 25 s, and 72°C for 30 s; and 30 cycles: 95°C for 5 s, 58°C for 15 s, and 72°C for 5 s; the last stage was performed at 72°C for 3 min. PCR products were then cleaved by *Hha*I or *BstHH*I (SibEnzyme, Russia) and restriction products were analyzed in 7.5% polyacrylamide gel.

The *rs11136000* polymorphism in *CLU* gene was tested with the following oligonucleotide primers: 5′_CTTTGTAATGATGTACC ATCTACCC and 5′_AGGCTGCAGACTCCCTGAAT. The PCR protocol was as follows: preliminary denaturation at 95°C for 1 min and 35 cycles: 94°C for 30 s, 57°C for 30 s, and 72°C for 1 min. The last stage was performed at 72°C. The 645 bp PCR products were then cleaved by *Acs*I restriction endonuclease (SibEnzyme, Russia) and restriction fragments were analyzed in 2% agarose gel.

STATISTICS

Differences in demographic scores between the groups (*CLU CC* young, *CLU CT*&*TT* young, *CLU CC* old, *CLU CT*&*TT* old) were tested using analysis of variance (ANOVA) for continuous variables (age, education), and the Mann–Whitney *U* test for categorical variables (sex).

Electroencephalography parameters from each group were tested for the normal distribution by the Wilk–Shapiro test, and in no cases were the data skewed. The significance of the differences between the log-transformed EEG parameters was estimated using repeated measures of ANOVA in the general linear model (GLM) separately for alpha1, alpha2, and alpha3 bands, with Genotype (*CLU CC* vs *CLU CT*&*TT*) and Age cohort (old vs. young) as between-subjects factors, and ROI: occipital (O2, O1), frontal 1 (F4, F3), frontal 2 (Fp2, Fp1), temporal 1 (T6, T5), temporal 2 (T4, T3), and hemisphere (right, left) as a within-subject factor. *Post hoc* comparisons for between-subject effects and within-subject effects were analyzed using the Duncan test, and the level of significance was set to $P < 0.05$ for *post hoc* comparisons.

RESULTS

Table 1 shows the demographic information for the participants. There were no differences in age and sex between the *CLU CC* and *CLU CT*&*TT* subgroups in either the young or the old subgroups and in the whole sample ($P > 0.05$). There were no significant differences in sex between the young and the old subgroups with the same *CLU* genotype.

Table 1 | Demographic characteristics of participants.

	Young cohort Age range: 20–50		Old cohort Age range: 51–80		All participants Age range: 20–80	
	CLU CC	***CLU CT&TT***	***CLU CC***	***CLU CT&TT***	***CLU CC***	***CLU CT&TT***
N	17	24	15	31	32	55
Age, years	28.4 ± 1.7	32.7 ± 2.0	64.1 ±2.4	62.6 ± 1.3	45.1 ± 3.5	49.6 ± 2.3
Sex (men/women)	9/8	9/15	5/10	10/21	14/18	19/36
Education, years	14.9 ± 0.2	14.7 ± 0.1	15.1 ± 0.1	14.9 ± 0.2	15.0 ± 0.1	14.8 ± 0.1

Data are presented as means and standard errors.

INFLUENCE OF AGING ON TOPOGRAPHIC DISTRIBUTION AND FREQUENCY OF ALPHA ACTIVITY IN HEALTHY ADULTS

The ANOVA revealed a significant effect of ROI on alpha1, alpha2, and alpha3 absolute power (for alpha1, $F[4,332] = 111.97$, $P = 0.0000$; for alpha2, $F([4,332] = 195.96$, $P = 0.0000$; for alpha3, $F[4,332] = 178.36$, $P = 0.0000$). *Post hoc* comparisons showed that in the entire sample, which included young and old cohorts, absolute power was higher in occipital than in frontal and temporal regions in the alpha1, alpha2, and alpha3 bands ($P < 0.0001$). Moreover, the power of all alpha bands was higher in frontal as compared to temporal areas ($P < 0.0001$).

There was no significant statistical Age × ROI interaction effect on alpha1 power (**Figure 1A**), but such an effect was observed on alpha2 and alpha3 bands ($F[4,332] = 6.33$, $P = 0.00006$ for alpha2; $F[4,332] = 15.30$, $P = 0.00000$ for alpha3). In the old cohort, the differences in alpha2 power between the ROI were reduced. Whereas in the young cohort, alpha2 power was higher in frontal Fp than in temporal posterior Tp areas (*post hoc* comparisons $P = 0.002$), in the old cohort the differences in these areas were not significant ($P = 0.11$). The differences between frontal Fp and temporal posterior Tp areas were significantly smaller in the old than in the young cohort ($P = 0.02$; **Figure 1B**).

Similarly, in the old cohort, the differences in alpha3 power between ROI were reduced as compared to the young cohort. In the young cohort, alpha3 power was higher in temporal posterior than in temporal areas ($P = 0.02$); in the old cohort these differences were not significant ($P = 0.1$), and age-related changes of these regional differences were also not significant. Alpha3 power was lower in the occipital ROI in the old cohort as compared to the young ($P < 0.01$; **Figure 1C**).

A significant interaction effect between the factors Age and Bands was observed ($F[2,166] = 4.51$, $P = 0.01$). In the young subjects, alpha2 power was significantly higher than alpha1 and alpha3 power ($P = 0.00001$), while in the old subjects the alpha1 power tended to increase and the differences between alpha1 and alpha2 power were not significant (**Figure 2**).

STATISTICAL ANALYSIS OF CLU EFFECT ON ALPHA ACTIVITY

The results of ANOVA showed that the main effect of *CLU* Genotype was significant on alpha3 ($F[1,83] = 5.57$, $P = 0.021$), but not on alpha1 ($F[1,83] = 2.10$, $P = 0.15$) or alpha2 ($F[1,83] = 2.81$, $P = 0.10$) absolute power. *Post hoc* comparison revealed that in the entire sample, which included old and young cohorts, alpha3 absolute power in the subjects with homozygous *CLU CC* genotype was significantly higher than in the subjects with heterozygous *CLU CT* and homozygous *CLU TT (CLU CT&TT)* genotypes ($P = 0.017$). Moreover, *post hoc* comparison showed that, in the old cohorts, alpha3 power was significantly higher in the CLU CC than in the *CLU CT&TT* carriers ($P = 0.016$), while in the young cohorts the differences in alpha3 power between the *CLU CC* and *CLU CT&TT* carriers did not reach a significant level (**Figure 3C**). There were no significant differences in alpha1 and alpha2 power between the young *CLU CC* and *CLU CT&TT* carriers (**Figures 3A,B**). In the old cohorts, alpha1 power was higher in the *CLU CC* than in the *CLU CT&TT* carriers ($P = 0.04$), while the differences of alpha2 power in the old *CLU CC* and *CLU CT&TT* carriers were not significant ($P = 0.1$; **Figures 3A,B**).

Topographic analysis demonstrated that the most pronounced differences between the homozygous *CLU CC* and *CLU CT&TT* carriers were observed in alpha3 power in the old cohorts. In the young cohorts, there were no significant differences in any ROI in alpha1, alpha2, and alpha3 power between *CLU CC* and *CLU CT&TT* carriers (**Figures 4A–C**). In the old cohort the differences between *CLU CC* and *CLU CT&TT* carriers were significant for alpha1 power in occipital ($P = 0.02$) and temporal posterior areas ($P = 0.02$), for alpha3 power – in frontal ($P = 0.04$), frontal poles ($P = 0.03$), and temporal posterior ($P = 0.02$) areas (**Figures 4A,C**).

A significant *CLU* × ROI interaction effect on the alpha1 power in the entire sample was observed ($F[4,332] = 3.43$, $P = 0.009$). In the *CLU CC* carriers alpha1 power was higher in occipital than in frontal areas ($P < 0.0001$) and in temporal posterior than in temporal areas ($P = 0.001$), while in the subjects with *CLU CT&TT* genotypes the differences in alpha1 power between occipital and frontal areas were smaller ($P = 0.01$), the differences between the temporal posterior and temporal areas were not significant ($P = 0.3$). There was a tendency toward higher alpha1 power in all ROI in the subjects with *CLU CC* genotype as compared to the subjects with *CLU CT&TT* genotype.

DISCUSSION

The main findings of this study show that the *CLU* genotype exerts a significant effect on alpha absolute power in the resting-state EEG of healthy adults. The homozygous presence of the AD risk variant *CLU CC* in non-demented subjects was associated with an increase of alpha3 and to a lesser, though significant, extent of alpha1 power in the subjects older than 50 years of age. *CLU* genotype-related differences were also found in the topographic

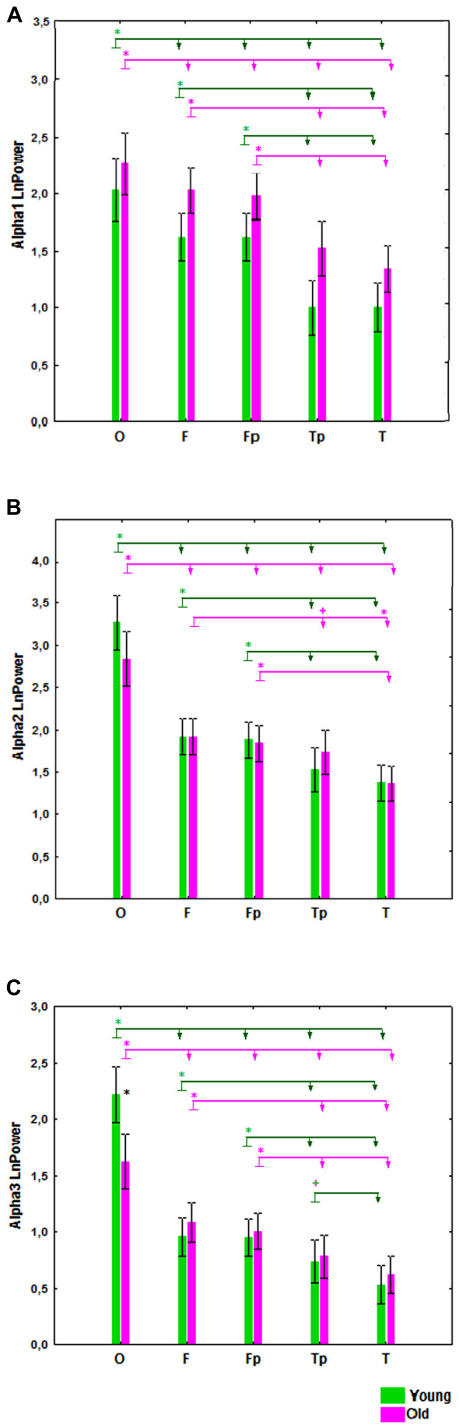

FIGURE 1 | Absolute power (mean and SE) of alpha1 (A), alpha2 (B), and alpha3 (C) bands in the young and old cohorts, for occipital (O), frontal (F), frontal poles (Fp), temporal posterior (Tp), and temporal (T) areas. Black asterisks (*) indicate a $P < 0.01$ significant difference in absolute spectral power between two cohorts in the same region of interest (ROI). The arrows labeled with green (for the young cohort) and purple (for the old cohort) asterisks compare different ROI in the same cohort. The ROI at the start of the arrow has either (+) $P < 0.05$ or (*) $P < 0.01$ significant differences in absolute spectral power compared the ROIs at the ends of the arrow.

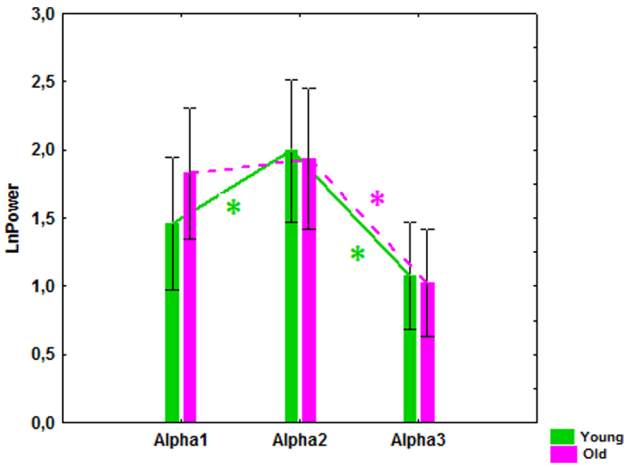

FIGURE 2 | Alpha1, alpha2, and alpha3 absolute power (mean and SE) in the healthy young and old cohorts. *$P \leq 0.01$, significant differences between the alpha bands in the young (green) and old (purple) cohorts.

distribution of alpha1 activity: in the subjects with homozygous *CLU CC* genotype, alpha1 power was higher in occipital than in frontal regions, while in the subjects with heterozygous *CLU CT* and homozygous *CLU TT (CLU CT&TT)* genotypes the differences in alpha1 power between occipital and frontal regions were not significant. The present study also showed age-related alterations of the topographic distribution of alpha2 and alpha3 activities, and an age-related increase in power of alpha1 relative to alpha2, all of which occurred in the subjects with *CLU CC* as well as with *CLU CT&TT* genotypes.

Alpha rhythm reflects the activity of dominant oscillatory neural networks in resting adults and represents a basic functional feature of the working brain (Klimesch, 2012). Alpha oscillations have been associated with essential cognitive functions, such as memory, intelligence quotient, internal attention (Cooper et al., 2006; Klimesch, 2012), and inhibitory control of motor programs (Pfurtscheller et al., 2000; Başar, 2012).

Inhibitory processes underlie alpha synchronization (Klimesch, 2012). During the awake resting condition, the voltage of the alpha rhythms is inversely correlated with the cortical activation. Alpha rhythm is modulated by thalamocortical and corticocortical interactions playing role in the transmission of sensorimotor information between subcortical and cortical pathways, and the retrieval of semantic information from cortical regions (Steriade and Llinás, 1988; Brunia, 1999; Pfurtscheller and Lopes da Silva, 1999).

According to prior research in this area, alpha rhythm is not a unitary phenomenon. Upper alpha (11–13 Hz) is more involved in cortical processes related to the semantic memory and low alpha (8–11 Hz) is more involved in attentional demands (Klimesch, 1999). Different neural networks have been suggested as generating low alpha and high alpha frequency bands. The modulation of the low alpha was proposed to be related to the corticosubcortical mechanisms, such as corticothalamic, corticostriatal, and corticobasal, while the upper alpha band is affected to a greater

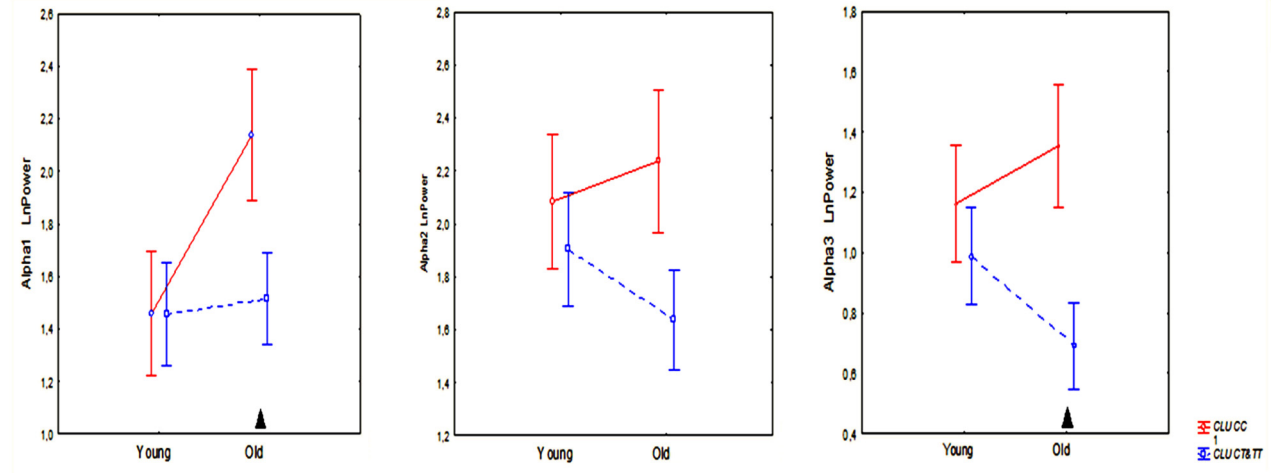

FIGURE 3 | The average absolute power of alpha1 (A), alpha2 (B), and alpha3 (C) bands (mean and SE) in young and old subjects with *CLU CC* and *CLU CT&TT* genotypes. Triangle indicates significant differences between the *CLU CC* and *CLU CT&TT* carriers $P < 0.05$.

extent by the hippocampus and other corticocortical interactions (Moretti et al., 2012a,b).

Recent study has shown an increase of the upper alpha power in patients with MCI and AD, when compared to normal elderly subjects (Moretti et al., 2012a,b). The increase in alpha3/alpha2 ratio in frontal and temporoparietal areas was associated with hippocampal atrophy in MCI (Moretti et al., 2007). The increase of alpha3/alpha2 ratio in subjects with MCI was suggested to reflect impairment of the anterior attentive mechanisms in subjects with MCI, in spite of the absence of overt clinical deficit (Moretti et al., 2012a,b). This increase was hypothesized to be due to a removal of excitatory, synaptic cholinergic inputs in intracortical networks, which would produce a decrease in synaptic efficacy and functional disconnection of cortical circuits (Steriade, 2006).

Healthy carriers of AD risk variant *CLU CC*, especially old subjects with this genotype, may have similar, though less pronounced, alterations underlying the increase of upper alpha activity to those found in MCI subjects. These alterations may include the dysregulation of excitatory synaptic inputs, especially cholinergic ones, in hippocampus and frontal intracortical networks. In the old *CLU CC* carriers we also found an increase in alpha1 power, though less pronounced, than in alpha3 power. These finding suggest that in the old *CLU CC* carriers the dysregulation may affect other mechanisms, such as corticothalamic, corticostriatal, and corticobasal ones, involved in low alpha generation (Moretti et al., 2012a,b).

Even normal aging is accompanied by a gradual loss of cholinergic function caused by dendritic, synaptic, and axonal degeneration as well as a decrease in trophic support. As a consequence, impairments in intracellular signaling and cytoskeletal transport may mediate cholinergic cell atrophy, finally leading to the known age-related functional decline in the brain, including aging-associated cognitive impairments (Schliebs and Arendt, 2011).

In line with previous studies, our results also demonstrated that in all individuals, independently of *CLU* genotype, aging is accompanied by changes in spectral power and topographic distribution of alpha activity (Tsuno et al., 2002; Babiloni et al., 2006a; Chiang et al., 2011). We found the decrease of alpha3 power in occipital areas, the reduction of the differences of alpha2 and alpha3 activity between posterior and anterior areas (anteriorization of alpha) and the trend toward the decrease of alpha2 power and increase of alpha1 power in the old cohort as compared to the young. It has been demonstrated that posterior cortical alpha rhythms decreases in magnitude during physiological aging (Babiloni et al., 2006a). A slowing of the alpha frequency peak in normal adults during physiological aging has also been reported (Klimesch, 1999). The anteriorization of alpha activity in elderly subjects was found to be related to a decreased level of vigilance (Tsuno et al., 2002). It was suggested that the anteriorization of alpha activity is related to the alterations in activation of posterior and anterior default mode networks (DMNs) and that these changes might be susceptible to dopaminergic influences (Knyazev, 2012). Chronic excessive neuronal activity during a resting-state condition in DMN can lead to Aβ deposition (Bero et al., 2011; de Haan et al., 2012). On the other hand, elevated level of Aβ elicits epileptiform activity, probably by enhancing synchrony among the glutamatergic synapses (Palop and Mucke, 2009). The brain regions of the DMN were shown to be preferentially vulnerable to neurodegenerative processes (Vlassenko et al., 2010; Hsiao et al., 2013).

The effect of aging on EEG is modulated by genetic factors (Babiloni et al., 2006b; Ponomareva et al., 2012). Several lines of evidence imply that the effect of *CLU* genotype on brain function may be observed before the onset of cognitive impairment. The *CLU* risk variant rs11136000 was found to be associated with reduced integrity of broad white matter regions, as observed with diffusion tensor imaging in young healthy adults (Braskie et al., 2011). fMRI study showed aberrant activation in the frontal and

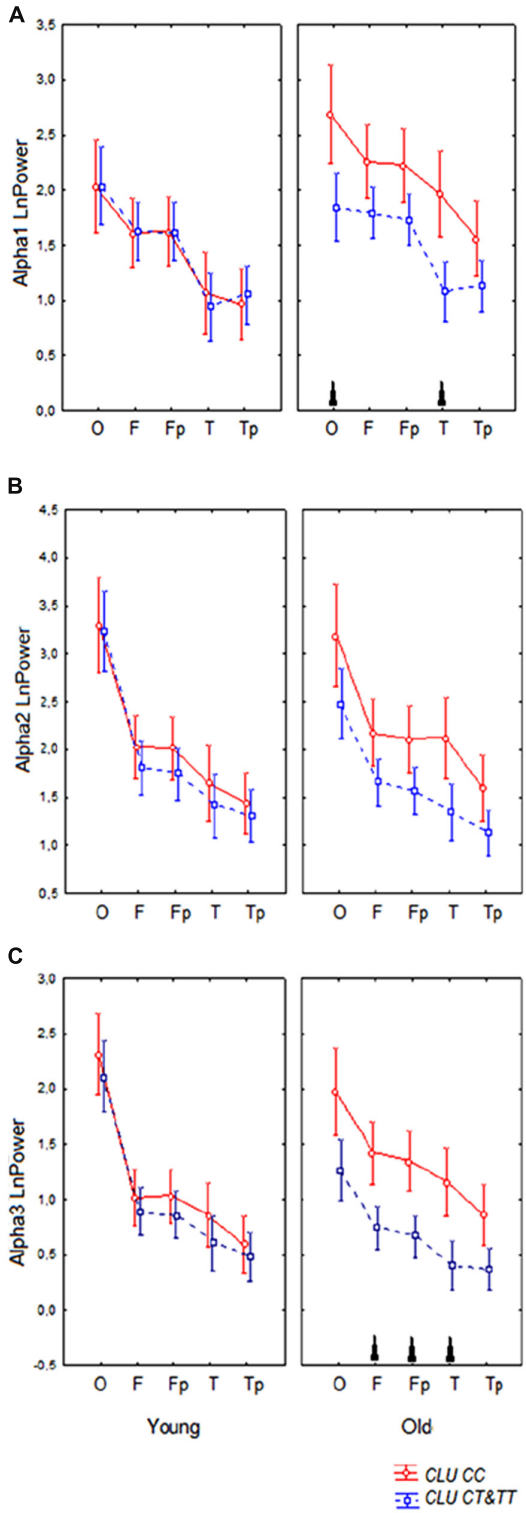

FIGURE 4 | Topographic distribution of alpha1 (A), alpha2 (B), and alpha3 (C) absolute power (mean and SE) in young and old carriers of *CLU CC* and *CLU CT&TT* genotypes in occipital O, frontal F, frontal poles Fp, temporal posterior Tp, and temporal T areas. Triangle indicates significant differences between the *CLU CC* and *CLU CT&TT* carriers $P < 0.05$.

posterior cingulate cortex and the hippocampus during working memory performance in healthy young individuals carrying *CLU* AD risk genotype (Lancaster et al., 2011).

Recently the robust changes in rCBF in cognitively normal old individuals carrying the *C*-allele of the rs11136000 SNP were revealed (Thambisetty et al., 2013). These changes consisted of significant longitudinal increases in rCBF in the hippocampus and anterior cingulated cortex. The authors suggested that the effect of *CLU CC* genotype may be related to the deposition of beta amyloid, and that affected regions are vulnerable to disruption by deposition of beta amyloid, even in the non-demented elderly.

The effect of *CLU* genotype on resting EEG in healthy subjects was not similar to the effect of *ApoE* genotype found in prior studies (Babiloni et al., 2006b; Lee et al., 2012). The differences are in line with the differing influence of *CLU* and *ApoE* genotype on resting rCBF in normal aging (Thambisetty et al., 2013). The authors reported longitudinal increase during aging of resting-state rCBF in the hippocampus and anterior cingulate cortex in the *CLU CC* carriers and the decrease in resting rCBF in the frontal, parietal, and temporal cortices and its increases in the insular cortex in the old *ApoE ε4* carriers.

Alpha rhythm slowing was found to occur in aging, and the alpha1 band of the young group might have some functional differences from the alpha1 band in the old subjects (Chiang et al., 2011). This is a potential limitation of our study. However, as *CLU* genotype-related differences were found in the age-adjusted groups, this possible confounding factor could not affect the results concerning the influence of *CLU* genotype on alpha power.

CONCLUSION

Our results show that the presence of the homozygous *CLU CC*, AD risk variant, is associated with increased absolute power of alpha3 activity and changes in topographical distribution of alpha1 activity and that this effect is more pronounced in the subjects older than 50 years of age. The increased synchronization of upper alpha activity may be related to the alterations in cholinergic hippocampal and cortical networks. The effect of *CLU* genotype on alpha activity can be superimposed to the other EEG alterations that occur across physiological aging.

ACKNOWLEDGMENTS

Research was supported by Grants from the Government of the Russian Federation (No 14.B25.31.0033), RFBR No 11-04-01896-a, and in part by the Ministry of Education and Science of the Russian Federation (Contract No 8053), RFBR (11-04-02106-a), Rosbiolab and NIH/NIA AG029360. We also thank Chikunov A. V. for support.

REFERENCES

Babiloni, C., Binetti, G., Cassarino, A., Dal Forno, G., Del Percio, C., Ferreri, F., et al. (2006a). Sources of cortical rhythms in adults during physiological aging: a multicentric EEG study. *Hum. Brain Mapp.* 27, 162–172. doi: 10.1002/hbm.20175

Babiloni, C., Benussi, L., Binetti, G., Cassetta, E., Dal Forno, G., Del Percio, C., et al. (2006b). Apolipoprotein E and alpha brain rhythms in mild cognitive impairment: a multicentric electroencephalogram study. *Ann. Neurol.* 59, 323–334. doi: 10.1002/ana.20724

Babiloni, C., Del Percio, C., Lizio, R., Marzano, N., Infarinato, F., Soricelli, A., et al. (2014). Cortical sources of resting state electroencephalographic alpha rhythms deteriorate across time in subjects with amnesic mild cognitive

impairment. *Neurobiol. Aging* 35, 130–142. doi: 10.1016/j.neurobiolaging.2013.06.019

Babiloni, C., Vecchio, F., Lizio, R., Ferri, R., Rodriguez, G., Marzano, N., et al. (2011a). Resting state cortical rhythms in mild cognitive impairment and Alzheimer's disease: electroencephalographic evidence. *J. Alzheimers Dis.* 26(Suppl. 3), 201–214. doi: 10.3233/JAD-2011-0051

Babiloni, C., Lizio, R., Carducci, F., Vecchio, F., Redolfi, A., Marino, S., et al. (2011b). Resting state cortical electroencephalographic rhythms and white matter vascular lesions in subjects with Alzheimer's disease: an Italian multicenter study. *J. Alzheimers Dis.* 26, 331–346. doi: 10.3233/JAD-2011-101710

Başar, E. (2012). A review of alpha activity in integrative brain function: fundamental physiology, sensory coding, cognition and pathology. *Int. J. Psychophysiol.* 86, 1–24. doi: 10.1016/j.ijpsycho.2012.07.002

Bero, A. W., Yan, P., Roh, J. H., Cirrito, J. R., Stewart, F. R., Raichle, M. E., et al. (2011). Neuronal activity regulates the regional vulnerability to amyloid-β deposition. *Nat. Neurosci.* 14, 750–756. doi: 10.1038/nn.2801

Bertram, L., McQueen, M. B., Mullin, K., Blacker, D., and Tanzi, R. E. (2007). Systematic meta-analyses of Alzheimer disease genetic association studies: the AlzGene database. *Nat. Genet.* 39, 17–23. doi: 10.1038/ng1934

Bettens, K., Brouwers, N., Engelborghs, S., Lambert, J. C., Rogaeva, E., Vandenberghe, R., et al. (2012). Both common variations and rare non-synonymous substitutions and small insertion/deletions in CLU are associated with increased Alzheimer risk. *Mol. Neurodegener.* 7, 3. doi: 10.1186/1750-1326-7-3

Bodenmann, S., Rusterholz, T., Dürr, R., Stoll, C., Bachmann, V., Geissler, E., et al. (2009). The functional Val158Met polymorphism of COMT predicts interindividual differences in brain alpha oscillations in young men. *J. Neurosci.* 29, 10855–10862. doi: 10.1523/JNEUROSCI.1427-09.2009

Braskie, M. N., Jahanshad, N., Stein, J. L., Barysheva, M., McMahon, K. L., de Zubicaray, G. I., et al. (2011). Common Alzheimer's disease risk variant within the CLU gene affects white matter microstructure in young adults. *J. Neurosci.* 31, 6764–6770. doi: 10.1523/JNEUROSCI.5794-10.2011

Brunia, C. H. (1999). Neural aspects of anticipatory behavior. *Acta Psychol. (Amst.)* 101, 213–242. doi: 10.1016/S0001-6918(99)00006-2

Chiang, A. K., Rennie, C. J., Robinson, P. A., van Albada, S. J., and Kerr, C. C. (2011). Age trends and sex differences of alpha rhythms including split alpha peaks. *Clin. Neurophysiol.* 122, 1505–1517. doi: 10.1016/j.clinph.2011.01.040

Cooper, N. R., Burgess, A. P., Croft, R. J., and Gruzelier, J. H. (2006). Investigating evoked and induced electroencephalogram activity in task-related alpha power increases during an internally directed attention task. *Neuroreport* 17, 205–208. doi: 10.1097/01.wnr.0000198433.29389.54

Dauwels, J., Vialatte, F., and Cichocki, A. (2010). Diagnosis of Alzheimer's disease from EEG signals: where are we standing? *Curr. Alzheimer Res.* 7, 487–505. doi: 10.2174/156720510792231720

de Haan, W., Mott, K., van Straaten, E. C., Scheltens, P., and Stam, C. J. (2012). Activity dependent degeneration explains hub vulnerability in Alzheimer's disease. *PLoS Comput. Biol.* 8:e1002582. doi: 10.1371/journal.pcbi.1002582

Enoch, M. A., Xu, K., Ferro, E., Harris, C. R., and Goldman, D. (2003). Genetic origins of anxiety in women: a role for a functional catechol-O-methyltransferase polymorphism. *Psychiatr. Genet.* 13, 33–41. doi: 10.1097/00041444-200303000-00006

Farrer, L. A., Cupples, A., Haines, J. L., Hyman, B., Kukull, W. A., Mayeux, R., et al. (1997). Effects of age, sex, and ethnicity on the association between apolipoprotein E genotype and Alzheimer's disease. A meta-analysis. APOE and Alzheimer Disease Meta Analysis Consortium. *JAMA* 278, 1349–1356. doi: 10.1001/jama.1997.03550160069041

Feigin, A., Tang, C., Ma, Y., Mattis, P., Zgaljardic, D., Guttman, M., et al. (2007). Thalamic metabolism and symptom onset in preclinical Huntington's disease. *Brain* 130, 2858–2867. doi: 10.1093/brain/awm217

Gatz, M., Reynolds, C. A., Fratiglioni, L., Johansson, B., Mortimer, J. A., Berg, S., et al. (2006). Role of genes and environments for explaining Alzheimer disease. *Arch. Gen. Psychiatry* 63, 168–174. doi: 10.1001/archpsyc.63.2.168

Goate, A., Chartier-Harlin, M. C., Mullan, M., Brown, J., Crawford, F., Fidani, L., et al. (1991). Segregation of missense mutation in the amyloid precursor protein gene with familial Alzheimer's disease. *Nature* 349, 704–706. doi: 10.1038/349704a0

Golenkina, S. A., Goltsov, A. Yu., Kuznetsova, I. L., Grigorenko, A. P., Andreeva, T. V., Reshetov, D. A., et al. (2010). Analysis of clusterin gene (CLU/APOJ) polymorphism in Alzheimer's disease patients and in normal cohorts from Russian populations. *Mol. Biol.* 44, 620–626. doi: 10.1134/S0026893310040072

Gottesman, I. I., and Gould, T. D. (2003). The endophenotype concept in psychiatry: etymology and strategic intentions. *Am. J. Psychiatry* 160, 636–645. doi: 10.1176/appi.ajp.160.4.636

Hamilton, M. (1960). A rating scale for depression. *J. Neurol. Neurosurg. Psychiatry* 23, 56–62. doi: 10.1136/jnnp.23.1.56

Harold, D., Abraham, R., Hollingworth, P., Sims, R., Gerrish, A., Hamshere, M. L., et al. (2009). Genome-wide association study identifies variants at CLU and PICALM associated with Alzheimer's disease. *Nat. Genet.* 41, 1088–1093. doi: 10.1038/ng.440

Hsiao, F. J., Wang, Y. J., Yan, S. H., Chen, W. T., and Lin, Y. Y. (2013). Altered oscillation and synchronization of default-mode network activity in mild Alzheimer's disease compared to mild cognitive impairment: an electrophysiological study. *PLoS ONE* 8:e68792. doi: 10.1371/journal.pone.0068792

Huang, C., Wahlund, L., Dierks, T., Julin, P., Winblad, B., and Jelic, V. (2000). Discrimination of Alzheimer's disease and mild cognitive impairment by equivalent EEG sources: a cross-sectional and longitudinal study. *Clin. Neurophysiol.* 111, 1961–1967. doi: 10.1016/S1388-2457(00)00454-5

Hughes, C. P., Berg, L., Danziger, W. L., Coben, L. A., and Martin, R. L. (1982). A new clinical scale for the staging of dementia. *Br. J. Psychiatry* 140, 566–572. doi: 10.1192/bjp.140.6.566

Illarioshkin, S. N., Ivanova-Smolenskaia, I. A., Markova, E. D., Shadrina, M. I., Kliushnikov, S. A., Zagorovskaia, T. V., et al. (2004). Molecular genetic analysis of hereditary neurodegenerative diseases. *Genetika* 4, 816–826.

Jann, K., Koenig, T., Dierks, T., Boesch, C., and Federspiel, A. (2010). Association of individual resting state EEG alpha frequency and cerebral blood flow. *Neuroimage* 51, 365–372. doi: 10.1016/j.neuroimage.2010.02.024

Jelic, V., Johansson, S. E., Almkvist, O., Shigeta, M., Julin, P., Nordberg, A., et al. (2000). Quantitative electroencephalography in mild cognitive impairment: longitudinal changes and possible prediction of Alzheimer's disease. *Neurobiol. Aging* 21, 533–540. doi: 10.1016/S0197-4580(00)00153-6

Jelic, V., Julin, P., Shigeta, M., Nordberg, A., Lannfelt, L., Winblad, B., et al. (1997). Apolipoprotein E epsilon 4 allele decreases functional connectivity in Alzheimer's disease as measured by EEG coherence. *J. Neurol. Neurosurg. Psychiatry* 63, 59–65. doi: 10.1136/jnnp.63.1.59

Jeong, J. (2004). EEG dynamics in patients with Alzheimer's disease. *Clin. Neurophysiol.* 115, 1490–1505. doi: 10.1016/j.clinph.2004.01.001

Jobert, M., Wilson, F. J., Ruigt, G. S., Brunovsky, M., Prichep, L. S., and Drinkenburg, W. H. (2012). IPEG Pharmaco-EEG Guidelines Committee: guidelines for the recording and evaluation of pharmaco-EEG data in man: the International Pharmaco-EEG Society (IPEG). *Neuropsychobiology* 66, 201–220. doi: 10.1159/000343478

John, E. R., Ahn, H., Prichep, L. S., Trepetin, M., Brown, D., Kaye, H., et al. (1980). Developmental equations for the electroencephalogram. *Science* 210, 1255–1258. doi: 10.1126/science.7434026

Killick, R., Ribe, E. M., Al-Shawi, R., Malik, B., Hooper, C., Fernandes, C., et al. (2012). Clusterin regulates β-amyloid toxicity via Dickkopf-1-driven induction of the wnt-PCP-JNK pathway. *Mol. Psychiatry*. doi: 10.1038/mp.2012.163 [Epub ahead of print].

Klimesch, W. (1999). EEG alpha and theta oscillations reflect cognitive and memory performance: a review and analysis. *Brain Res. Brain Res. Rev.* 29, 169–195. doi: 10.1016/S0165-0173(98)00056-3

Klimesch, W. (2012). Alpha-band oscillations, attention, and controlled access to stored information. *Trends Cogn. Sci.* 16, 606–617. doi: 10.1016/j.tics.2012.10.007

Knyazev, G. G. (2012). Extraversion and anterior vs. posterior DMN activity during self-referential thoughts. *Front. Hum. Neurosci.* 6:348. doi: 10.3389/fnhum.2012.00348

Koenig, T., Prichep, L., Dierks, T., Hubl, D., Wahlund, L. O., John, E. R., et al. (2005). Decreased EEG synchronization in Alzheimer's disease and mild cognitive impairment. *Neurobiol. Aging* 26, 165–171. doi: 10.1016/j.neurobiolaging.2004.03.008

Lambert, J. C., Heath, S., Even, G., Campion, D., Sleegers, K., Hiltunen, M., et al. (2009). Genome-wide association study identifies variants at CLU and CR1 associated with Alzheimer's disease. *Nat. Genet.* 41, 1094–1099. doi: 10.1038/ng.439

Lancaster, T. M., Baird, A., Wolf, C., Jackson, M. C., Johnston, S. J., Donev, R., et al. (2011). Neural hyperactivation in carriers of the Alzheimer's risk variant on the clusterin gene. *Eur. Neuropsychopharmacol.* 21, 880–884. doi: 10.1016/j.euroneuro.2011.02.001

Lee, T. W., Yu, Y. W., Hong, C. J., Tsai, S. J., Wu, H. C., and Chen, T. J. (2012). The influence of apolipoprotein E Epsilon4 polymorphism on qEEG profiles in healthy young females: a resting EEG study. *Brain Topogr.* 25, 431–442. doi: 10.1007/s10548-012-0229-y

Lehtovirta, M., Partanen, J., Könönen, M., Hiltunen, J., Helisalmi, S., Hartikainen, P., et al. (2000). A longitudinal quantitative EEG study of Alzheimer's disease: relation to apolipoprotein E polymorphism. *Dement. Geriatr. Cogn. Disord.* 11, 29–35. doi: 10.1159/000017210

Levy-Lahad, E., Wasco, W., Poorkaj, P., Romano, D., Oshima, J., Pettingell, W., et al. (1995). Candidate gene for the chromosome 1 familial Alzheimer's disease locus. *Science* 269, 973–977. doi: 10.1126/science.7638622

Ling, I.-F., Bhongsatiern, J., Simpson, J. F., Fardo, D. W., and Estus, S. (2012). Genetics of clusterin isoform expression and Alzheimer's disease risk. *PLoS ONE* 7:e33923. doi: 10.1371/journal.pone.0033923

Lizio, R., Vecchio, F., Frisoni, G. B., Ferri, R., Rodriguez, G., and Babiloni, C. (2011). Electroencephalographic rhythms in Alzheimer's disease. *Int. J. Alzheimers Dis.* 2011, 927573. doi: 10.4061/2011/927573

Masdeu, J. C., Kreisl, W. C., and Berman, K. F. (2012). The neurobiology of Alzheimer disease defined by neuroimaging. *Curr. Opin. Neurol.* 25, 410–420. doi: 10.1097/WCO.0b013e3283557b36

Moretti, D. V., Babiloni, F., Carducci, F., Cincotti, F., Remondini, E., Rossini, P. M., et al. (2003). Computerized processing of EEG-EOG-EMG artifacts for multi-centric studies in EEG oscillations and event-related potentials. *Int. J. Psychophysiol.* 47, 199–216. doi: 10.1016/S0167-8760(02)00153-8

Moretti, D. V., Frisoni, G. B., Binetti, G., and Zanetti, O. (2011). Anatomical substrate and scalp EEG markers are correlated in subjects with cognitive impairment and Alzheimer's disease. *Front. Psychiatry* 1:152. doi: 10.3389/fpsyt.2010.00152

Moretti, D. V., Miniussi, C., Frisoni, G. B., Geroldi, C., Zanetti, O., Binetti, G., et al. (2007). Hippocampal atrophy and EEG markers in subjects with mild cognitive impairment. *Clin. Neurophysiol.* 118, 2716–2729. doi: 10.1016/j.clinph.2007.09.059

Moretti, D. V., Prestia, A., Fracassi, C., Binetti, G., Zanetti, O., and Frisoni, G. B. (2012a). Specific EEG changes associated with atrophy of hippocampus in subjects with mild cognitive impairment and Alzheimer's disease. *Int. J. Alzheimers Dis.* 2012, 253153. doi: 10.1155/2012/253153

Moretti, D. V., Zanetti, O., Binetti, G., and Frisoni, G. B. (2012b). Quantitative EEG markers in mild cognitive impairment: degenerative versus vascular brain impairment. *Int. J. Alzheimers Dis.* 2012, 917537. doi: 10.1155/2012/917537

Palop, J. J., and Mucke, L. (2009). Epilepsy and cognitive impairments in Alzheimer disease. *Arch. Neurol.* 66, 435–440. doi: 10.1001/archneurol.2009.15

Pfurtscheller, G., and Lopes da Silva, F. H. (1999). Event-related EEG/MEG synchronization and desynchronization: basic principles. *Clin. Neurophysiol.* 110, 1842–1857. doi: 10.1016/S1388-2457(99)00141-8

Pfurtscheller, G., Neuper, C., and Krausz, G. (2000). Functional dissociation of lower and upper frequency mu rhythms in relation to voluntary limb movement. *Clin. Neurophysiol.* 111, 1873–1879. doi: 10.1016/S1388-2457(00)00428-4

Ponomareva, N. V., Goltsov, A. Y., Kunijeva, S. S., Scheglova, N. S., Malina, D. D., Mitrofanov, A. A., et al. (2012). Age- and genotype-related neurophysiologic reactivity to oxidative stress in healthy adults. *Neurobiol. Aging* 33, 839.e11–839.e21. doi: 10.1016/j.neurobiolaging.2011.11.013

Ponomareva, N. V., Korovaitseva, G. I., and Rogaev, E. I. (2008). EEG alterations in non-demented individuals related to apolipoprotein E genotype and to risk of Alzheimer disease. *Neurobiol. Aging* 29, 819–827. doi: 10.1016/j.neurobiolaging.2006.12.019

Prichep, L. S., John, E. R., Ferris, S. H., Rausch, L., Fang, Z., Cancro, R., et al. (2006). Prediction of longitudinal cognitive decline in normal elderly with subjective complaints using electrophysiological imaging. *Neurobiol. Aging* 27, 471–481. doi: 10.1016/j.neurobiolaging.2005.07.021

Rogaev, E. I. (1999). Genetic factors and a polygenic model of Alzheimer's disease. *Genetika* 35, 1558–1571.

Rogaev, E. I., Sherrington, R., Rogaeva, E. A., Levesque, G., Ikeda, M., Liang, Y., et al. (1995). Familial Alzheimer's disease in kindreds with missense mutations in a gene on chromosome 1 related to the Alzheimer's disease type 3 gene. *Nature* 376, 775–778. doi: 10.1038/376775a0

Saunders, A. M., Strittmatter, W. J., Schmechel, D., George-Hyslop, P. H., Pericak-Vance, M. A., Joo, S. H., et al. (1993). Association of apolipoprotein E allele ε4 with late-onset familial and sporadic Alzheimer's disease. *Neurology* 43, 1467–1472. doi: 10.1212/WNL.43.8.1467

Schliebs, R., and Arendt, T. (2011). The cholinergic system in aging and neuronal degeneration. *Behav. Brain Res.* 221, 555–563. doi: 10.1016/j.bbr.2010.11.058

Schmechel, D. E., Saunders, A. M., Strittmatter, W. J., Crain, B. J., Hulette, C. M., Joo, C. H., et al. (1993). Increased amyloid β-peptide deposition in cerebral cortex as a consequence of an apolipoprotein E genotype in late-onset Alzheimer disease. *Proc. Natl. Acad. Sci. U.S.A.* 90, 9649–9653. doi: 10.1073/pnas.90.20.9649

Sherrington, R., Rogaev, E. I., Liang, Y., Rogaeva, E. A., Levesque, G., Ikeda, M., et al. (1995). Cloning of a gene bearing missense mutations in early-onset familial Alzheimer's disease. *Nature* 375, 754–760. doi: 10.1038/375754a0

Song, F., Poljak, A., Crawford, J., Kochan, N. A., Wen, W., Cameron, B., et al. (2012). Plasma apolipoprotein levels are associated with cognitive status and decline in a community cohort of older individuals. *PloS ONE* 7:e34078. doi: 10.1371/journal.pone.0034078

Spielberger, C. D. (1983). *Manual for the State-Trait Anxiety Inventory: STAI (Form Y)*. Palo Alto: Consulting Psychologists Press.

Stam, C. J., van der Made, Y., Pijnenburg, Y. A., and Scheltens, P. (2003). EEG synchronization in mild cognitive impairment and Alzheimer's disease. *Acta Neurol. Scand.* 108, 90–96. doi: 10.1034/j.1600-0404.2003.02067.x

Steriade, M. (2006). Grouping of brain rhythms in corticothalamic systems. *Neuroscience* 137, 1087–1106. doi: 10.1016/j.neuroscience.2005.10.029

Steriade, M., and Llinás, R. R. (1988). The functional states of the thalamus and the associated neuronal interplay. *Physiol. Rev.* 68, 649–742.

Suslina, Z. A. (2012). Neurology at the border of centuries: achievements and prospects. *Vestn. Ross. Akad. Med. Nauk* 57–65.

Tang, M., Li, J., Liu, B., Song, N., Wang, Z., and Yin, C. (2013). Clusterin expression and human testicular seminoma. *Med. Hypotheses* 81, 635–637. doi: 10.1016/j.mehy.2013.07.019

Tatum, W. O., Dworetzky, B. A., and Schomer, D. L. (2011). Artifact and recording concepts in EEG. *J. Clin. Neurophysiol.* 28, 252–263. doi: 10.1097/WNP.0b013e31821c3c93

Thambisetty, M., Beason-Held, L. L., An, Y., Kraut, M., Nalls, M., Hernandez, D. G., et al. (2013). Alzheimer risk variant CLU and brain function during aging. *Biol. Psychiatry* 73, 399–405. doi: 10.1016/j.biopsych.2012.05.026

Tsuno, N., Shigeta, M., Hyoki, K., Kinoshita, T., Ushijima, S., Faber, P. L., et al. (2002). Spatial organization of EEG activity from alertness to sleep stage 2 in old and younger subjects. *J. Sleep Res.* 11, 43–51. doi: 10.1046/j.1365-2869.2002.00288.x

van Beijsterveldt, C. E., Molenaar, P. C., de Geus, E. J., and Boomsma, D. I. (1996). Heritability of human brain functioning as assessed by electroencephalography. *Am. J. Hum. Genet.* 58, 562–573.

Van der Hiele, K., Bollen, E. L., Vein, A. A., Reijntjes, R. H., Westendorp, R. G., van Buchem, M. A., et al. (2008). EEG markers of future cognitive performance in the elderly. *J. Clin. Neurophysiol.* 25, 83–89. doi: 10.1097/WNP.0b013e31816a5b25

Versavel, M., Leonard, J. P., and Herrmann, W. M. (1995). Standard operating procedure for registration and computer-supported evaluation of pharmaco-EEG data. *Neuropsychobiology* 32, 166–170. doi: 10.1159/000119230

Vlassenko, A. G., Vaishnavi, S. N., Couture, L., Sacco, D., Shannon, B. J., Mach, R. H., et al. (2010). Spatial correlation between brain aerobic glycolysis and amyloid-β (Aβ) deposition. *Proc. Natl. Acad. Sci. U.S.A.* 107, 17763–17767. doi: 10.1073/pnas.1010461107

Winterer, G., Mahlberg, R., Smolka, M. N., Samochowiec, J., Ziller, M., Rommelspacher, H. P., et al. (2003). Association analysis of exonic variants of the GABA(B)-receptor gene and alpha electroencephalogram voltage in normal subjects and alcohol-dependent patients. *Behav. Genet.* 33, 7–15. doi: 10.1023/A:1021043315012

Conflict of Interest Statement: The authors declare that the research was conducted in the absence of any commercial or financial relationships that could be construed as a potential conflict of interest.

Received: 10 September 2013; paper pending published: 29 September 2013; accepted: 19 November 2013; published online: 13 December 2013.

Citation: Ponomareva N, Andreeva T, Protasova M, Shagam L, Malina D, Goltsov A, Fokin V, Mitrofanov A and Rogaev E (2013) Age-dependent effect of Alzheimer's risk

variant of CLU on EEG alpha rhythm in non-demented adults. Front. Aging Neurosci. ***5****:86. doi: 10.3389/fnagi.2013.00086*
This article was submitted to the journal Frontiers in Aging Neuroscience.
Copyright © 2013 Ponomareva, Andreeva, Protasova, Shagam, Malina, Goltsov, Fokin, Mitrofanov and Rogaev. This is an open-access article distributed under the terms of the Creative Commons Attribution License (CC BY). The use, distribution or reproduction in other forums is permitted, provided the original author(s) or licensor are credited and that the original publication in this journal is cited, in accordance with accepted academic practice. No use, distribution or reproduction is permitted which does not comply with these terms.

frontiers in
AGING NEUROSCIENCE

ORIGINAL RESEARCH ARTICLE
published: 19 February 2013
doi: 10.3389/fnagi.2013.00002

Cerebellar theta burst stimulation modulates short latency afferent inhibition in Alzheimer's disease patients

Francesco Di Lorenzo[1], Alessandro Martorana[1,2], Viviana Ponzo[1], Sonia Bonnì[1], Egidio D'Angelo[3], Carlo Caltagirone[1,2] and Giacomo Koch[1,2]*

[1] *Neurologia Clinica e Comportamentale, Fondazione Santa Lucia IRCCS, Rome, Italy*
[2] *Dipartimento di Neuroscienze, Policlinico Tor Vergata, Università di Roma Tor Vergata, Rome, Italy*
[3] *Dipartimento di Sanità Pubblica e Neuroscienze, Università di Pavia, and IRCCS C. Mondino, Pavia, Italy*

Edited by:
Davide V. Moretti, IRCCS Centro San Giovanni di Dio Fatebenefratelli, Italy

Reviewed by:
Vincenzo Di Lazzaro, Università Campus Biomedico di Roma, Italy
Masashi Hamada, University College London, UK

***Correspondence:**
Giacomo Koch, Laboratorio di Neurologia Clinica e Comportamentale, IRCCS Fondazione Santa Lucia, Via Ardeatina 306, 00179 Rome, Italy.
e-mail: g.koch@hsantalucia.it

The dysfunction of cholinergic neurons is a typical hallmark in Alzheimer's disease (AD). Previous findings demonstrated that high density of cholinergic receptors is found in the thalamus and the cerebellum compared with the cerebral cortex and the hippocampus. We aimed at investigating whether activation of the cerebello-thalamo-cortical pathway by means of cerebellar theta burst stimulation (TBS) could modulate central cholinergic functions evaluated *in vivo* by using the neurophysiological determination of Short-Latency Afferent Inhibition (SLAI). We tested the SLAI circuit before and after administration of cerebellar continuous TBS (cTBS) in 12 AD patients and in 12 healthy age-matched control subjects (HS). We also investigated potential changes of intracortical circuits of the contralateral primary motor cortex (M1) by assessing short intracortical inhibition (SICI) and intracortical facilitation (ICF). SLAI was decreased in AD patients compared to HS. Cerebellar cTBS partially restored SLAI in AD patients at later inter-stimulus intervals (ISIs), but did not modify SLAI in HS. SICI and ICF did not differ in the two groups and were not modulated by cerebellar cTBS. These results demonstrate that cerebellar magnetic stimulation is likely to affect mechanisms of cortical cholinergic activity, suggesting that the cerebellum may have a direct influence on the cholinergic dysfunction in AD.

Keywords: transcranial magnetic stimulation, cortical plasticity, cholinergic, cerebellum, Alzheimer's disease

INTRODUCTION

Alzheimer's disease (AD) pathophysiology is dominated by a dysfunction of the central cholinergic system. In AD patients, the impairment of central cholinergic functions can be evaluated *in vivo* by using a neurophysiological effect called Short-Latency Afferent Inhibition (SLAI) (Tokimura et al., 2000). SLAI consists in the inhibition of the Motor Evoked Potentials (MEPs) by afferent sensory impulses. SLAI can be easily measured by applying an electric conditioning pulse on the median nerve at wrist that precedes the TMS test pulse applied over the contralateral primary motor cortex (M1) by 20–25 ms. SLAI is abolished by scopolamine, a potent muscarinic antagonist (Di Lazzaro et al., 2002), and it has therefore been suggested that the inhibitory effect of peripheral stimulation is mediated by cholinergic projections over the primary motor cortex. In AD patients, SLAI is reduced to various degrees depending on the severity of the disease, so that the decreased inhibitory effect of peripheral stimulation is thought to reflect the cholinergic dysfunction in AD (Di Lazzaro et al., 2002; Martorana et al., 2009).

Although the cerebellum is not among the most renown brain structures to be affected by the pathology, recent evidence suggested that it undergoes degenerative changes in AD: the posterior cerebellar lobes are significantly smaller in AD patients when compared to HC, and atrophy of the posterior cerebellar regions is associated with poorer cognitive performance (Thomann et al., 2008). Moreover, the cerebellum is strongly involved in cholinergic functions. A recent PET study demonstrated that intravenously administered [^{11}C]-donepezil, an acetyl-cholinesterase (AChE) inhibitor used in AD therapy, rapidly enters the brain and mainly distributes to the striatum, thalamus, and cerebellum, which are known to contain high densities of AChE compared with the cerebral cortex and hippocampus (Okamura et al., 2008). The regional distribution of [^{11}C]-donepezil was consistent with regional AChE activity determined in a human postmortem study (Finkelstein et al., 1988). Moreover, nicotinic cholinergic receptors (nAChRs) are widely distributed in the mammalian cerebellum and are known to regulate synaptic efficacy at two major classes of cerebellar neurons (Turner et al., 2011; D'Angelo and Casali, 2012).

In humans, the neural activity of the cerebellum can be explored *in vivo* by means of repetitive transcranial magnetic stimulation (Ugawa et al., 1995; Del Olmo et al., 2007; Koch et al., 2008). Therefore, in the current study, we sought to investigate whether cerebellar magnetic stimulation could modulate the altered SLAI circuits described in AD patients. We reasoned that given that the cerebellar activity is involved in the cholinergic system, cerebellar continuous TBS (cTBS) could provide novel information regarding the interactions between the cerebello-thalamo-cortical circuits and the central cholinergic functioning in AD patients.

MATERIALS AND METHODS

SUBJECTS

We examined 12 patients with a new diagnosis of probable AD according to the NINCDS-ADRDA criteria (Varma et al., 1999) and 12 neurologically healthy age-matched control subjects (HS). The mean (±SD) age of the patients was 69.8 (±4.9) years, whereas that of controls was 71.7 (±4.4) years. All patients underwent a complete clinical investigation, including medical history, neurological examination, mini mental state examination (MMSE), a complete blood screening (including routine exams, thyroid hormones, level of B12), neuropsychological examination, a complete neuropsychiatric evaluation, and morphological magnetic resonance imaging (1.5 T MRI). Exclusion criteria were the following: patients with isolated deficits and/or unmodified MMSE (≥25/30) on revisit (6, 12, and 18 months follow-up), patients with clinically manifest acute stroke in the last 6 months showing Hachinsky scale score >4, and a radiological evidence of sub-cortical lesions. None of patients revealed pyramidal and/or extrapyramidal signs at the neurological examination. At the time of enrolment, in the 30 days before participating in this study, none of the patients had been treated with drugs that might have modulated cerebral cortex excitability such as antidepressants, or any other neuroactive drugs (i.e., benzodiazepines, anti-epileptic drugs, or neuroleptics), and they had not been treated with cholinesterase inhibitors. All AD patients showed a cognitive profile consistent with moderate dementia, as assessed by a neuropsychological evaluation including the MMSE and a standardized neuropsychological battery (Carlesimo et al., 1996). On the MMSE, AD patients scored a mean of 21.08 (±3.9) and Clinical Dementia Rating (CDR) was 1.21 (±1.1). All participants or their legal guardian gave the written informed consent after receiving an extensive disclosure of study. The study was performed according to the Declaration of Helsinki and approved by the ethics committee of the Tor Vergata University in Rome.

EXPERIMENT 1: EFFECTS OF CEREBELLAR cTBS ON SLAI, SICI, AND ICF CIRCUITS

SLAI

Magnetic stimulation was performed using an high power Magstim 200 magnetic stimulator (Magstim Co, Whitland, Dyfed, UK). The magnetic stimuli had a nearly monophasic pulse configuration, with a rise time of 0.1 ms, decaying back to zero over 0.8 ms. A figure of eight coil with external loop diameters of 9 cm was held over the left motor cortex at the optimum scalp position to elicit motor responses in the contralateral first dorsal interosseous (FDI) muscle. The optimal position was marked on the scalp with a felt pen to ensure identical placement of the coil throughout the experiment. The handle of the coil pointed backward and was perpendicular to the presumed direction of the central sulcus, about 45° to the midsagittal line. The direction of the induced current was from posterior to anterior and was optimal to activate the motor cortex transsynaptically. Surface muscle responses were recorded via two 9 mm diameter Ag–AgCl electrodes with the active electrode over the motor point of the muscle and the reference on the metacarpophalangeal joint of the index finger. Muscle responses were amplified and filtered (bandwidth 3–3000 Hz) by D150 amplifiers (Digitimer, Welwyn Garden City, Hertfordshire, UK). Data were collected on a computer with a sampling rate of 10 kHz per channel and stored for later analysis using a CED 1401 A–D converter (Cambridge Electronic Design, Cambridge, UK). All the AD patients selected were able to understand and carry out the simple task required for this electrophysiological study—that is, to keep fully relaxed.

The resting motor threshold (RMT) was defined as the lowest intensity that produced MEPs of >50 μV in at least five out of 10 trials with the muscles relaxed (Rossini et al., 1994). Determination of RMT was done in step width of 1% of maximal stimulator output (MSO). Short latency inhibition was studied using the technique that has been recently described (Tokimura et al., 2000) (see **Figure 1**). Conditioning stimuli were single pulses (200 μs) of electrical stimulation applied through bipolar electrodes to the right median nerve at the wrist (cathode proximal). The intensity of the conditioning stimulus was set at just over motor threshold for evoking a visible twitch of the thenar muscles. The intensity of the test cortical magnetic stimulus was adjusted to evoke a muscle response in relaxed right FDI with amplitude of approximately 1 mV peak to peak. The conditioning stimulus to the peripheral nerve preceded the magnetic test stimulus by different interstimulus intervals (ISIs). ISIs were determined relative to the latency of the N20 component of the somatosensory evoked potential induced by stimulation of the right median nerve. The active electrode for recording the N20 potential was attached 3 cm posterior to C3 (10–20 system) and the reference was 3 cm posterior to C4. Five hundred responses were averaged to identify the latency of the N20 peak. ISIs from N20 −4 ms to N20 +8 ms were investigated in 4 ms steps. Ten stimuli were delivered at each ISI. The subject was given audiovisual feedback at high gain to assist in maintaining complete relaxation. The intertrial interval was set at 5 s (±10%), for a total duration of approximately 5 min. Measurements were made on each individual trial. The mean peak-to peak amplitude of the conditioned MEP at each ISI was expressed as a percentage of the mean peak-to-peak amplitude size of the unconditioned test pulse in that block.

SICI-ICF

We used a 7 cm figure-of-eight coil connected with two Magstim 200 stimulators to apply paired TMS over the motor cortex. In order to investigate M1 intracortical circuits such as short intracortical inhibition (SICI) and intracortical facilitation (ICF). The magnetic stimuli had a nearly monophasic pulse configuration. The coil was placed at the optimal position for eliciting MEPs from the left contralateral FDI muscle. SICI and ICF were tested using paired TMS with a conditioning stimulus (CS) preceding a test stimulus (TS) by 1–15 ms (Kujirai et al., 1993; Ziemann et al., 1996). CS was set at 80% AMT (Huang and Rothwell, 2004) while the intensity of TS was adjusted to evoke a MEP of approximately 1 mV peak to peak in the relaxed FDI. The amplitude of the conditioned MEP at each ISI was expressed as a percentage of the mean peak-to-peak amplitude size of the unconditioned TS in that block.

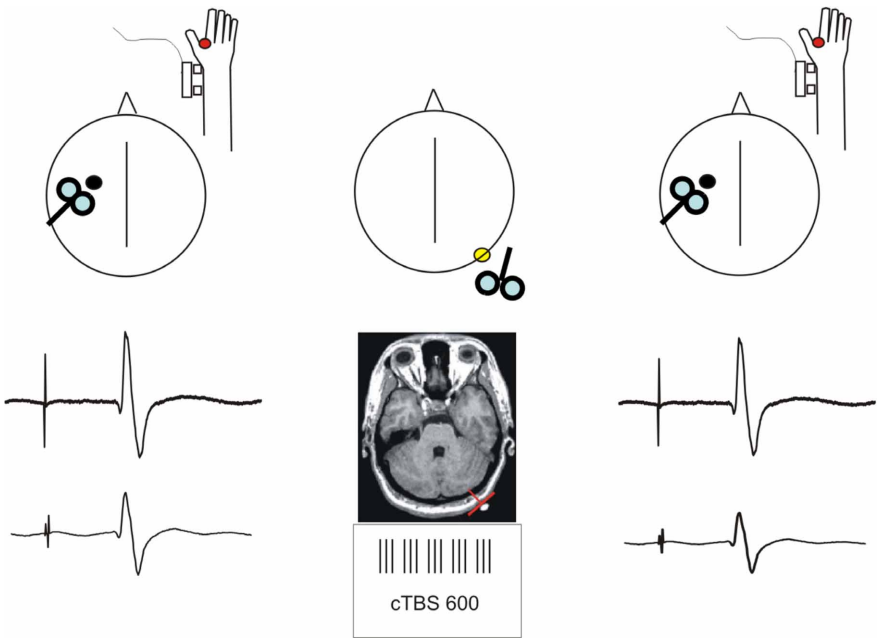

FIGURE 1 | Schematic description of the experimental procedure. Short-latency afferent inhibition (SLAI) was recorded by measuring the inhibitory effects of the peripheral median nerve stimulation over the amplitude of the MEP recorded from the right FDI at different interstimulus intervals in AD patients and age matched healthy controls. SLAI was measured at baseline and after a session of cTBS over the left lateral cerebellum in both groups.

cTBS

A MagStim Super Rapid magnetic stimulator (Magstim Company, Whitland, Wales, UK), connected with a figure-of-eight coil with a diameter of 70 mm was used to deliver cTBS. Three-pulse bursts at 50 Hz repeated every 200 ms for 40 s were delivered at 80% of the active motor threshold (AMT) over the lateral cerebellum (600 pulses) (Huang et al., 2005). cTBS was applied over the right lateral cerebellum using the same scalp co-ordinates (1 cm inferior and 3 cm left/right to the inion) adopted in previous MRI studies showing that this site target the posterior and superior lobules of the lateral cerebellum (Del Olmo et al., 2007). We used the figure-of-eight coil, since this approach has been adopted in previous investigations in which cerebellar rTMS was shown to be effective in modulating the excitability of the contralateral motor cortex (Del Olmo et al., 2007). The coil was positioned tangentially to the scalp, with the handle pointing superiorly.

SLAI and SICI/ICF were tested before in two different blocks and immediately after the application of cTBS over the right lateral cerebellum. The order of presentation of the blocks before and after cTBS was pseudo-randomized across subjects.

EXPERIMENT 2: EFFECTS OF CEREBELLAR cTBS ON SLAI INPUT-OUTPUT CURVES IN HEALTHY SUBJECTS

SLAI is already different between groups (less in AD) at baseline. Therefore, it is unclear how to interpret the effects of cerebellar cTBS. From the reported data, the possibility cannot be excluded that the modulating cTBS effect was not seen in the healthy controls merely due to SLAI saturation (floor effect). To disentangle this, we performed an experiment in which we studied SLAI input-output curves by systematic variation of the intensity of the peripheral nerve stimulus to compare the effects of cTBS at equivalent SLAI levels as those obtained in the AD patients group. In a group of eight healthy controls SLAI was tested as in Experiment 1, but three different blocks were applied. In each block the intensity of the peripheral nerve stimulation was set at 100, 200, and 300% of the sensory threshold (ST) (note that an intensity of 300% is close to the one necessary for evoking a visible twitch of the thenar muscles as in Experiment 1). SLAI blocks were tested before and immediately after the application of cTBS over the right lateral cerebellum. The order of presentation of the blocks before and after cTBS was pseudo-randomized across subjects.

EXPERIMENT 3: EFFECTS OF OCCIPITAL cTBS ON SLAI, SICI, AND ICF CIRCUITS

We performed an additional experiment in order to exclude that the cTBS effects obtained in the AD patients could be non-specific. Therefore, we performed the same experiment as in Experiment 1 but we varied the site of application of cTBS, by choosing the occipital cortex as a control area. The occipital TMS site was 3 cm above the inion and 1 cm right of midline (Romei et al., 2012). SLAI and SICI/ICF were tested before in two different blocks and immediately after the application of cTBS over the right lateral cerebellum. The order of presentation of the blocks before and after cTBS was pseudo-randomized across subjects.

STATISTICAL ANALYSIS

In Experiment 1 SLAI parameters of AD patients were compared with those of controls by means of repeated measures ANOVA with GROUP (AD vs. healthy subjects) as between subjects factor

and ISI (−4, 0, +4, and +8 ms plus the latency of the N20) and PROTOCOL (pre vs. post cTBS) as within subjects factors. For SICI we performed a repeated measures analysis ANOVA with GROUP (AD vs. healthy subjects) as between subjects' factor and ISI (1, 2, 3, 5, 7, 10, and 15 ms) and PROTOCOL (pre vs. post cTBS) as within subjects factors. In experiment 2 we performed a repeated measures ANOVA with INTENSITY (100, 200, and 300% of ST), ISI (−4, 0, +4, and +8 ms plus the latency of the N20) and PROTOCOL (pre vs. post cTBS) as within subjects factors. In Experiment 3 SLAI parameters of AD patients were analysed by means of repeated measures ANOVA with ISI (−4, 0, +4, and +8 ms plus the latency of the N20) and PROTOCOL (pre vs. post cTBS) as within subjects factors. When a significant main effect was reached, paired *t*-tests with Bonferroni correction were employed to characterize the different effects of the specific ISIs. For all statistical analyses, a p value of <0.05 was considered to be significant. Mauchley's test examined for sphericity. The Greenhouse–Geisser correction was used for non-spherical data.

RESULTS

EXPERIMENT 1

The N20 latency and amplitude were within normal limits in all AD patients and control subjects and did not differ between the two groups (20.5 ± 3.2 ms vs. 20.8 ± 2.9 ms). The mean (SD) RMT to TMS was significantly lower in AD patients than in controls (45.9% ± 2.1 vs. 49.9 ± 1.1%) of MSO; $t = 3.14$; $p < 0.05$ (see **Table 1**). RMT was not significantly modified following cerebellar cTBS ($p = 0.48$ at paired *t*-test analysis). For unconditioned, TS MEPs amplitude pre and post cTBS did not differ being, respectively, 1.08 ± 0.33 mV and 1.04 ± 0.31 mV in AD and 1.13 ± 0.25 mV and 1.14 ± 0.34 mV in controls. Repeated ANOVA performed on SLAI measures revealed significant main effects of PROTOCOL ($F = 5.66$; $p = 0.027$) and ISI ($F = 19.14$; $p = 0.0001$), as well significant GROUP × PROTOCOL ($F = 4.26$; $p = 0.041$) interaction. The triple interaction GROUP × ISI × PROTOCOL was not significant. *Post hoc* analysis revealed that at baseline the amount of SLAI inhibition was smaller in AD patients than in normal controls at +4 and +8 ms (all $p < 0.05$) (**Figure 2**). The amount of SLAI inhibition increased in AD patients following cTBS at 0 and +4 ms ISIs (all $p < 0.05$) (**Figure 3A**). On the other hand when the same analysis was performed in the HS group, no significant difference emerged (**Figure 3B**). No effects were found for SICI and ICF in both groups. (**Figures 4A,B**).

Table 1 | Parameters of corticospinal excitability before and after cTBS.

Measures	AD	HS
rMT (%)	45.9 ± 2.1	49.9 ± 1.1
aMT (%)	34 ± 1.3	37 ± 1.9
1mV (%)	52.41 ± 2.8	55.4 ± 2.2
PRE cTBS		
ICI 2 ms (%)	42.85 ± 7.2	65 ± 10.6
ICF 15 ms (%)	99.22 ± 9.0	136.9 ± 9.1
SLAI 24 ms (%)	75.4 ± 13.5	57.7 ± 9.8
POST cTBS		
ICI 2 ms (%)	41.77 ± 6.1	60.32 ± 9.6
ICF 15 ms (%)	118 ± 12.1	136.5 ± 27
SLAI 24 ms (%)	53.147 ± 4.9	63.4 ± 8.8

rMT, resting motor threshold; aMT, active motor threshold; 1mV, intensity of magnetic stimulus adjusted to evoke 1 mV peak to peak MEP; ICI, intracortical inhibition; SLAI, short-latency afferent inhibition. For the threshold values, "%" are related to the maximal stimulator output (MSO); for SICI, ICF and SLAI values, "%" are related to the control MEP amplitude.

EXPERIMENT 2

Repeated ANOVA performed on SLAI measures revealed significant main effects of INTENSITY ($F = 2.14$; $p = 0.036$) and ISI ($F = 2.64$; $p = 0.04$), but no a significant cTBS effect (**Figure 5**). All the interactions were not significant. These data indicate that the cTBS effects observed in Experiment 1 were specific for the AD patients and did not depend on a different basal level of SLAI.

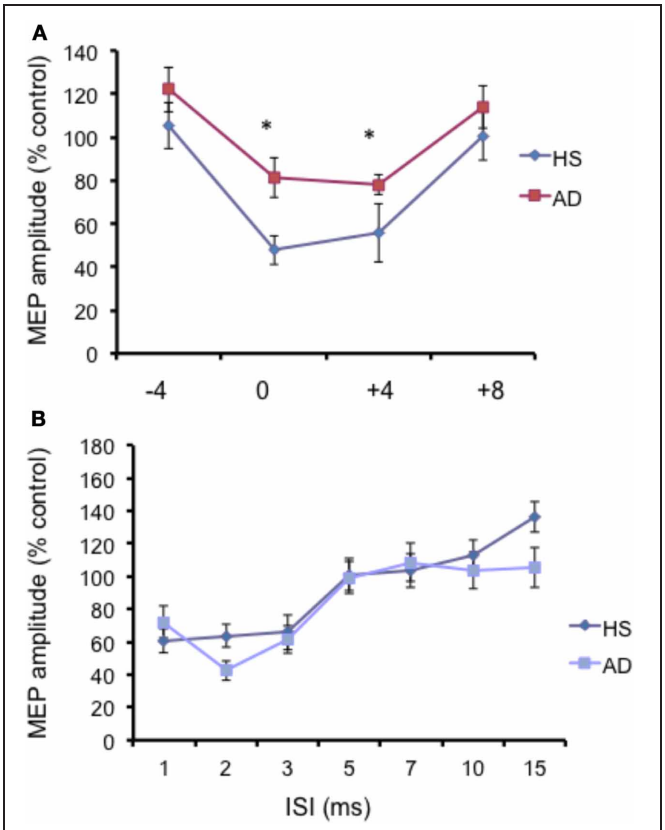

FIGURE 2 | (A) Short-latency afferent inhibition (SLAI) at different interstimulus intervals in AD patients (open squares) and control (black diamonds) subjects. The interval between median nerve stimulation and cortical stimuli was corrected for the latency of the N20 component of the somatosensory evoked potential in each subject (see text). The size of MEPs is expressed as a percentage of the MEP evoked by magnetic stimulation alone. **(B)** Short intracortical inhibition (SICI) and intracortical facilitation (ICF) at different interstimulus intervals in AD patients (open squares) and control subjects (black diamonds). The size of MEPs is expressed as a percentage of the MEP evoked by magnetic stimulation alone. Error bars indicate mean standard errors. *$p < 0.05$.

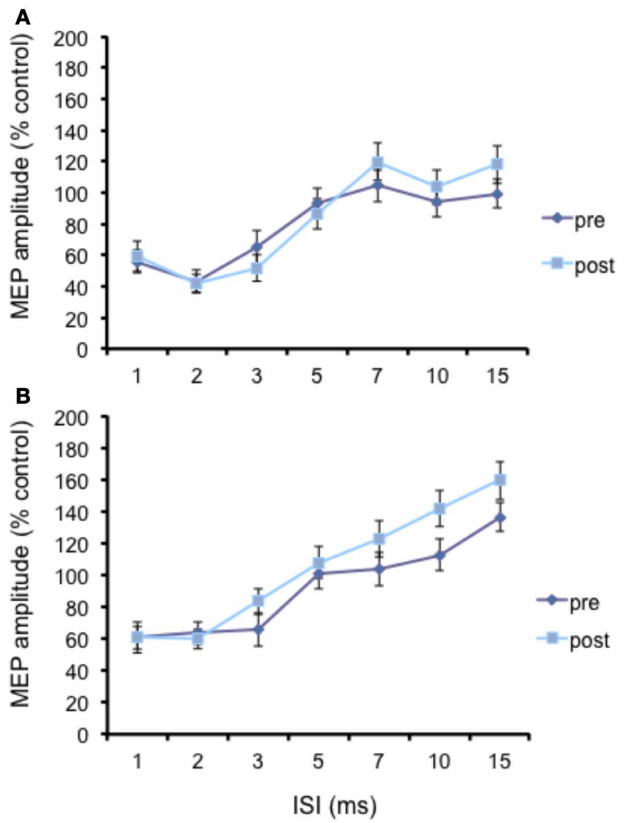

FIGURE 3 | Effects of cerebellar cTBS on SLAI (A) and SICI (B) in AD patients. Error bars indicate standard deviations. The size of MEPs is expressed as a percentage of the MEP evoked by magnetic stimulation alone. Error bars indicate mean standard errors.

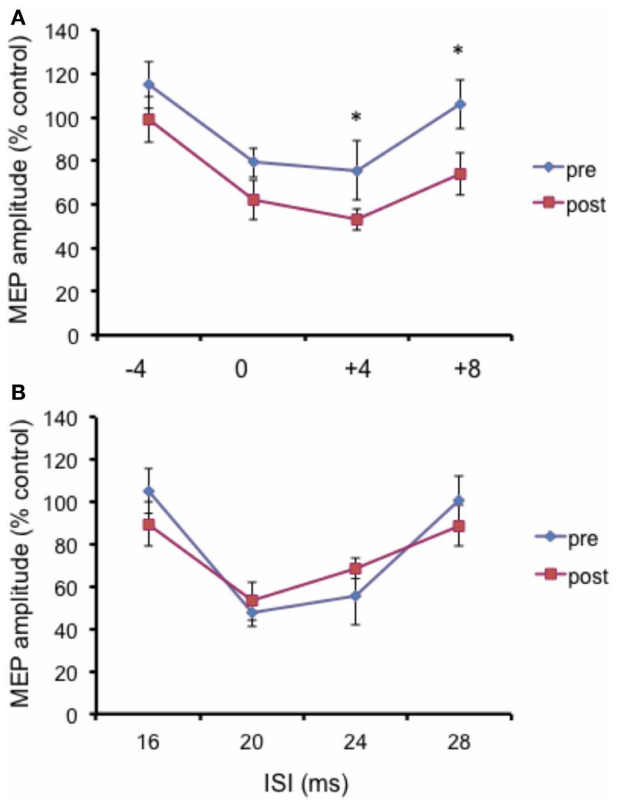

FIGURE 4 | Effects of cerebellar cTBS on SLAI (A) and SICI and ICF (B) in healthy subjects. Error bars indicate standard deviations. The size of MEPs is expressed as a percentage of the MEP evoked by magnetic stimulation alone. Error bars indicate mean standard errors. $^{*}p < 0.05$.

EXPERIMENT 3

Repeated ANOVA performed on SLAI measures revealed a significant main effect of ISI ($F = 4.04$; $p = 0.023$), but no effect for cTBS main factor and for the cTBS × ISI interaction (**Figure 6**).

DISCUSSION

The current results confirmed previous studies showing that SLAI of the motor cortex is significantly reduced in AD patients compared to age matched normal subjects (i.e., Di Lazzaro et al., 2002; Freitas et al., 2011). Notably, we found that such SLAI dis-inhibition is restored following a single session of cerebellar cTBS. Our results therefore seem to suggest that the activation of cerebello-thalamo-cortical pathway by means of cerebellar cTBS is able to modulate SLAI function in AD patients. Although SLAI is considered a hallmark of central cholinergic function that is thought to depend on the integrity of cortico-cortical inhibitory circuits (Tokimura et al., 2000), its current interpretation is still debated. Acetylcholine is thought to be involved in modulation of intracortical circuits mediated by groups of GABAergic interneurons, rather than directly acting on pyramidal cells (Di Lazzaro et al., 2002, 2004). At this regard, Di Lazzaro and co-workers (Di Lazzaro et al., 2005) demonstrated that different types of benzodiazepines such as diazepam and lorazepam resulted in distinct effects on both SICI and SLAI. In particular diazepam increased both SLAI and SICI, while lorazepam reduced SLAI but increased SICI, suggesting that the interactions between cholinergic and GABAergic circuits may require the activation of a variety of different receptor subtypes. Moreover we recently showed that dopamine also plays a critical role in modulating cortical cholinergic activity, presumably interacting with such GABAergic intracortical circuits (Martorana et al., 2009). SLAI starts only a few milliseconds after the arrival of the somatosensory input at the cortex, and implies a relatively direct pathway from sensory input to motor output (Tokimura et al., 2000). The dorsomedial nucleus and intralaminar nuclei (thalamic paramedian structures) are under control of excitatory projections from pontomesencephalic cholinergic neurons (peduncolopontine and laterodorsal tegmental cholinergic nuclei) through muscarinic receptors (Jones, 2003; Steriade, 2004). These pontomesencephalic cholinergic neurons have no direct projection to the cortex but they do have a prominent indirect effect on the functional state (and excitability) of cortical neurons as they activate thalamocortical neurons (Steriade, 2004). Consistently with these premises, Oliviero et al. (2005) reported that, after a thalamic stroke that had destroyed the dorsomedian and intralaminar nuclei, a patient showed a selective attenuation of the SLAI in the ipsilesional M1.

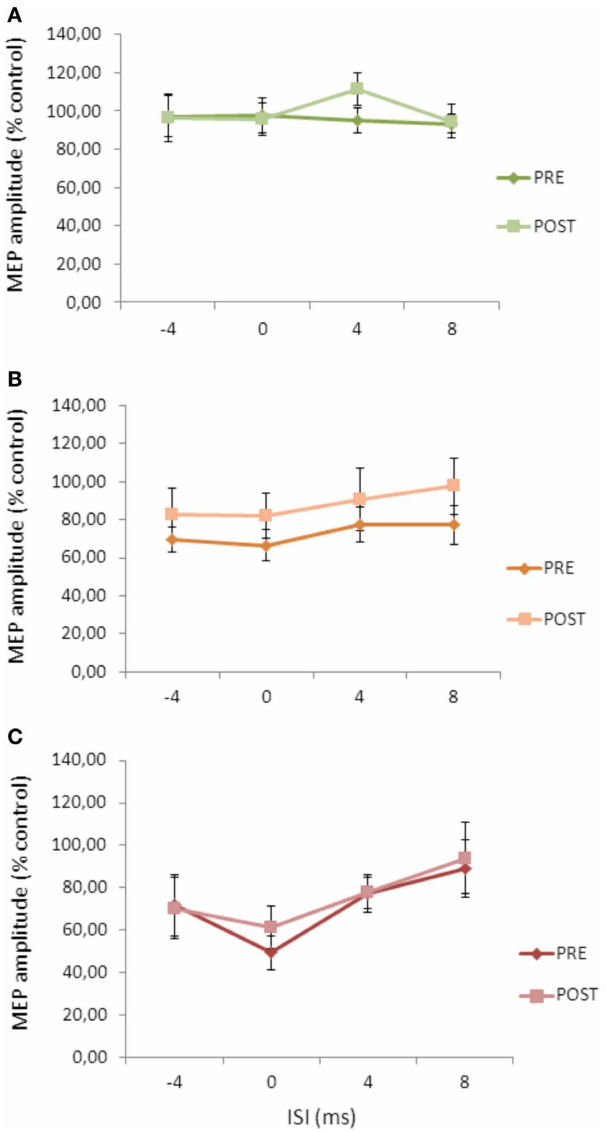

FIGURE 5 | Effects of cerebellar cTBS on SLAI applied with different intensities of peripheral nerve stimulation in healthy subjects (A) = 100%; (B) = 200%; (C) = 300% of the sensory threshold. Error bars indicate standard deviations. The size of MEPs is expressed as a percentage of the MEP evoked by magnetic stimulation alone. Error bars indicate mean standard errors.

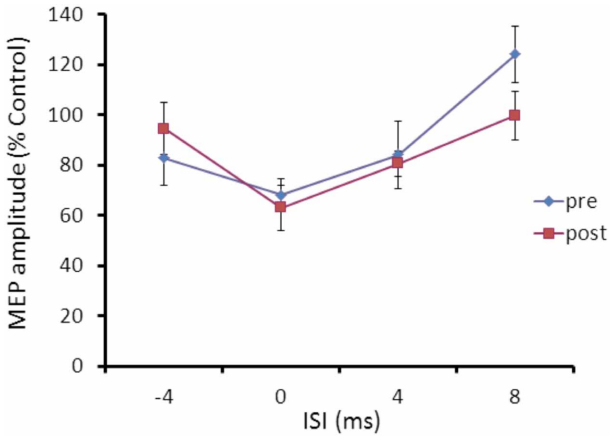

FIGURE 6 | Effects of occipital cTBS on SLAI in AD patients. Error bars indicate standard deviations. The size of MEPs is expressed as a percentage of the MEP evoked by magnetic stimulation alone. Error bars indicate mean standard errors.

Moreover, cerebellar cTBS is known to modulate the activation of cerebello-thalamo-cortical circuits (Koch et al., 2008, 2009). A recent PET study performed in order to detect the effects induced by cerebellar cTBS revealed that metabolic changes occur not only in the cerebellar cortex below the stimulated portion of the cortex but also in the deep cerebellar nuclei reflecting the activation of a pathway connecting these regions and likely projecting to the thalamus (Brusa et al., 2012).

Therefore, one possibility is that cerebellar cTBS could have increased SLAI efficacy by modulating the gating of the afferent input at the level of the thalamic nuclei. In fact, the physiology of the cerebellar-thalamo-cortical pathway activated by magnetic stimulation has been recently clarified. It has been proposed that cerebellar TMS activates the Purkinje cells of the superior cerebellum; such activation results in an inhibition of the dentate nucleus, which is known to exert a background tonic facilitatory drive onto the contralateral motor cortex (M1) through synaptic relay in the ventral lateral thalamus (Dum and Strick, 2003). This in turn leads to an inhibition of the contralateral M1, due to a reduction in dentato-thalamo-cortical facilitatory drive (Ugawa et al., 1994, 1997; Pinto and Chen, 2001; Daskalakis et al., 2004). Although apparently SLAI and the cerebello-thalamo-cortical pathway activated by cerebellar TMS act on different thalamic nuclei, it has to be considered that intrathalamic connections have been recently described between thalamic nuclei such as the ventroposterior and the medial posterior nucleus (Crabtree et al., 1998). At this regard, one could argue that the thalamus could be a plausible site for the interaction occurring between these two pathways. In alternative, it is possible that the effects that we observe could depend on an interaction occurring at the level of the primary motor cortex. Here, complex interactions of intracortical circuits that mediate both the afferent volleys from the thalamus could be responsible for the observed effects induced by cerebellar cTBS on SLAI in AD patients.

Another final possibility is that the observed results could depend on the modulation of cerebellar activity itself, not involving necessarily interconnected pathways. Notably, the effects of cerebellar cTBS were evident at later delays (ISIs = +4 and +8 ms). It has been proposed that sensory signals to the motor cortex arriving at later delays around 25 ms (corresponding approximately to the ISI = 4 ms in the current study) are transmitted by a longer polysynaptic pathway which includes the cerebellum. This view is supported by the literature showing that the cerebellum receives sensory information (Dean et al., 2010), and that patients with cerebellar degeneration have abnormal sensory-motor integration (Tamburin et al., 2003). Accordingly, recent studies performed in healthy subjects showed that both transcranial direct stimulation (TDCS) and cTBS applied over

the cerebellum interfered with the long lasting effects induced by protocols of paired associative stimulation (PAS) using an electrical stimulus to the median nerve with a TMS pulse given 25 ms later to the motor cortex (Hamada et al., 2012a,b; Popa et al., 2013). This would explain why in the current study the interaction of cerebellar stimulation with sensory-motor integration is evident only for those stimuli that have longer delays. At this regard, a large limitation of the current study is that we did not investigate to which extent the observed SLAI modulation was eventually associated by changes in cerebello-thalamo-cortical inhibition (CBI). Thus, it remains to be clarified if there are any physiological relationships among CBI and SLAI circuits in AD patients. Moreover we did not even assess changes in MEP sizes after cerebellar cTBS because our main aim was to study modulation of cholinergic circuits. It has to be acknowledged that this lack of systematic investigation of test MEP sizes as well as conditioning stimulus intensities for SAI, SICI, and ICF limits the scientific quality of this paper.

It is important to notice that we did not find the expected modulation of some intracortical circuits such as SICI in the primary motor cortex that we previously described following cerebellar theta burst stimulation (TBS) (Koch et al., 2008). This could possibly depend on the older age of the healthy controls. Further experiments would be necessary to better clarify the interplay between cerebellar cTBS and cortical excitability. Moreover, we did not find any difference for SICI and ICF measurements at baseline between the two groups. This is consistent with the data presented in a recent review that considers all the studies evaluating SICI in AD (Freitas et al., 2011): some reductions of SICI to paired-pulse TMS were found by some investigators, but most (7 of 11) studies did not find differences in SICI between AD patients and controls.

Indeed, the effects of cerebellar cTBS were evident only in AD patients and not in healthy age matched controls. It could well be that we detected any change in the healthy controls because SLAI inhibition reached a floor level or, in alternative that such modulation would occur only when a deficient cholinergic innervation coexists such as in AD patients.

As expected, we found lower RMT in the AD patients group. It is therefore likely that the I-wave component of the test MEP sizes (Hamada et al., 2012a,b) would be different between AD patients and healthy controls. This different amount of I-waves could have been involved in determining the amount of SLAI and hence affected the present results. Besides, the conditioning stimulus intensity of SICI and ICF would also be different between the two groups, and therefore this could be another potential confounding factor.

Whatever the neurophysiological mechanisms underlying these complex interactions, the current data suggest that cerebellar magnetic stimulation could be effective in modulating central cholinergic activity in AD patients. Further studies aimed to investigate systematically the impact of this protocol on different cognitive functions would be important to further understand the potential clinical importance of the current findings.

ACKNOWLEDGMENTS

This work was supported by a grant of the Italian Ministry of Health **RF08.18** "Markers of cortico-cerebellar dysfunction associated with cognitive impairment in brain aging" to Giacomo Koch.

REFERENCES

Brusa, L., Ceravolo, R., Kiferle, L., Monteleone, F., Iani, C., Schillaci, O., et al. (2012). Metabolic changes induced by theta burst stimulation of the cerebellum in dyskinetic Parkinson's disease patients. *Parkinsonism Relat. Disord.* 18, 59–62.

Carlesimo, G. A., Caltagirone, C., and Gainotti, G. (1996). The Mental Deterioration Battery: normative data, diagnostic reliability and qualitative analyses of cognitive impairment. The Group for the Standardization of the Mental Deterioration Battery. *Eur. Neurol.* 36, 378–384.

Crabtree, J. W., Collingridge, G. L., and Isaac, J. T. (1998). A new intrathalamic pathway linking modality-related nuclei in the dorsal thalamus. *Nat. Neurosci.* 1, 389–394.

D'Angelo, E., and Casali, S. (2012). Seeking a unified framework for cerebellar function and dysfunction: from circuit operations to cognition. *Front. Neural Circuits* 6:116. doi: 10.3389/fncir.2012.00116

Daskalakis, Z. J., Paradiso, G. O., Christensen, B. K., Fitzgerald, P. B., Gunraj, C., and Chen, R. (2004). Exploring the connectivity between the cerebellum and motor cortex in humans. *J. Physiol.* 557, 689–700.

Dean, P., Porrill, J., Ekerot, C. F., and Jorntell, H. (2010). The cerebellar microcircuit as an adaptive filter: experimental and computational evidence. *Nat. Rev. Neurosci.* 11, 30–43.

Del Olmo, M. F., Cheeran, B., Koch, G., and Rothwell, J. C. (2007). Role of the cerebellum in externally paced rhythmic finger movements. *J. Neurophysiol.* 9, 145–152.

Di Lazzaro, V., Oliviero, A., Pilato, F., Saturno, E., Dileone, M., and Tonali, P. A. (2004). Motor cortex hyperexcitability to transcranial magnetic stimulation in Alzheimer's disease. *J. Neurol. Neurosurg. Psychiatry* 75, 555–559.

Di Lazzaro, V., Oliviero, A., Tonali, P. A., Marra, C., Daniele, A., Profice, P., et al. (2002). Noninvasive *in vivo* assessment of cholinergic cortical circuits in AD using transcranial magnetic stimulation. *Neurology* 59, 392–397.

Di Lazzaro, V., Pilato, F., Dileone, M., Tonali, P. A., and Ziemann, U. (2005). Dissociated effects of diazepam and lorazepam on short-latency afferent inhibition. *J. Physiol.* 569, 315–323.

Dum, R. P., and Strick, P. L. (2003). An unfolded map of the cerebellar dentate nucleus and its projections to the cerebral cortex. *J. Neurophysiol.* 89, 634–639.

Finkelstein, Y., Wolff, M., and Biegon, A. (1988). Brain acetylcholinesterase after parathion poisoning: a comparative quantitative histochemical analysis post-mortem. *Toxicology* 49, 165–169.

Freitas, C., Mondragon-Llorca, H., and Pascual-Leone, A. (2011). Noninvasive brain stimulation in Alzheimer's disease: systematic review and perspectives for the future. *Exp. Gerontol.* 46, 611–627.

Hamada, M., Murase, N., Hasan, A., Balaratnam, M., and Rothwell, J. C. (2012a). The role of interneuron networks in driving human motor cortical plasticity. *Cereb. Cortex*. doi: 10.1093/cercor/bhs147. [Epub ahead of print].

Hamada, M., Strigaro, G., Murase, N., Sadnicka, A., Galea, J. M., Edwards, M. J., et al. (2012b). Cerebellar modulation of human associative plasticity. *J. Physiol.* 1, 2365–2374.

Huang, Y. Z., Edwards, M. J., Rounis, E., Bhatia, K. P., and Rothwell, J. C. (2005). Theta burst stimulation of the human motor cortex. *Neuron* 45, 201–206.

Huang, Y. Z., and Rothwell, J. C. (2004). The effect of short-duration bursts of high-frequency, low-intensity transcranial magnetic stimulation on the human motor cortex. *Clin. Neurophysiol.* 115, 1069–1075.

Jones, B. E. (2003). Arousal systems. *Front. Biosci.* 8, 438–451.

Koch, G., Brusa, L., Carrillo, F., Lo Gerfo, E., Torriero, S., Oliveri, M., et al. (2009). Cerebellar magnetic stimulation decreases levodopa-induced dyskinesias in Parkinson disease. *Neurology* 73, 113–119.

Koch, G., Mori, F., Marconi, B., Codecà, C., Pecchioli, C., Salerno, S., et al. (2008). Changes in intracortical circuits of the human motor cortex following theta burst stimulation of the lateral cerebellum. *Clin. Neurophysiol.* 119, 2559–2569.

Kujirai, T., Caramia, M. D., Rothwell, J. C., Day, B. L., Thompson, P. D., Ferbert, A., et al. (1993). Corticocortical inhibition in human motor cortex. *J. Physiol.* 471, 501–519.

Martorana, A., Mori, F., Esposito, Z., Kusayanagi, H., Monteleone, F., Codecà, C., et al. (2009). Dopamine modulates cholinergic cortical excitability in Alzheimer's disease patients. *Neuropsychopharmacology* 34, 2323–2328.

Okamura, N., Funaki, Y., Tashiro, M., Kato, M., Ishikawa, Y., Maruyama, M., et al. (2008). *In vivo* visualization of donepezil binding in the brain of patients with Alzheimer's disease. *Br. J. Clin. Pharmacol.* 65, 472–479.

Oliviero, A., Leon, A. M., Holler, I., Vila, J. F., Siebner, H. R., Della Marca, G., et al. (2005). Reduced sensorimotor inhibition in the ipsilesional motor cortex in a patient with chronic stroke of the paramedian thalamus. *Clin. Neurophysiol.* 116, 2592–2598.

Pinto, A. D., and Chen, R. (2001). Suppression of the motor cortex by magnetic stimulation of the cerebellum. *Exp. Brain Res.* 140, 505–510.

Popa, T., Velayudhan, B., Hubsch, C., Pradeep, S., Roze, E., Vidailhet, M., et al. (2013). Cerebellar processing of sensory inputs primes motor cortex plasticity. *Cereb. Cortex* 23, 305–314.

Romei, V., Gross, J., and Thut, G. (2012). Sounds reset rhythms of visual cortex and corresponding human visual perception. *Curr. Biol.* 8, 807–813.

Rossini, P. M., Barker, A. T., Berardelli, A., Caramia, M. D., Caruso, G., Cracco, R. Q., et al. (1994). Non-invasive electrical and magnetic stimulation of the brain, spinal cord and roots: basic principles and procedures for routine clinical application. Report of an IFCN committee. *Electroencephalogr. Clin. Neurophysiol.* 91, 79–92.

Steriade, M. (2004). Acetylcholine systems and rhythmic activities during the waking–sleep cycle. *Prog. Brain Res.* 145, 179–196.

Tamburin, S., Fiaschi, A., Andreoli, A., Forgione, A., Manganotti, P., and Zanette, G. (2003). Abnormal cutaneomotor integration in patients with cerebellar syndromes: a transcranial magnetic stimulation study. *Clin. Neurophysiol.* 114, 643–651.

Thomann, P. A., Schlafer, C., Seidl, U., Santos, V. D., Essig, M., and Schroder, J. (2008). The cerebellum in mild cognitive impairment and Alzheimer's disease– a structural MRI study. *J. Psychiatr. Res.* 42, 1198–1202.

Tokimura, H., Di Lazzaro, V., Tokimura, Y., Oliviero, A., Profice, P., Insola, A., et al. (2000). Short latency inhibition of human hand motor cortex by somatosensory input from the hand. *J. Physiol.* 523, 503–513.

Turner, J. R., Ortinski, P. I., Sherrard, R. M., and Kellar, K. J. (2011). Cerebellar nicotinic cholinergic receptors are intrinsic to the cerebellum: implications for diverse functional roles. *Cerebellum* 10, 748–757.

Ugawa, Y., Hanajima, R., and Kanazawa, I. (1994). Motor cortex inhibition in patients with ataxia. *Electroencephalogr. Clin. Neurophysiol.* 93, 225–229.

Ugawa, Y., Uesaka, Y., Terao, Y., Hanajima, R., and Kanazawa, I. (1995). Magnetic stimulation over the cerebellum in humans. *Ann. Neurol.* 37, 703–713.

Ugawa, Y., Terao, Y., Hanajima, R., Sakai, K., Furubayashi, T., Machii, K., et al. (1997). Magnetic stimulation over the cerebellum in patients with ataxia. *Electroencephalogr. Clin. Neurophysiol.* 104, 453–458.

Varma, A. R., Snowden, J. S., Lloyd, J. J., Talbot, P. R., Mann, D. M., and Neary, D. (1999). Evaluation of the NINCDS-ADRDA criteria in the differentiation of Alzheimer's disease and frontotemporal dementia. *J. Neurol. Neurosurg. Psychiatry* 66, 84–88.

Ziemann, U., Lonnecker, S., Steinhoff, B. J., and Paulus, W. (1996). Effects of antiepileptic drugs on motor cortex excitability in humans: a transcranial magnetic stimulation study. *Ann. Neurol.* 40, 367–378.

Conflict of Interest Statement: The authors declare that the research was conducted in the absence of any commercial or financial relationships that could be construed as a potential conflict of interest.

Received: 13 December 2012; accepted: 25 January 2013; published online: 19 February 2013.

*Citation: Di Lorenzo F, Martorana A, Ponzo V, Bonnì S, D'Angelo E, Caltagirone C and Koch G (2013) Cerebellar theta burst stimulation modulates short latency afferent inhibition in Alzheimer's disease patients. Front. Ag. Neurosci. **5**:2. doi: 10.3389/fnagi.2013.00002*

Copyright © 2013 Di Lorenzo, Martorana, Ponzo, Bonnì, D'Angelo, Caltagirone and Koch. This is an open-access article distributed under the terms of the Creative Commons Attribution License, which permits use, distribution and reproduction in other forums, provided the original authors and source are credited and subject to any copyright notices concerning any third-party graphics etc.

frontiers in Aging Neuroscience

ORIGINAL RESEARCH
published: 29 February 2016
doi: 10.3389/fnagi.2016.00035

Progranulin Mutations Affects Brain Oscillatory Activity in Fronto-Temporal Dementia

Davide V. Moretti[1], Luisa Benussi[2], Silvia Fostinelli[2], Miriam Ciani[2], Giuliano Binetti[3] and Roberta Ghidoni[2]*

[1] Alzheimer Rehabilitation Research Unit, IRCCS Istituto Centro San Giovanni di Dio Fatebenefratelli, Brescia, Italy, [2] Molecular Markers Laboratory, IRCCS Istituto Centro San Giovanni di Dio Fatebenefratelli, Brescia, Italy, [3] Memory Clinic, IRCCS Istituto Centro San Giovanni di Dio Fatebenefratelli, Brescia, Italy

Background: Mild cognitive impairment (MCI) is a clinical stage indicating a prodromal phase of dementia. This practical concept could be used also for fronto-temporal dementia (FTD). Progranulin (PGRN) has been recently recognized as a useful diagnostic biomarker for fronto-temporal lobe degeneration (FTLD) due to *GRN* null mutations. Electroencephalography (EEG) is a reliable tool in detecting brain networks changes. The working hypothesis of the present study is that EEG oscillations could detect different modifications among FTLD stages (FTD-MCI versus overt FTD) as well as differences between *GRN* mutation carriers versus non-carriers in patients with overt FTD.

Materials and Methods: EEG in all patients and PGRN dosage in patients with a clear FTD were detected. The cognitive state has been investigated through mini mental state examination (MMSE).

Results: MCI-FTD showed a significant lower spectral power in both alpha and theta oscillations as compared to overt FTD. *GRN* mutations carriers affected by FTLD show an increase in high alpha and decrease in theta oscillations as compared to non-carriers.

Conclusion: EEG frequency rhythms are sensible to different stage of FTD and could detect changes in brain oscillatory activity affected by *GRN* mutations.

Keywords: EEG, FTD, PGRN positive, PGRN negative, MCI FTD

OPEN ACCESS

Edited by:
Jean Mariani, Université Pierre et Marie Curie, France

Reviewed by:
Eugenia Rota, Ospedale Guglielmo da Saliceto di Piacenza, Italy
Laura Lorenzo-López, University of A Coruña, Spain

****Correspondence:***
Davide V. Moretti
davide.moretti@afar.it;
dmoretti@fatebenefratelli.eu

Received: *05 November 2015*
Accepted: *10 February 2016*
Published: *29 February 2016*

Citation:
Moretti DV, Benussi L, Fostinelli S, Ciani M, Binetti G and Ghidoni R (2016) Progranulin Mutations Affects Brain Oscillatory Activity in Fronto-Temporal Dementia. Front. Aging Neurosci. 8:35. doi: 10.3389/fnagi.2016.00035

INTRODUCTION

Fronto-temporal lobar degeneration (FTLD) is a neurodegenerative disorder characterized by behavioral abnormalities, language impairment, and deficits in executive functions as the most typical clinical features (Seelaar et al., 2011). FTLD is clinically heterogeneous, as different clinical variants have been carefully described. On the basis of presenting clinical symptoms, behavioural variant FTD (bvFTD), agrammatic variant of Primary Progressive Aphasia (avPPA), and semantic variant of PPA (svPPA) represent the most common phenotypes (Benussi et al., 2015). Each one presents specific neuroimaging hallmarks; bvFTD is characterized by mesial and dorsolateral frontal damage, prevalent on the right side, avPPA is defined by involvement of Broca's area and left insula, whilst svPPA usually presents left rostral temporal involvement (Lashley et al., 2015).

Moreover, FTD is chacterized also by early stages, usually named mild cognitive impairment (MCI), that are still not completely characterized. Unfortunately, the diagnosis of FTD can be

difficult because of its insidious and gradual onset and can also be misdiagnosed as Alzheimer's disease (AD) (Rankin et al., 2005; Walker et al., 2005).

The discovery of mutations in *GRN* as a genetic determinant for FTLD resulted in the rapid identification of a large number of families carrying *GRN* mutations, inherited in an autosomal dominant pattern. At present, 77 different mutations in more than 240 unrelated families have been described (Ghidoni et al., 2012a). Mutations in *GRN* have been associated with a broad spectrum of clinical phenotypic variability (Benussi et al., 2008; Rohrer et al., 2010a,b).

GRN null mutations cause protein haploinsufficiency, leading to a significant decrease in progranulin (PGRN) levels that can be detected in plasma, serum, and cerebrospinal fluid of mutation carriers (Ghidoni et al., 2008, 2012b; Finch et al., 2009; Sleegers et al., 2009). It has been reported that PGRN promotes neuronal survival and neurite outgrowth in cultured neurons (Van Damme et al., 2008) and enhances neuronal survival under stress conditions (Kessenbrock et al., 2008). Data from GRN knockout experimental models suggest that PGRN deficiency leads to reduced synaptic connectivity and impaired plasticity, which may be contributing factors to FTLD pathology in human patients (Tapia et al., 2011; Petkau et al., 2012). Brain activity could be widely and variously affected in FTLD patients with *GRN* mutations. Neuroimaging studies have shown that the topography of brain atrophy is frequently asymmetric, and predominantly involves the frontal, temporal, and parietal cortex (Whitwell et al., 2012). Nevertheless, a recent study (Caroppo et al., 2014) have demonstrated that a diffuse and bilateral white matter involvement is common in patients with *GRN* mutations. The presence of white matter lesions is not surprising since expression of PGRN, not only in neurons but also in activated microglia, in astrocytes and oligodendroglia, has been previously ascertained (Ahmed et al., 2010). As a consequence, cortical and subcortical loop are both implicated in the disruption of intrinsic brain networks in *GRN* mutations carriers.

Electroencephalography is a reliable and non-invasive tool for the study of brain networks in dementia. Relationship of the brain oscillations with intrinsic brain network like default mode network (DMN) have been extensively studied (Nishida et al., 2015). In particular, alpha and theta field potentials are deeply involved in tuning the large and local scale networks interactions in cognitive and psychiatric illnesses (Koenig et al., 2001; Tenke et al., 2011). Previous EEG studies have demonstrated peculiar modifications in brain oscillations in patients with MCI due to AD as compared to non-AD converters (Moretti et al., 2011a). Moreover, these changes in brain oscillations have been correlated with temporo-parietal and hippocampal atrophy (Moretti et al., 2007a, 2008a, 2009a,b, 2011a, 2012) as well as to white matter lesions (Moretti et al., 2007b, 2008b). In the present explorative study, we test the working hypothesis that changes in EEG oscillations could specifically detect different stages of FTLD, namely MCI-FTD versus overt FTD, as well as differences between *GRN* mutation carriers versus non- carriers. The search for new biomarkers is of great importance for an early diagnosis and for monitoring the effectiveness of new therapies.

MATERIALS AND METHODS

Subjects

Diagnostic Criteria

Clinical diagnosis of FTLD and LBD were made according to international guidelines (McKeith et al., 1996; Neary et al., 1998) as well as more recent revised criteria for the diagnosis of frontotemporal dementia (Gorno-Tempini et al., 2011; Rascovsky et al., 2011). MCI-FTD patients were recruited with mini mental state examination (MMSE) score higher than 24/30. Eleven patients with MCI-FTD, eight FTLD patients carrying GRN mutations, and 20 FTLD patients not carrying *GRN* mutations were included in the present study (**Table 1**). The diagnosis of the enrolled subjects is reported in **Table 2**. All patients underwent a series of standardized diagnostic and severity instruments, including: the MMSE (Folstein et al., 1975), the Clinical Dementia Rating Scale (CDRS; Hughes et al., 1982), the Hachinski Ischemic Scale (HIS; Rosen et al., 1980), the Instrumental and Basic Activities of Daily Living (IADL, BADL; Lawton and Brody, 1969) and a comprehensive neuropsychological battery (Lezak et al., 2004). The patients were recruited only with apparently primary cognitive deficits excluding psychic comorbid conditions like anxiety, depression, psychosis etc., or physical comorbidities like hypothiroidism, uncontrolled diabetes, vitamin B12, and folate deficiency, uncontrolled heart disease or hypertension, drug addiction, or alcohol abuse. Moreover, none of the patients was taking any drugs that might affect the EEG, namely psychoactive drugs, including acetylcholinesterase inhibitors or other drugs enhancing brain cognitive functions. In addition, patients underwent diagnostic neuroimaging procedures (magnetic resonance imaging, MRI), and laboratory testing to rule out other causes of cognitive impairment. In particular, MRI was able to exclude patients with major cerebrovascular diseases or other diseases (like tumors) that might influence EEG frequency rhythms. On the whole, 13 patients with primary progressive non-fluent aphasia (PNFA), 12 patients with the behavioral variant of FTD (FTD-bv), one patient with the semantic variant of FTD (FTD-sv), and one patient with Lewy Body Disease (LBD) were recruited. Demographic and clinical features of the sample in study are reported in **Table 2**. All experimental protocols had been approved by the local ethics committee of Scientific Institute for Research and Care (IRCCS) of Alzheimer's and psychiatric diseases 'Fatebenefratelli' in Brescia, Italy (Protocol numbers: 26/2014; 50/2015). Written informed consent was obtained from all participants or their caregivers, according to the Code of Ethics of the World Medical Association (Declaration of Helsinki).

EEG Recordings

The EEG activity was recorded continuously from 19 sites by using electrodes set in an elastic cap (Electro-Cap International,

TABLE 1 | ANOVA results of demographic variable (age, education) MMSE score, and of PGRN dosage, high alpha, and theta EEG power of the study sample.

	GRN positive	GRN negative	MCI FTD	*p*
Number of subjects	8	20	11	–
Age, years	65,7 ± 9,3	67,2 ± 9,2	64,8 ± 4,2	0,07
Education, years	7,4 ± 2,8	7,6 ± 4,2	7,6 ± 3,1	0,9
MMSE	21,3 ± 5,6	20,5 ± 4,3	26,2 ± 5,1	0,11
PGRN dosage	33,6 ± 18,5	142,4 ± 72,1	n.a.	0.001
High alpha EEG power	15,2 ± 3,5	10,6 ± 3,2	8,7 ± 2,8	0,003
Theta EEG power	13,8 ± 5,1	21,1 ± 2,1	4,3 ± 8,3	0,002

TABLE 2 | Clinical diagnosis of the patients recuited in the study.

DIAGNOSIS	PGRN positive	PGRN negative
FTD PPA	4	9
FTDbv	2	10
FTD	1	1
LBD	1	

FTD, fronto-temporale dementia; PPA, primary progressive aphasia; bv, behavioral variant; LBD, Lewy body dementia

Inc. Eaton, OH, USA) and positioned according to the 10–20 international system (Fp1, Fp2, F7, F3, Fz, F4, F8, T3, C3, Cz, C4, T4, T5, P3, Pz, P4, T6, O1, and O2). All recordings were obtained in the morning with subjects resting comfortably. The patients were instructed to sit with closed eyes and relax and vigilance was continuously monitored in order to avoid drowsiness by an operator. The ground electrode was placed in front of Fz. The left and right mastoids served as the reference points for all electrodes. The recordings were used off-line to re-reference the scalp recordings to the common average. Re-referencing was done prior to the EEG artifact detection and analysis. Data were recorded with a band-pass filter of 0.3–70 Hz and digitized at a sampling rate of 250 Hz (BrainAmp, BrainProducts, Munich, Germany). Electrode-skin impedance was set below 5 kΩ. Horizontal and vertical eye movements were detected by electrooculogram (EOG). The recording lasted 5 min with the subjects' eyes closed. EEG data were then analyzed and fragmented off-line in consecutive epochs of 2 s with a frequency resolution of 0.5 Hz. The average number of epochs analyzed was 140, ranging from 130 to 150. The epochs with ocular, muscular, and other types of artifacts were discarded by two skilled electroencephalographists. The spectral power we obtained is an estimation of a spectrum collapsed all over the scalp electrodes. In this way, the eventual contribution of the muscular or other artifacts is strongly reduced. Moreover, two skilled electroencephalographists checked separately the EEG traces (Moretti et al., 2003, 2004).

Analysis of Frequency Bands

A digital FFT-based power spectrum analysis (Welch technique, Hanning windowing function, no phase shift) computed the power density of EEG rhythms (ranging from 2 to 45 Hz) with a 0.5 Hz frequency resolution. The frequency bands range was computed on fixed limit as follows: (1) delta, 1–3 Hz; (2) theta, 4–7 Hz; (3) alpha 1 ore low alpha, 8–10,5 Hz; (4) alpha 2 ore high alpha, 10.5–14 Hz. These frequencies were computed on the power spectra averaged across all recording electrodes. This "collapsed spectrum method," being a normalized scalp spectrum, determined a global field power (Moretti et al., 2003, 2004).

Genetic Analysis

GRN gene was analyzed in patients with FTLD and LBD by direct sequencing of all exonic and flanking intronic regions as previously described (Benussi et al., 2008). Plasma PGRN levels were measured in duplicate using an ELISA kit (Human PGRN ELISA Kit, AdipoGen Inc., Seoul, Korea) as previously reported (Ghidoni et al., 2012b). *GRN* positive carriers belongs to different families. This choice has been made to avoid that EEG patterns could be due to familial relationships. **Tables 2** and **3** shows the clinical diagnosis and related genetic mutations of *GRN* positive carriers.

Statistical Analysis

One-way analysis of variance (ANOVA) has been performed to compute the differences between groups (independent variables) in sociodemographic, MMSE score, PGRN dosage, and EEG oscillations (dependent variables) and neuropsychological tests. Age, education, and MMSE score have been used as covariates in ANOVA of brain rhythms to avoid confounding factors.

RESULTS

Table 1 shows ANOVA significant results. As expected, the PGRN dosage was significantly different, with an impressive decrease in *GRN* null mutation carrier patients [$F(19,77)$, df = 1, $p < 0.001$], confirming previous results (Ghidoni et al., 2012b). As about the EEG rhythms, results show: 1) a significant increase of high alpha power in *GRN* positive mutations carriers [$F(4,22)$, df = 2, $p = 0.003$]; (2) a significant increase of theta power in *GRN* negative patients [$F(3,14)$, df = 2, $p = 0.002$].

ANOVA analysis showed a decrease of the theta and alpha spectral power in MCI-FTD as compared to both PGRN positive

TABLE 3 | Genetic mutations identified in the GRN mutations carriers group and related clinical diagnosis.

	PGRN identified mutations	Diagnosis
1	PGRN Leu271LeufsX10	FTDsv
2	PGRN Leu271LeufsX10 (g.1977_1980delCACT)	FTD-PPA
3	PGRN Leu271LeufsX10	FTD-PPA
4	PGRN Leu271LeufsX10	FTD-PPA
5	PGRN Thr276SerfsX7	FTD-PPA
6	PGRN Leu271LeufsX10	FTDbv
7	PGRN Leu271LeufsX10	FTDbv
8	PGRN Leu 271LeufsX10	LBD

FTDsv, fronto-temporal dementia semantic variant; FTDbv, fronto-temporal dementia behavioral variant; FTD-PPA, fronto-temporal dementia primary progressive aphasia; LBD, Lewy, body disease.

and negative FTD patients. Given that the difference between PGRN positive and negative FTD patients were limited to theta and alpha power spectra, other frequency bands were not considered in the analysis.

The only significant results about neuropsychological battery were obtained in Token test, fluency for letters and working memory test. The results showed a general better performance in MCI-FTD patients as compared to both negative and positive PGRN mutations carriers ($p < 0.01$). No significant differences resulted between the comparison between negative and positive mutations PGRN carriers.

DISCUSSION

Our results show that FTLD patients carrying GRN mutations have different changes of EEG rhythms when compared to patients negative for GRN mutations. Specifically, GRN mutations carriers demonstrate an increment of the high alpha and a decreased of the theta power spectra. In this view, the presence of PGRN, which is a trophic factor for the nervous system, would allow a reorganization of the neural networks in a compensatory or adaptive way: accordingly, it has been reported that PGRN promotes neuronal survival and neurite outgrowth in cultured neurons (Van Damme et al., 2008) Likewise, under stress conditions it has been exhibited that PGRN improves neuronal survival (Kessenbrock et al., 2008). Data from GRN knockout experimental models suggest that PGRN deficiency leads to reduced synaptic connectivity and impaired plasticity, which may be contributing factors to FTLD pathology in human patients (Tapia et al., 2011; Xu et al., 2011). On the other hand, the white matter impairment in *GRN* mutation carriers has been directly proved in a recent study (Caroppo et al., 2014). In this study, four patients carrying *GRN* mutation were investigated and in all of them mostly confluent white matter lesions, affecting the periventricular subcortical white matter and U-fibers, were found mainly in the frontal and parietal lobes. This trophic activity could be shown by the maintenance of theta brain oscillations. Of note, fronto-parietal network are well recognized potential generators of theta oscillations (Beck et al., 2008; Ghetti et al., 2008; Whitwell et al., 2009), traveling on long pathway bundles of the white matter of fronto-parietal lobes and related subcortical structures like brainstem, and corpus callosum systems (Rohrer et al., 2010a,b). In particular, a recent study investigating the cortical generators of theta brain rhythm, through intracranial electrode recordings, have found that the higher percentage of cortical gated theta oscillations is situated in parieto-occipital regions (Raghavachari et al., 2006). So, a possible explanation of the spared maintenance of theta power in FTLD patients negative for GRN mutations as compared to GRN mutations carriers could be related to the relative integrity of parieto-occipital areas, embedded in the DMN.

Not surprisingly, in case of PGRN deficiency, the high alpha frequency spectral power increments. The alpha oscillation is the rhythm that mirrors the brain electrical signal of the parietal-occipital default system, profoundly connoted with higher cognitive abilities (Klimesch, 2012; Moretti, 2015a). Recent studies have shown that mutations in GRN are correlated with atrophy of the parietal lobes (Pickering-Brown et al., 2008; Seeley, 2008; Van Swieten and Heutink, 2008). In particular, a recent study investigating brain network connectivity with functional resting state MRI (Premi et al., 2014) utilizing three measures of both local and global connectivity (the regional homogeneity, the fractional amplitude of low frequency fluctuation and the degree centrality) has shown that parietal lobes are affected very early in *GRN* mutation carriers, so that the notion of fronto-parietal dementia for PGRN related disease should be considered. The parietal lobes are well-recognized core regions of the DMN (Sala-Llonch et al., 2015). Previous studies have demonstrated that high alpha rhythm synchronization (or increase) is a marker of loss of function in the default system, as exhibited in patients with prodromal or overt AD (Moretti et al., 2011b, 2013a,b, 2014a,b; Moretti, 2015b,c,d). The increase of high alpha oscillation in FTD patients, characterized by the loss of PGRN, confirms the reliability of this biomarker as a sign of DMN impairment. Moreover, the lack of PGRN is confirmed to be connected to the disruptive of the default system, determining real reverberations on cognitive capacity.

As expected, MCI-FTD have better cognitive performance, especially in frontal function assessment tests, as compare to overt FTD patients both carriers and non-carriers of GRN mutation. Moreover, in MCI-FTD the lower spectral power of theta and alpha power could be explained with an initial stage of the disease in which EEG changes are not still clear. A possible fingerprint of this stage could be the ratio between alpha and theta power spectra. The progression of disease could modify the EEG oscillations, as observed in overt FTD and more strongly in GRN mutation positive patients. Anyway, future studies will clarify if the presence or absence of PGRN mutations also in MCI-FTD could unveil more peculiar brain oscillations changes.

Study Limitations

It should be remarked a main limitation of the study that is the small sample size. We want to highlight that it should be considered the exploratory nature of the study. In this view, the choice criteria and statistical outcomes are sufficiently robust to be confident in the overall reliability of the results. In particular, the straight difference between MCI-FTD and overt FTD patients confirm that results are not due to mere random chance results. Despite this limitation, it provides important results for future studies. Up to date, for the first time in this paper, the particular aspect of a neurophysiological EEG biomarker in GRN mutation carriers and non-carriers have been investigated. Most important, the detection of a neuropshysiological biomarker, related to functional, and structural changes, could open new windows on integrated research strategy about the molecular nexopathies shedding light on the way through which different proteinopathies could differently affect neural networks (Warren et al., 2013). Finally, the finding of a new biomarker could be helpful for early diagnosis, to monitor the progression of disease and to test disease-modifying drugs. Anyway, we are well aware

of the need to correlate the results with a wider morphological and neuropathological characterization as well as with other risk factors.

CONCLUSION

GRN mutations affect brain oscillatory activity. A better understanding of the complexity of PGRN biology in the brain will help guide the development of PGRN-modulating therapies for neurodegenerative disease. Further studies with a larger number of subjects are needed to confirm the present results.

AUTHOR CONTRIBUTIONS

DVM: Substantial contributions to the conception or design of the work. LB: substantial contribution for the acquisition, analysis, or interpretation of data for the work; and drafting the work. SF: substantial contribution for the acquisition, analysis, or interpretation of data for the work; AND drafting the work. MC: substantial contribution for the acquisition, analysis, or interpretation of data for the work; and drafting the work. GB: substantial contribution for the acquisition, analysis, or interpretation of data for the work; and drafting the work. RG: substantial contribution for the acquisition, analysis, or interpretation of data for the work; and drafting the work.

ACKNOWLEDGMENT

This work was supported by grants from Ricerca Corrente, Italian Ministry of Health.

REFERENCES

Ahmed, Z., Sheng, H., Xu, Y. F., Lin, W. L., Innes, A. E., Gass, J., et al. (2010). Accelerated lipofuscinosis and ubiquitination in granulin knockout mice suggest a role for progranulin in successful aging. *Am. J. Pathol.* 177, 311–324. doi: 10.2353/ajpath.2010.090915

Beck, J., Rohrer, J. D., Campbell, T., Isaacs, A., Morrison, K. E., Goodall, E. F., et al. (2008). A distinct clinical, neuropsychological and radiological phenotype is associated with progranulin gene mutations in a large UK series. *Brain* 131, 706–720. doi: 10.1093/brain/awm320

Benussi, A., Padovani, A., and Borroni, B. (2015). Phenotypic heterogeneity of monogenic frontotemporal dementia. *Front. Aging Neurosci.* 7:171. doi: 10.3389/fnagi.2015.00171

Benussi, L., Binetti, G., Sina, E., Gigola, L., Bettecken, T., Meitinger, T., et al. (2008). A novel deletion in progranulin gene is associated with FTDP-17 and CBS. *Neurobiol. Aging* 29, 427–435. doi: 10.1016/j.neurobiolaging.2006.10.028

Caroppo, P., Le Ber, I., Camuzat, A., Clot, F., Naccache, L., Lamari, F., et al. (2014). Extensive white matter involvement in patients with frontotemporal lobar degeneration: think progranulin. *JAMA Neurol.* 71, 1562–1566. doi: 10.1001/jamaneurol.2014.1316

Finch, N., Baker, M., Crook, R., Swanson, K., Kuntz, K., Surtees, R., et al. (2009). Plasma progranulin levels predict progranulin mutation status in frontotemporal dementia patients and asymptomatic family members. *Brain* 132, 583–591. doi: 10.1093/brain/awn352

Folstein, M. F., Folstein, S. E., and McHugh, P. R. (1975). "Mini-mental state". A practical method for grading the cognitive state of patients for the clinician. *J. Psychiatr. Res.* 12, 189–198. doi: 10.1016/0022-3956(75)90026-6

Ghetti, B., Spina, S., Murrell, J. R., Huey, E. D., Pietrini, P., Sweeney, B., et al. (2008). In vivo and postmortem clinicoanatomical correlations in frontotemporal dementia and parkinsonism linked to chromosome 17. *Neurodegener. Dis.* 5, 215–217. doi: 10.1159/000113706

Ghidoni, R., Benussi, L., Glionna, M., Franzoni, M., and Binetti, G. (2008). Low plasma progranulin levels predict progranulin mutations in frontotemporal lobar degeneration. *Neurology* 71, 1235–1239. doi: 10.1212/01.wnl.0000325058.10218.fc

Ghidoni, R., Paterlini, A., and Benussi, L. (2012a). Circulating progranulin as a biomarker for neurodegenerative diseases. *Am. J. Neurodegener. Dis.* 1, 180–190.

Ghidoni, R., Stoppani, E., Rossi, G., Piccoli, E., Albertini, V., Paterlini, A., et al. (2012b). Optimal plasma progranulin cutoff value for predicting null progranulin mutations in neurodegenerative diseases: a multicenter Italian study. *Neurodegener. Dis.* 9, 121–127. doi: 10.1159/000333132

Gorno-Tempini, M. L., Hillis, A. E., Weintraub, S., Kertesz, A., Mendez, M., Cappa, S. F., et al. (2011). Classification of primary progressive aphasia and its variants. *Neurology* 76, 1006–1014. doi: 10.1212/WNL.0b013e31821103e6

Hughes, C. P., Berg, L., Danziger, W. L., Coben, L. A., and Martin, R. L. (1982). A new clinical scale for the staging of dementia. *Br. J. Psychiatry* 140, 566–572. doi: 10.1192/bjp.140.6.566

Kessenbrock, K., Frohlich, L., Sixt, M., Lammermann, T., Pfister, H., Bateman, A., et al. (2008). Proteinase 3 and neutrophil elastase enhance inflammation in mice by inactivating antiinflammatory progranulin. *J. Clin. Invest.* 118, 2438–2447. doi: 10.1172/JCI34694

Klimesch, W. (2012). Alpha-band oscillations, attention, and controlled access to stored information. *Trends Cogn. Sci.* 16, 606–617. doi: 10.1016/j.tics.2012.10.007

Koenig, T., Lehmann, D., Saito, N., Kuginuki, T., Kinoshita, T., and Koukkou, M. (2001). Decreased functional connectivity of EEG theta-frequency activity in first-episode, neuroleptic-naive patients with schizophrenia: preliminary results. *Schizophr. Res.* 50, 55–60. doi: 10.1016/S0920-9964(00)00154-7

Lashley, T., Rohrer, J. D., Mead, S., and Revesz, T. (2015). Review: an update on clinical, genetic and pathological aspects of frontotemporal lobar degenerations. *Neuropathol. Appl. Neurobiol.* 41, 858–881. doi: 10.1111/nan.12250

Lawton, M. P., and Brody, E. M. (1969). Assessment of older people: self-maintaining and instrumental activities of daily living. *Gerontologist* 9, 179–186. doi: 10.1093/geront/9.3_Part_1.179

Lezak, M., Howieson, D., and Loring, D. W. (2004). *Neuropsychological Assessment*, 4th Edn. Oxford: Oxford University Press.

McKeith, I. G., Galasko, D., Kosaka, K., Perry, E. K., Dickson, D. W., Hansen, L. A., et al. (1996). Consensus guidelines for the clinical and pathologic diagnosis of dementia with Lewy bodies (DLB): report of the consortium on DLB international workshop. *Neurology* 47, 1113–1124. doi: 10.1212/WNL.47.5.1113

Moretti, D. V. (2015a). Electroencephalography reveals lower regional blood perfusion and atrophy of the temporoparietal network associated with memory deficits and hippocampal volume reduction in mild cognitive impairment due to Alzheimer's disease. *Neuropsychiatr. Dis. Treat.* 11, 461–470. doi: 10.2147/NDT.S78830

Moretti, D. V. (2015b). Theta and alpha EEG frequency interplay in subjects with mild cognitive impairment: evidence from EEG, MRI, and SPECT brain modifications. *Front. Aging Neurosci.* 7:31. doi: 10.3389/fnagi.2015.00031

Moretti, D. V. (2015c). Mild cognitive impairment: structural, metabolical, and neurophysiological evidence of a novel EEG biomarker. *Front. Neurol.* 6:152. doi: 10.3389/fneur.2015.00152

Moretti, D. V. (2015d). Association of EEG, MRI, and regional blood flow biomarkers is predictive of prodromal Alzheimer's disease. *Neuropsychiatr. Dis. Treat.* 11, 2779–2791. doi: 10.2147/NDT.S93253

Moretti, D. V., Babiloni, C., Binetti, G., Cassetta, E., Dal Forno, G., Ferreric, F., et al. (2004). Individual analysis of EEG frequency and band power in mild Alzheimer's disease. *Clin. Neurophysiol.* 115, 299–308. doi: 10.1016/S1388-2457(03)00345-6

Moretti, D. V., Babiloni, F., Carducci, F., Cincotti, F., Remondini, E., Rossini, P. M., et al. (2003). Computerized processing of EEG-EOG-EMG artifacts for multi-centric studies in EEG oscillations and event-related potentials. *Int. J. Psychophysiol.* 47, 199–216. doi: 10.1016/S0167-8760(02)00153-8

Moretti, D. V., Frisoni, G. B., Fracassi, C., Pievani, M., Geroldi, C., Binetti, G., et al. (2011b). MCI patients' EEGs show group differences between those who progress and those who do not progress to AD. *Neurobiol. Aging* 32, 563–571. doi: 10.1016/j.neurobiolaging.2009.04.003

Moretti, D. V., Frisoni, G. B., Pievani, M., Rosini, S., Geroldi, C., Binetti, G., et al. (2008a). Cerebrovascular disease and hippocampal atrophy are differently linked to functional coupling of brain areas: an EEG coherence study in MCI subjects. *J. Alzheimers Dis.* 14, 285–299. PMID: 18599955

Moretti, D. V., Miniussi, C., Frisoni, G., Zanetti, O., Binetti, G., Geroldi, C., et al. (2007b). Vascular damage and EEG markers in subjects with mild cognitive impairment. *Clin. Neurophysiol.* 118, 1866–1876. doi: 10.1016/j.clinph.2007.05.009

Moretti, D. V., Miniussi, C., Frisoni, G. B., Geroldi, C., Zanetti, O., Binetti, G., et al. (2007a). Hippocampal atrophy and EEG markers in subjects with mild cognitive impairment. *Clin. Neurophysiol.* 118, 2716–2729. doi: 10.1016/j.clinph.2007.05.009

Moretti, D. V., Paternico, D., Binetti, G., Zanetti, O., and Frisoni, G. B. (2013a). EEG upper/low alpha frequency power ratio relates to temporo-parietal brain atrophy and memory performances in mild cognitive impairment. *Front. Aging Neurosci.* 5:63. doi: 10.3389/fnagi.2013.00063

Moretti, D. V., Paternico, D., Binetti, G., Zanetti, O., and Frisoni, G. B. (2014a). Electroencephalographic upper/low alpha frequency power ratio relates to cortex thinning in mild cognitive impairment. *Neurodegener. Dis.* 14, 18–30. doi: 10.1159/000354863

Moretti, D. V., Paternico, D., Binetti, G., Zanetti, O., and Frisoni, G. B. (2014b). EEG upper/low alpha frequency power ratio and the impulsive disorders network in subjects with mild cognitive impairment. *Curr. Alzheimer Res.* 11, 192–199. doi: 10.2174/1567205011021403131555546

Moretti, D. V., Pievani, M., Fracassi, C., Binetti, G., Rosini, S., Geroldi, C., et al. (2009a). Increase of theta/gamma and alpha3/alpha2 ratio is associated with amygdalo-hippocampal complex atrophy. *J. Alzheimers Dis.* 17, 349–357. doi: 10.3233/JAD-2009-1059

Moretti, D. V., Pievani, M., Fracassi, C., Geroldi, C., Calabria, M., De Carli, C. S., et al. (2008b). Brain vascular damage of cholinergic pathways and EEG markers in mild cognitive impairment. *J. Alzheimers Dis.* 15, 357–372. PMID: 18997289

Moretti, D. V., Pievani, M., Geroldi, C., Binetti, G., Zanetti, O., Cotelli, M., et al. (2009b). Increasing hippocampal atrophy and cerebrovascular damage is differently associated with functional cortical coupling in MCI patients. *Alzheimer Dis. Assoc. Disord.* 23, 323–332. doi: 10.1097/WAD.0b013e31819d4a9d

Moretti, D. V., Prestia, A., Binetti, G., Zanetti, O., and Frisoni, G. B. (2013b). Increase of theta frequency is associated with reduction in regional cerebral blood flow only in subjects with mild cognitive impairment with higher upper alpha/low alpha EEG frequency power ratio. *Front. Behav. Neurosci.* 7:188. doi: 10.3389/fnbeh.2013.00188

Moretti, D. V., Prestia, A., Fracassi, C., Binetti, G., Zanetti, O., and Frisoni, G. B. (2012). Specific EEG changes associated with atrophy of hippocampus in subjects with mild cognitive impairment and Alzheimer's disease. *Int. J. Alzheimers Dis.* 2012, 253153. doi: 10.1155/2012/253153

Moretti, D. V., Prestia, A., Fracassi, C., Geroldi, C., Binetti, G., Rossini, P. M., et al. (2011a). Volumetric differences in mapped hippocampal regions correlate with increase of high alpha rhythm in Alzheimer's disease. *Int. J. Alzheimers Dis.* 2011, 208218. doi: 10.4061/2011/208218

Neary, D., Snowden, J. S., Gustafson, L., Passant, U., Stuss, D., Black, S., et al. (1998). Frontotemporal lobar degeneration: a consensus on clinical diagnostic criteria. *Neurology* 51, 1546–1554. doi: 10.1212/WNL.51.6.1546

Nishida, K., Razavi, N., Jann, K., Yoshimura, M., Dierks, T., Kinoshita, T., et al. (2015). Integrating different aspects of resting brain activity: a review of electroencephalographic signatures in resting state networks derived from functional magnetic resonance imaging. *Neuropsychobiology* 71, 6–16. doi: 10.1159/000363342

Petkau, T. L., Neal, S. J., Milnerwood, A., Mew, A., Hill, A. M., Orban, P., et al. (2012). Synaptic dysfunction in progranulin-deficient mice. *Neurobiol. Dis.* 45, 711–722. doi: 10.1016/j.nbd.2011.10.016

Pickering-Brown, S. M., Rollinson, S., Du Plessis, D., Morrison, K. E., Varma, A., Richardson, A. M., et al. (2008). Frequency and clinical characteristics of progranulin mutation carriers in the Manchester frontotemporal lobar degeneration cohort: comparison with patients with MAPT and no known mutations. *Brain* 131, 721–731. doi: 10.1093/brain/awm331

Premi, E., Cauda, F., Gasparotti, R., Diano, M., Archetti, S., Padovani, A., et al. (2014). Multimodal FMRI resting-state functional connectivity in granulin mutations: the case of fronto-parietal dementia. *PLoS ONE* 9:e106500. doi: 10.1371/journal.pone.0106500

Raghavachari, S., Lisman, J. E., Tully, M., Madsen, J. R., Bromfield, E. B., and Kahana, M. J. (2006). Theta oscillations in human cortex during a working-memory task: evidence for local generators. *J. Neurophysiol.* 95, 1630–1638. doi: 10.1152/jn.00409.2005

Rankin, K. P., Baldwin, E., Pace-Savitsky, C., Kramer, J. H., and Miller, B. L. (2005). Self awareness and personality change in dementia. *J. Neurol. Neurosurg. Psychiatry* 76, 632–639. doi: 10.1136/jnnp.2004.042879

Rascovsky, K., Hodges, J. R., Knopman, D., Mendez, M. F., Kramer, J. H., Neuhaus, J., et al. (2011). Sensitivity of revised diagnostic criteria for the behavioural variant of frontotemporal dementia. *Brain* 134, 2456–2477. doi: 10.1093/brain/awr179

Rohrer, J. D., Geser, F., Zhou, J., Gennatas, E. D., Sidhu, M., Trojanowski, J. Q., et al. (2010b). TDP-43 subtypes are associated with distinct atrophy patterns in frontotemporal dementia. *Neurology* 75, 2204–2211. doi: 10.1212/WNL.0b013e318202038c

Rohrer, J. D., Ridgway, G. R., Modat, M., Ourselin, S., Mead, S., Fox, N. C., et al. (2010a). Distinct profiles of brain atrophy in frontotemporal lobar degeneration caused by progranulin and tau mutations. *Neuroimage* 53, 1070–1076. doi: 10.1016/j.neuroimage.2009.12.088

Rosen, W. G., Terry, R. D., Fuld, P. A., Katzman, R., and Peck, A. (1980). Pathological verification of ischemic score in differentiation of dementias. *Ann. Neurol.* 7, 486–488. doi: 10.1002/ana.410070516

Sala-Llonch, R., Bartres-Faz, D., and Junque, C. (2015). Reorganization of brain networks in aging: a review of functional connectivity studies. *Front. Psychol.* 6:663. doi: 10.3389/fpsyg.2015.00663

Seelaar, H., Rohrer, J. D., Pijnenburg, Y. A., Fox, N. C., and van Swieten, J. C. (2011). Clinical, genetic and pathological heterogeneity of frontotemporal dementia: a review. *J. Neurol. Neurosurg. Psychiatry* 82, 476–486. doi: 10.1136/jnnp.2010.212225

Seeley, W. W. (2008). Selective functional, regional, and neuronal vulnerability in frontotemporal dementia. *Curr. Opin. Neurol.* 21, 701–707. doi: 10.1097/WCO.0b013e3283168e2d

Sleegers, K., Brouwers, N., Van Damme, P., Engelborghs, S., Gijselinck, I., van der Zee, J., et al. (2009). Serum biomarker for progranulin-associated frontotemporal lobar degeneration. *Ann. Neurol.* 65, 603–609. doi: 10.1002/ana.21621

Tapia, L., Milnerwood, A., Guo, A., Mills, F., Yoshida, E., Vasuta, C., et al. (2011). Progranulin deficiency decreases gross neural connectivity but enhances transmission at individual synapses. *J. Neurosci.* 31, 11126–11132. doi: 10.1523/JNEUROSCI.6244-10.2011

Tenke, C. E., Kayser, J., Manna, C. G., Fekri, S., Kroppmann, C. J., Schaller, J. D., et al. (2011). Current source density measures of electroencephalographic alpha predict antidepressant treatment response. *Biol. Psychiatry* 70, 388–394. doi: 10.1016/j.biopsych.2011.02.016

Van Damme, P., Van Hoecke, A., Lambrechts, D., Vanacker, P., Bogaert, E., van Swieten, J., et al. (2008). Progranulin functions as a neurotrophic factor to regulate neurite outgrowth and enhance neuronal survival. *J. Cell Biol.* 181, 37–41. doi: 10.1083/jcb.200712039

Van Swieten, J. C., and Heutink, P. (2008). Mutations in progranulin (GRN) within the spectrum of clinical and pathological phenotypes of frontotemporal dementia. *Lancet Neurol.* 7, 965–974. doi: 10.1016/S1474-4422(08)70194-7

Walker, A. J., Meares, S., Sachdev, P. S., and Brodaty, H. (2005). The differentiation of mild frontotemporal dementia from Alzheimer's disease and

healthy aging by neuropsychological tests. *Int. Psychogeriatr.* 17, 57–68. doi: 10.1017/S1041610204000778

Warren, J. D., Rohrer, J. D., Schott, J. M., Fox, N. C., Hardy, J., and Rossor, M. N. (2013). Molecular nexopathies: a new paradigm of neurodegenerative disease. *Trends Neurosci.* 36, 561–569. doi: 10.1016/j.tins.2013.06.007

Whitwell, J. L., Jack, C. R. Jr., Boeve, B. F., Senjem, M. L., Baker, M., Rademakers, R., et al. (2009). Voxel-based morphometry patterns of atrophy in FTLD with mutations in MAPT or PGRN. *Neurology* 72, 813–820. doi: 10.1212/01.wnl.0000343851.46573.67

Whitwell, J. L., Weigand, S. D., Boeve, B. F., Senjem, M. L., Gunter, J. L., DeJesus-Hernandez, M., et al. (2012). Neuroimaging signatures of frontotemporal dementia genetics: C9ORF72, tau, progranulin and sporadics. *Brain* 135, 794–806. doi: 10.1093/brain/aws001

Xu, J., Xilouri, M., Bruban, J., Shioi, J., Shao, Z., Papazoglou, I., et al. (2011). Extracellular progranulin protects cortical neurons from toxic insults by activating survival signaling. *Neurobiol. Aging* 32, 2326.e5–2326.e16. doi: 10.1016/j.neurobiolaging.2011.06.017

Conflict of Interest Statement: The authors declare that the research was conducted in the absence of any commercial or financial relationships that could be construed as a potential conflict of interest.

Copyright © 2016 Moretti, Benussi, Fostinelli, Ciani, Binetti and Ghidoni. This is an open-access article distributed under the terms of the Creative Commons Attribution License (CC BY). The use, distribution or reproduction in other forums is permitted, provided the original author(s) or licensor are credited and that the original publication in this journal is cited, in accordance with accepted academic practice. No use, distribution or reproduction is permitted which does not comply with these terms.

Advantages of publishing in Frontiers

OPEN ACCESS
Articles are free to read, for greatest visibility

COLLABORATIVE PEER-REVIEW
Designed to be rigorous – yet also collaborative, fair and constructive

FAST PUBLICATION
Average 85 days from submission to publication (across all journals)

COPYRIGHT TO AUTHORS
No limit to article distribution and re-use

TRANSPARENT
Editors and reviewers acknowledged by name on published articles

SUPPORT
By our Swiss-based editorial team

IMPACT METRICS
Advanced metrics track your article's impact

GLOBAL SPREAD
5'100'000+ monthly article views and downloads

LOOP RESEARCH NETWORK
Our network increases readership for your article

Frontiers
EPFL Innovation Park, Building I • 1015 Lausanne • Switzerland
Tel +41 21 510 17 00 • Fax +41 21 510 17 01 • info@frontiersin.org
www.frontiersin.org

Find us on